TECHNICAL REPORT H-75-17

TYPE 16 FLOOD INSURANCE STUDY: TSUNAMI PREDICTIONS FOR MONTEREY AND SAN FRANCISCO BAYS AND PUGET SOUND

by

Andrew W. Garcia, James R. Houston

Hydraulics Laboratory
U. S. Army Engineer Waterways Experiment Station
P. O. Box 631, Vicksburg, Miss. 39180

November 1975

Final Report

Prepared for Federal Insurance Administration,
Department of Housing and Urban Development
Washington, D. C. 20314

Unclassified

SECURITY CLASSIFICATION OF THIS PAGE *(When Data Entered)*

REPORT DOCUMENTATION PAGE

READ INSTRUCTIONS BEFORE COMPLETING FORM

1. REPORT NUMBER: Technical Report H-75-17

2. GOVT ACCESSION NO.:

3. RECIPIENT'S CATALOG NUMBER:

4. TITLE *(and Subtitle)*: TYPE 16 FLOOD INSURANCE STUDY: TSUNAMI PREDICTIONS FOR MONTEREY AND SAN FRANCISCO BAYS AND PUGET SOUND

5. TYPE OF REPORT & PERIOD COVERED: Final report

6. PERFORMING ORG. REPORT NUMBER:

7. AUTHOR(s): Andrew W. Garcia
James R. Houston

8. CONTRACT OR GRANT NUMBER(s):

9. PERFORMING ORGANIZATION NAME AND ADDRESS:
U. S. Army Engineer Waterways Experiment Station
Hydraulics Laboratory
P. O. Box 631, Vicksburg, MS 39180

10. PROGRAM ELEMENT, PROJECT, TASK AREA & WORK UNIT NUMBERS:

11. CONTROLLING OFFICE NAME AND ADDRESS:
Federal Insurance Administration
Department of Housing and Urban Development
Washington, D. C. 20314

12. REPORT DATE: November 1975

13. NUMBER OF PAGES: 263

14. MONITORING AGENCY NAME & ADDRESS *(if different from Controlling Office)*:

15. SECURITY CLASS. *(of this report)*: Unclassified

15a. DECLASSIFICATION/DOWNGRADING SCHEDULE:

16. DISTRIBUTION STATEMENT *(of this Report)*

Approved for public release; distribution unlimited.

17. DISTRIBUTION STATEMENT *(of the abstract entered in Block 20, if different from Report)*

18. SUPPLEMENTARY NOTES

19. KEY WORDS *(Continue on reverse side if necessary and identify by block number)*

Flood insurance
Monterey Bay, Calif.
Predictions
Puget Sound
San Francisco Bay
Tsunamis

20. ABSTRACT *(Continue on reverse side if necessary and identify by block number)*

Calculations of runup due to seismic sea waves (tsunamis) of distant origin were made for Monterey and San Francisco Bays and the greater part of Puget Sound. Those areas which are specifically included and excluded are listed. The values presented are interpreted as being equaled or exceeded on the average of once per 100 (R_{100}) or once per 500 (R_{500}) yr, whichever is indicated. All runup values, R_{100} and R_{500}, are referenced to the mean sea

(Continued)

DD FORM 1 JAN 73 1473 EDITION OF 1 NOV 65 IS OBSOLETE

Unclassified

SECURITY CLASSIFICATION OF THIS PAGE *(When Data Entered)*

20. ABSTRACT (Continued).

level datum. The combined effects of astronomical tides and tsunamis are incorporated into the analysis as are certain local effects. The effects of wind waves superimposed on the tsunami have been neglected. The simultaneous occurrence of a storm surge and tsunami is considered highly improbable and therefore unlikely to constitute a 1 in 100- or 1 in 500-yr event.

Analysis of the error attributed to each of the various steps in the procedure results in an estimated maximum average error of about ±40 percent.

PREFACE

The investigation reported herein was authorized by the Office, Chief of Engineers (OCE), U. S. Army, in a letter dated 14 February 1974 and was performed for the Federal Insurance Administration, Department of Housing and Urban Development, under Inter-Agency Agreements IAA-H-19-74, Project Order No. 9, and IAA-H-19-75, Project Order No. 4. Project coordinator was Mr. Jerome Peterson of OCE.

The investigation was conducted from March 1974 to January 1975 by personnel of the Hydraulics Laboratory (HL), U. S. Army Engineer Waterways Experiment Station (WES), under the direction of Mr. H. B. Simmons, Chief of HL, Dr. R. W. Whalin, Chief of the Wave Dynamics Division, and Mr. D. D. Davidson, Chief of the Wave Research Branch. Messrs. A. W. Garcia, Research Oceanographer, and J. R. Houston, Research Physicist, both of HL, conducted the study, and this report was prepared by Mr. Houston with the aid of Mr. Garcia.

A significant portion of the numerical computations was performed on a CDC-7600 computer at the Los Alamos Scientific Laboratory through the cooperation and under the supervision of Dr. Kenneth Olsen of Group J-9. Also, Mr. H. L. Butler of the Harbor Wave Action Section, WES, provided valuable assistance in the performance of these calculations. Drs. Dean McManus and Warren Thompson of the University of Washington and the U. S. Naval Postgraduate School, respectively, provided unpublished data which greatly aided in the performance of this study, as did the staff of the National Ocean Survey, National Oceanic and Atmospheric Administration.

Attendees of the Type 16 Flood Insurance Study Tsunami Coordination meeting held at the U. S. Army Engineer Division, South Pacific, Office in San Francisco, California, on 11 and 12 November 1974 are listed below.

Name	Affiliation
John Ritter	U. S. Geological Survey
Jerome Peterson	Flood Plain Management Services, Office, Chief of Engineers

Name	Affiliation
Robert Whalin	U. S. Army Engineer Waterways Experiment Station
Andrew Garcia	U. S. Army Engineer Waterways Experiment Station
James Houston	U. S. Army Engineer Waterways Experiment Station
Robert Cook	Flood Plain Management Services, South Pacific Division
Warren Viets	Flood Plain Management Services, South Pacific Division
Gerald Gardner	Flood Plain Management Services, Seattle District
Romain Repair	Flood Plain Management Services, San Francisco District
Bill McCaleb	Flood Plain Management Services, San Francisco District
Scott Terry	Flood Plain Management Services, Los Angeles District
Orville Magoon	Coastal Engineering Branch, South Pacific Division
Henry M. DeGraca	Navigation and Shoreline Planning, San Francisco District
Benjamin Wells	Engineering Division, Water Resources Branch, San Francisco District
Claude Wong	Coastal Resources Branch, Los Angeles District
Bob Easley	Hydrologic Engineering Branch, South Pacific Division
Bob Edminsten	Coastal Engineering Branch, South Pacific Division

Director of WES during the investigation and the publication of this report was COL G. H. Hilt, CE. Technical Director was Mr. F. R. Brown.

CONTENTS

TYPE 16 FLOOD INSURANCE STUDY: TSUNAMI PREDICTIONS FOR MONTEREY AND SAN FRANCISCO BAYS AND PUGET SOUND

PART I: INTRODUCTION

1. This study was conducted to determine 100- and 500-yr runup due to tsunamis of distant origin for parts of Monterey Bay, San Francisco Bay, and the Straits of Juan de Fuca and Puget Sound (Table 1). A 100-yr runup is one that is equaled or exceeded with an average frequency of once every 100 yr; a 500-yr runup has a corresponding definition. Runup values in this report are referenced to the mean sea level (msl) datum.

2. A finite-difference numerical computer program was used to simulate tsunamis and propagate them across the deep ocean to the mouths of the above-mentioned water bodies. The governing equations used in the program were the linearized long-wave equations. In order to simulate the generation of a tsunami, an uplift deformation of the water surface at a selected tsunami source site was used as an initial condition in the finite-difference program. As discussed in Reference 1, the large size of the generation areas considered and the short time interval during which displacement occurs cause the water surface deformation to display the same topographic features as the permanent vertical displacement of the ocean floor resulting from the earthquake.

3. The responses of San Francisco Bay and the Straits of Juan de Fuca and Puget Sound to an incoming tsunami were determined using a computerized numerical scheme which employs a finer spatial mesh grid than that used in the numerical scheme for propagating the tsunami across the deep ocean. This numerical solution cannot be validly applied to Monterey Bay, however, because this bay has a mouth that is wide relative to the length of the bay. Therefore, an analytic solution in the form of a standing wave for the linearized long-wave equations was used to propagate a tsunami across the continental shelf of Monterey Bay.

4. Although tsunamis are generated in many areas along the perimeter of the Pacific Basin, only the Aleutian Trench generates tsunamis

capable of causing significant runup in the study areas of this report with sufficient frequency to influence 100- and 500-yr runup values. Historical evidence, tsunami source characteristics and orientation, and numerical computer programs discussed in Reference 1 were used in the selection of the Aleutian Trench as the sole tsunamigenic area. The hypothetical uplift of the water surface used and the dimensional parameters which can be varied to represent tsunamis of different intensities in the selected tsunamigenic areas were also formulated therein.

5. The probability of generation of tsunamis of different intensities and the maximum height of the uplift deformation for the standard source were defined for these different intensities in Reference 1. The Aleutian Trench was divided into 12 segments and the wave amplitudes resulting from locating sources of varying intensities in each of the segments were calculated for points near the mouths of the bays considered. The responses of the bays were determined by the numerical and analytical solutions mentioned earlier. Each wave amplitude inside the bays has an associated probability, and the totality of wave amplitudes defines a probability distribution from which the cumulative probability distribution for a wave amplitude being greater than or equal to a particular value is obtained. Runup is set equal to wave amplitude at the shore.

6. A cumulative probability distribution, $P(z)$, for runup at a given site being equal to or exceeding a particular value due to the astronomical tide and a tsunami was determined using an approach discussed in Reference 1. This approach makes use of the following relationships:

$$P(z) = \int_{-\infty}^{\infty} f_{\beta}(\lambda) P_S(z - \lambda)\, d\lambda \qquad (1)$$

where $f_{\beta}(\lambda)$* is the probability for the astronomical tide.

---

* For convenience, all unusual symbols used in this report are listed and defined in the Notation (Appendix A).

This equation was solved numerically by superimposing tsunami wave trains on the tides for a 1-yr period.

7. A previous San Francisco Bay tsunami study of the U. S. Geological Survey is discussed and results are compared herein.

PART II: LOCATION AND USE OF BACKUP DATA

8. The numerical calculations used in determining the runup values will be retained at the U. S. Army Engineer Waterways Experiment Station (WES) for an indefinite period of time. These calculations by themselves are of limited usefulness in direct determination of runup at a particular coastal site because each raw calculation applies only to a specific intensity tsunami originating at a particular source. Probability distributions, tide analyses, and local effects are calculated using these data but they comprise a number of different and subsequent operations.

9. The user of the information contained in this report will have to judge for his purposes the adequacy of topographic information displayed within, i.e. the accuracy and spacing of contour intervals, the currentness of indicated features, etc.

PART III: EXPLANATION OF RESULTS

10. Table 2 lists the names of the topographic quadrangles contained in this report by groups, according to their geographical location. Because of the geographic complexity of the Monterey and San Francisco Bays and Puget Sound areas, it was not feasible to arrange the section of quadrangles in a continuous sequence following the shoreline of the areas. It was decided instead to arrange the quadrangle sections into subgroups by alphabetical order. Figures 1a and 1b are sections of indices to topographic maps of California and Washington, respectively. To locate the applicable subgroup of quad-sections, locate the area of interest in Figure 1a or 1b; these figures give the name of the topographic quad. The figure number for each quad can be found by referring to Table 2.

11. Located within each figure (Figures 2-239) is the estimated runup with the appropriate subscript designating the runup due to a 100- and 500-yr tsunami. It is specified in the form

$$R_{100} = \_\_ \text{ ft}$$
$$R_{500} = \_\_ \text{ ft}$$

The datum for all runup computations (R_{100} and R_{500}) is msl. As in Reference 1 the runup estimates will be applicable to those reaches of coastline indicated between the solid lines extending from the shoreline. Where only one pair of runup values is displayed, those values will apply to the entire reach of coastline shown in that figure.

12. The figure titles also follow the form used in Reference 1 but the explanation will be repeated here for the convenience of the reader. Using Figure 2 as an example:

Figure 2 - figure number.
Marina - name of topographic quadrangle from which illustration was taken.
Calif. - state in which area is located.
53+N to 57+N - digits indicating the 100-metre* Universal Transverse Mercator grid ticks used to delineate the

---

* 3.2808 converts metres to feet.

approximate boundaries of the section of quadrangle illustrated. (Letter following digits will be either N or E indicating north-south directed or east-west directed tick marks, respectively. A plus (+) or minus (-) sign indicates that the illustration extends slightly beyond or falls slightly short of the indicated tick mark.)

L - last letter indicating which boundary of the topographic quadrangle the grid tick marks are referenced to, i.e. R-right, L-Left, T-top, B-bottom.

Unless otherwise indicated, the scale of all the topographic figures is 1:24,000

PART IV: METHODOLOGY FOR RUNUP PREDICTIONS

Tsunami Sources

13. As described in Reference 1, the Aleutian Trench is divided into 12 segments. Ground displacements which produce tsunamis with intensities ranging from 2 to 5 in intensity increments of 1/2 are centered at the midpoint of each segment. As discussed in Reference 1, an investigation of tsunamigenic sites in the Pacific indicates that tsunamis generated along the Aleutian or Peru-Chile Trenches only cause significant runup along the western coast of the United States. Furthermore, it was found that the 100- and 500-yr runup values for the study areas reported herein are determined by tsunamigenic sites in the Aleutian Trench alone and are not significantly influenced by tsunamis generated in the Peru-Chile Trench.

14. As stated previously, a computer program for a finite-difference numerical scheme was used in Reference 1 to generate a tsunami (using a given ground displacement as input) and to propagate it across the deep ocean. The linearized long-wave equations were the governing equations in the program. This program uses a commonly available tape which contains bathymetric data at intervals of 1 deg of latitude and longitude. The program then interpolates these data to create another bathymetric grid for computational purposes that has 15 bathymetric data points per degree of latitude and longitude. While this procedure is adequate for those regions of the ocean that are relatively featureless, it is not satisfactory for wave propagation across the continental rise and portions of the continental shelf. To avoid this difficulty, the program was modified to include bathymetric data obtained from National Ocean Survey bathymetric charts. These data were smoothed from a minimum of 180 points to 15 points (compatible with the grid used for computation) per degree of latitude and longitude. This was done for both the previous[1] and present studies.

15. The program was used in this study to propagate tsunamis to the vicinities of Monterey and San Francisco Bays and the Straits of

Juan de Fuca. Local bathymetric irregularities (shoals and channels, for example) which might not be resolved by the large mesh grid covering part of the Pacific Ocean near the continental shelf, along with non-linear terms and vertical accelerations which are neglected in the linearized long-wave equations, produce effects which must be determined by calibration. Results of a computer simulation of the generation and propagation of the 1964 Alaska tsunami were compared with tide gage records obtained near the mouths of San Francisco Bay and the Straits of Juan de Fuca; differences in comparison are attributed to these local bathymetric irregularities and the neglected terms in the equations of motion. In this manner, the simulation of the 1964 tsunami was calibrated to reproduce the effects observed at the bay mouths.

Bay Response

16. Once the tsunami wave amplitudes at the mouths of San Francisco Bay and the Straits of Juan de Fuca were known, the responses of these partially enclosed bodies of water to the incoming tsunami were determined by using a computerized numerical scheme[2] which employs a fine mesh spatial grid. The numerical method used is that described by Leendertse.[3] Variable bathymetry and Chezy frictional coefficients in the bay were allowed as input to the program. The ratio of tsunami amplitude to water depth in parts of the bay is great enough that non-linear advective terms may be significant and are therefore included in the equations of motion. The period of the tsunami waves entering the bays was chosen to be 38 min for San Francisco Bay and 1.8 hr for Puget Sound; these periods were observed during the 1964 tsunami.[2] The reasons different locations can observe different tsunami wave periods are discussed in Reference 1.

17. The numerical solution discussed above cannot be validly applied to Monterey Bay because this bay has a mouth that is wide relative to its length. Wave recordings of the 1964 tsunami obtained at Monterey, California, indicate that resonance of the bay resulting from tsunami excitation is not significant in determining the maximum

runup; a number of major waves of approximately the same amplitude were observed during the 1964 Alaska tsunami.*

18. The analytical solution employed in Reference 1 to determine the modification of a tsunami after its propagation across the continental shelf was used at Monterey Bay to determine runup. A computer simulation of the generation and propagation of the 1964 tsunami across the deep ocean was coupled with the above analytical solution and the results were compared with gage recordings of the 1964 tsunami at Monterey to calibrate the techniques.

Effect of Astronomical Tides

19. As mentioned earlier, the statistical effect of astronomical tides on tsunami runup was determined in Reference 1 by an analytical solution of the convolution integral.[4]

$$P(z) = \int_{-\infty}^{\infty} f_{\beta}(\lambda) P_S(z - \lambda)\, d\lambda \qquad (1 \text{ bis})$$

where

z = the runup at any time above local mean sea level

$P_S(z)$ = the cumulative probability distribution for runup at a given site being equal to or exceeding z due only to the maximum wave of the tsunami

$P_{\beta}(z)$ = the probability of the runup at the same location being equal to or exceeding z due only to the astronomical tide, here approximated by a Gaussian distribution (tidal runup equals the tidal level)

$P(z)$ = the cumulative probability distribution for runup at a given site being equal to or exceeding z due to the maximum wave of the tsunami and the astronomical tide

and where

$$f_{\beta}(z) = - \frac{dP_{\beta}(z)}{dz}$$

---

* Prof. W. C. Thompson, personal communication.

and $f_\beta(z)$ is the probability density for the astronomical tide.

20. Tsunamis arriving at Monterey Bay, San Francisco Bay, and Puget Sound have, in the past, exhibited characteristic wave trains consisting of a number of waves of significant amplitude. The statistical effect of astronomical tides on tsunami runup for such a situation when more than a single maximum tsunami wave is important must be determined through a numerical solution because an analytical solution is intractable. A numerical approach similar to that used by Petrauskas and Borgman[5] to randomly combine the effects of astronomical tides and tsunamis recorded at Crescent City, California, was used to solve this problem. Data obtained during the 1960 and 1964 tsunamis were combined with tides at random times during a year by Petrauskas and Borgman. In this study, the combination at random times during a year of a wave train consisting of a specified number of waves of equal amplitude and period and the astronomical tides was considered. The amplitudes of the wave trains are not fixed, however, but are specified by probability distributions.

21. A time history of the tide for a year at any location of interest was determined by a computer program which used the techniques of Reference 6 and tide information from Reference 7. The period and number of significant waves of a tsunami which could be expected at a site were determined by analyzing wave records obtained during the 1964 tsunami. It is assumed here that the number and period of waves observed during the 1964 tsunami are indicative of the respective response of these areas to other high-intensity tsunamis. Five waves with a period of 38 min were chosen for the tide effect analysis for San Francisco Bay, three waves with a period of 1.8 hr for Puget Sound, and ten waves with a period of 36 min for Monterey Bay.

22. A tsunami with an intensity between 2 and 5 in increments of one-half is generated in one of the 12 segments of the Aleutian Trench and arrives at a site on the western coast of the United States with its significant waves having an amplitude which can be determined by the techniques described earlier in this report. The probability of such an event occurring is equal to the probability of a tsunami of some particular intensity being generated somewhere in the Aleutian Trench, given by

$$n(i) = 0.065e^{-0.71i} \quad (2)$$

multiplied by 1/12, because it is assumed that earthquakes occur uniformly throughout the length of the 12-segment trench.[1,8]

23. Each of the possible tsunami wave trains of intensity range 2-5 from 1 of the 12 segments is then superimposed upon the astronomical tide occurring at a site during a year. For example, the 10 significant wave crests of period 36 min of a tsunami arriving at Monterey Bay are superimposed on the tides over a 360-min interval; the maximum tsunami plus tide elevation for the period is assigned a probability equal to 1/12 multiplied by Equation 2, for a particular intensity i, multiplied by q (360 min/number of minutes per year = 6.85×10^{-4}). The tsunami is superimposed upon the astronomical tide for 360-min intervals for the entire year. By following this procedure for all tsunamis of intensity 2-5 for the 12 segments, a cumulative probability distribution for runup at a given site equal to or exceeding some value due to the superposition of the tsunami and the astronomical tide was determined. The 1 in 100-yr and 1 in 500-yr runup values at a site were determined from this probability distribution.

Results

24. By applying the methodology described in the previous sections and in Reference 1, 100- and 500-yr runup values were calculated for Monterey Bay, San Francisco Bay, and the Puget Sound area. The runup values (referenced to msl) are shown in Figures 2-239 which are sections of topographic quadrangle maps published by the U. S. Geological Survey.

25. The effect of the astronomical tides on runup varied from location to location. The more pronounced the tidal range, the more significant was the increase in runup due to the influence of the astronomical tides. For example, tsunami waves in Puget Sound had small amplitudes, and runup values were governed largely by the effect of astronomical tides. Therefore, although waves had larger amplitudes at Port Townsend, Washington, than at Seattle, Washington, the greater

tidal range at Seattle resulted in larger combined runup values there.

26. The effect of the astronomical tides on runup was also dependent upon the probability distribution of tsunami wave amplitudes at a location. The tidal contribution to runup is usually greater for locations protected from tsunamis than for those exposed. This can readily be seen for an analytic solution of Equation 1.

27. For simplicity consider only a single source region (e.g. the Aleutian Trench) and let $P_S^{(1)}(z)$ be represented by an exponential function

$$P_S^{(1)}(z) = A_1 e^{-\alpha_1 z} \tag{3}$$

where the superscript (1) denotes location 1.

28. Suppose that tsunamis at a second location occur with the same frequency as that for the first location but always produce twice as great a runup. Then

$$P_S^{(1)}(z) = P_S^{(2)}(\hat{z}) \tag{4}$$

where

$$\hat{z} = 2z$$

and

$$P_S^{(2)}(\hat{z}) = A_2 e^{-\alpha_2 \hat{z}}$$

$$= A_2 e^{-2\alpha_2 z} \tag{5}$$

Therefore

$$A_1 e^{-\alpha_1 z} = A_2 e^{-2\alpha_2 z}$$

$$A_1 = A_2 \quad \text{and} \quad \alpha_1 = 2\alpha_2 \tag{6}$$

29. In Reference 1 it was found that the net effect of the astronomical tide is to produce a $P(z)$ identical with $P_S(z)$ except for a shift of z by an amount $(\sigma^2/2)\alpha$. σ^2 is the tidal variance and equals $\sum_{m=1}^{\infty} C_m^2$ where C_m is equal to the m^{th} tidal constituent. To

evaluate Equation 1

$$P_\beta(z) \approx f_\beta(z) = \frac{1}{\sqrt{(\pi\sigma)}} e^{-z^2/2\sigma^2}$$

30. Since σ^2 varies very little between two locations, the effect of the astronomical tide on runup is approximately twice as large for location 1 as for location 2.

31. As an example of this effect note that although a tsunami at the easterly end of San Pablo Bay in San Francisco Bay is reduced to less than one-tenth its height at the Presidio, the 100-yr runup including the effect of astronomical tide is reduced only by a factor of between 2 and 3.

San Francisco Bay Tsunami Study by the U. S. Geological Survey

32. An earlier study of tsunami runup in the San Francisco Bay region was performed in cooperation with the Department of Housing and Urban Development by John R. Ritter and William R. Dupre of the U. S. Geological Survey of the Department of the Interior.[9] This previous investigation determined a 200-yr tsunami runup at the Presidio in San Francisco (Figure 240) by extrapolating a frequency of occurrence curve for the maximum tsunami waves at the Presidio which was developed by Wiegel[10] and based on historical data for the years 1900-1965. Tsunami attenuation inside San Francisco Bay was based on data of the May 1960 and March 1964 tsunamis collected by Magoon.[11] The maps of this earlier study delineated areas which would be subject to inundation in the event of a 200-yr tsunami occurring during the mean higher high water tidal stage.

33. The 100-yr tsunami maximum wave height predicted by the extended frequency curve (Figure 2 of Reference 9) is approximately 11 ft.* The ordinate axis of this graph is erroneously labeled "Maximum

---

* 0.3048 converts feet to metres.

Wave Height or Runup." Wiegel[10] plotted maximum wave height versus recurrence interval for Crescent City and San Francisco, California. Runup was plotted versus recurrence interval for Hilo, Hawaii, in the same figure. The word "Runup" was intended to be the ordinate axis label for Hilo only. Maximum wave height in this case refers to what is sometimes called range, the sum of runup plus drawdown, and thus runup does not refer to wave height.

34. Assuming that tsunami waves are approximately sinusoidal (as noted by Wilson,[12] the 100-yr tsunami would have an amplitude of 5.5 ft at the Presidio according to Ritter and Dupre's analysis. Neglecting tidal effects, this is a 5.5-ft runup above mean sea level. The 100-yr runup at the Presidio calculated in this report is 7.0 ft (predictions in Figure 54 include tidal effects) above mean sea level if tidal effects are neglected. The Geological Survey analysis also predicts a 500-yr runup of 15 ft. This compares with a 14.6-ft runup value, neglecting astronomical tides, calculated in this report.

35. Tsunami attenuation inside San Francisco Bay as calculated in this report is similar to the attenuation noted by Magoon (Reference 11) for the May 1960 and March 1964 tsunamis. The tsunami wave amplitude at Richmond on the north and Hunter's Point on the south is approximately half the height at the Presidio. The attenuation noted by Magoon and the attenuation calculated in this report are compared in Figure 240b.

36. The numerical method used herein allows prediction of tsunami runup in San Francisco Bay over an area bounded laterally by Point San Pablo on the north and Point San Bruno on the south. The limits of these boundaries are dictated by a combination of small grid size required to adequately define the incoming wave at the bay entrance and maximum storage available using the WES Honeywell 635 computer. It is doubtful that the numerical technique used would give meaningful results in very shallow areas of the bay because the tsunami wave height becomes a significant fraction of the water depth. For those areas of the bay not covered by the numerical grid, the tsunami wave was linearly decayed with distance from the values at the boundary of the numerical grid to

the normalized value of 0.1 at the ends of the bay. The fact that the numerical grid did not include the entire San Francisco Bay is not felt to be a deficiency with serious consequences because the wave has decayed to less than half its height in the distance from the bay entrance to the boundaries of the numerical grid.

Conclusions

37. The resonance problem of Monterey and San Francisco Bays has required particular attention and individual treatment. The physical configuration of these bays is such that similar techniques could not be used for both. For example, while San Francisco Bay is characterized as being very elongated with a relatively small mouth, Monterey Bay is more or less semicircular with a relatively wide mouth. Moreover, Monterey Bay is bisected by a deep submarine canyon which effectively partitions it into separate basins.[13] In contrast, the overall problem in the Straits of Juan de Fuca and Puget Sound is not primarily one of resonance but of the decay of the leading waves of the tsunami as they progress along a narrow body of water.

38. The adoption and modification of techniques described by Petrauskas and Borgman[5] for combining tsunami and astronomical tide effects permits a series of waves (of the same tsunami) to arrive at different times during a tidal cycle; in contrast, an earlier report[1] allowed only the leading wave (assumed to be the largest) to be combined with the astronomical tide. This approach results in greater accuracy, especially in areas in which the tsunami is small relative to the tidal range.

39. Use of the latest (in some instances unpublished) bathymetric information for the Pacific coast of the United States allowed significant improvement in the detailing of the coastline and continental shelf area. The finite difference numerical program normally interpolates information available from the 1-deg-square bathymetric tape from one point per square degree to nine points per square degree. However, for this area, the interpolation process was not used; instead,

bathymetric data compatible with the numerical program were inserted.

40. For the three areas considered, analysis of the error attributed to each of the various steps in the procedure results in an estimated maximum average uncertainty of about ±40 percent.

REFERENCES

1. Houston, J. R. and Garcia, A. W., "Type 16 Flood Insurance Study: Tsunami Predictions for Pacific Coastal Communities," Technical Report H-75-3, May 1974, U. S. Army Engineer Waterways Experiment Station, CE, Vicksburg, Miss.

2. Butler, H. L., "Notes on the Usage of a Code for the Numerical Simulation of 'Bay Hydrodynamics'" (unpublished memorandum), Mar 1974, U. S. Army Engineer Waterways Experiment Station, CE, Vicksburg, Miss.

3. Leendertse, J. J., "Aspects of a Computational Model for Long-Period Water-Wave Propagation," Memorandum RM-5204-PR, May 1967, The Rand Corporation, Santa Monica, Calif.

4. Chandrasekhar, S., "Stochastic Problems in Physics and Astronomy," Reviews of Modern Physics, Vol 15, Jan 1943, pp 1-89.

5. Petrauskas, C. and Borgman, L. E., "Frequencies of Crest Heights for Random Combinations of Astronomical Tides and Tsunamis Recorded at Crescent City, California," Technical Report HEL 16-8, Mar 1971, Hydraulic Engineering Laboratory, University of California, Berkeley, Calif.

6. U. S. Coast and Geodetic Survey, "Manual of Harmonic Analysis and Prediction of Tides," Special Publication No. 98, 1958, Washington, D. C.

7. _____, "Tidal Harmonic Constants; Pacific and Indian Oceans," Apr 1942, Washington, D. C.

8. Kelleher, J. et al., "Why and Where Great Thrust Earthquakes Occur Along Island Arcs," Journal of Geophysical Research, Vol 79, No. 32, Nov 1974, pp 4889-4899.

9. Ritter, J. R. and Dupre, W. R., "Maps Showing Areas of Potential Inundation by Tsunamis in the San Francisco Bay Region, California," Miscellaneous Field Studies Map MF-480, 1972, San Francisco Bay Region Environment and Resources Planning Study, U. S. Department of the Interior and U. S. Department of Housing and Urban Development, Washington, D. C.

10. Wiegel, R. L., "Protection of Crescent City, California, from Tsunami Waves," Mar 1965, Redevelopment Agency of the City of Crescent City, Berkeley, Calif.

11. Magoon, O. T., "Structural Damage by Tsunamis," Coastal Engineering - Santa Barbara Specialty Conference, American Society of Civil Engineers, 1965, pp 35-68.

12. Wilson, B. W. and Tørum, A., "The Tsunami of the Alaskan Earthquake, 1964: Engineering Evaluation," Technical Memorandum No. 25, May 1968, U. S. Army Coastal Engineering Research Center, CE, Washington, D. C.

13. Wilson, B. W., Hendrickson, J. A., and Kilmer, R. E., "Feasibility Study for a Surge-Action Model of Monterey Harbor, California," Contract Report 2-136, October 1965, U. S. Army Engineer Waterways Experiment Station, CE, Vicksburg, Miss.

Table 1

Areas Definitely Included or Excluded

Included	Excluded
Monterey Bay	
Santa Cruz Harbor and Small Craft Harbor	Salinas River
Monterey Harbor	Pajaro River
The beaches of Monterey Bay extending from Pt. Pinos to Pt. Terrence	Moss Landing Harbor
San Francisco Bay	
San Pablo Bay	Carquinez Strait
San Francisco Bay	Napa River
Richardson Bay	Petaluma River
Golden Gate as far seaward as Pt. Bonita and Pt. Lobos	Sonoma Creek
	Redwood Creek
Straits of Juan de Fuca, Puget Sound	
Seattle and vicinity	Hood Canal
Tacoma and vicinity	Saratoga Passage
Victoria and vicinity	Skagit Bay and Holmes Harbor
Everett and vicinity	Port Susan
Port Angeles and vicinity	Sooke Harbor
Port Townsend	

Table 2

Topographic Quadrangles

Quad Name	Applicable Figure No. (Inclusive)
Monterey Bay	
Marina	2-5
Monterey	6-7
Moss Landing	8-11
Santa Cruz	12-13
Sea Side	14
Soquel	15-17
Watsonville W.	18-19
San Francisco Bay	
Benicia	20
Hunters Point	21-23
Mountain View	24-26
Newark	27-28
Oakland E.	29
Oakland W.	30-35
Petaluma Point	36-40
Redwood Point	41-47
Richmond	48-50
San Francisco N.	51-57
San Francisco S.	58-60
San Leandro	61-65
San Mateo	66-68
San Quentin	69-76
San Rafael	77-78
Sears Point	79
Puget Sound Area	
Anacortes	80-81
Angeles Point	82-84
Bremerton E.	85-88
Camano	89
Cape Flattery	90-91
Clallam Bay	92-93
Coupeville	94-95
Deception Pass	96-99

Quad Name	Applicable Figure No. (Inclusive)
Puget Sound Area (Continued)	
Des Moines	100-103
Disque	104-105
Dungeness	106-110
Duwamish Head	111-117
Edmonds E.	118-119
Edmonds W.	120-123
Everett	124
False Bay	125-128
Freeland	129-132
Friday Harbor	133-138
Gardiner	139-144
Hansville	145-149
Joyce	150-151
Langley	152
Marysville	153-155
Maxwelton	156-159
Mukilteo	160-165
Nordland	166-171
Orcas Island	172-175
Port Angeles	176-177
Port Gamble	178-182
Port Townsend	183-187
Port Townsend S.	188-189
Port Townsend N.	190-192
Poverty Bay	193-194
Pysht	195-196
Richardson	197-199
Roche Harbor	200-203
Seattle N.	204
Seattle S.	205-206
Sequim	207-210
Shilshole Bay	211-216
Suquamish	217-220
Tacoma N.	221-228
Tulalip	229-232
Twin River	233-234
Vashon	235-239

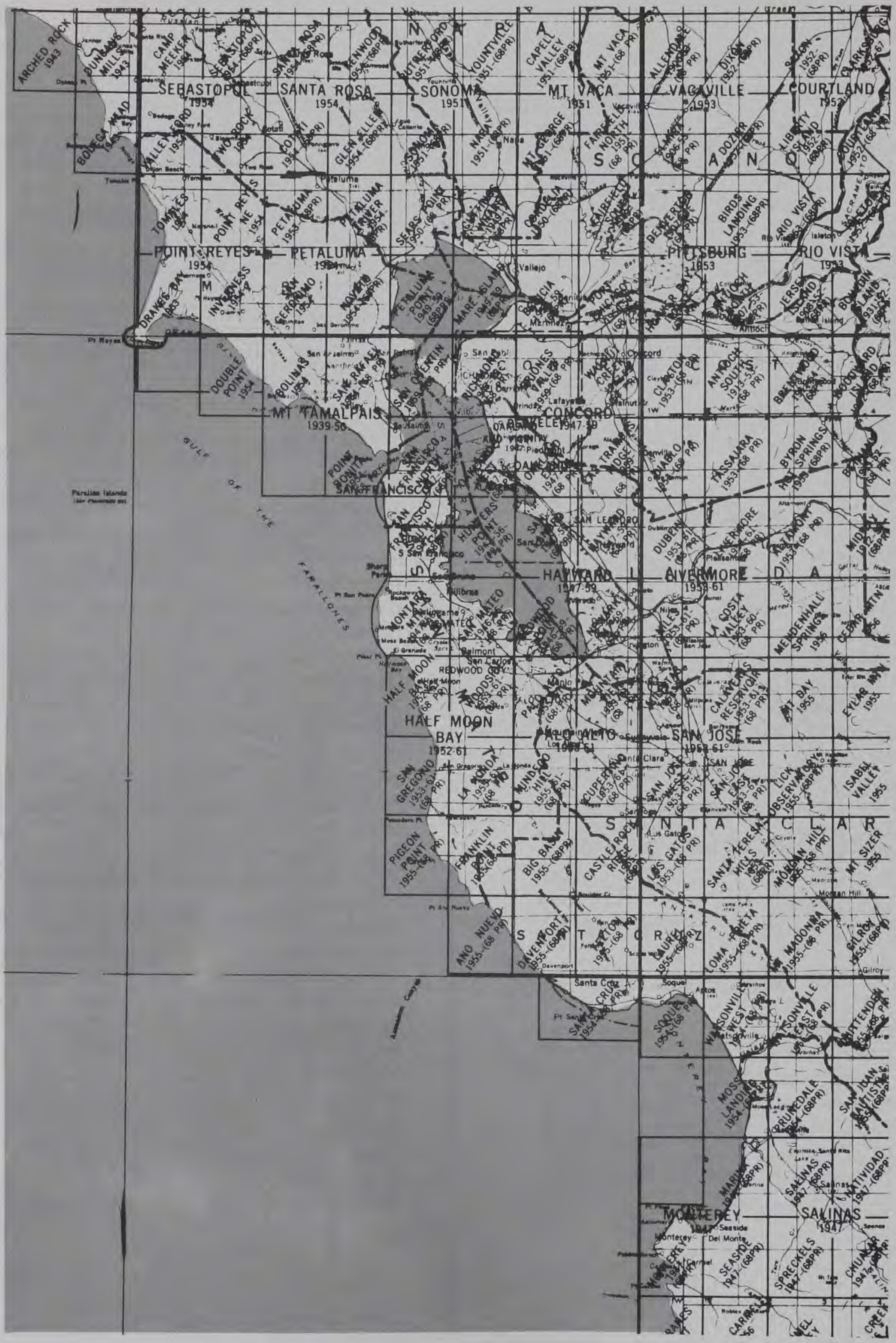

Figure 1a. Portion of index to topographic quadrangles of the State of California

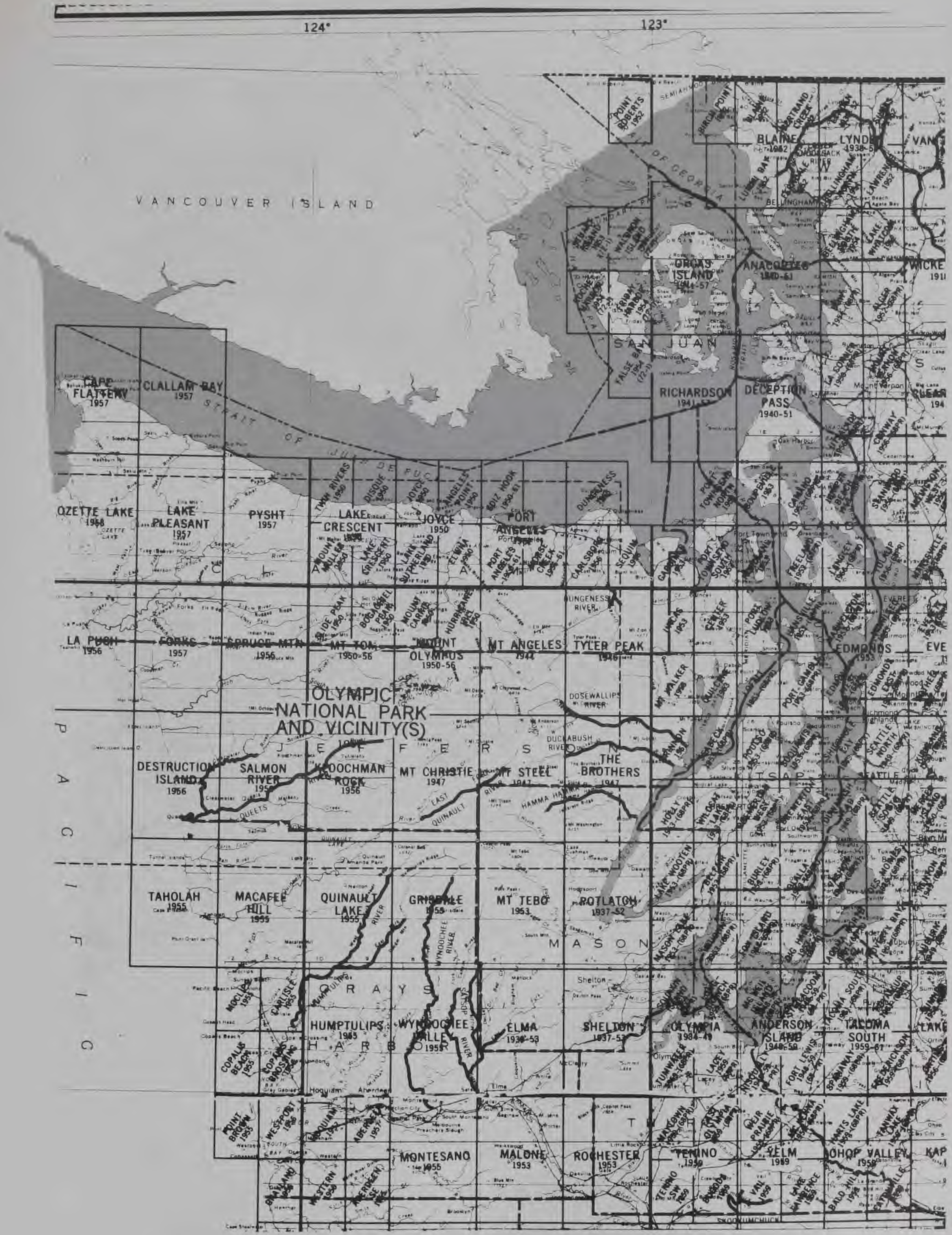

Figure 1b. Portion of index to topographic quadrangles of the State of Washington

$R_{100} = 5.9$

$R_{500} = 11.5$

Figure 2. Marina, Calif., 53+N to 57+N, L

Figure 3. Marina, Calif., 57+N to 61N, R

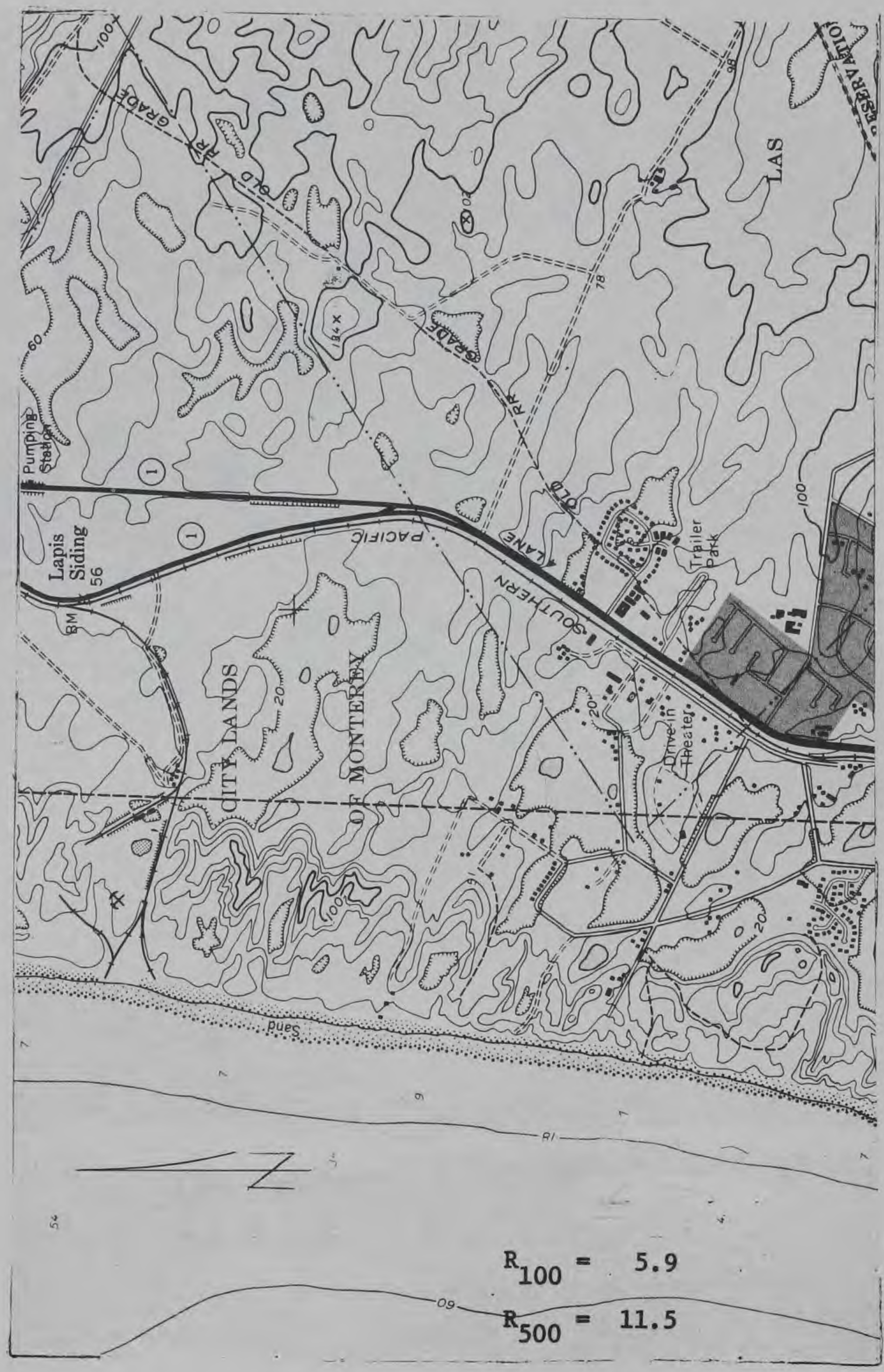

Figure 4. Marina, Calif., 61N to 64N, R

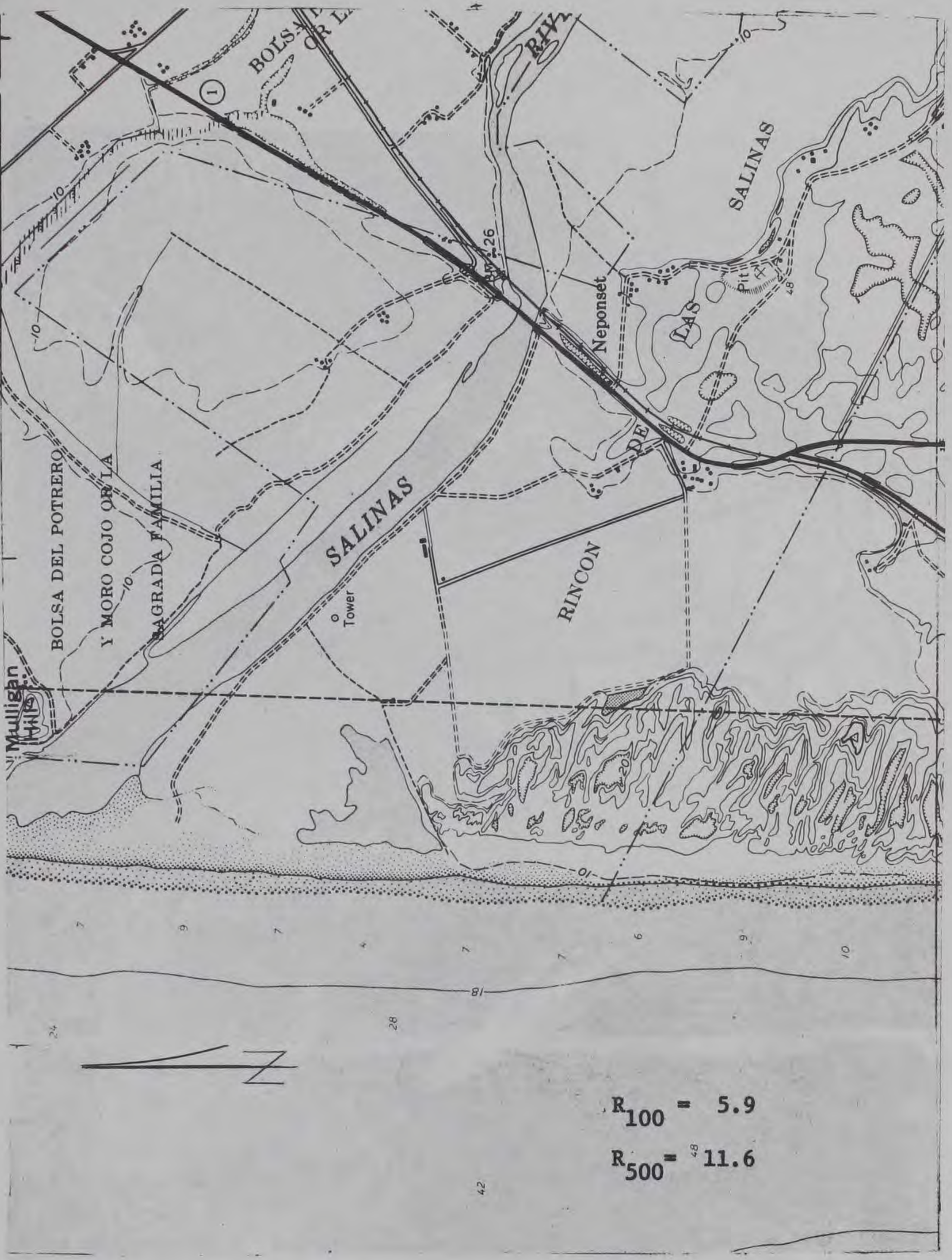

Figure 5. Marina, Calif., 64N to 67+N, R

Figure 6. Monterey, Calif., 93+E to 97E, T

Figure 7. Monterey, Calif., 50N to 54+N, R

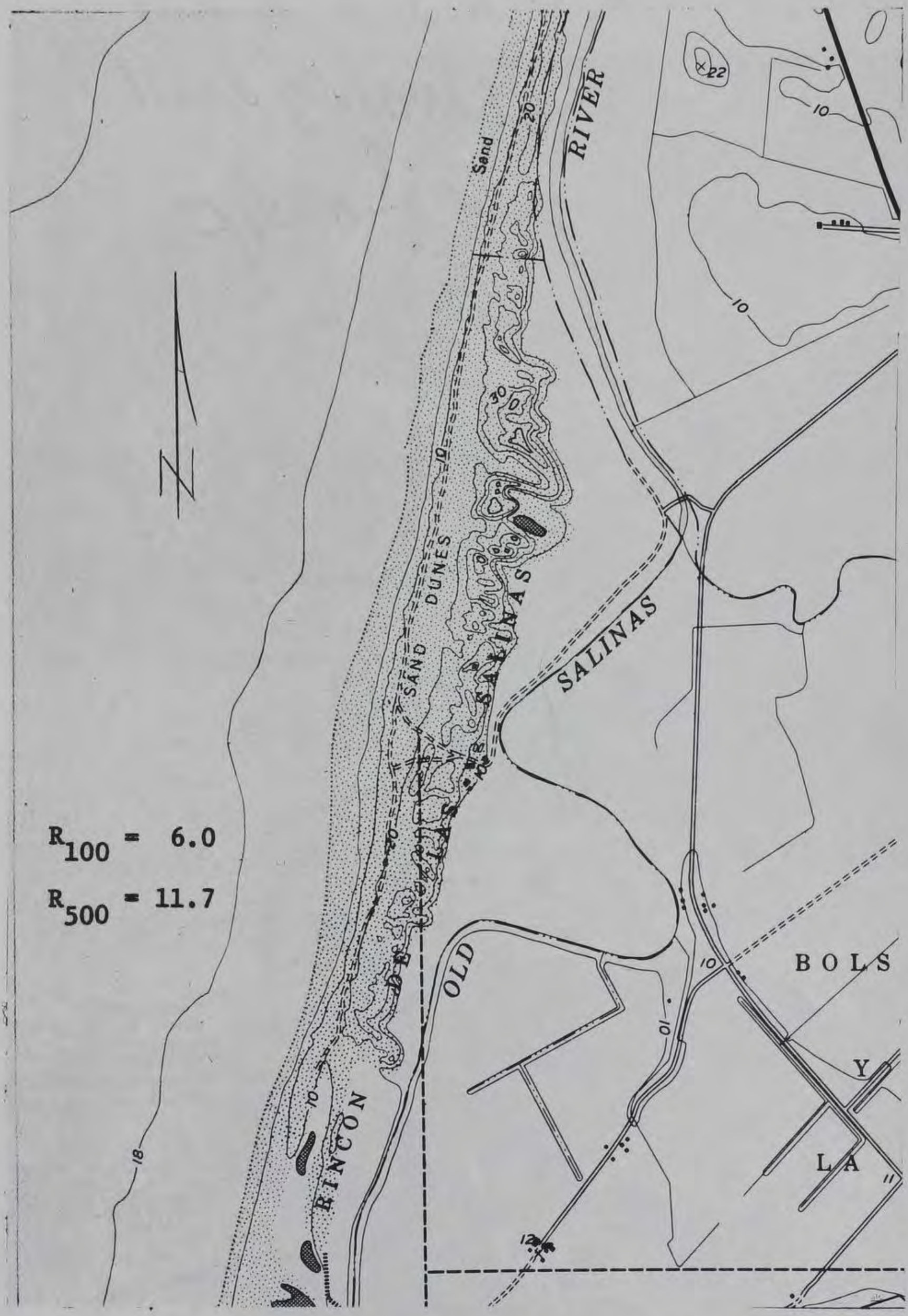

Figure 8. Moss Landing, Calif., 06E to 09E, B

Figure 9. Moss Landing, Calif., 72N to 75+N, R

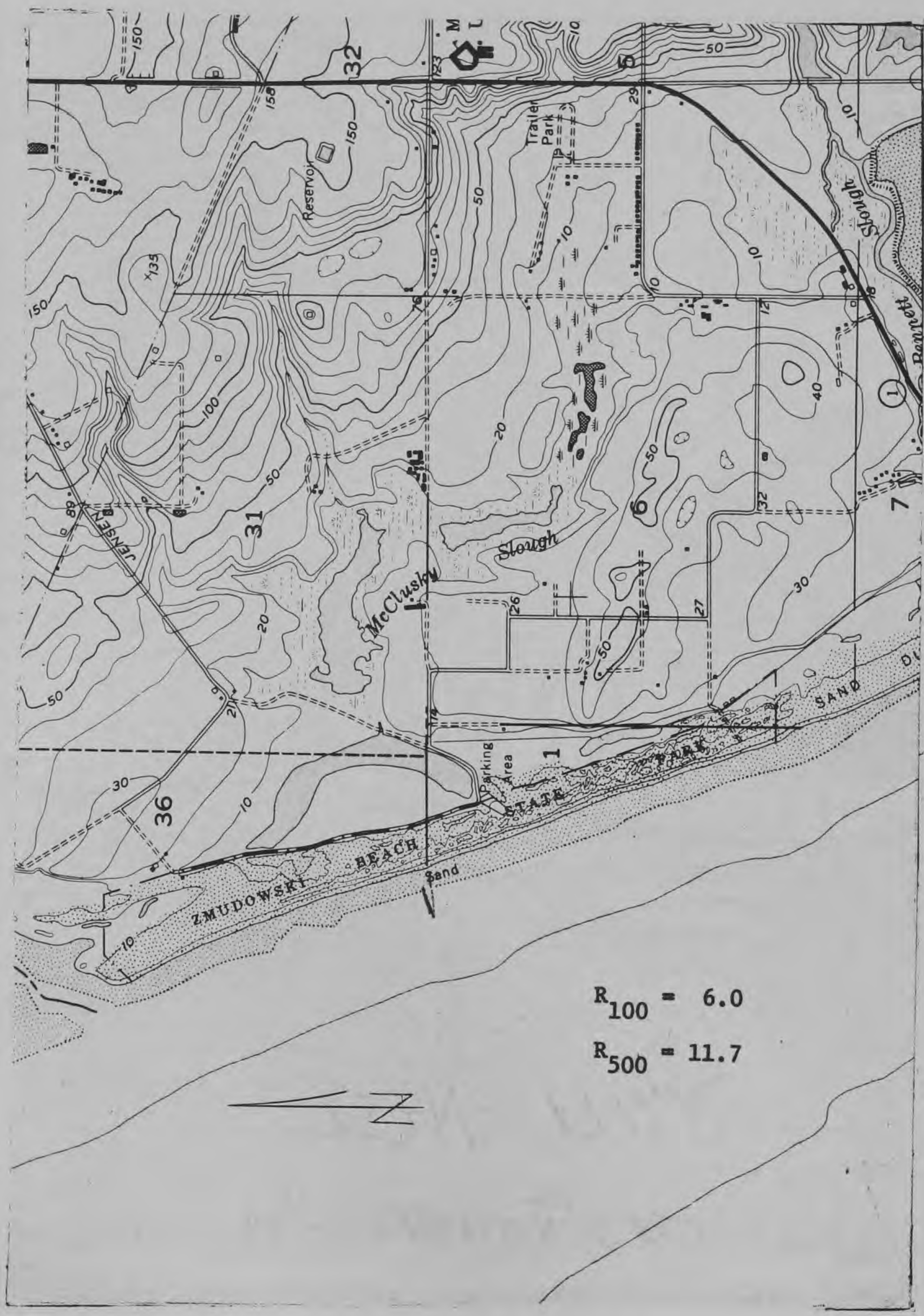

Figure 10. Moss Landing, Calif., 75+N to 79N, R

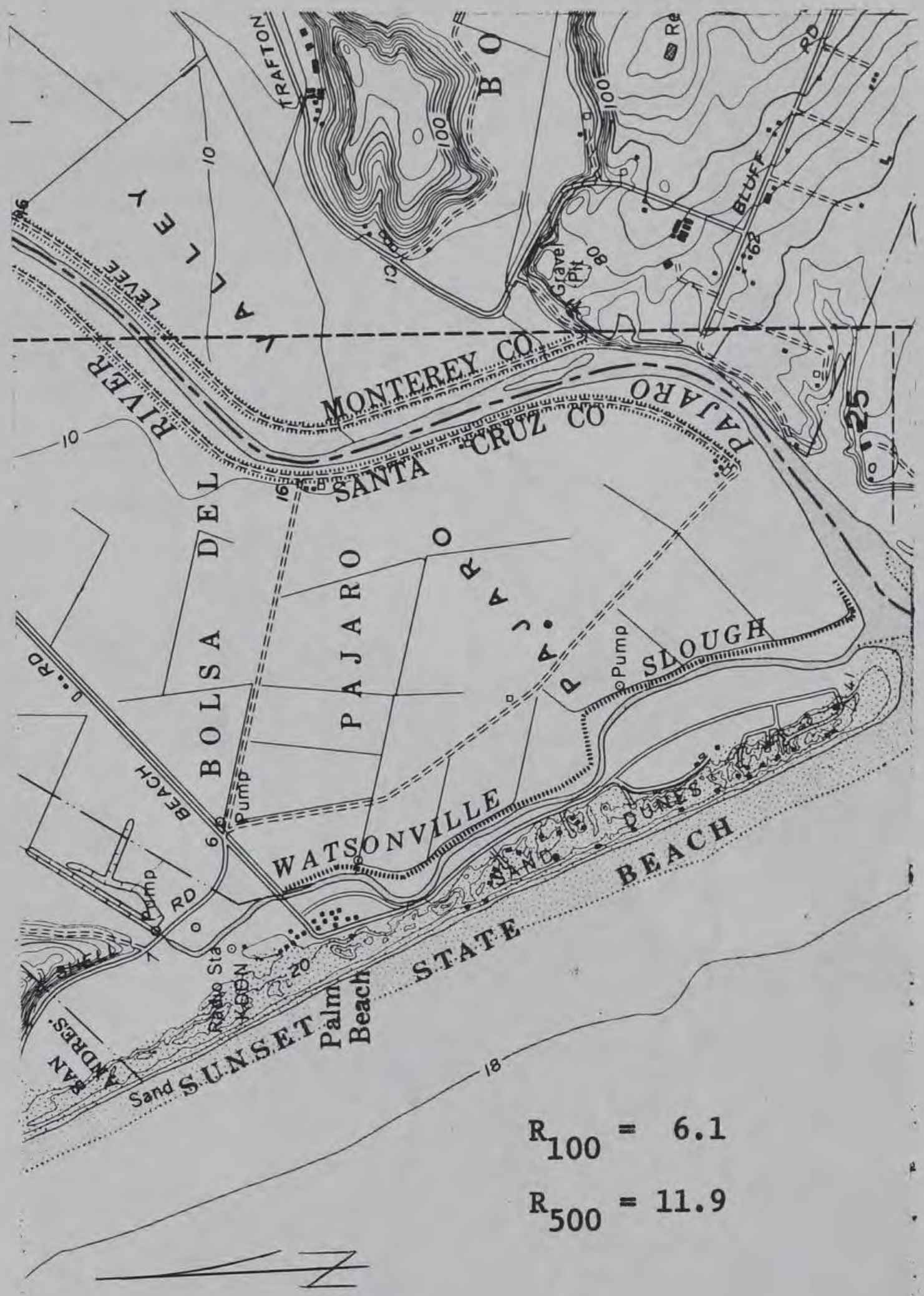

Figure 11. Moss Landing, Calif., 04E to 08E, T

Figure 12. Santa Cruz, Calif., 89N to 92N, R

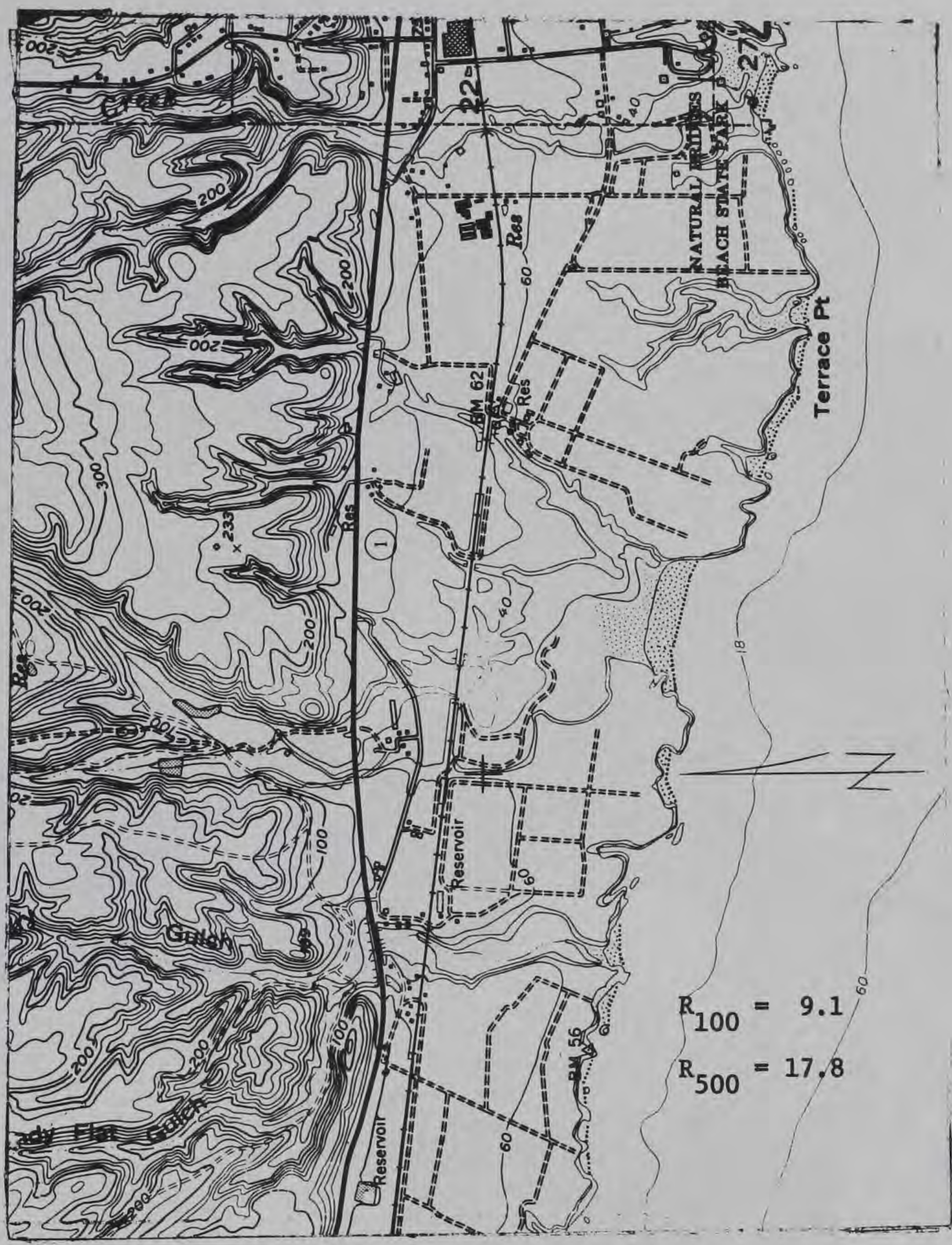

Figure 13. Santa Cruz, Calif., 80E to 84E, T

Figure 14. Sea Side, Calif., 49N to 53+N, L

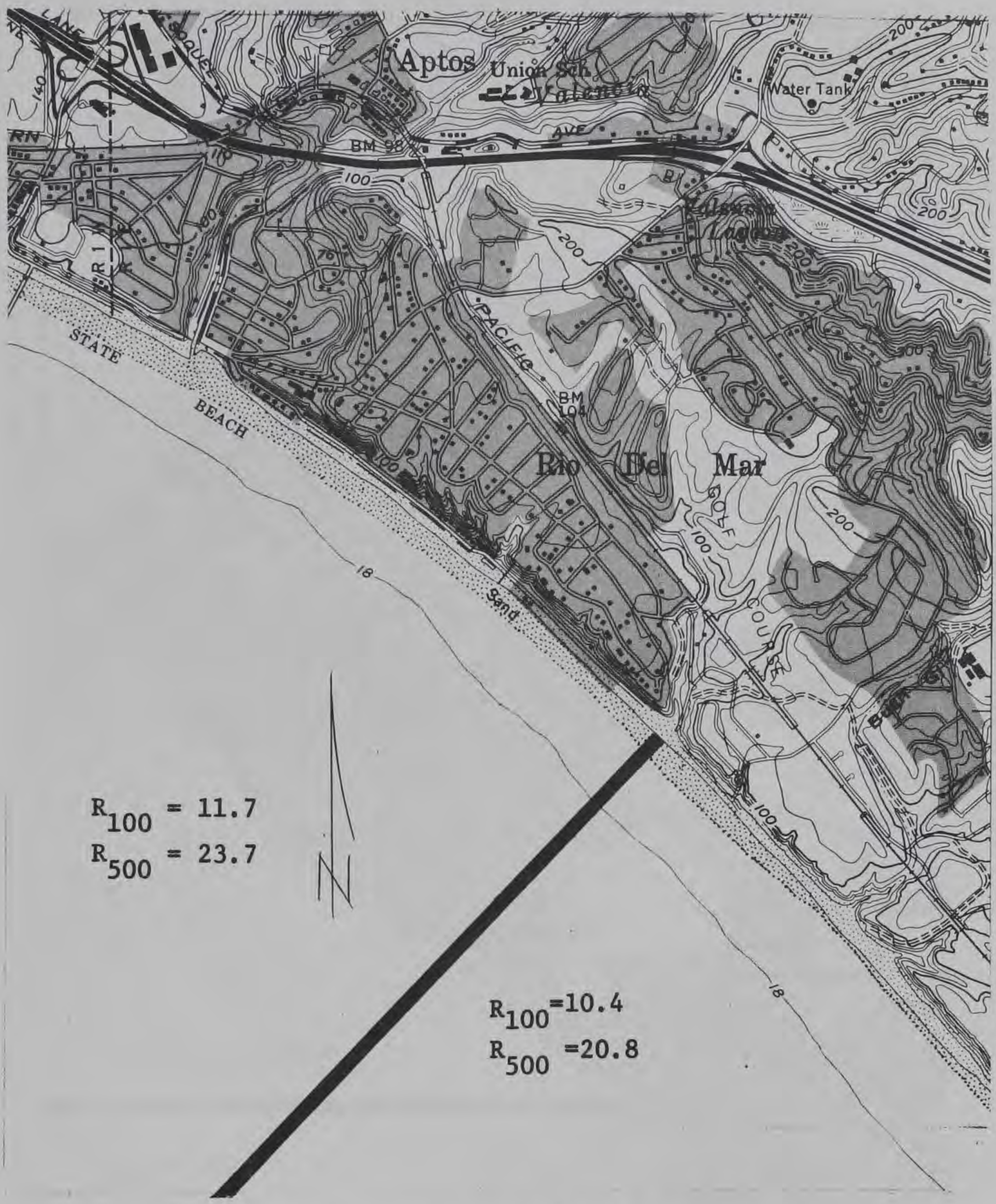

Figure 15. Soquel, Calif., 89N to 93N, R

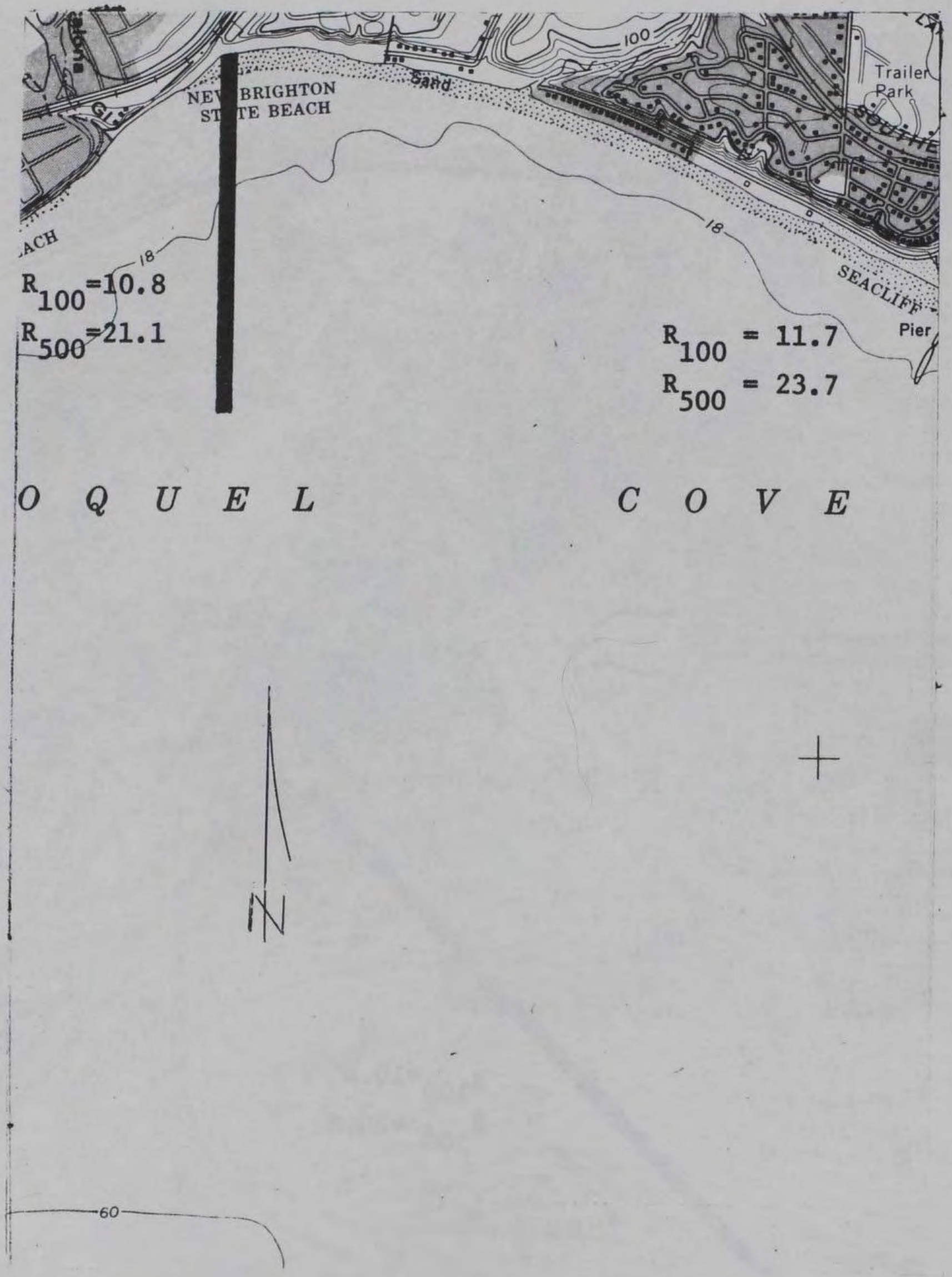

Figure 16. Soquel, Calif., 89N to 93N, R

Figure 17. Soquel, Calif., 90N to 93N, L

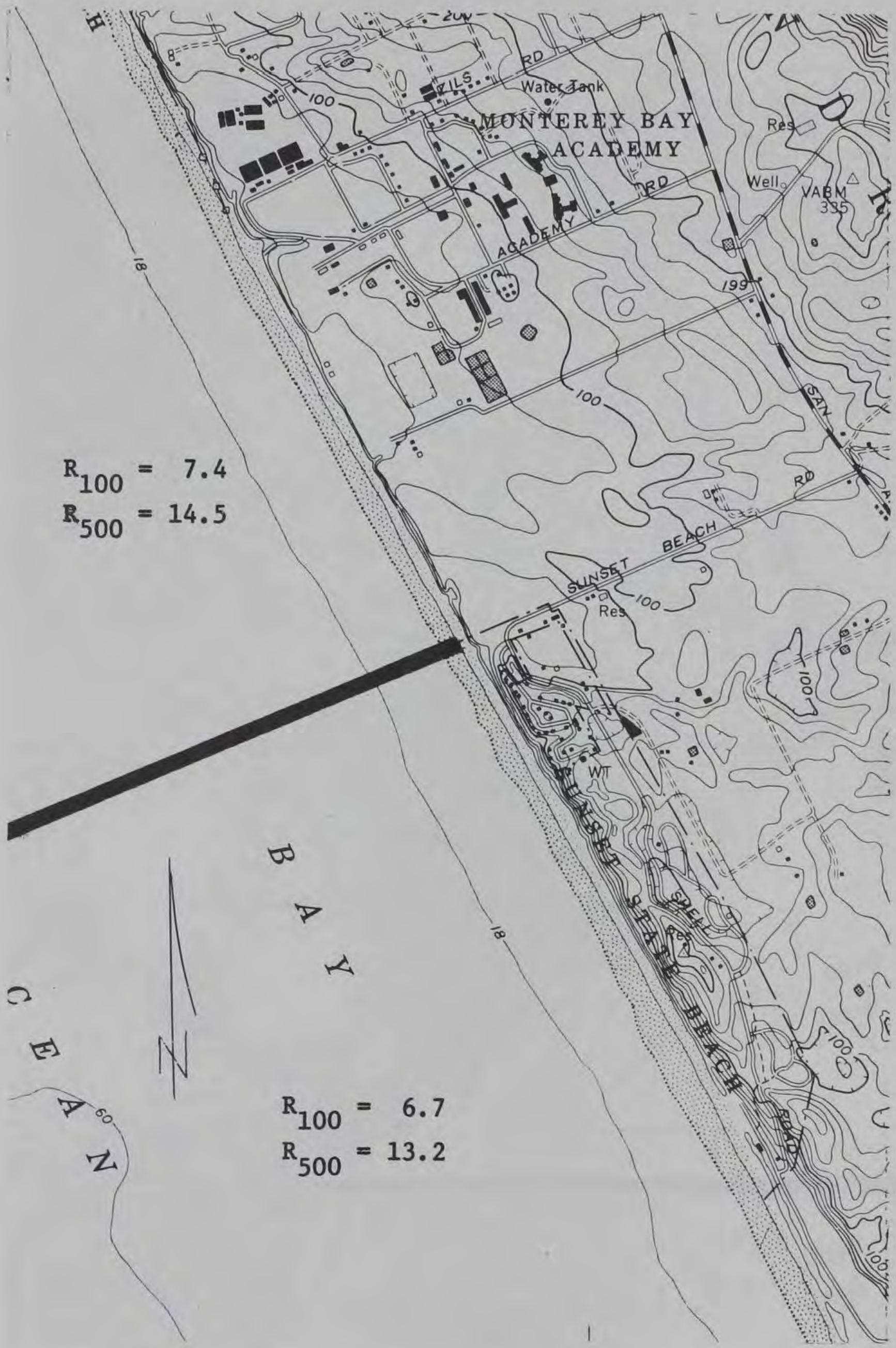

Figure 18. Watsonville West, Calif., 02E to 05E, B

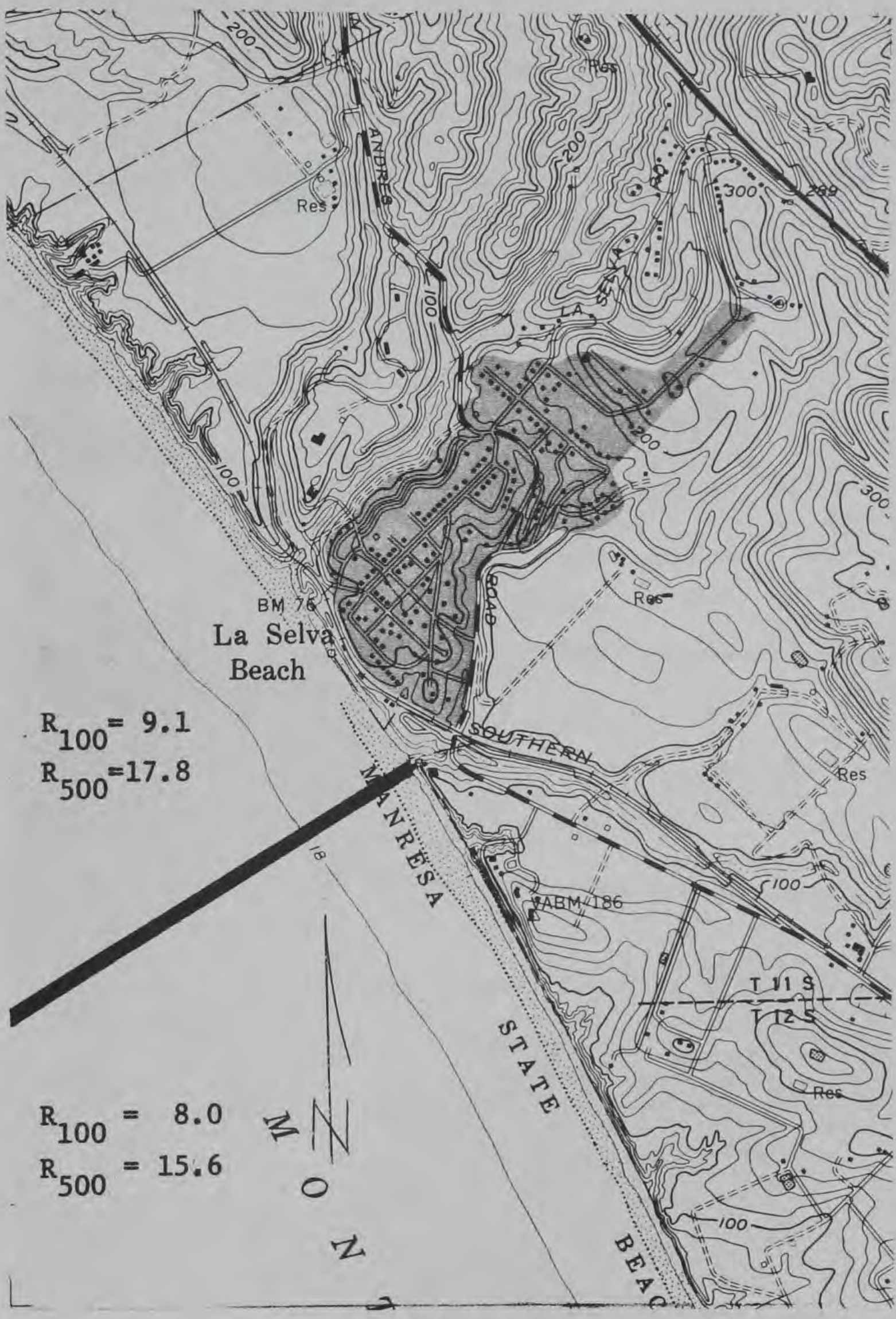

Figure 19. Watsonville West, Calif., 86N to 90N, L

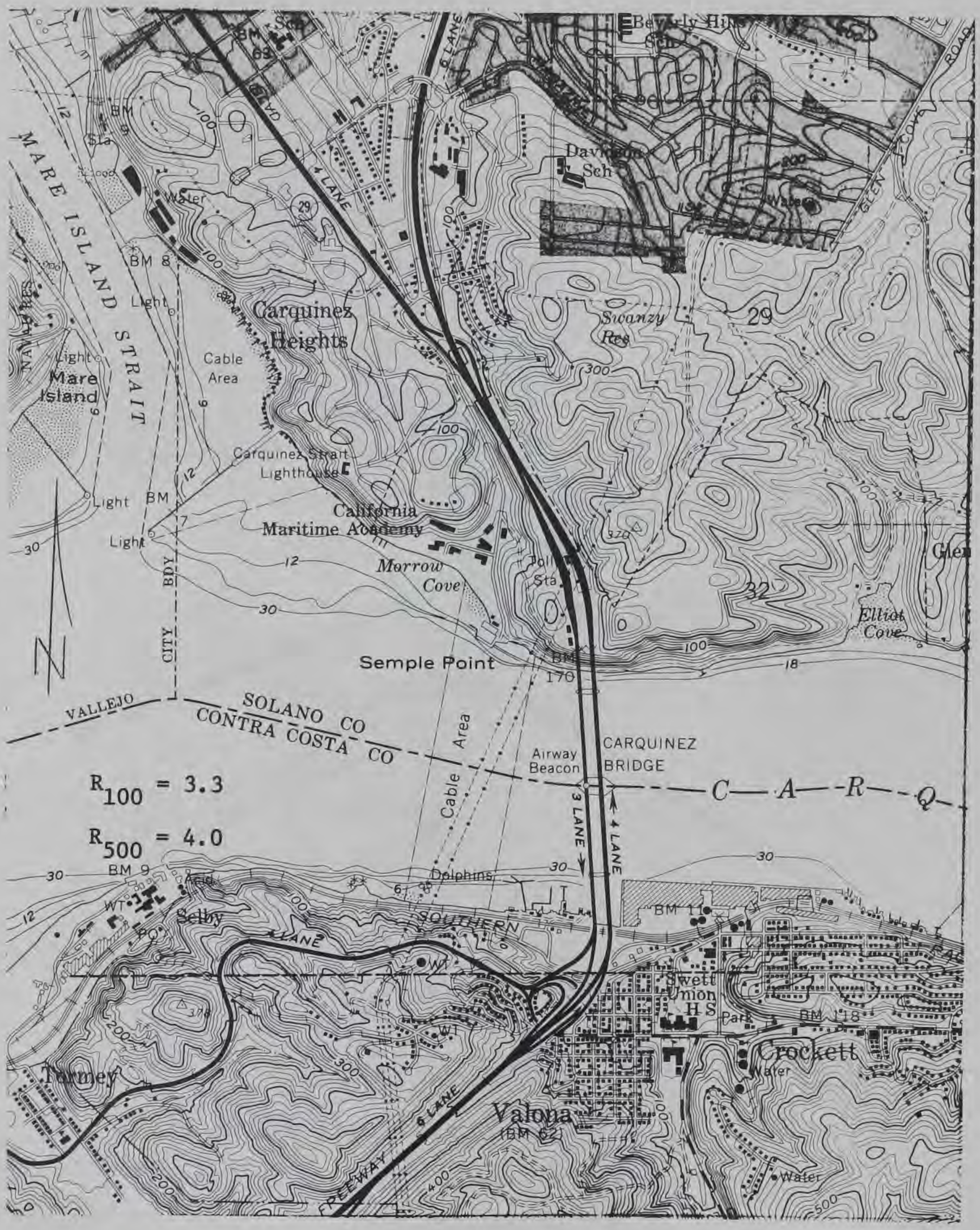

Figure 20. Benicia, Calif., 11N to 15+N, L

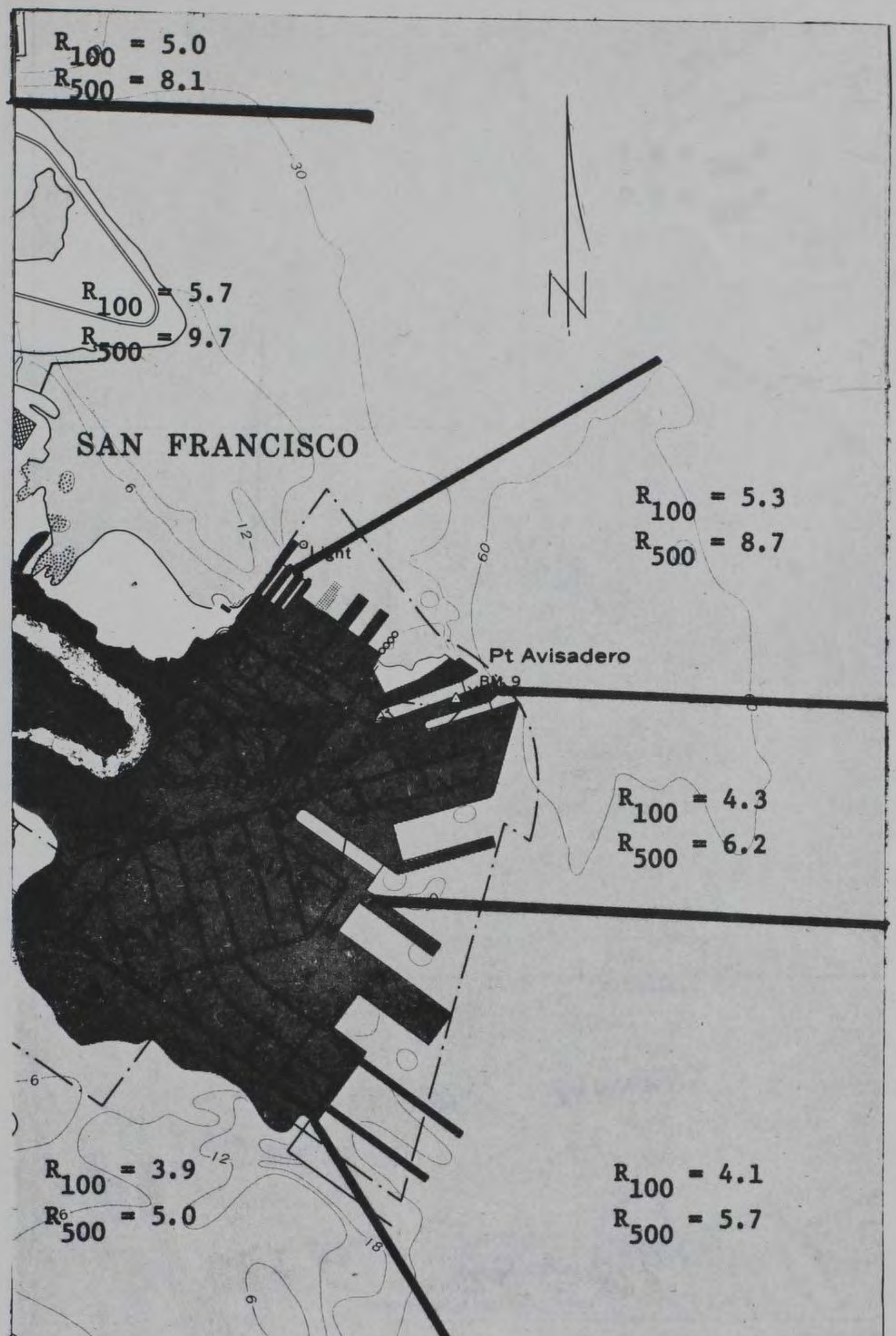

Figure 21. Hunters Point, Calif., 55+E to 58E, T

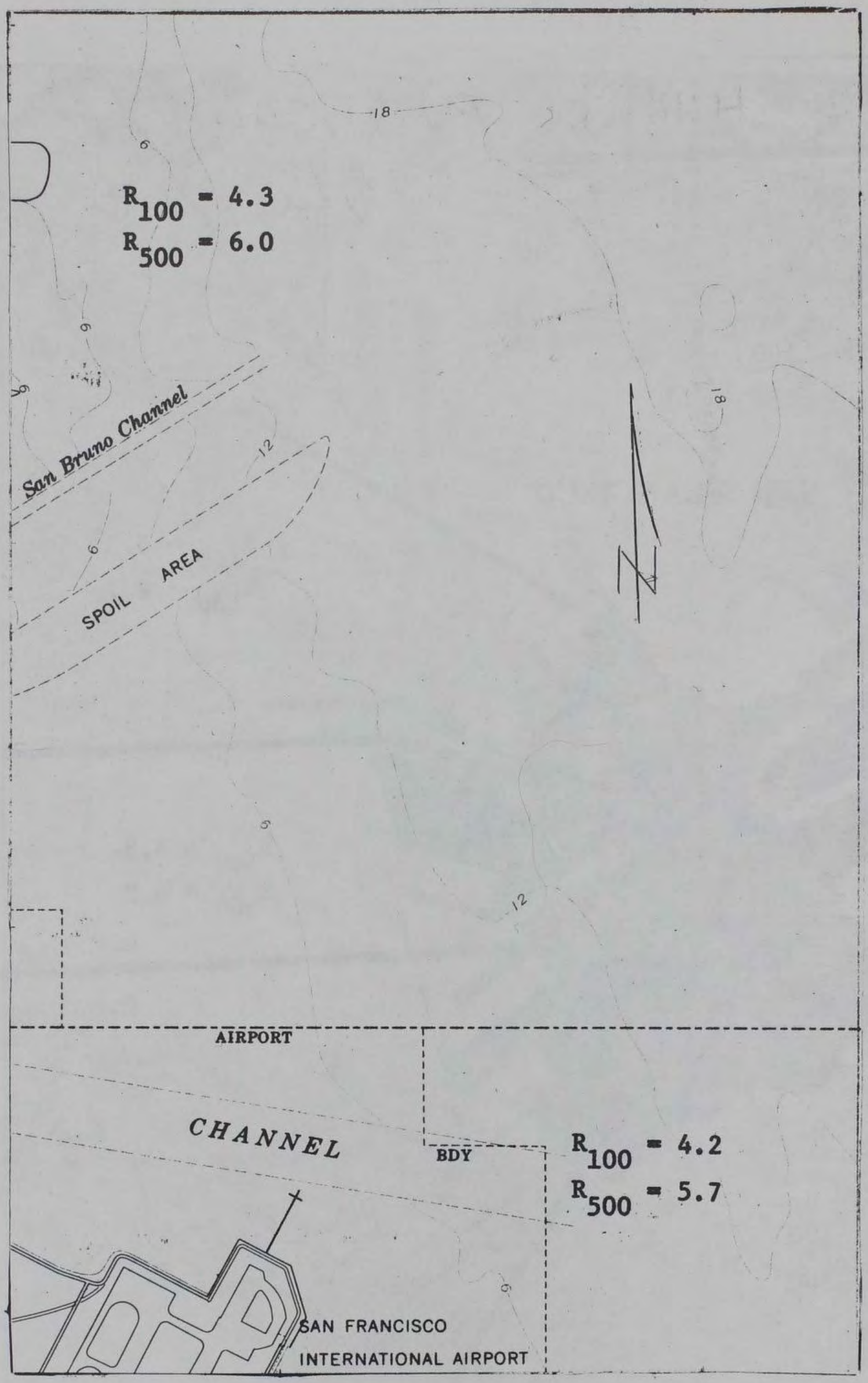

Figure 22. Hunters Point, Calif., 55+E to 58E, B

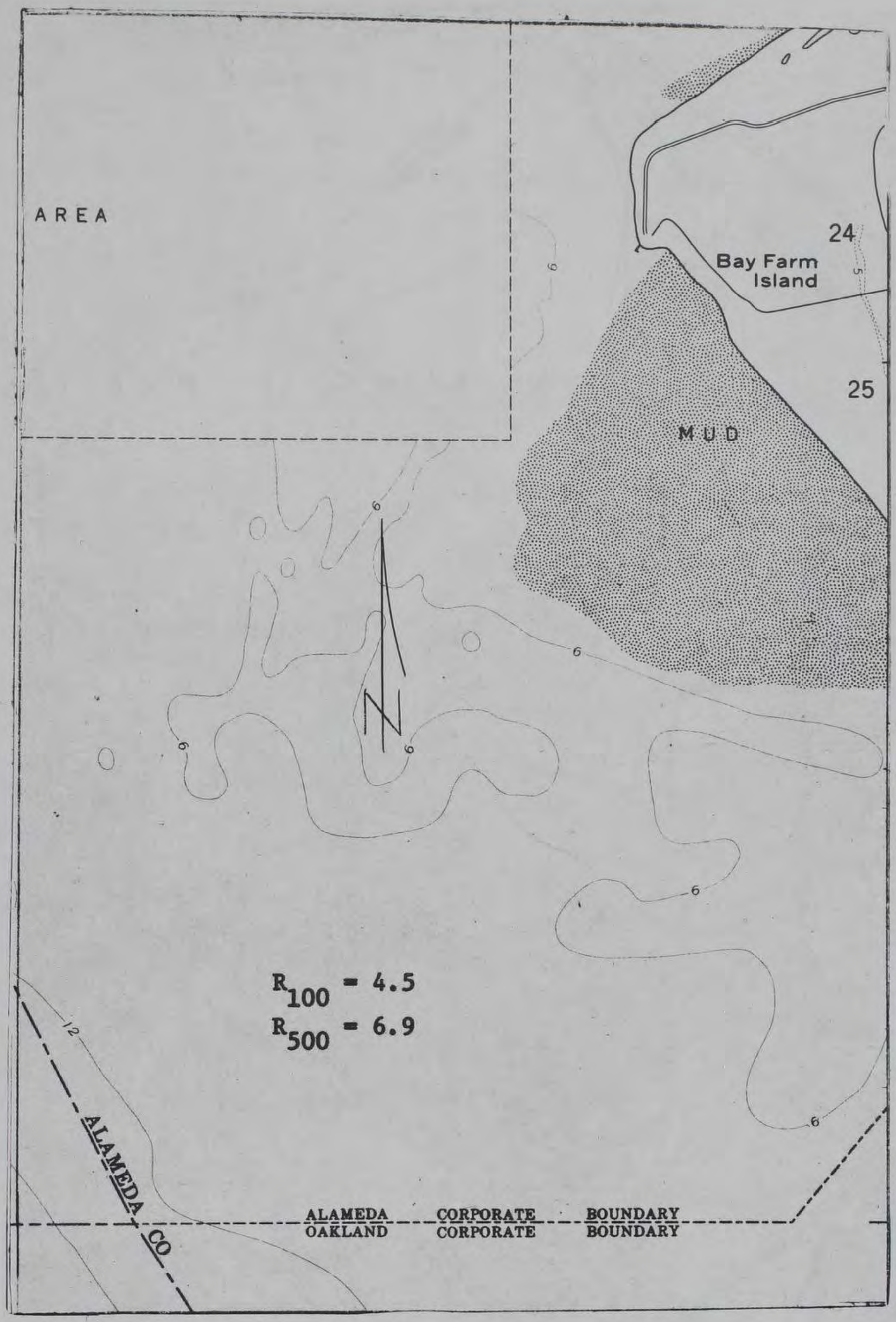

Figure 23. Hunters Point, Calif., 63E - 66+E, T

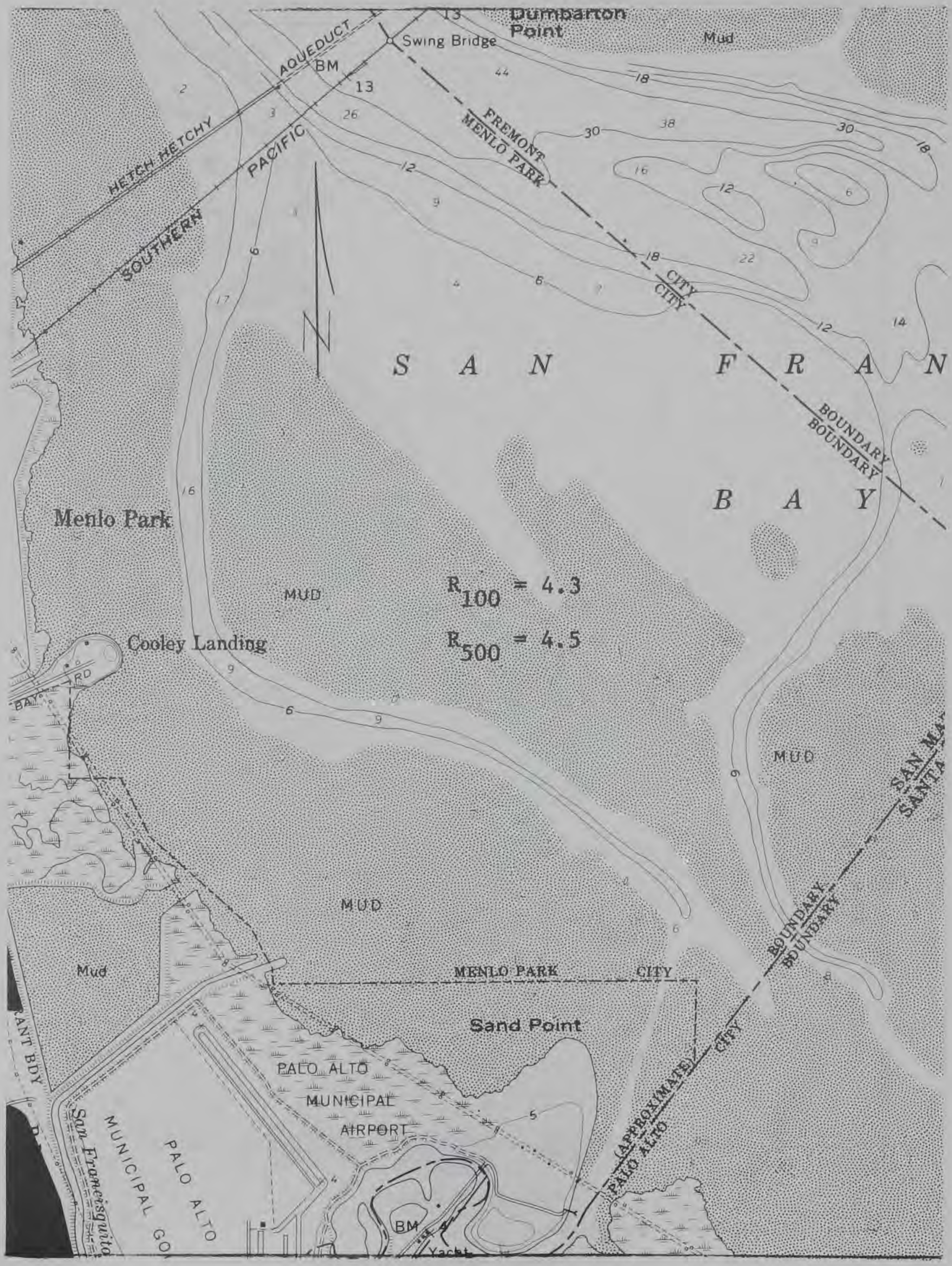

Figure 24. Mountain View, Calif., 45+N to 50+N, L

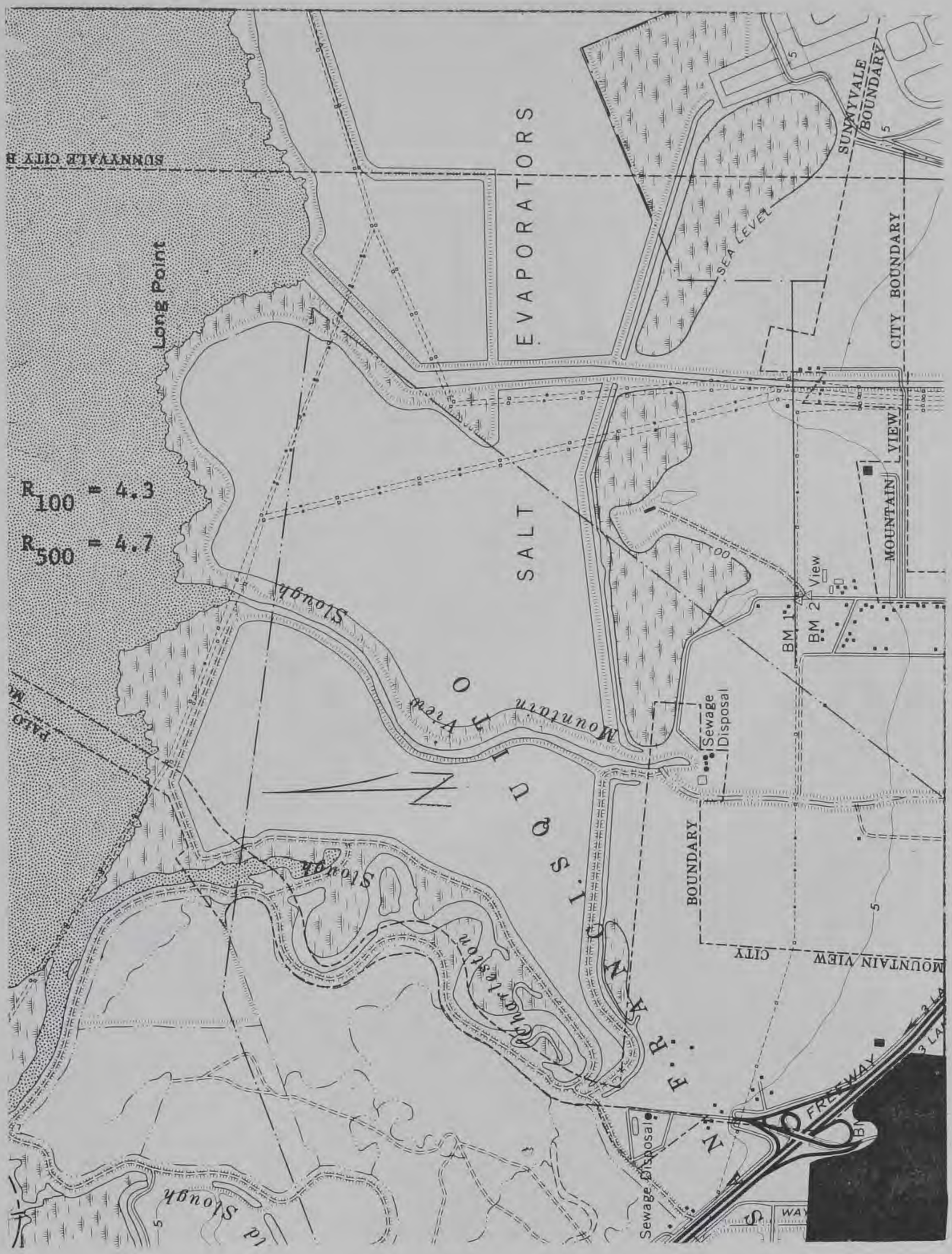

Figure 25. Mountain View, Calif., 42N to 45+N, L

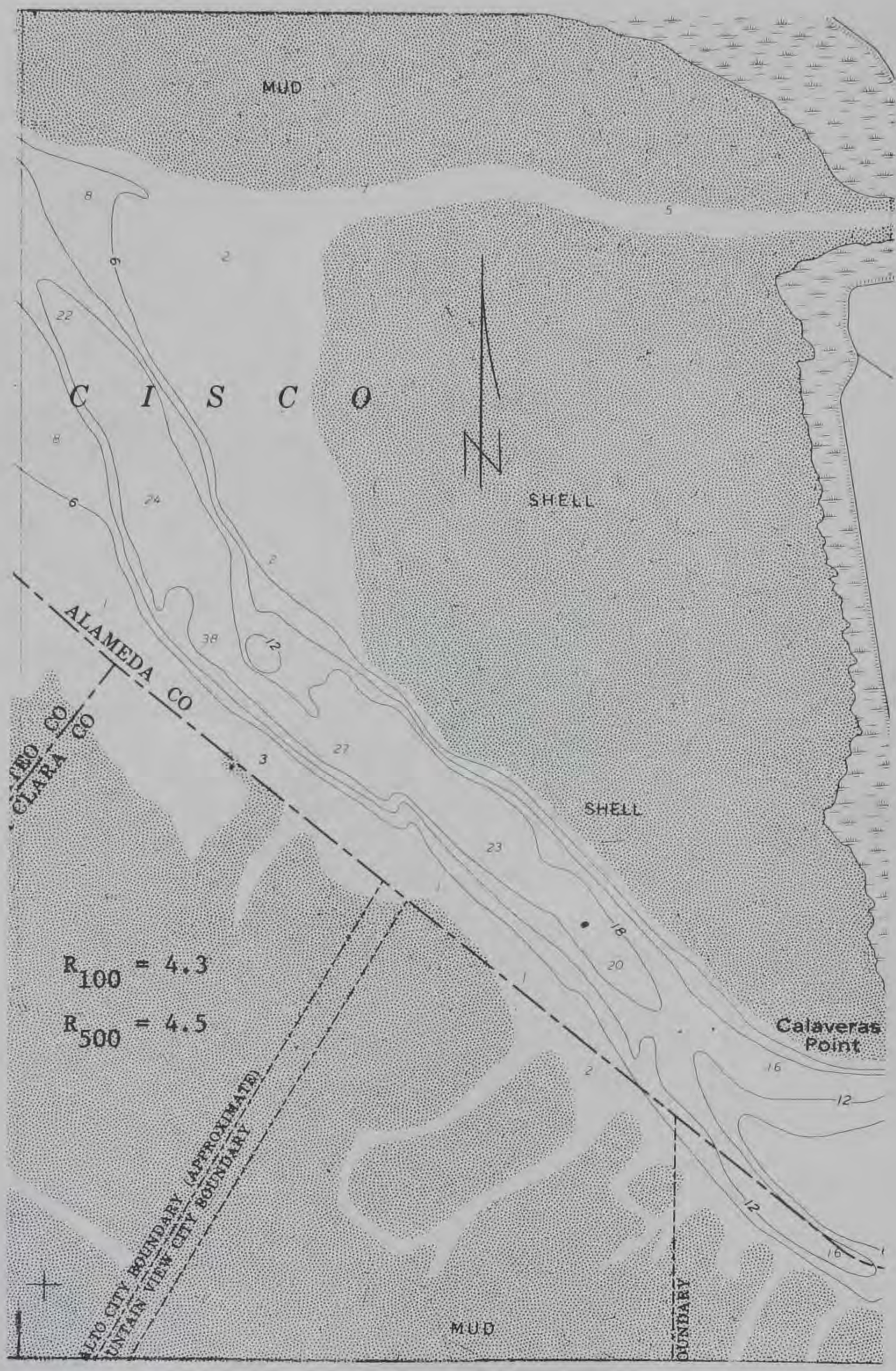

Figure 26. Mountain View, Calif., 80+E to 84E, T

Figure 27. Newark, Calif., 77+E to 82E, B

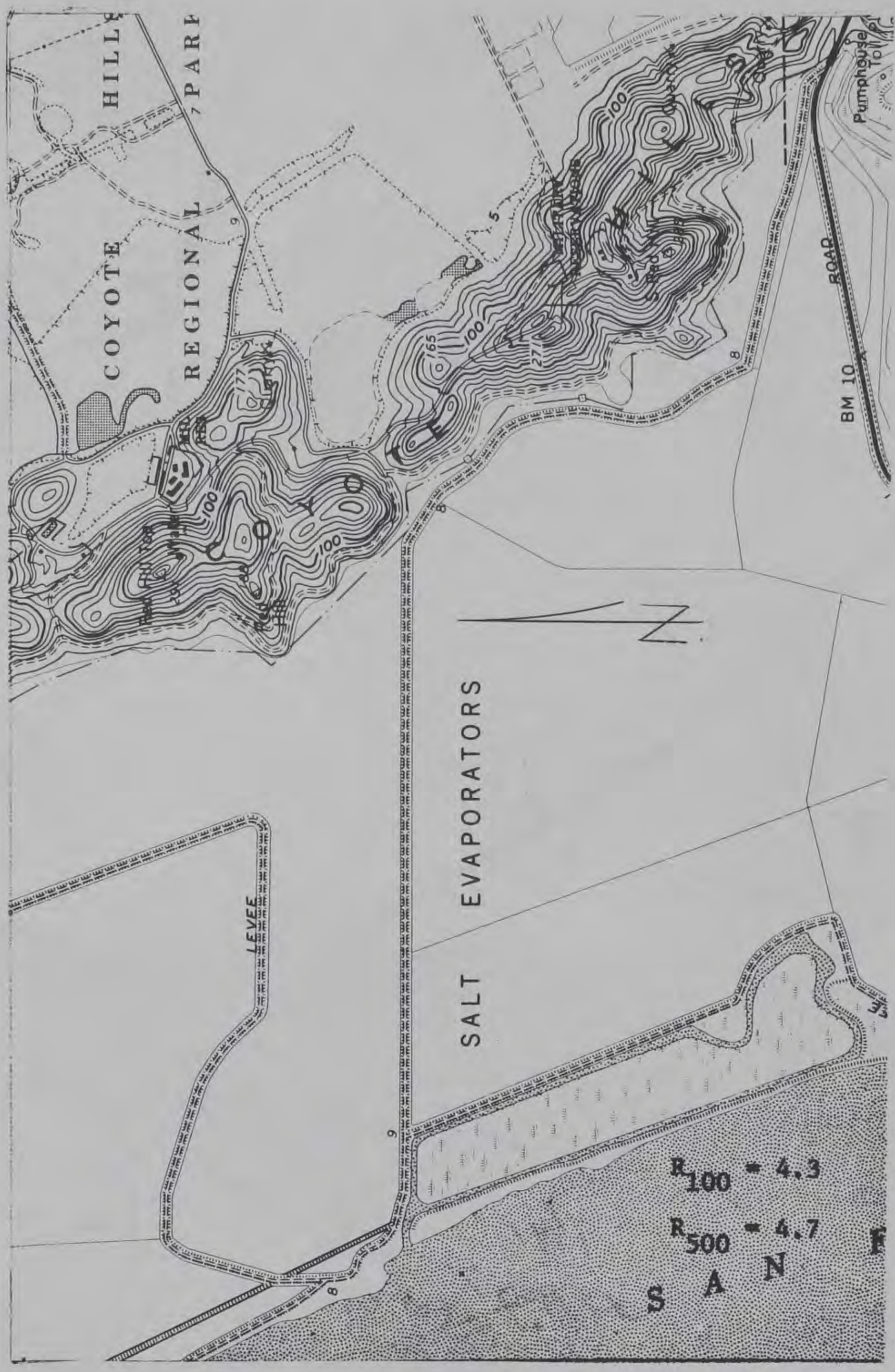

Figure 28. Newark, Calif., 54N to 57N, L

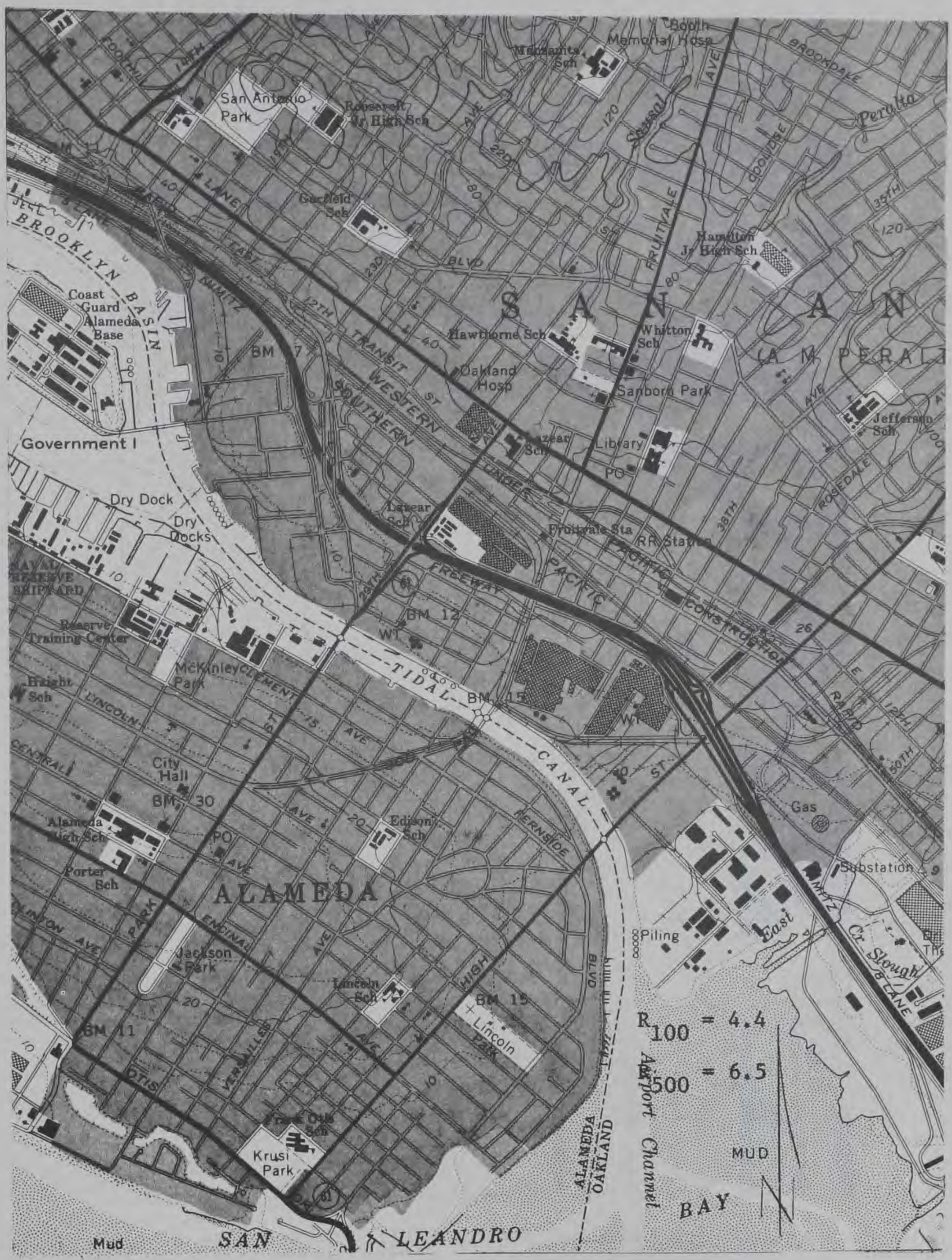

Figure 29. Oakland East, Calif., 78+N to 83N, L

Figure 30. Oakland West, Calif., 78+N to 81N, R

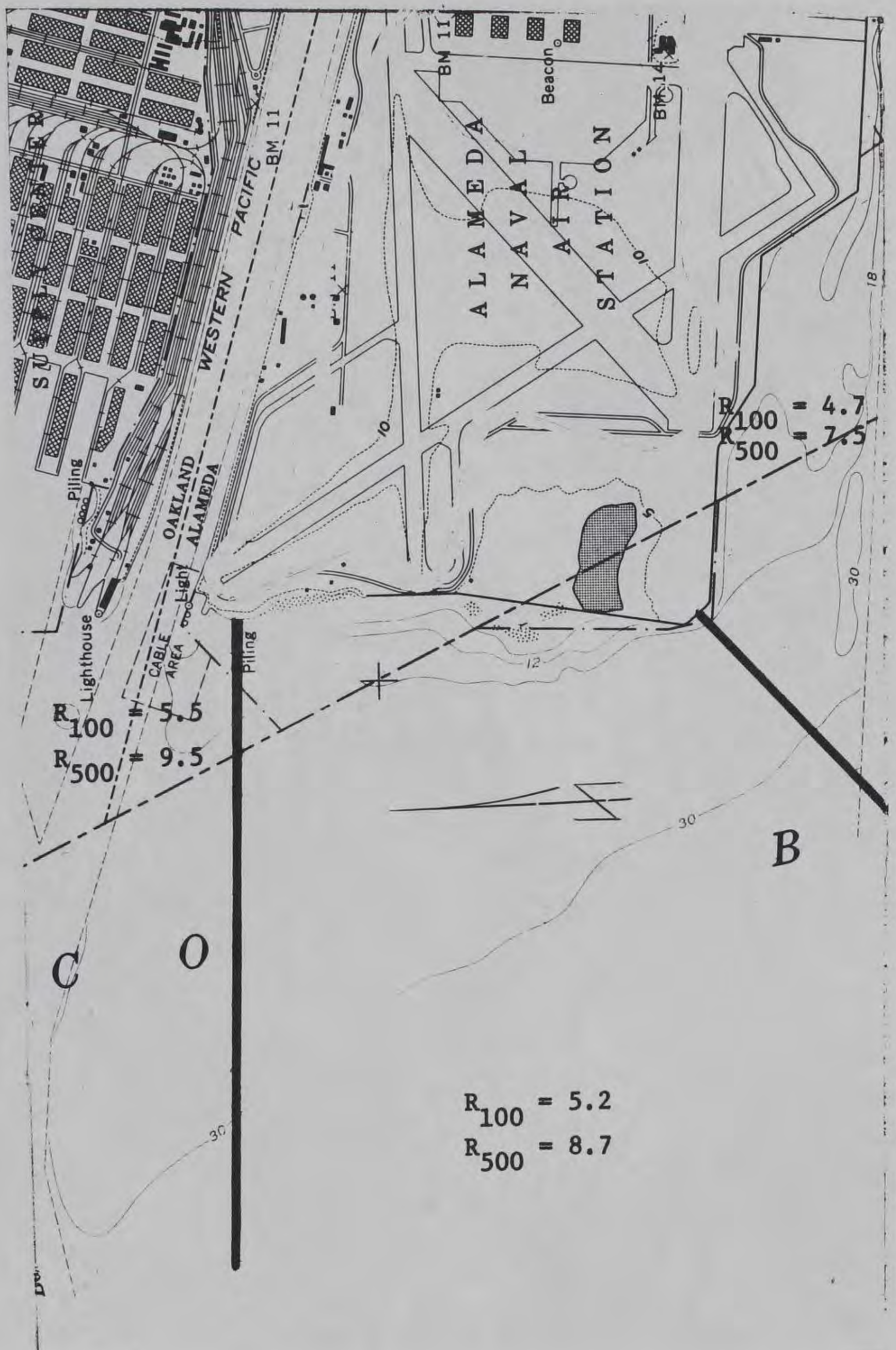

Figure 31. Oakland West, Calif., 81N to 84N, R

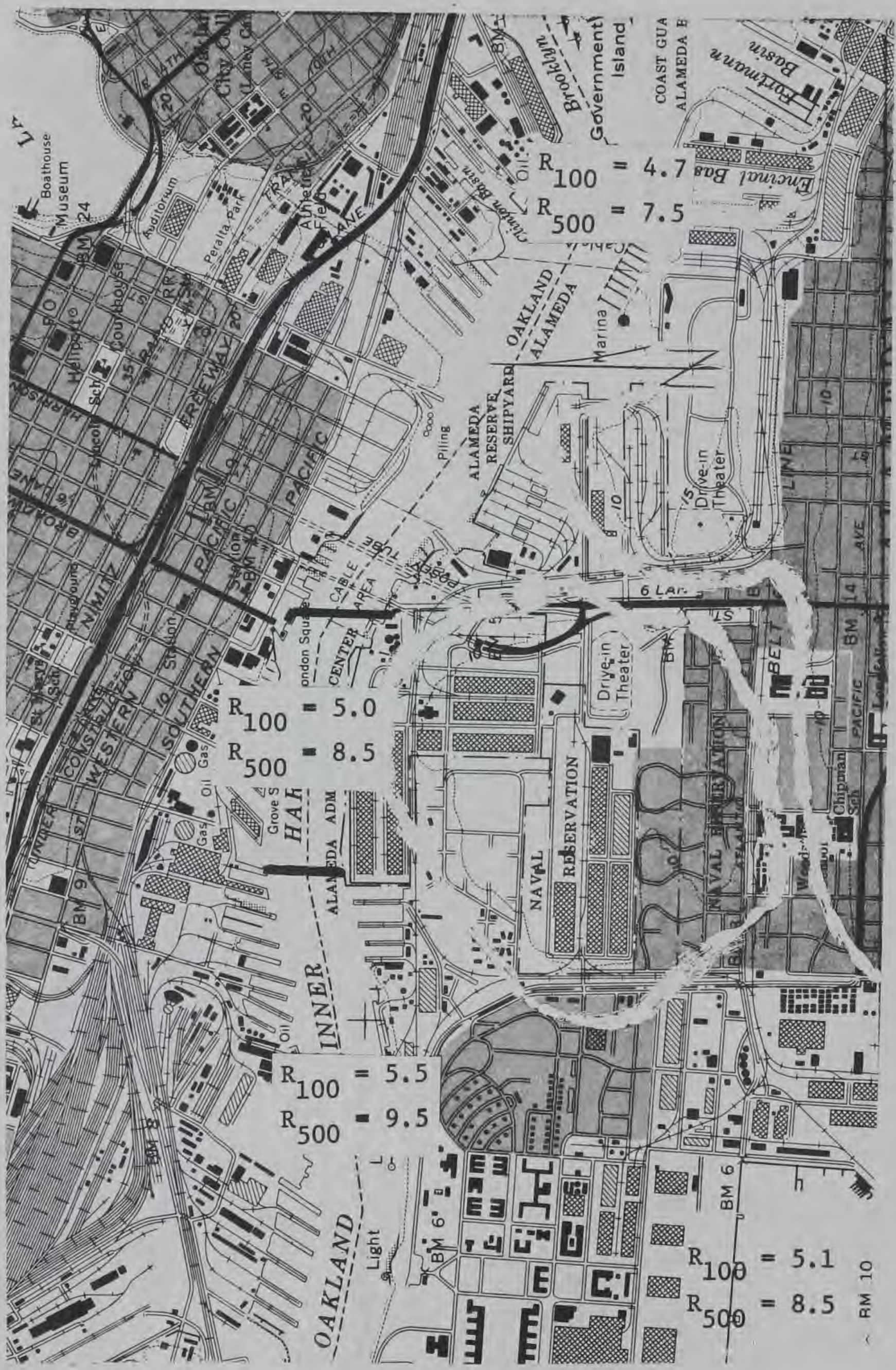

Figure 32. Oakland West, Calif., 81N to 84N, R

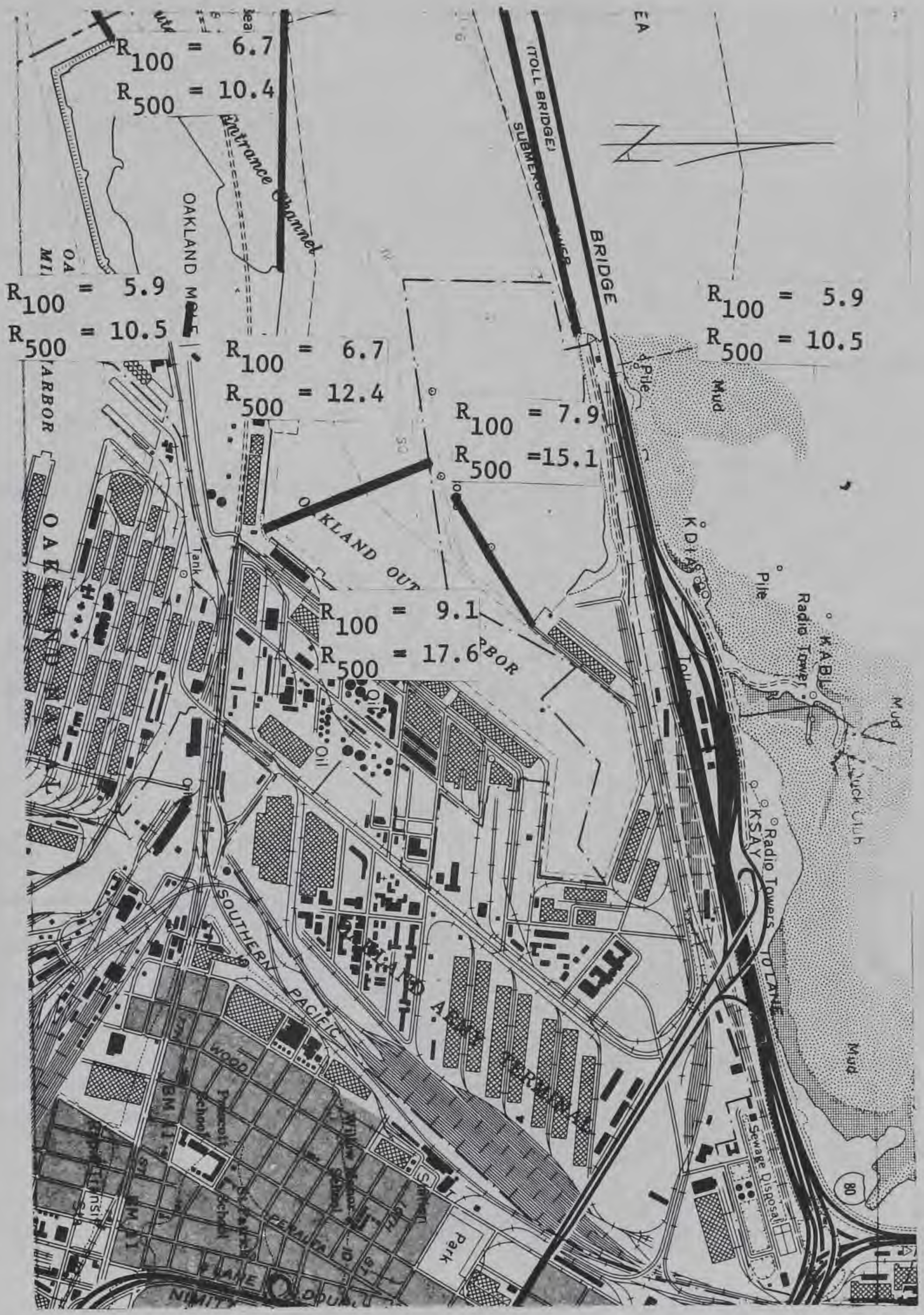

Figure 33. Oakland West, Calif., 84N to 86+N, L

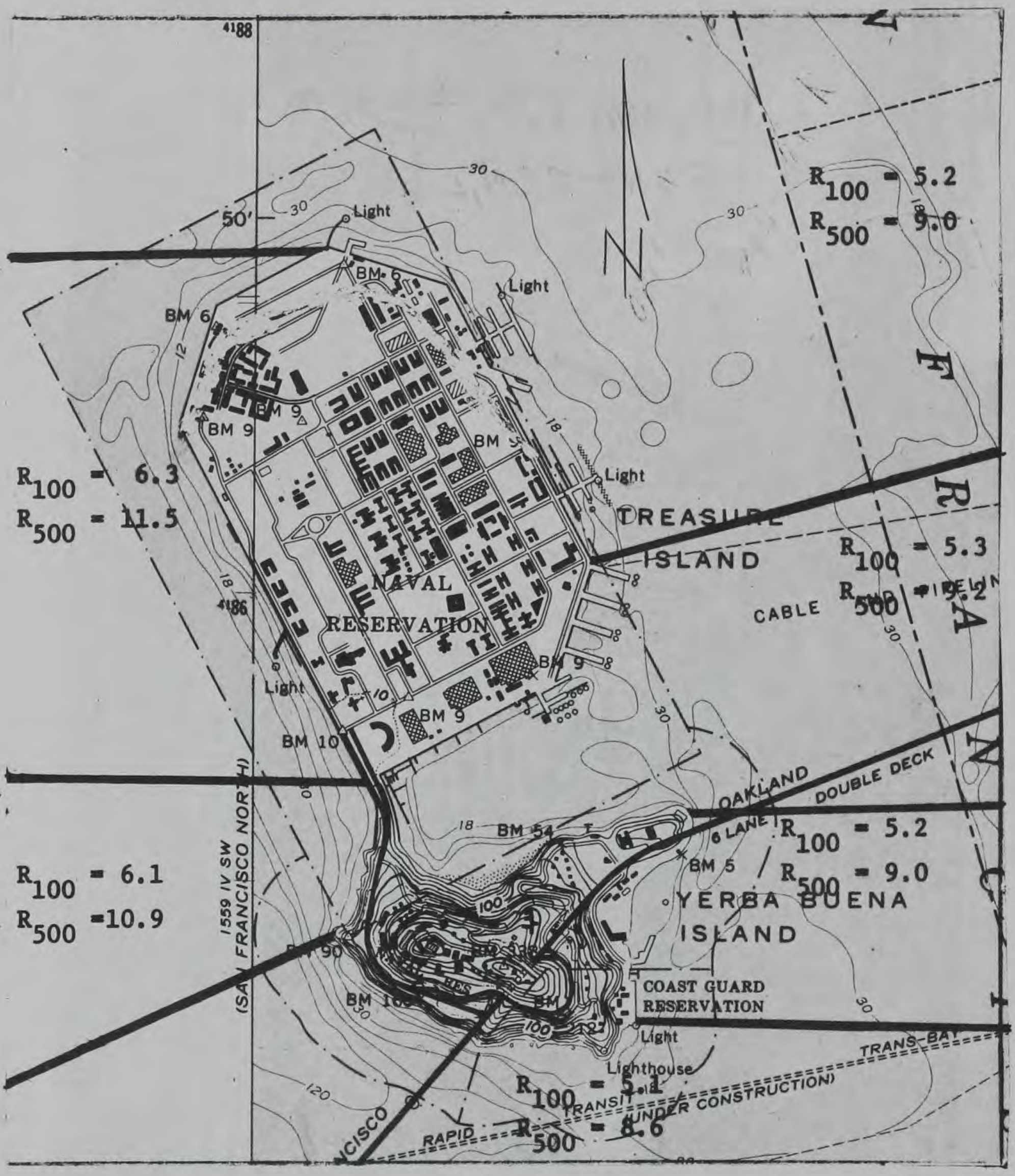

Figure 34. Oakland West, Calif., 84N to 88N, L

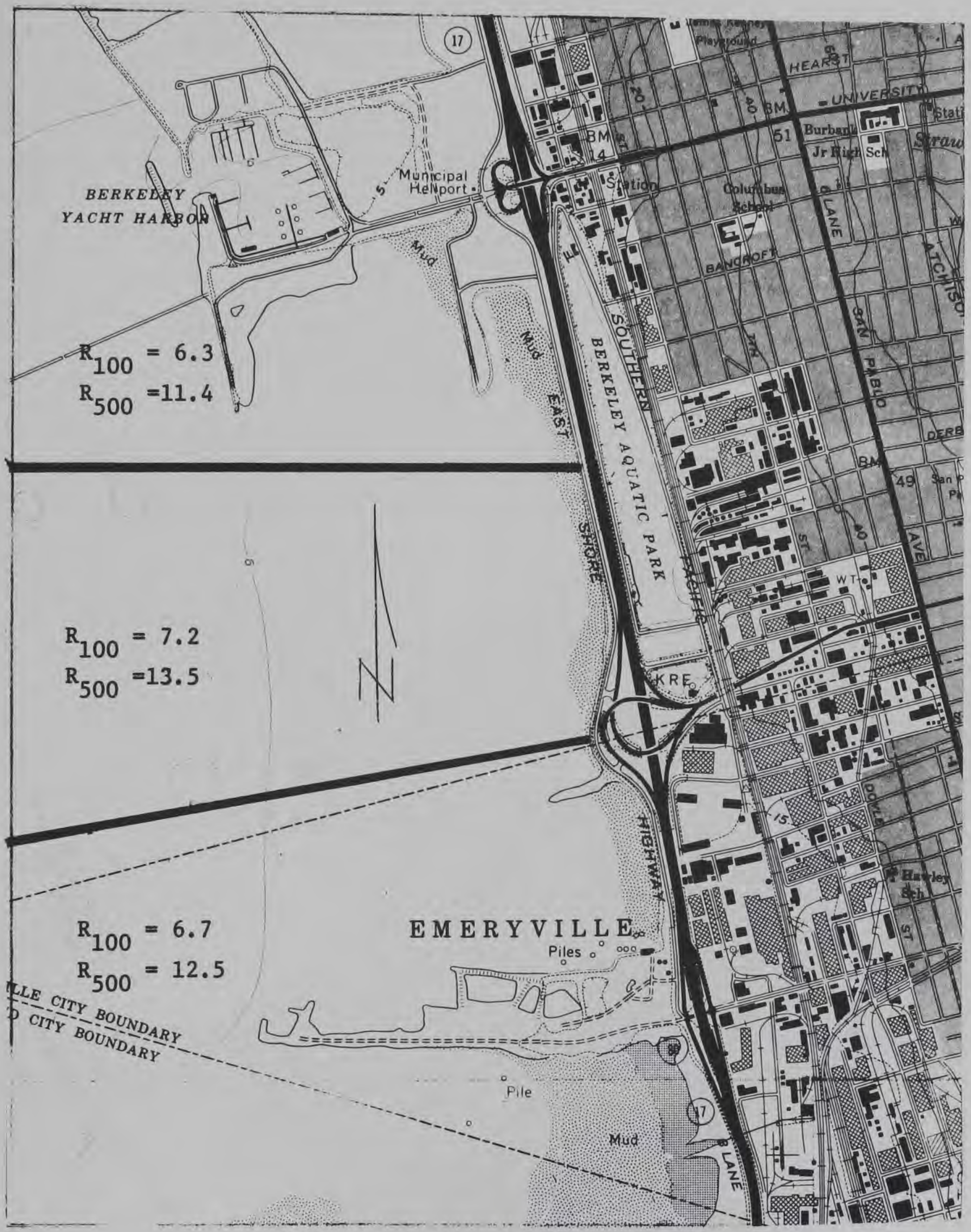

Figure 35. Oakland West, Calif., 86+N to 91+N, L

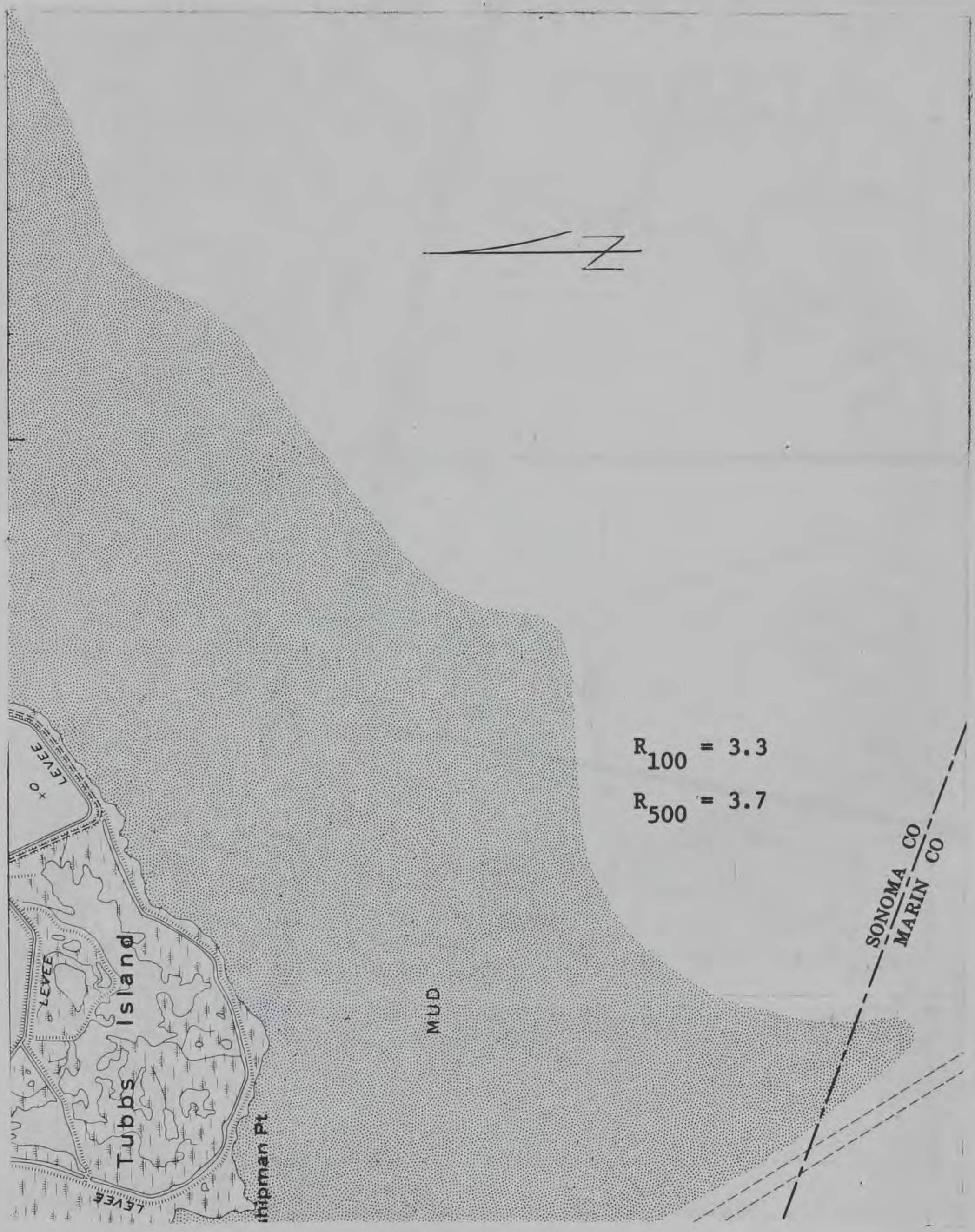

Figure 36. Petaluma Point, Calif., 16N to 19+N, R

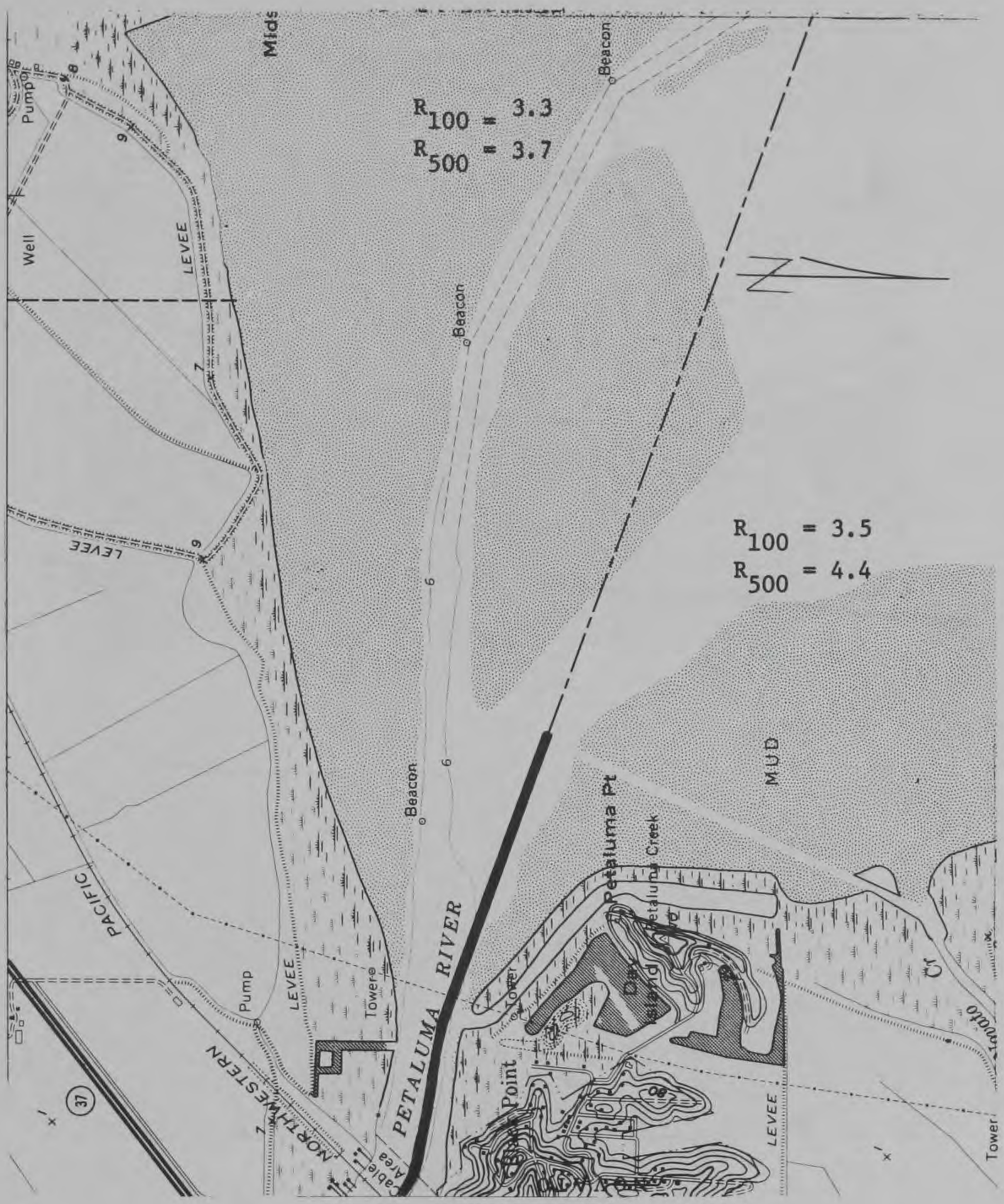

Figure 37. Petaluma Point, Calif., 16N to 19+N, L

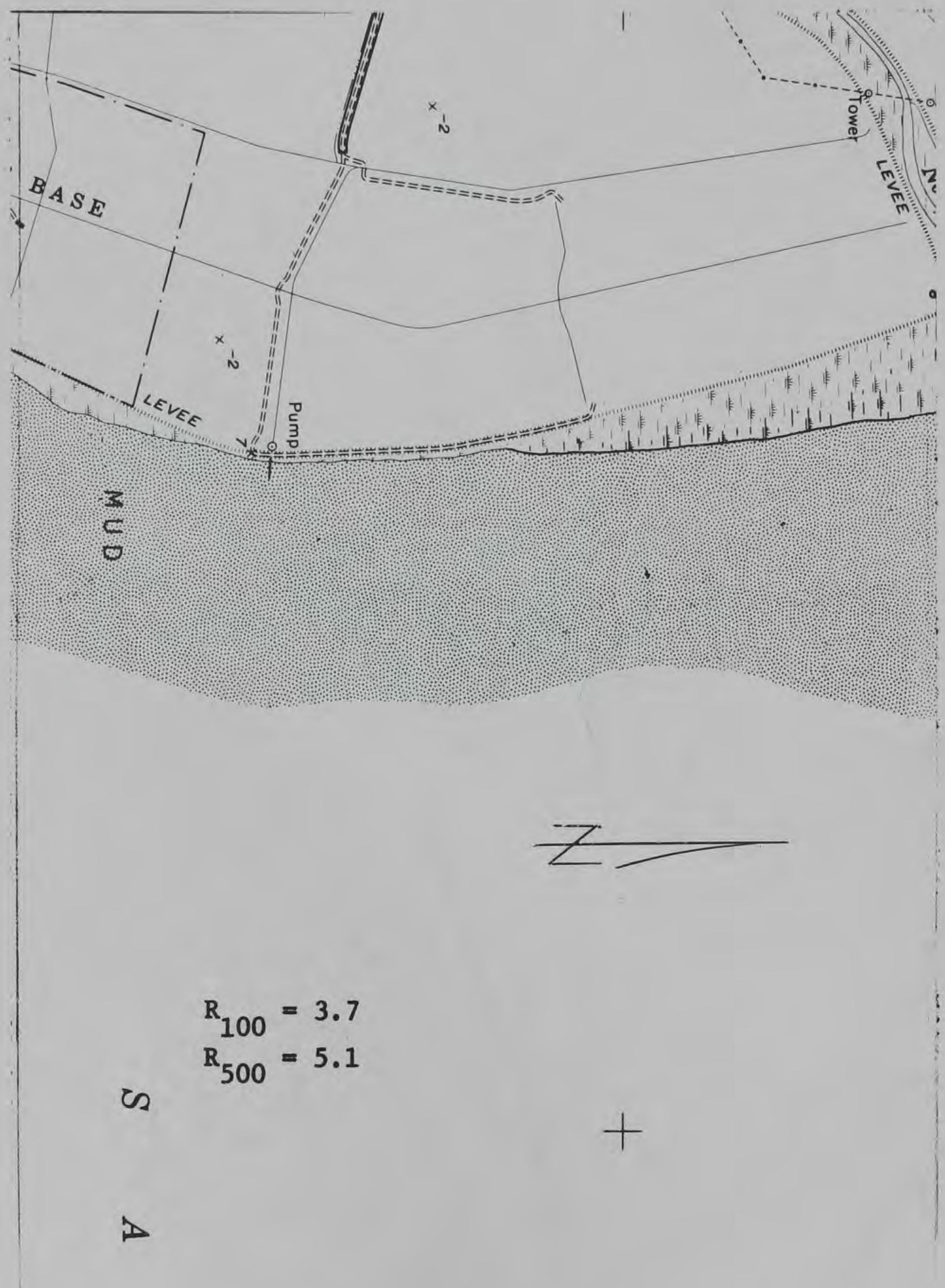

Figure 38. Petaluma Point, Calif., 13N to 16N, L

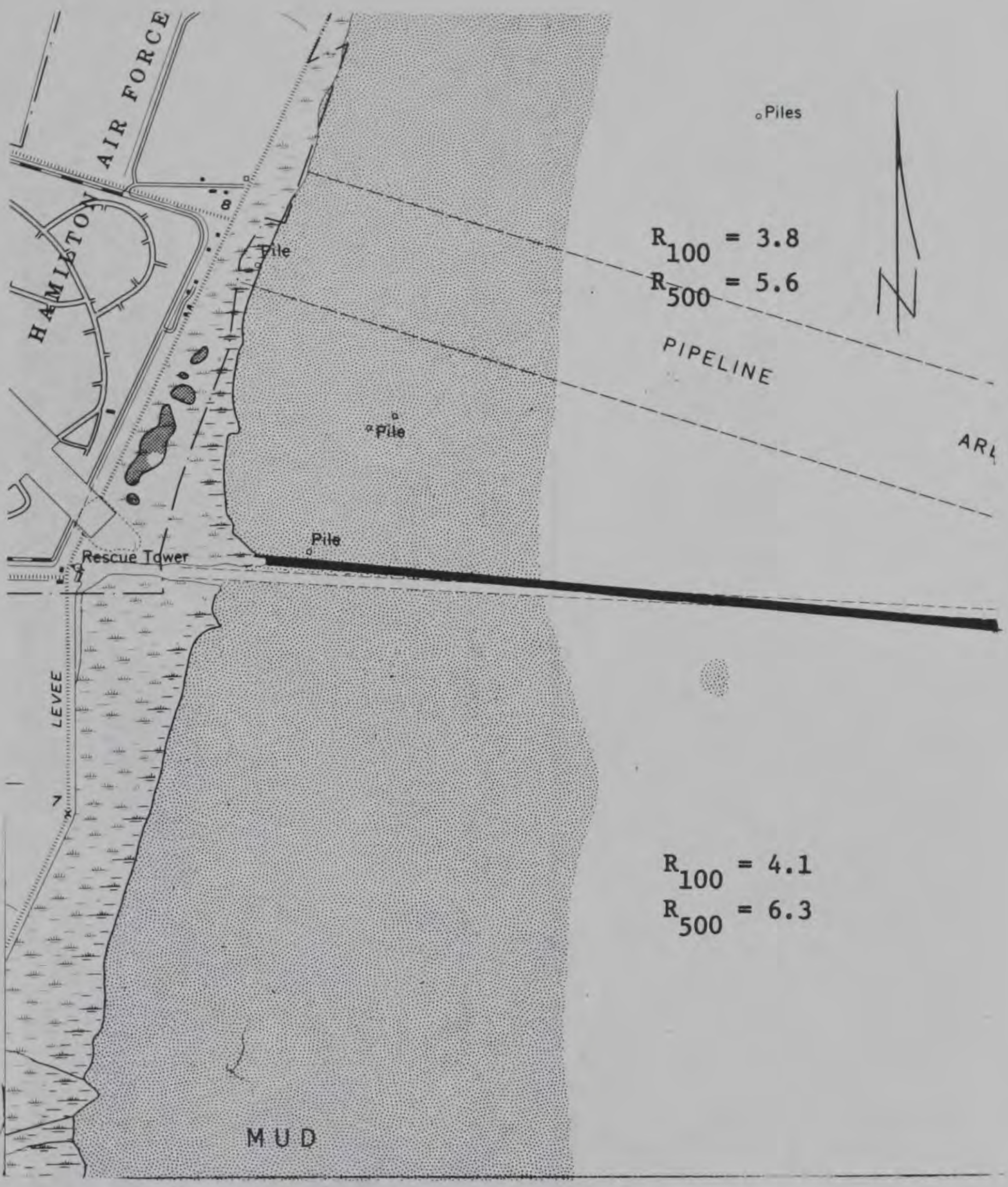

Figure 39. Petaluma Point, Calif., 09N to 13N, L

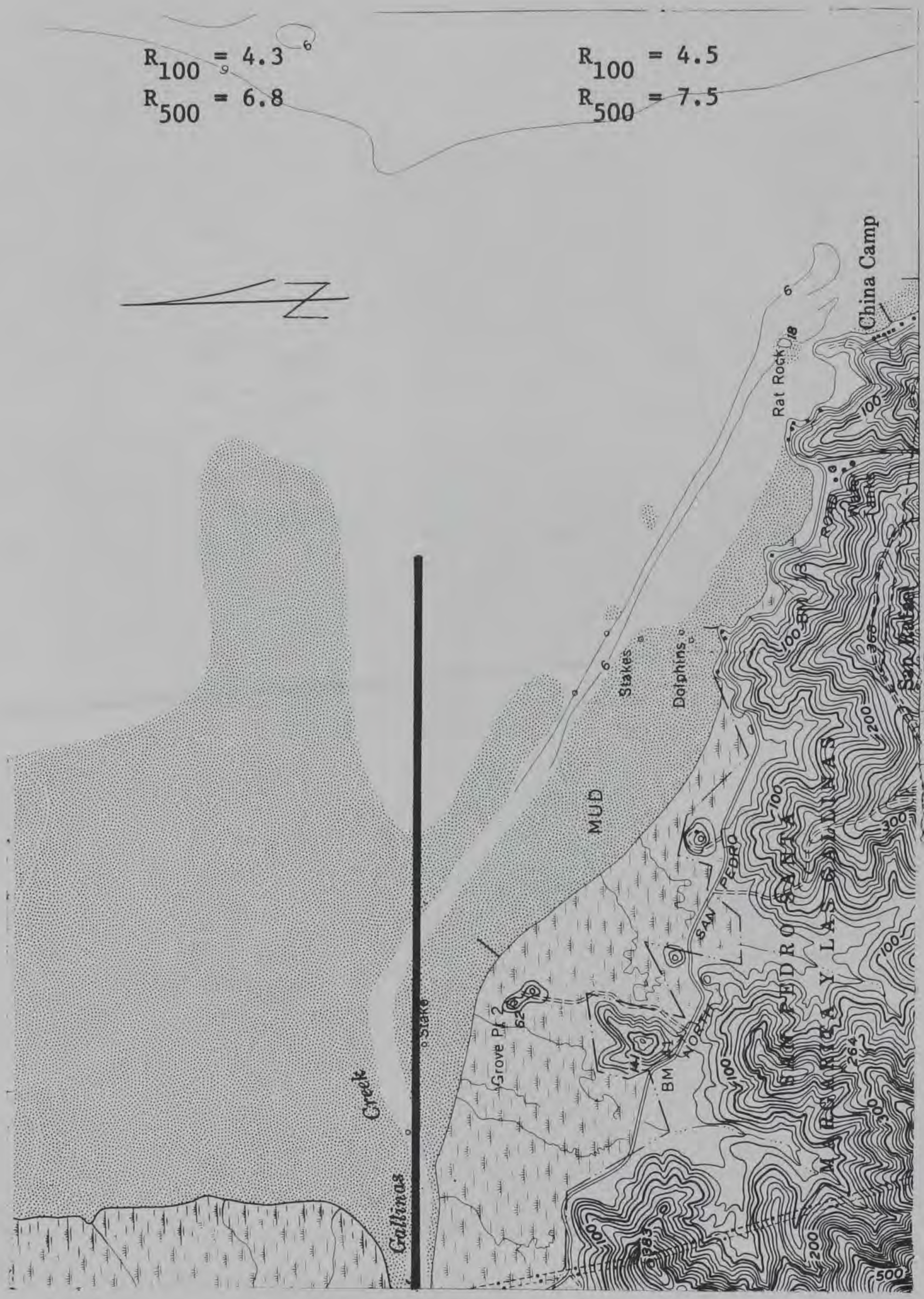

Figure 40. Petaluma Point, Calif., 05+N to 09N, L

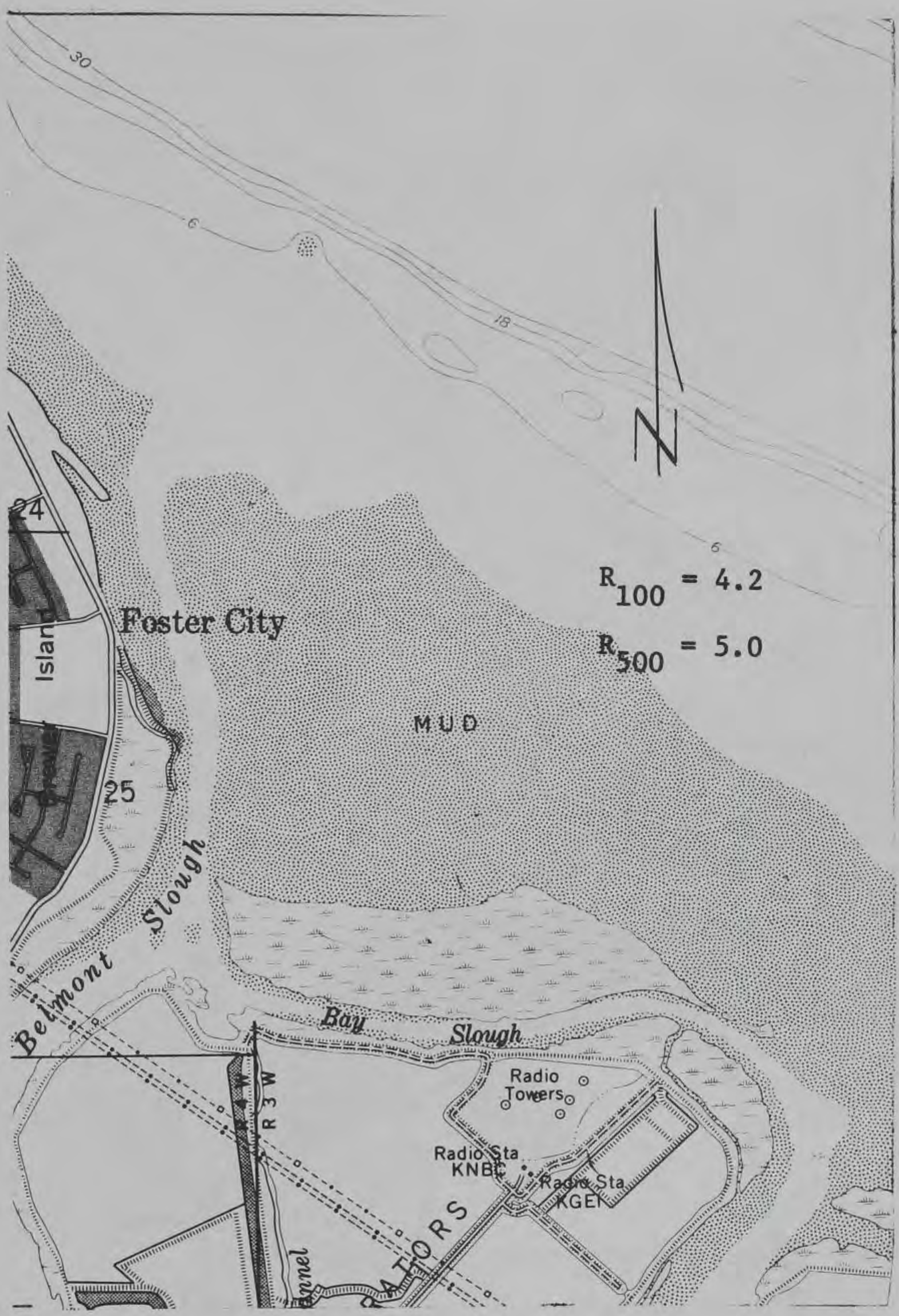

Figure 41. Redwood Point, Calif., 55N to 59N, L

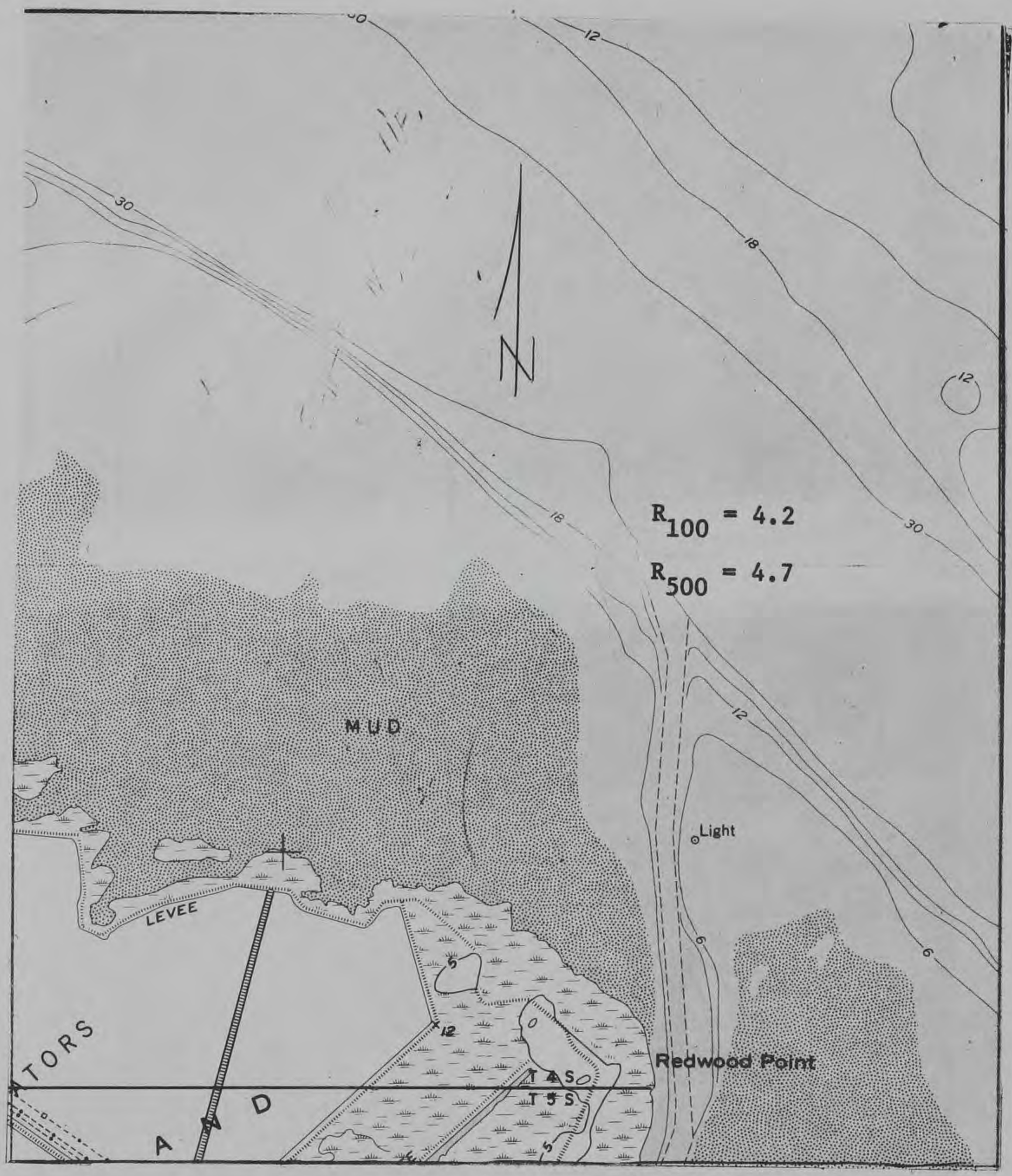

Figure 42. Redwood Point, Calif., 53+N to 58N, L

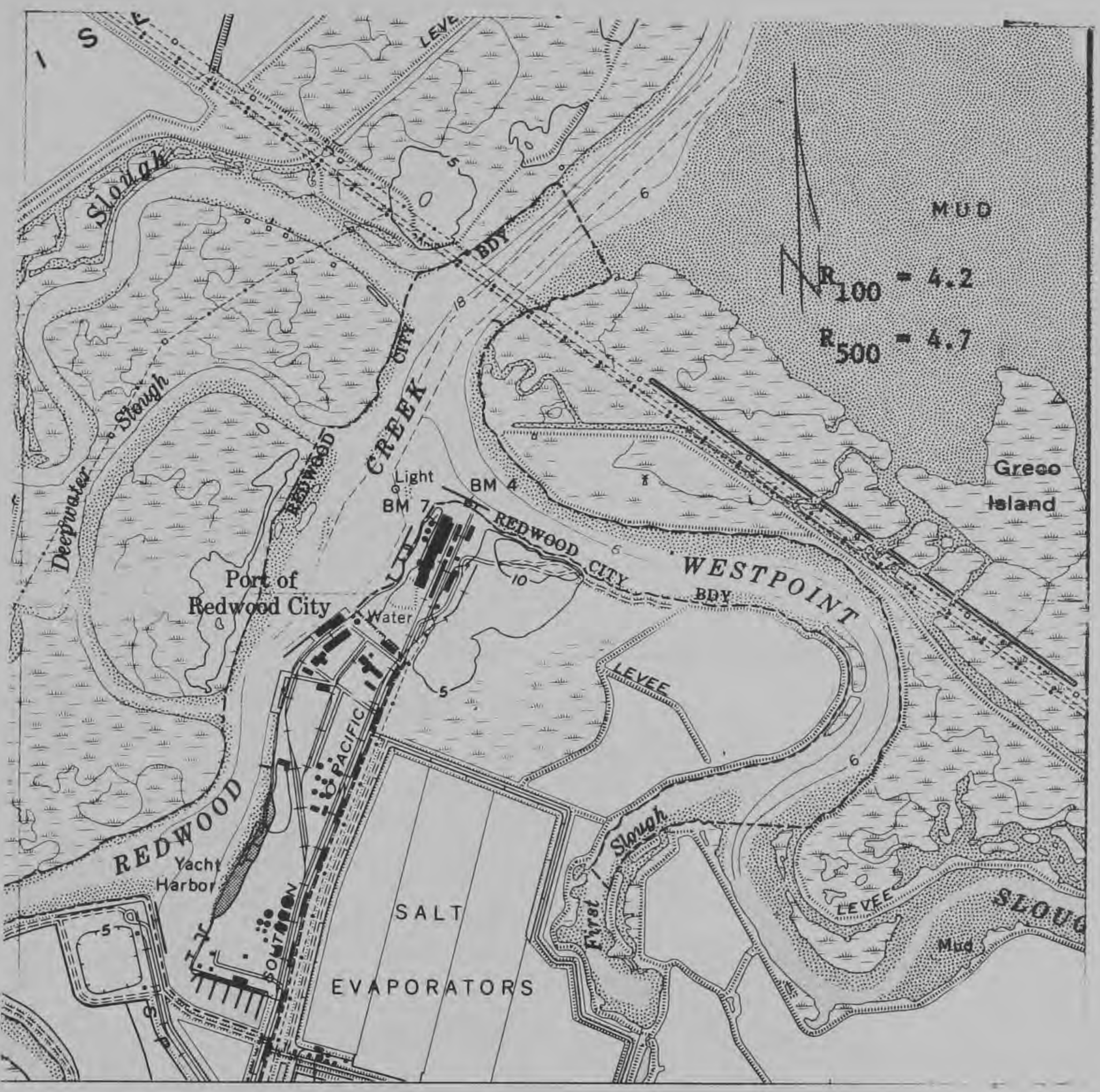

Figure 43. Redwood Point, Calif., 67E to 72+E, B

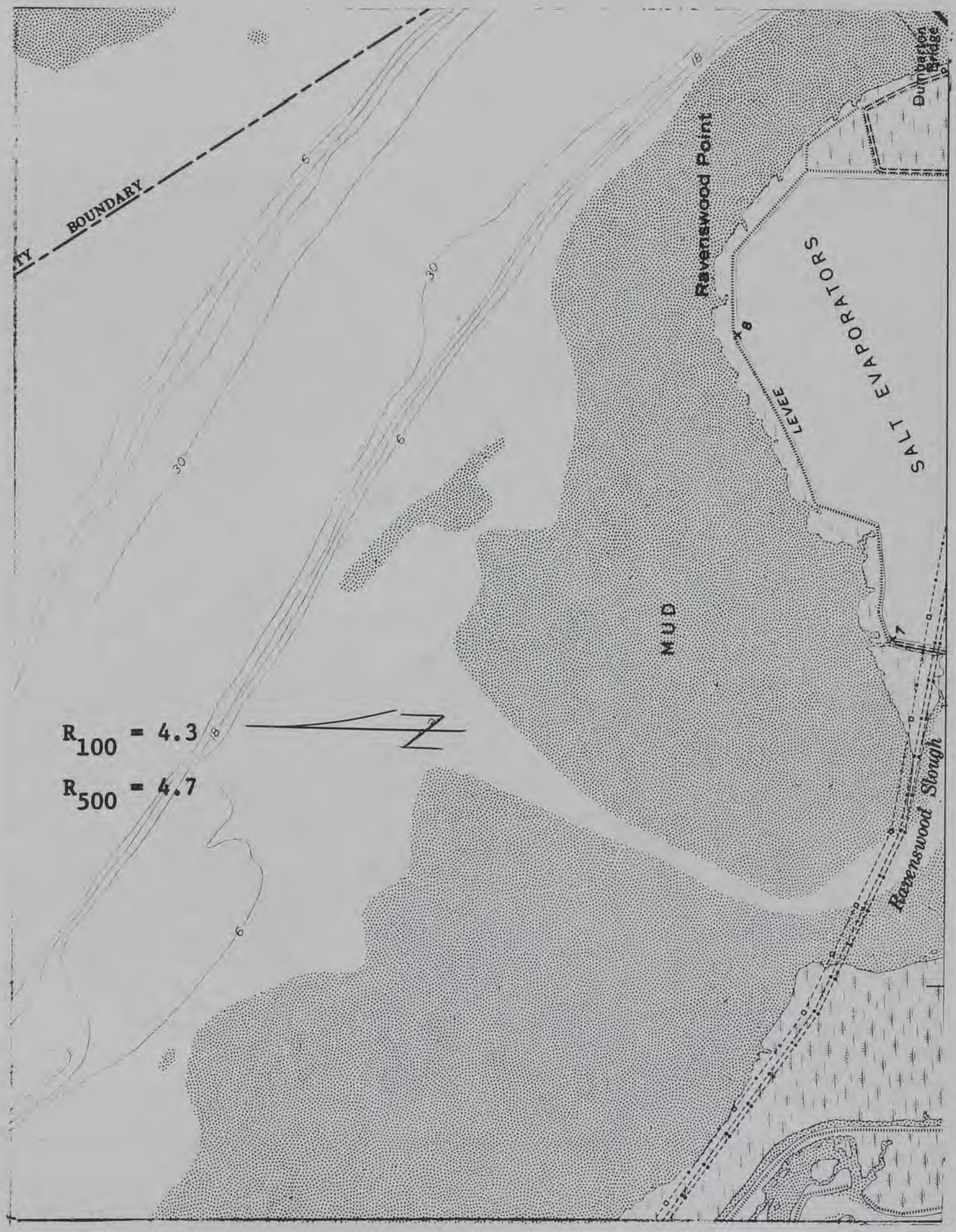

Figure 44. Redwood Point, Calif., 50+N to 54N, R

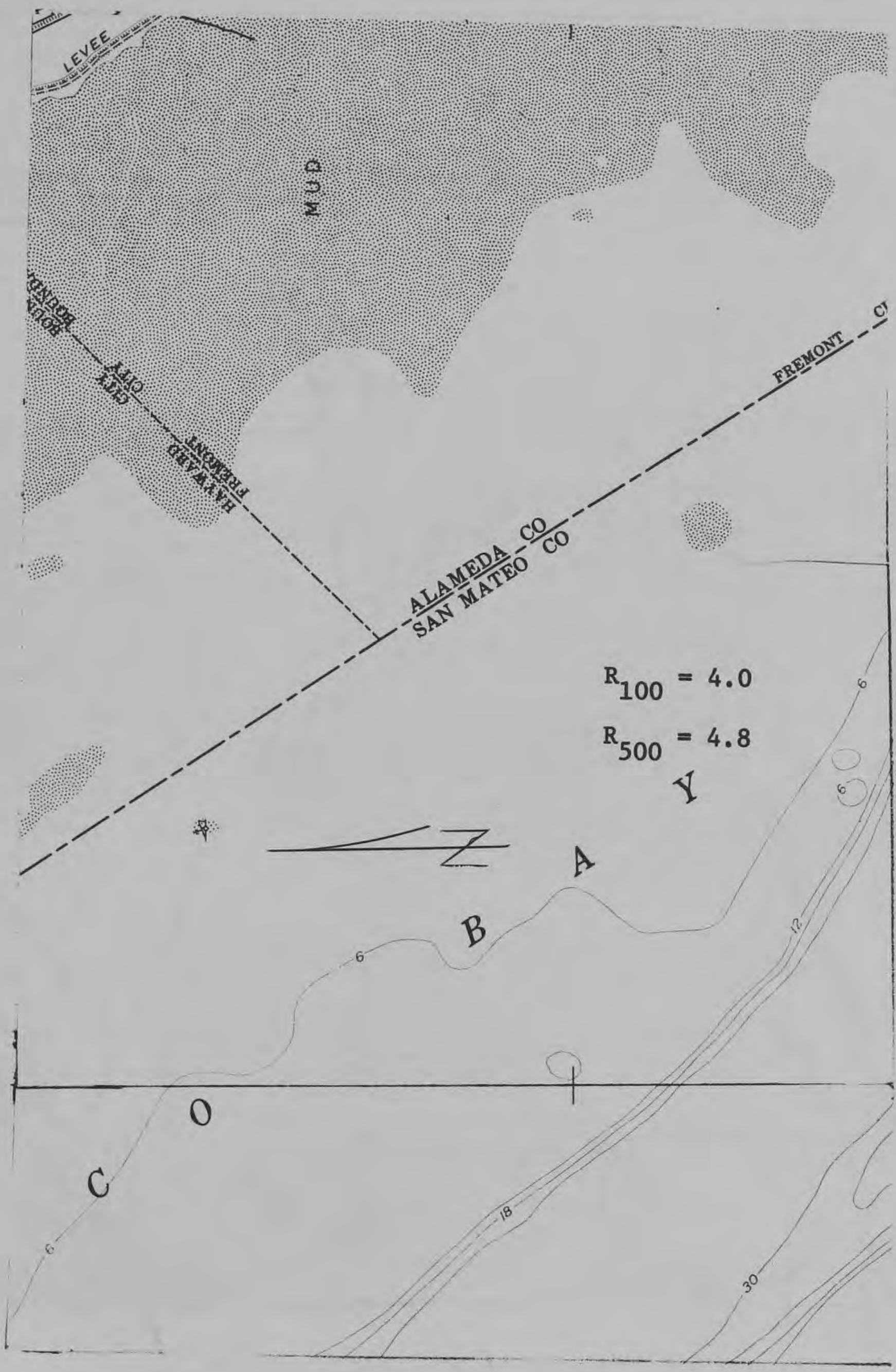

Figure 45. Redwood Point, Calif., 54N to 57N, R

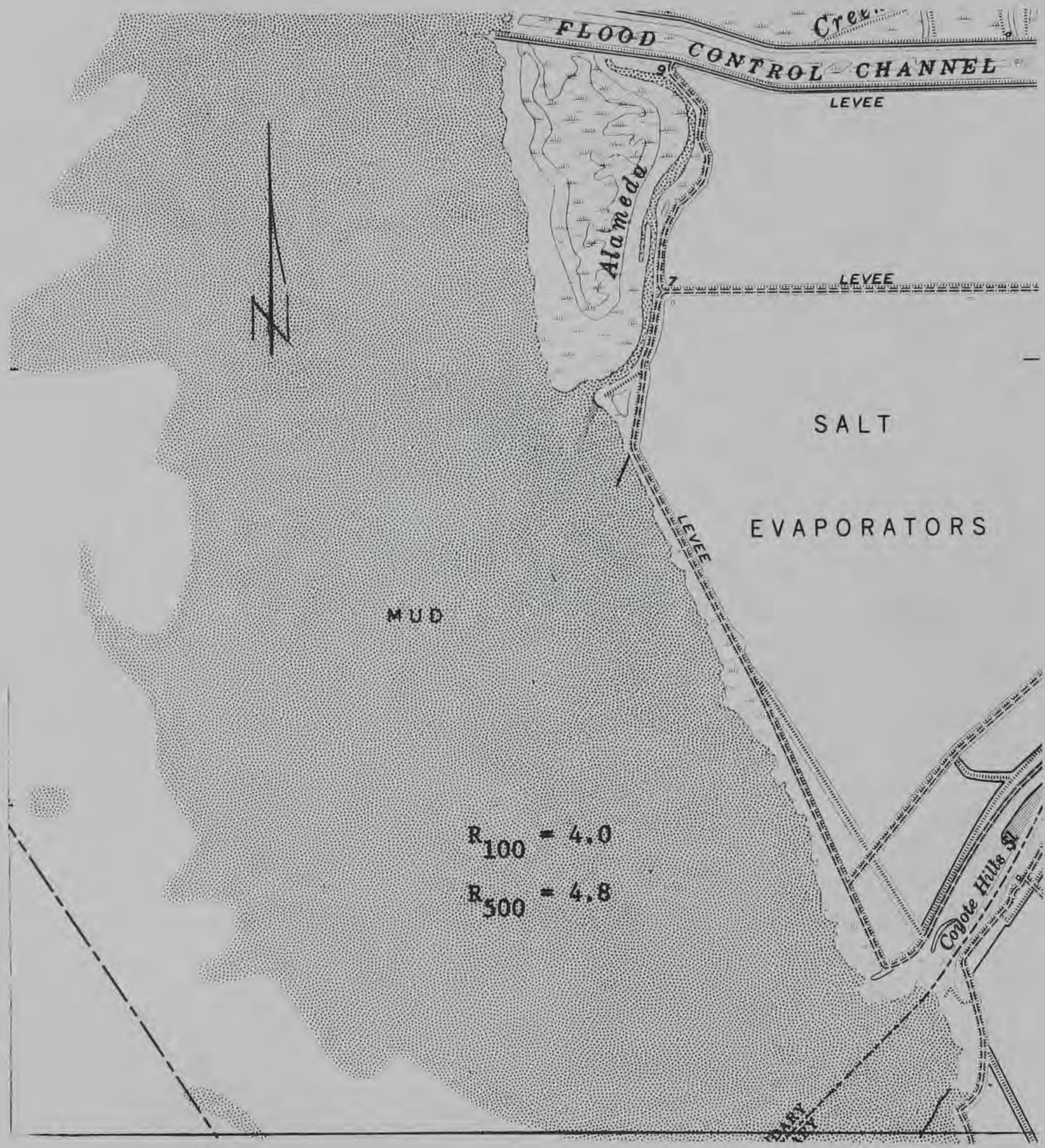

Figure 46. Redwood Point, Calif., 57N to 61N, R

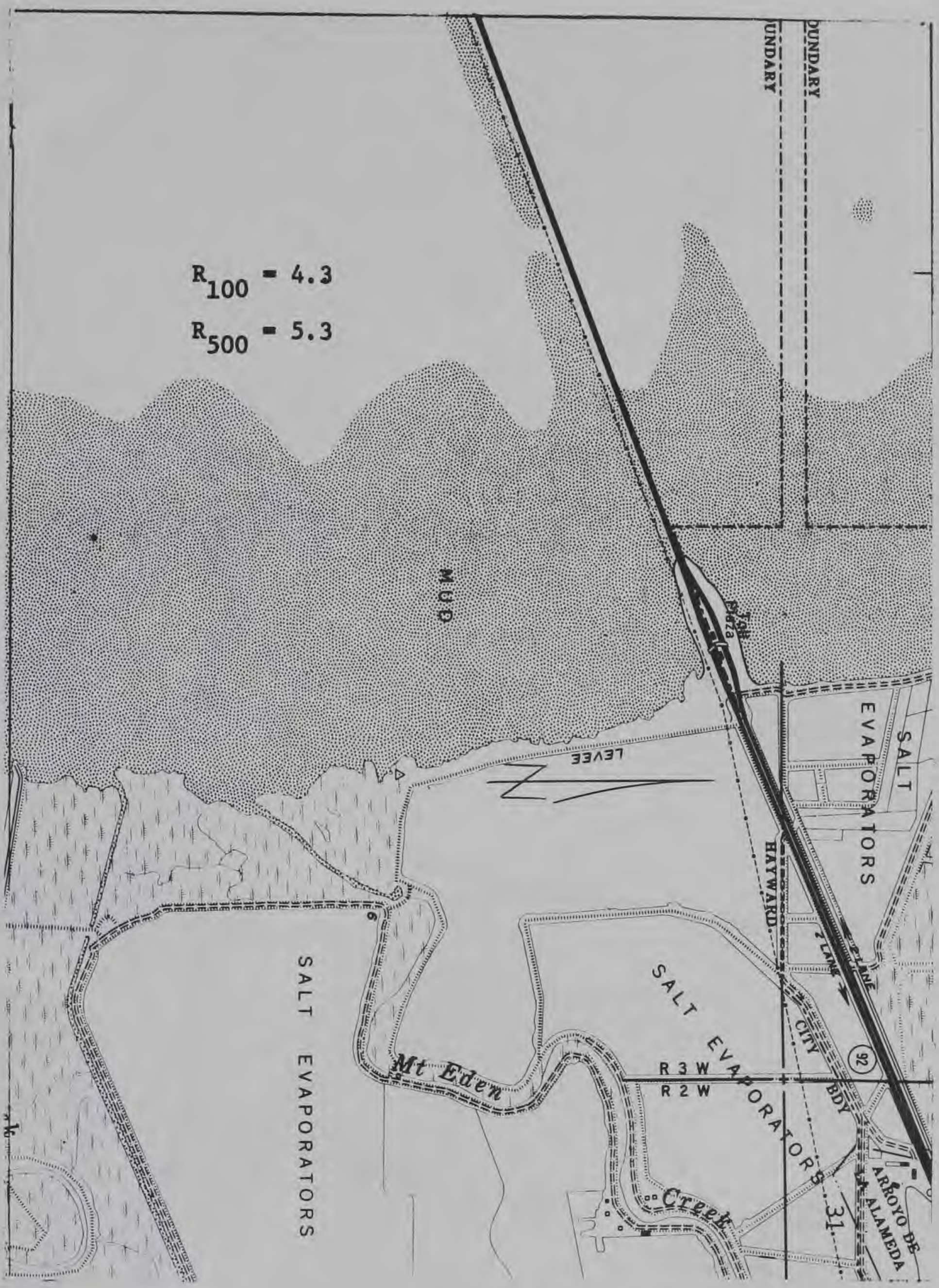

Figure 47. Redwood Point, Calif., 61N to 64+N, R

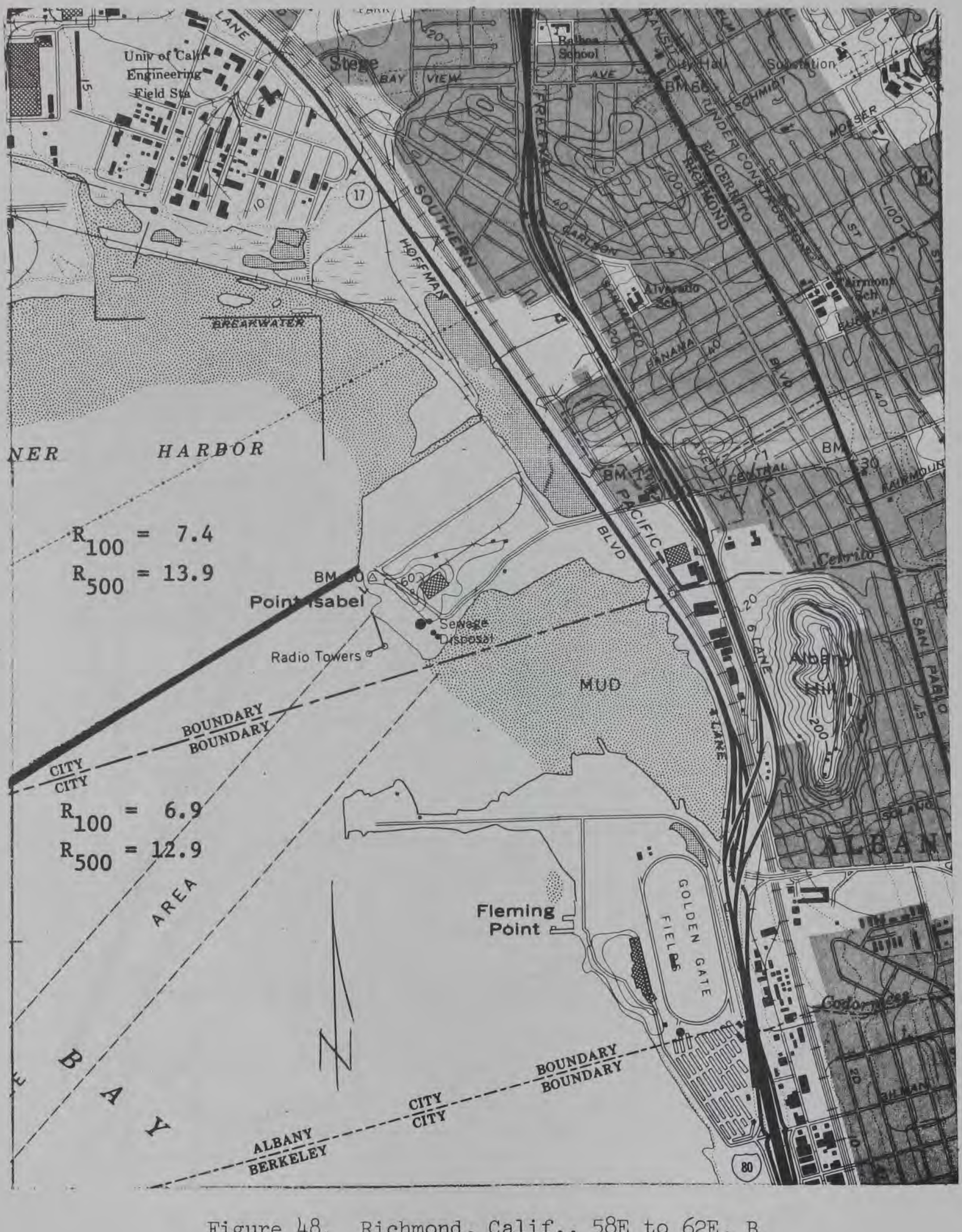

Figure 48. Richmond, Calif., 58E to 62E, B

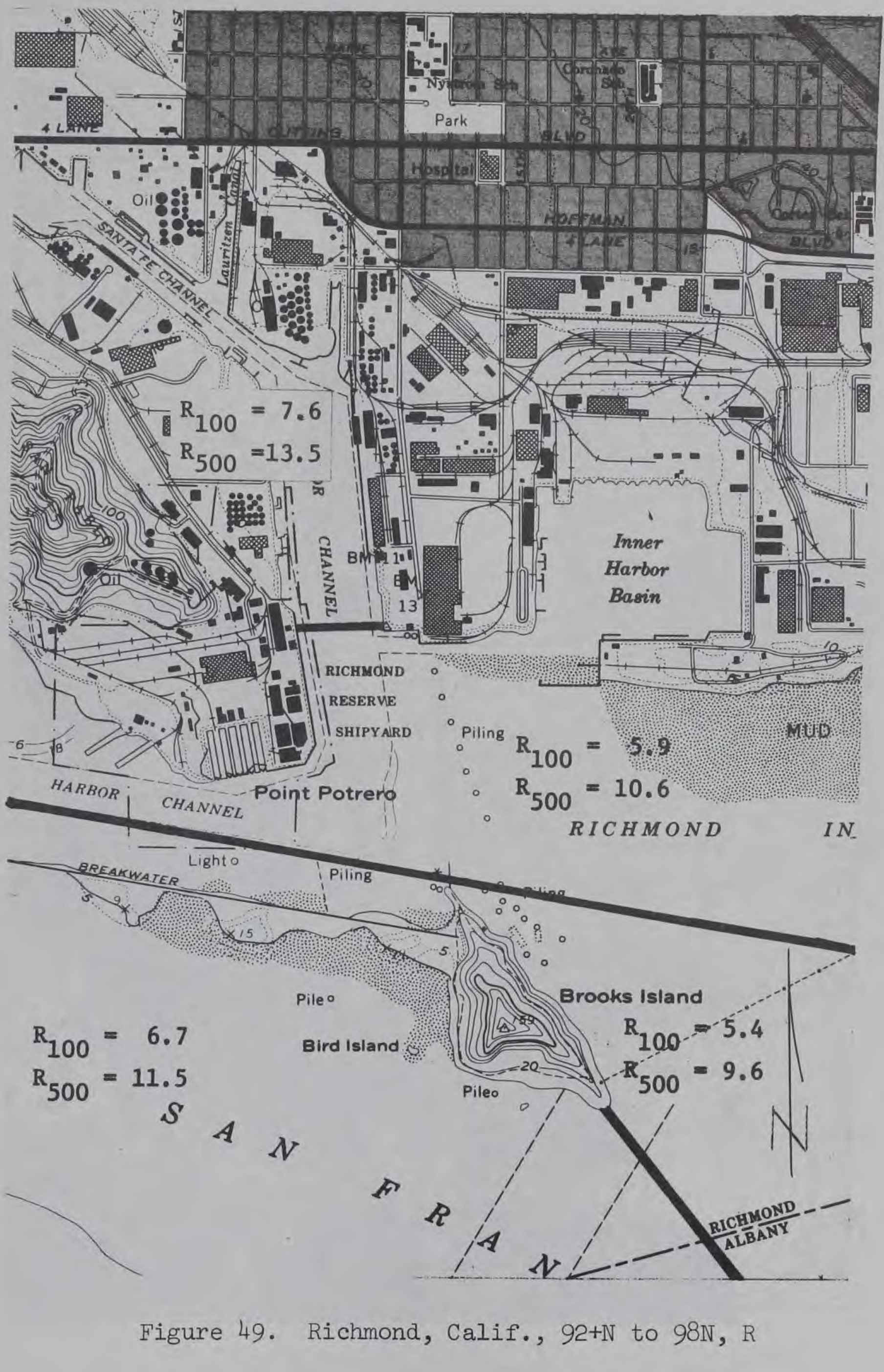

Figure 49. Richmond, Calif., 92+N to 98N, R

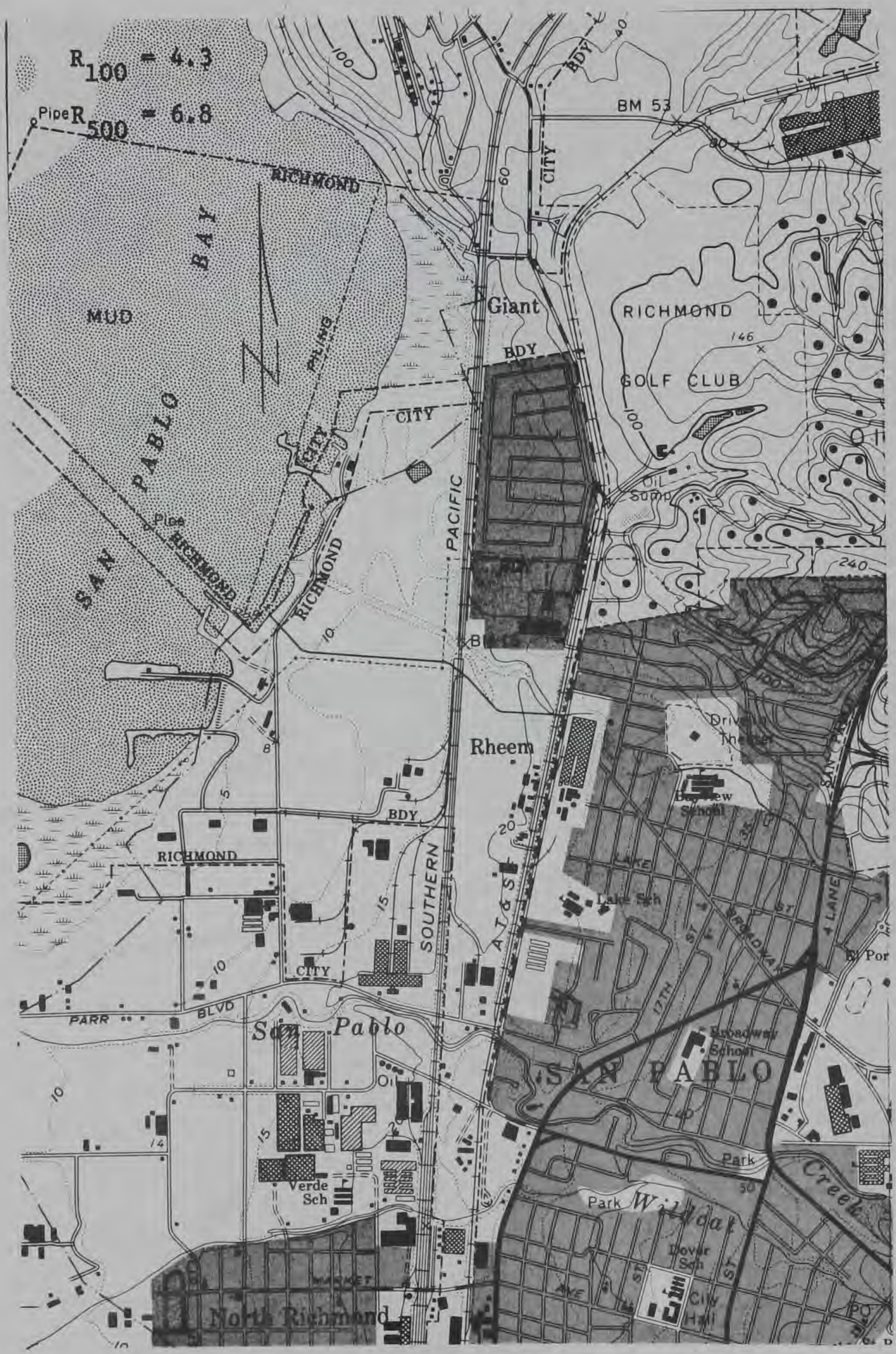

Figure 50. Richmond, Calif., O1N to O5+N, L

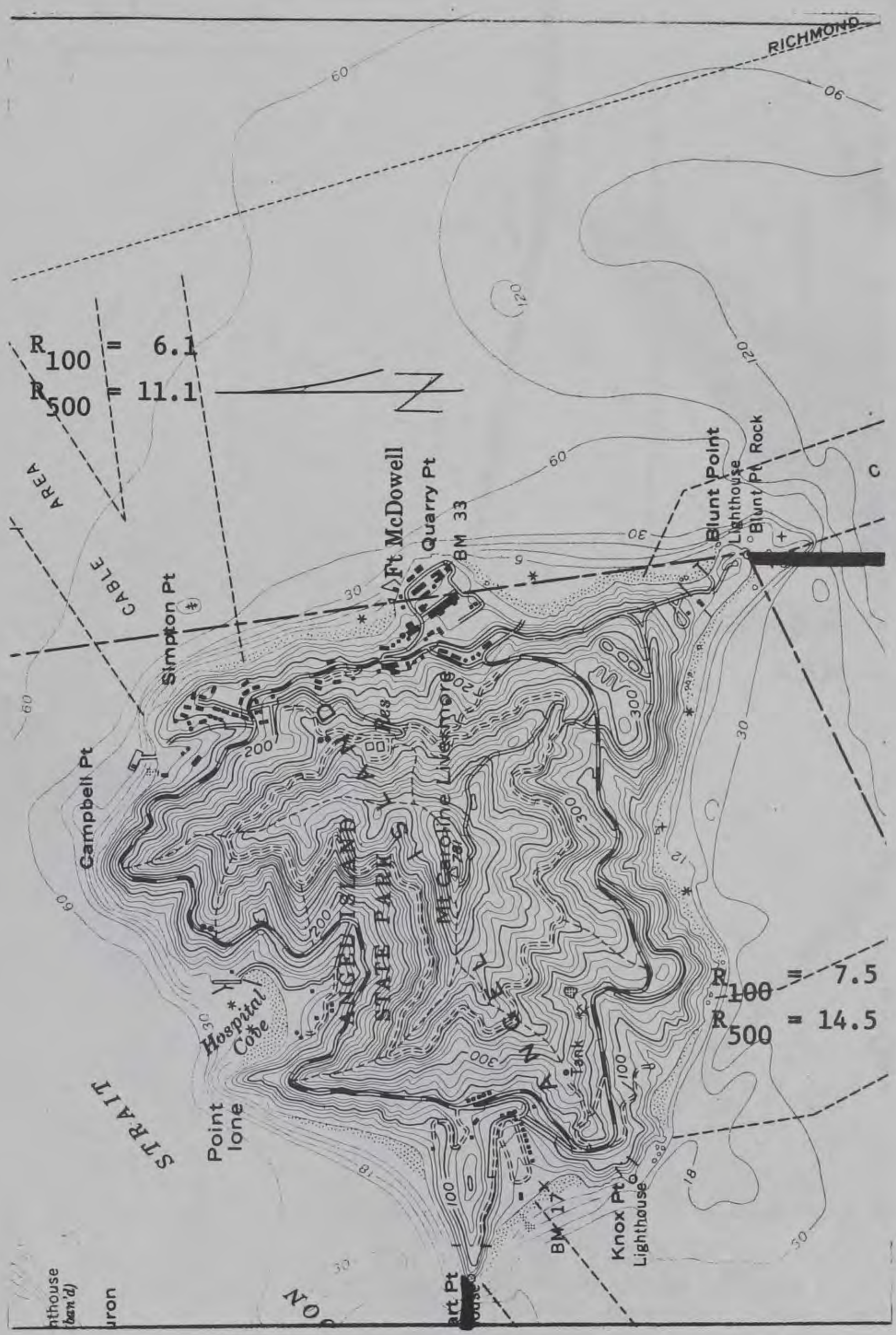

Figure 51. San Francisco North, Calif., 89N to 91+N, R

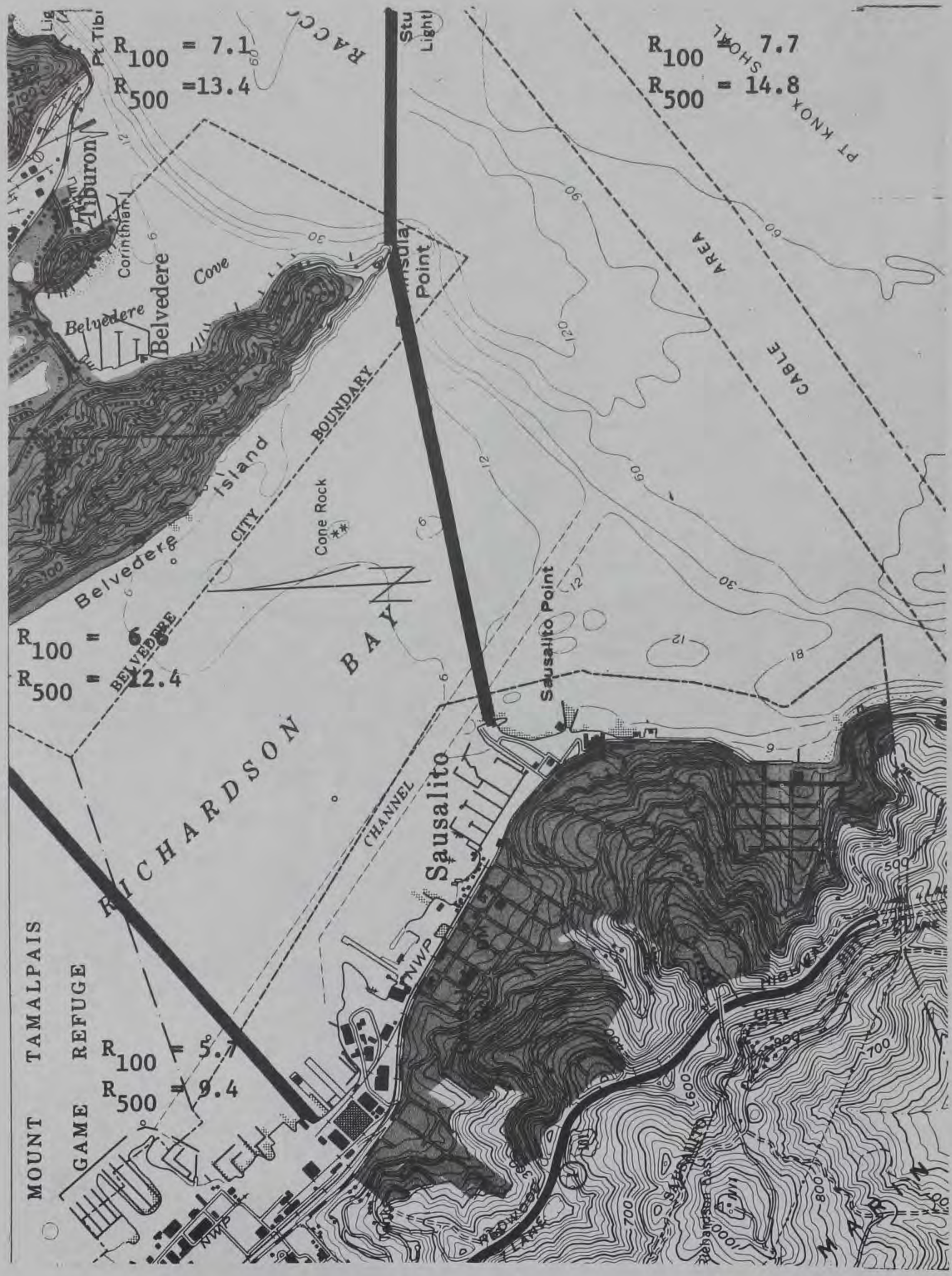

Figure 52. San Francisco North, Calif., 44E to 48+E, T

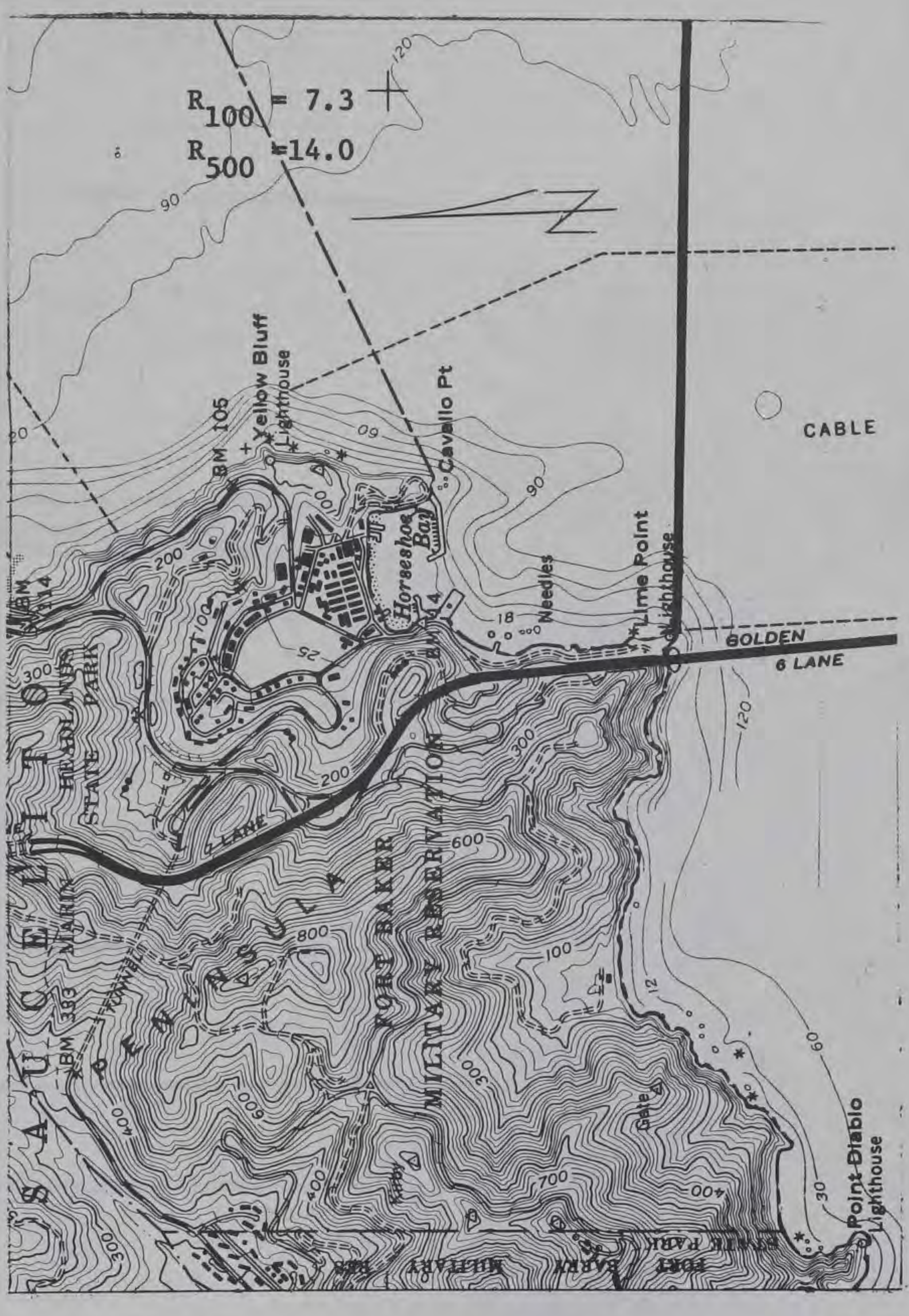

Figure 53. San Francisco North, Calif., 85N to 88+N, L

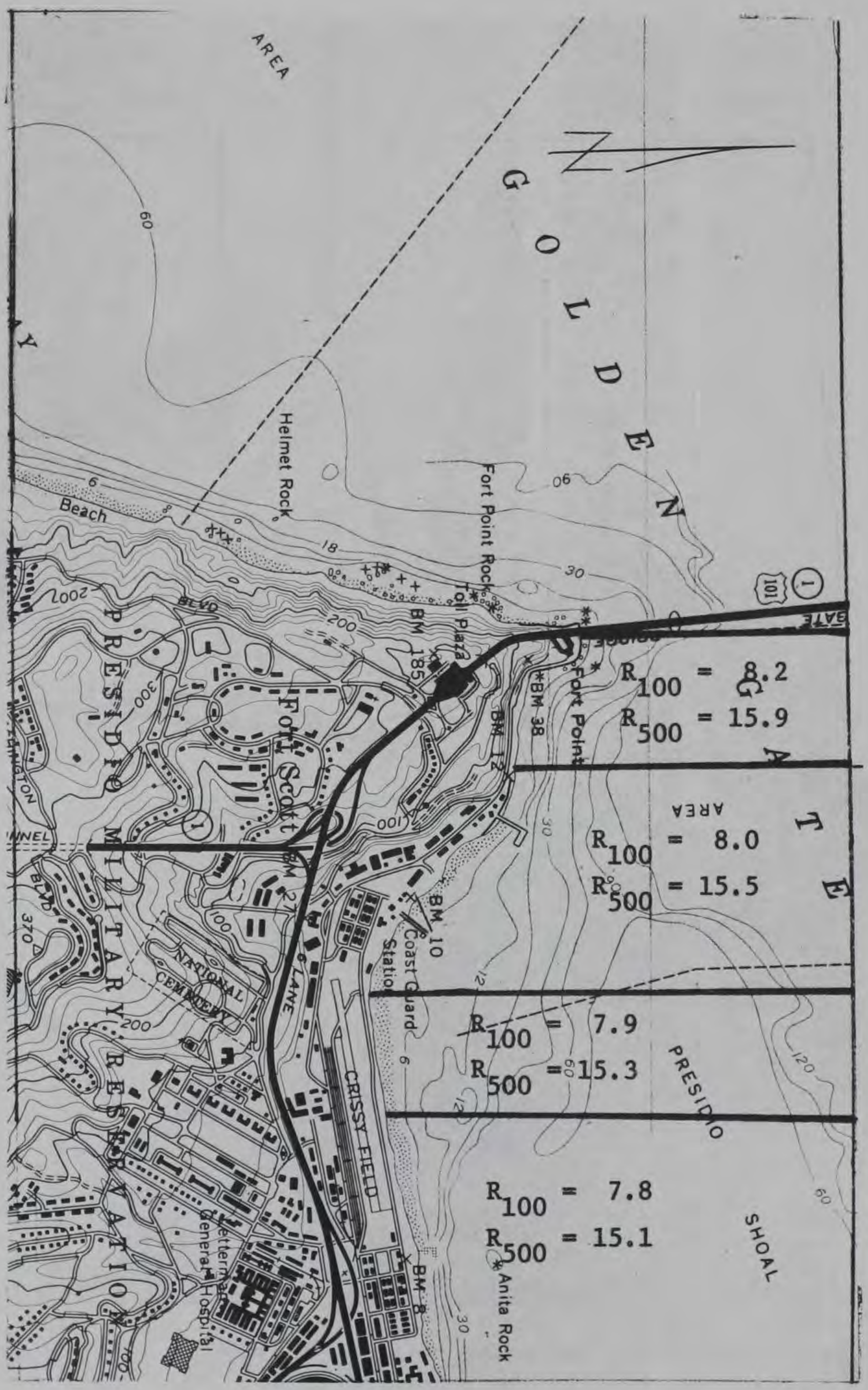

Figure 54. San Francisco North, Calif., 82+N to 85+N, L

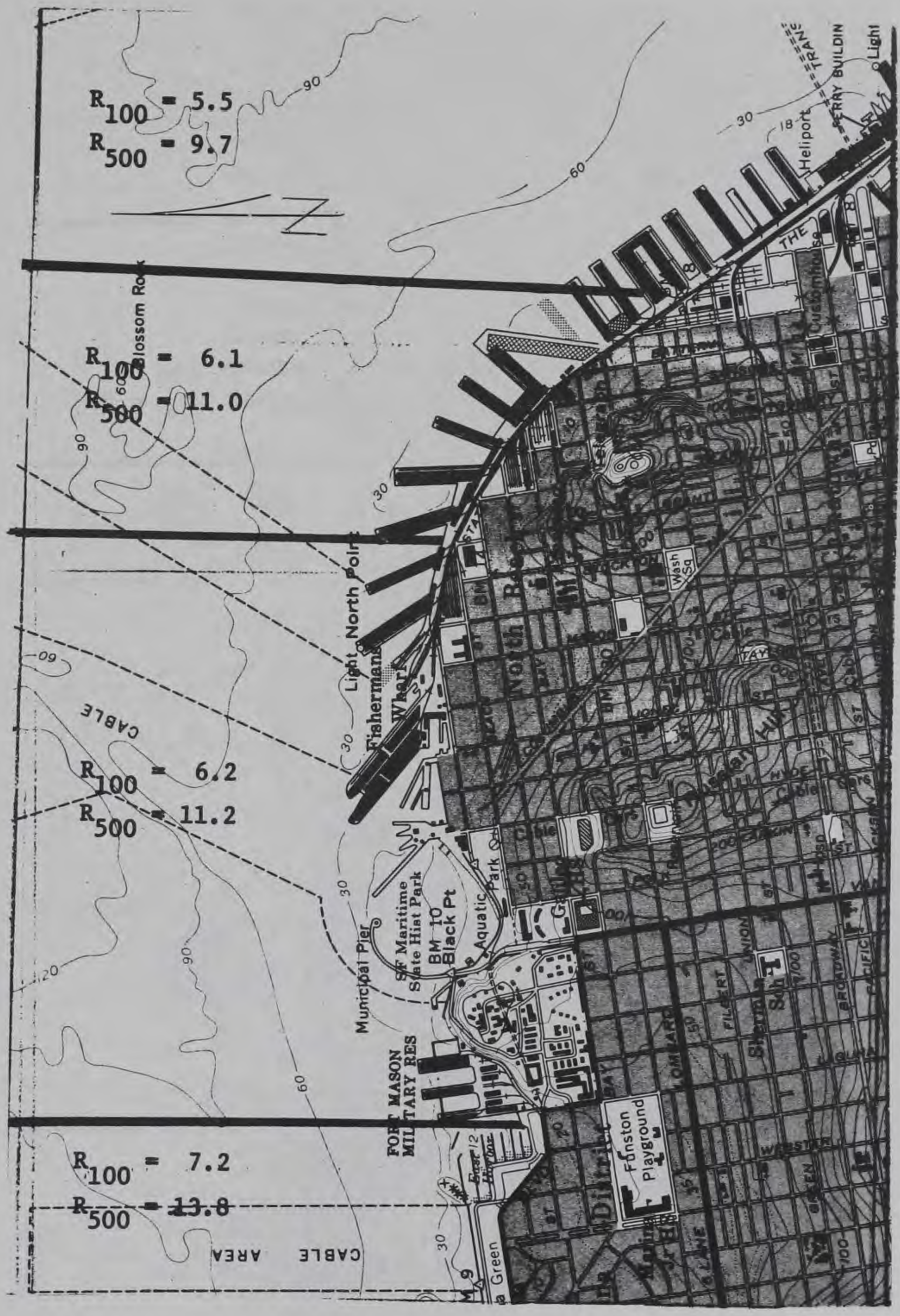

Figure 55. San Francisco North, Calif., 82+N to 86N, R

Figure 56. San Francisco North, Calif., 78+N to 82+N, R

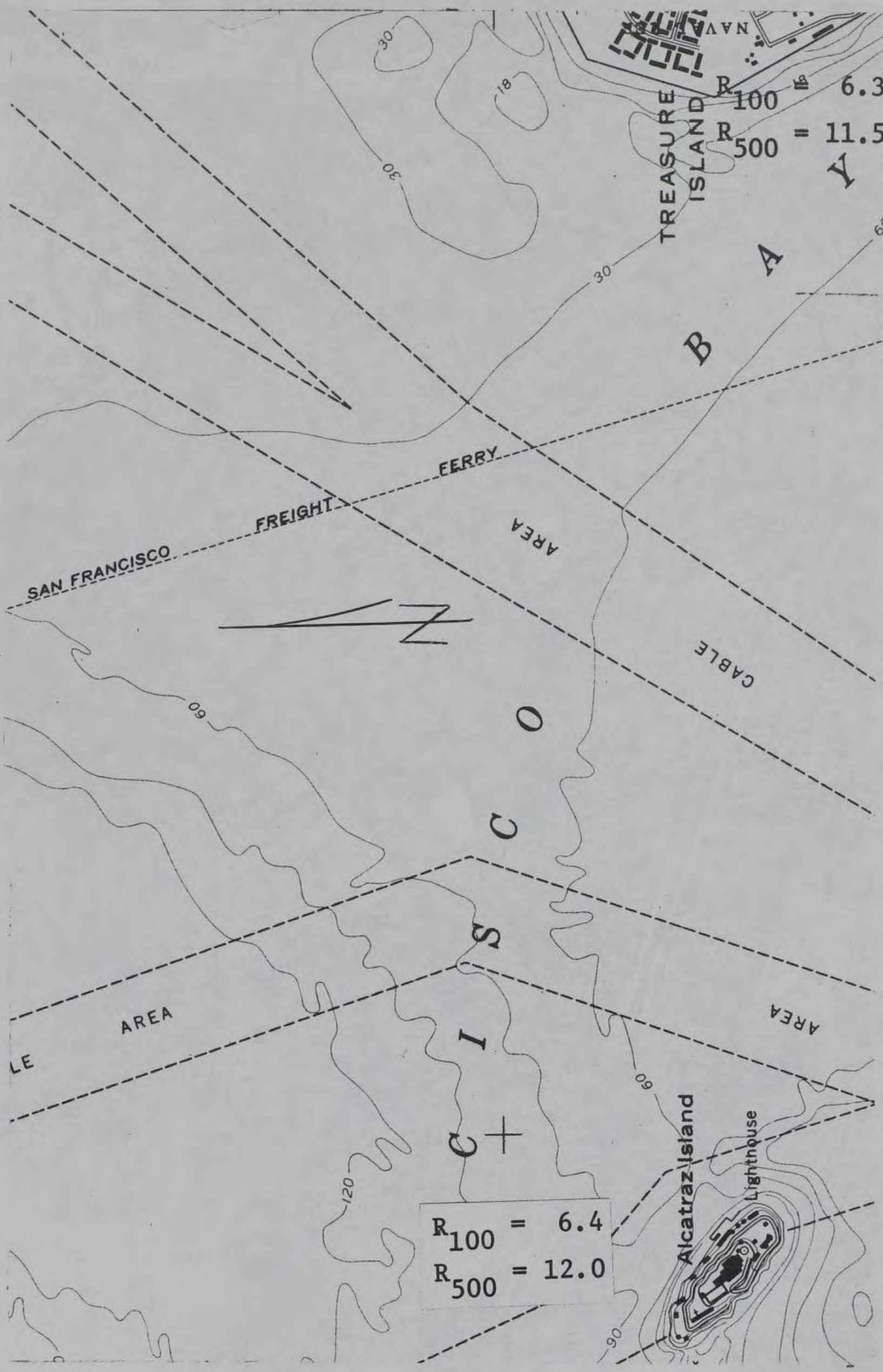

Figure 57. San Francisco North, Calif., 86N to 89N, R

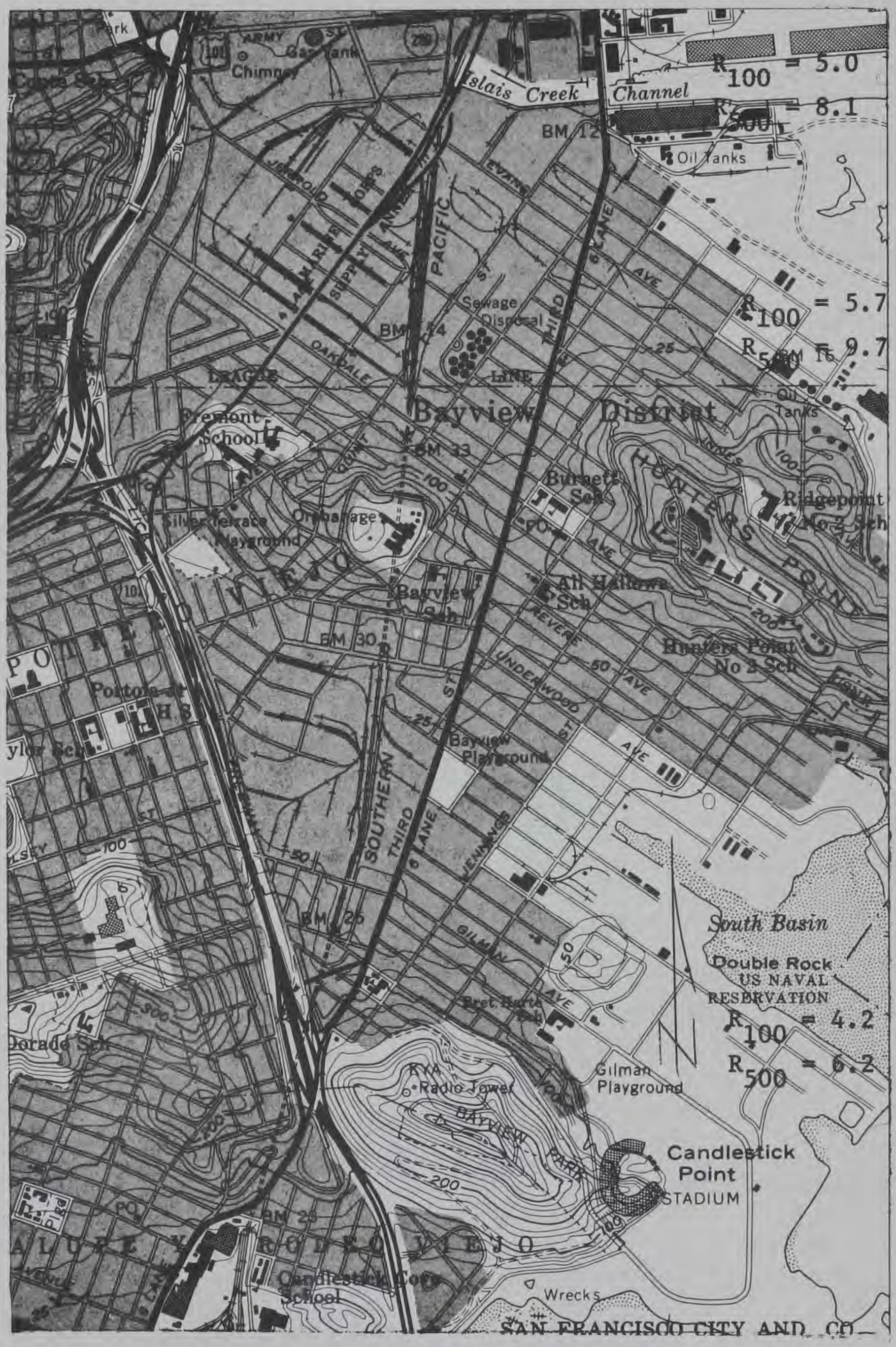

Figure 58. San Francisco South, Calif., 52E to 55E, T

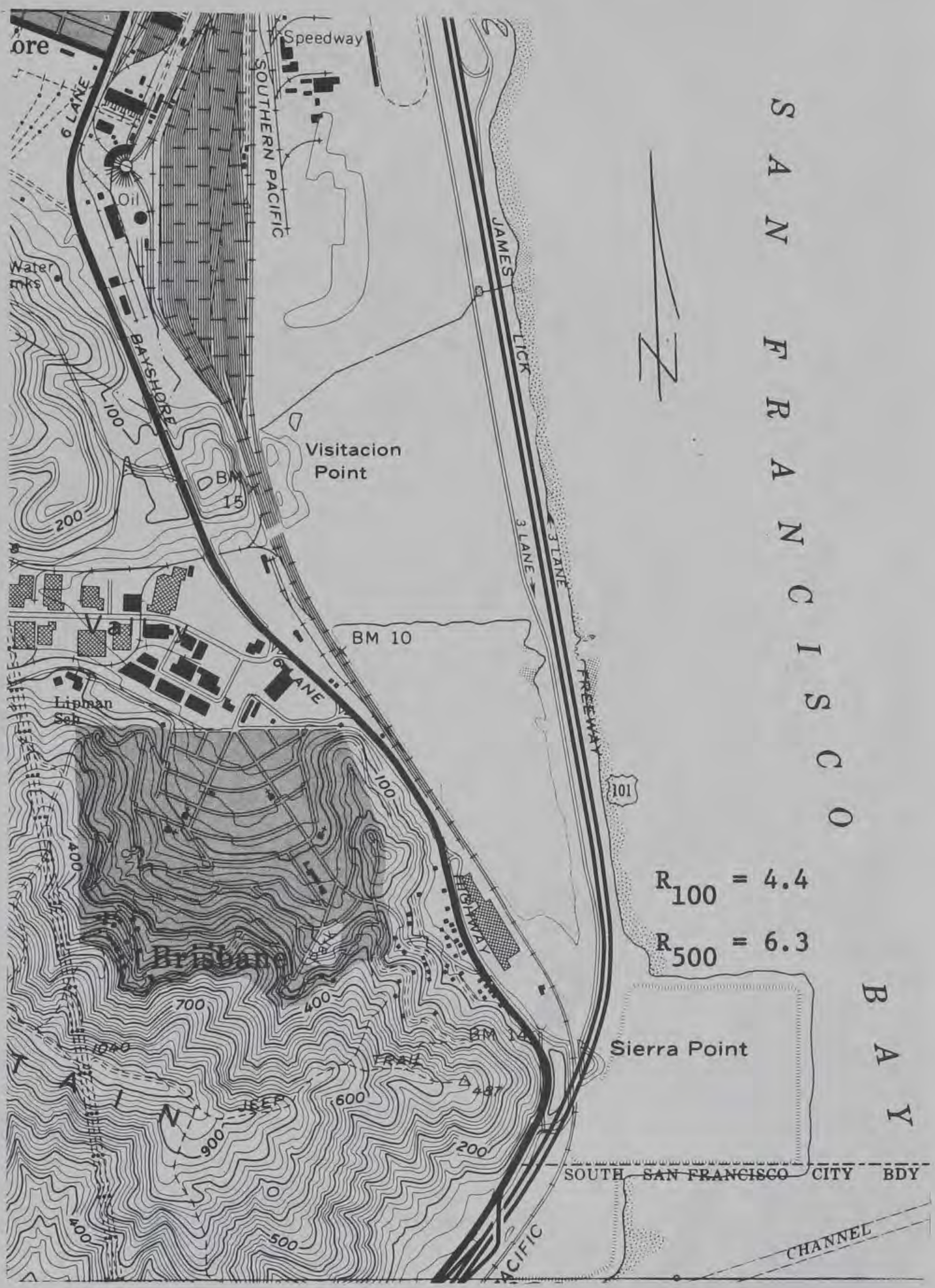

Figure 59. San Francisco South, Calif., 69N to 73+N, R

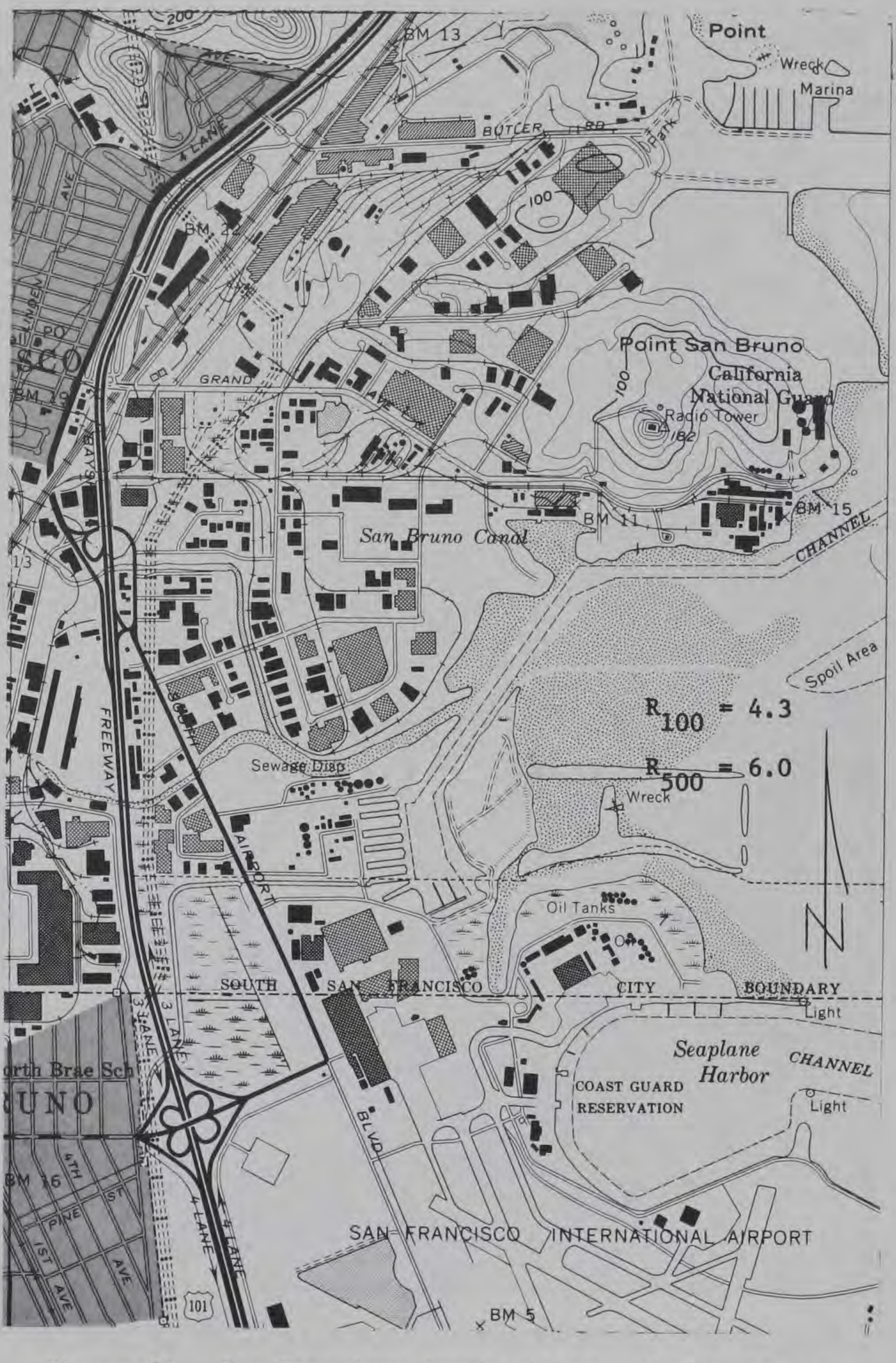

Figure 60. San Francisco South, Calif., 65N to 69N, R

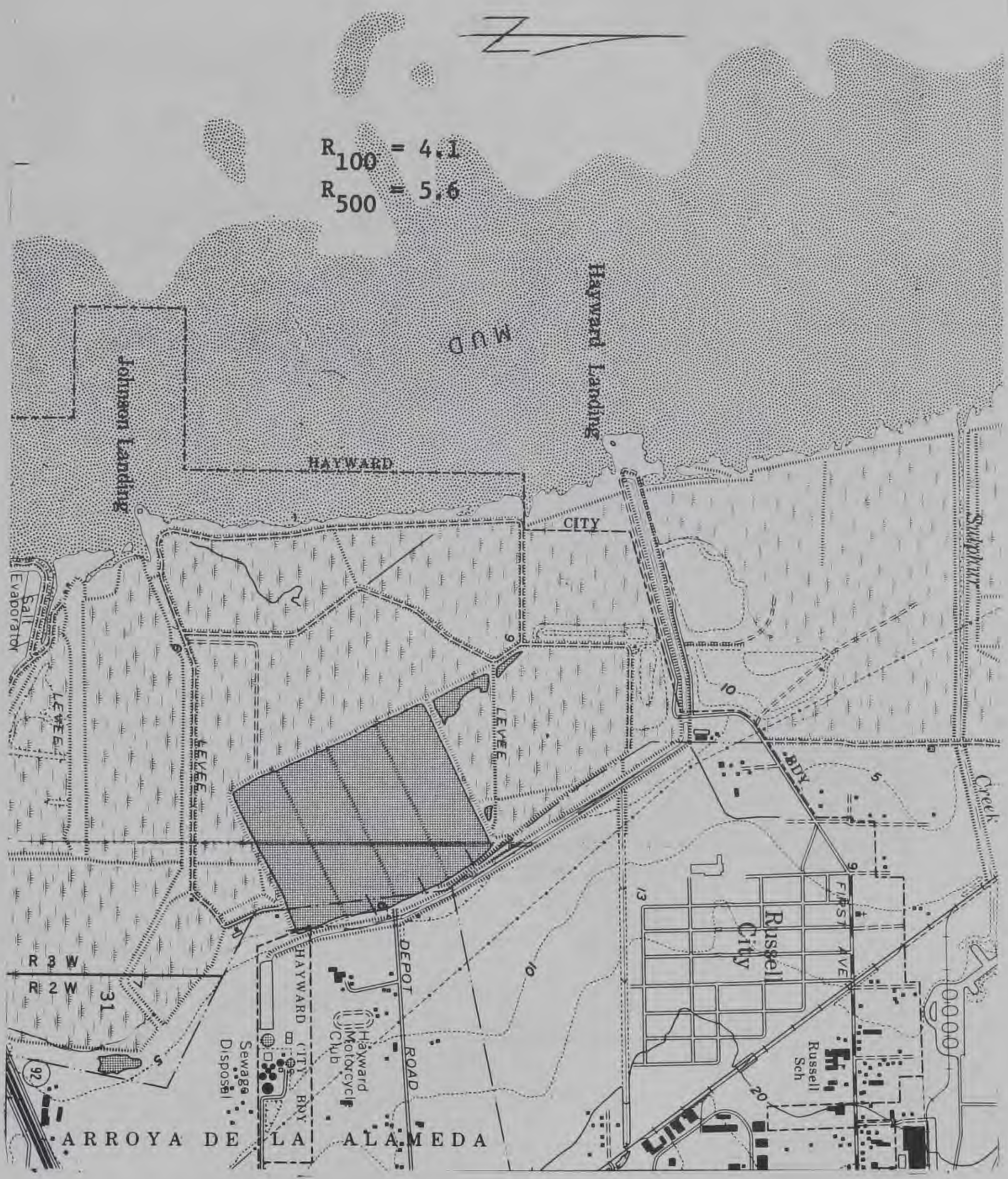

Figure 61. San Leandro, Calif., 72E to 76E, B

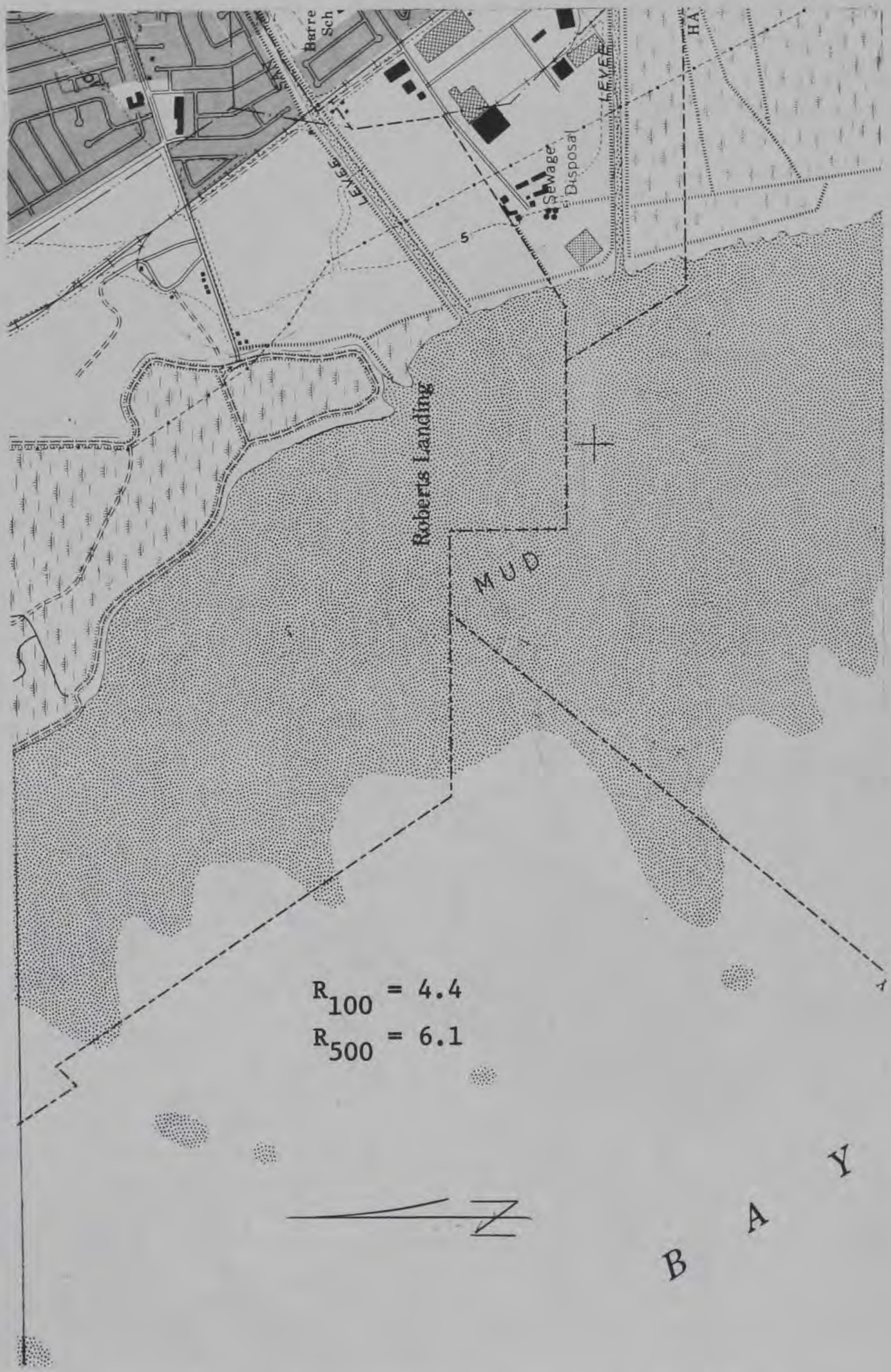

Figure 62. San Leandro, Calif., 68N to 71N, R

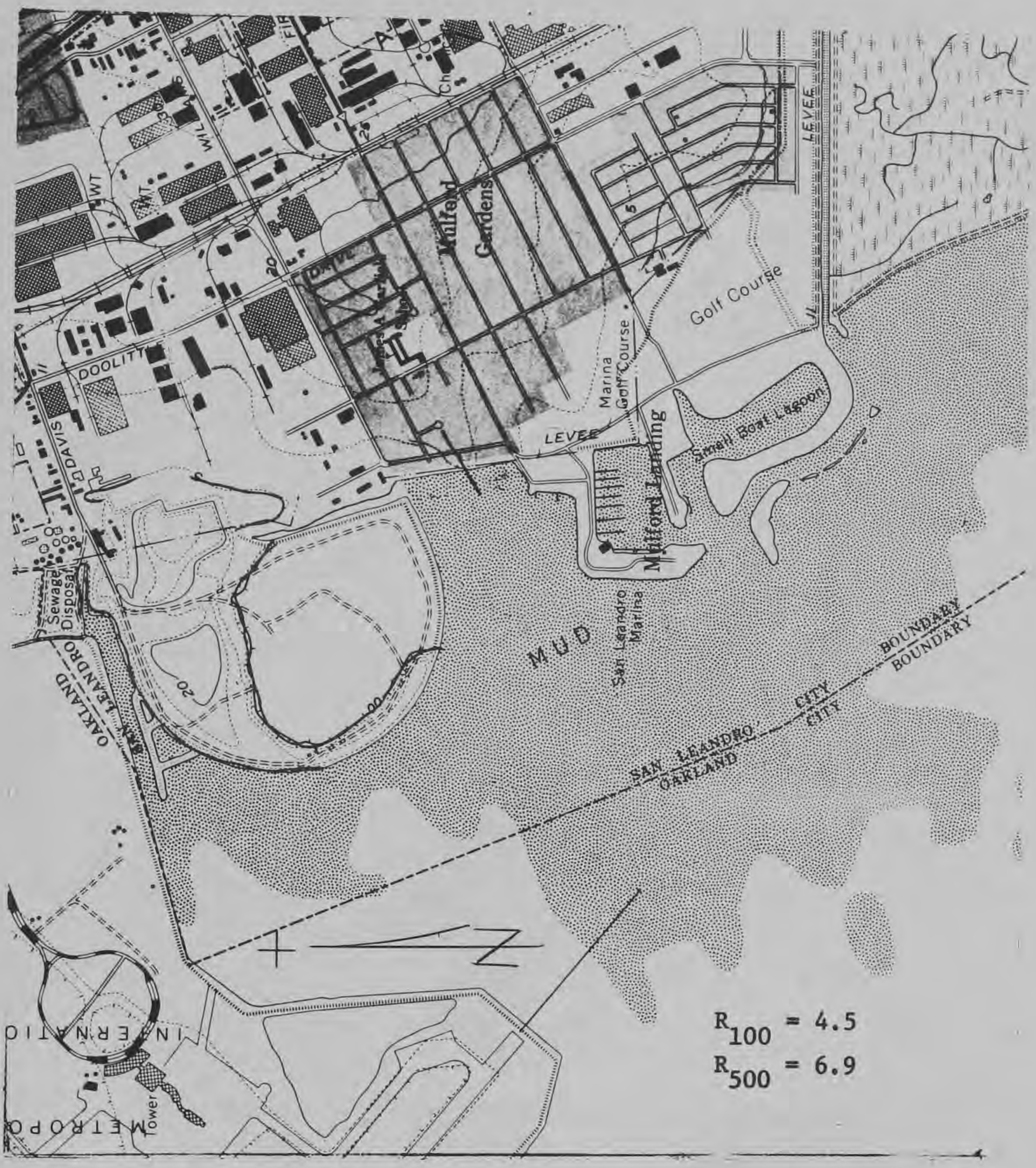

Figure 63. San Leandro, Calif., 71N to 74+N, R

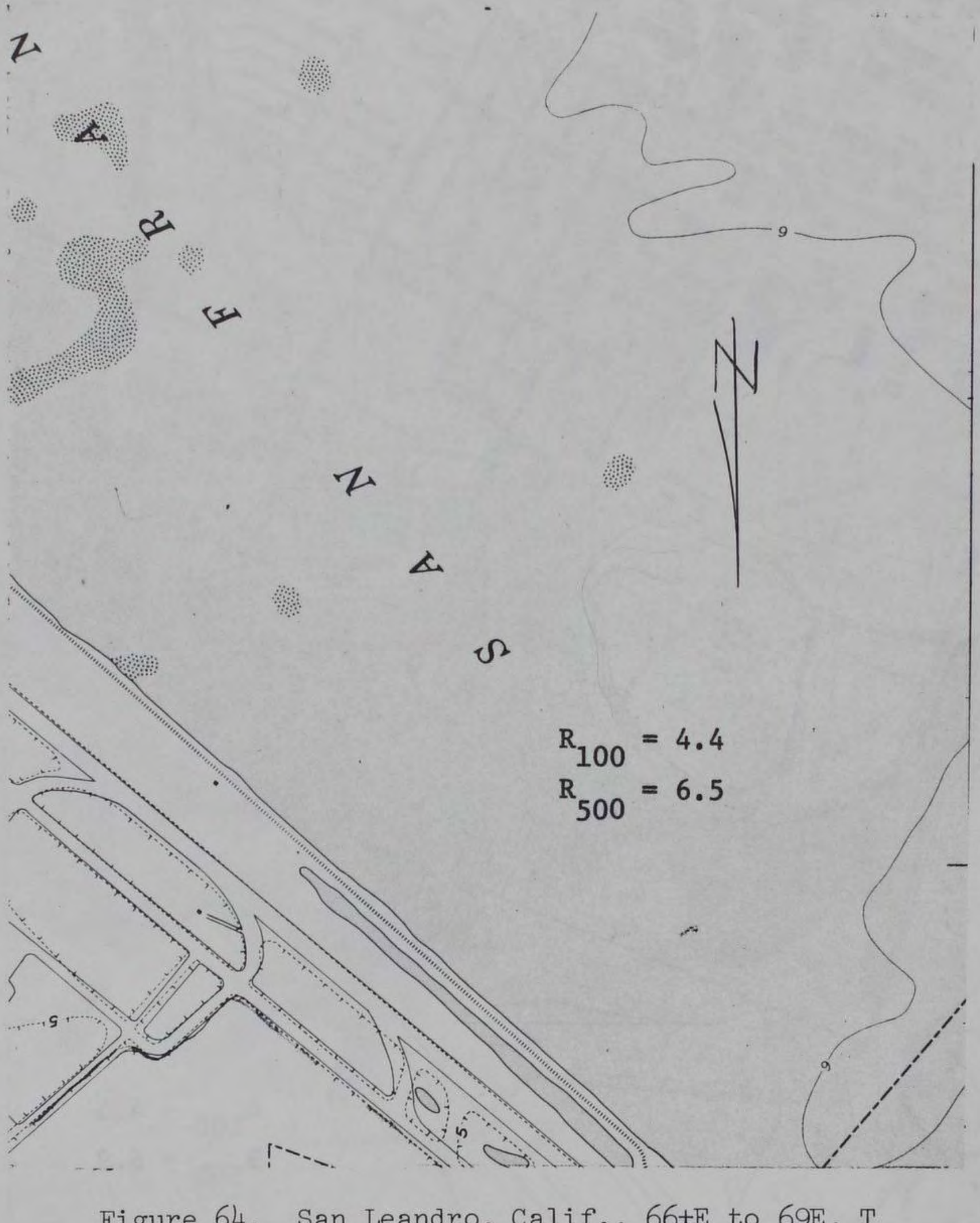

Figure 64. San Leandro, Calif., 66+E to 69E, T

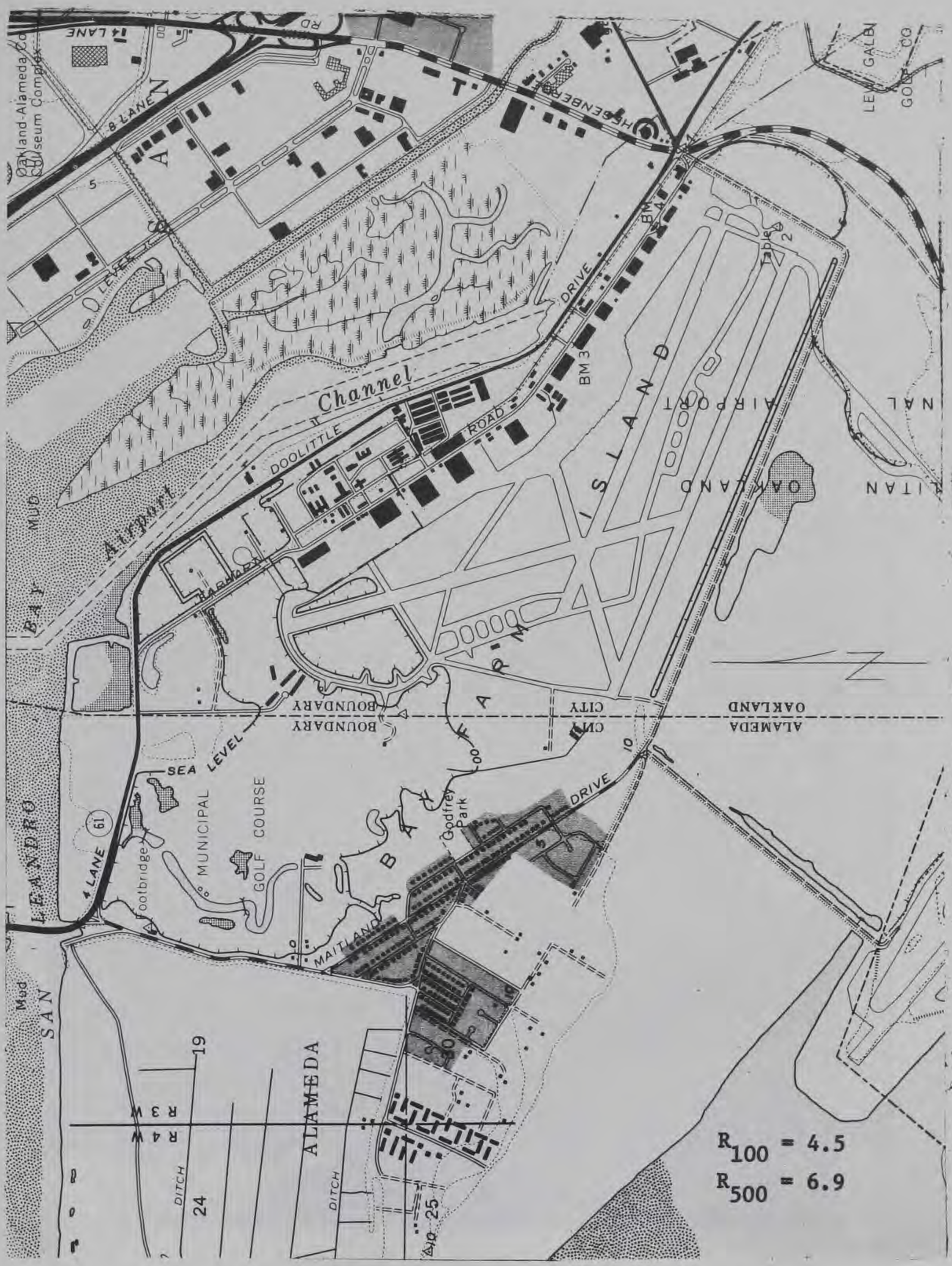

Figure 65. San Leandro, Calif., 66+E to 70+E, T

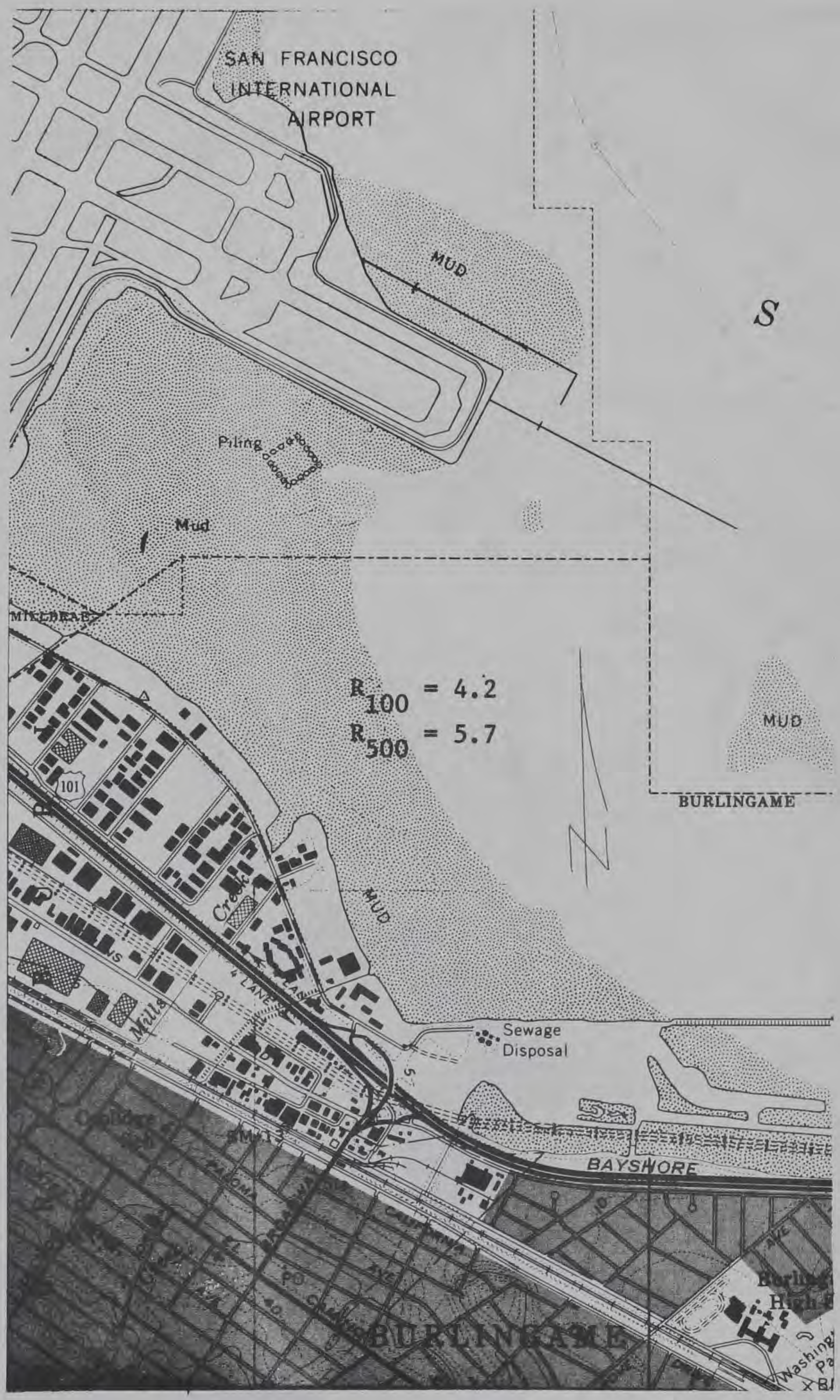

Figure 66. San Mateo, Calif., 59+N to 64+N, L

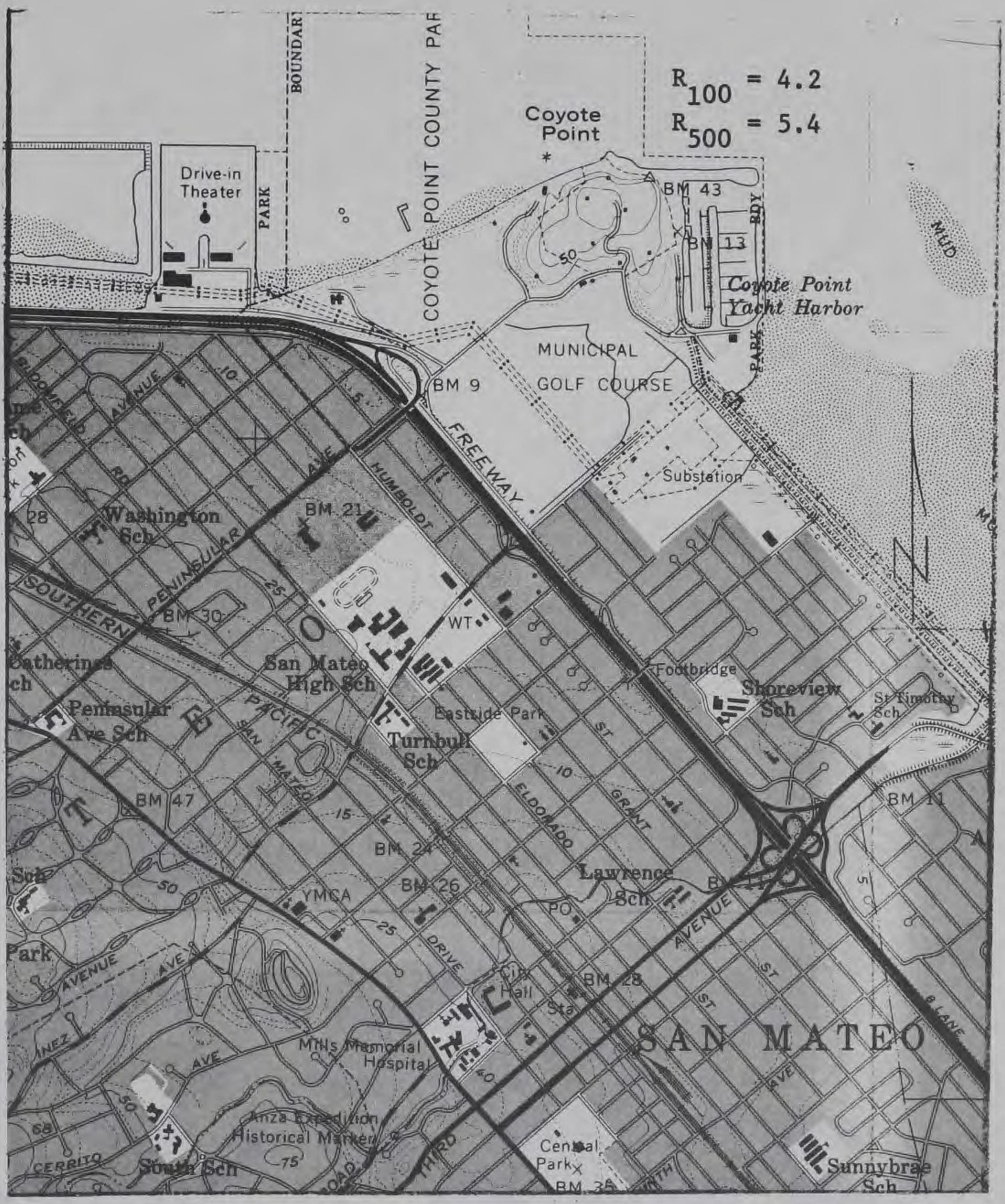

Figure 67. San Mateo, Calif., 58E to 61+E, T

Figure 68. San Mateo, Calif., 55+N to 59N, R

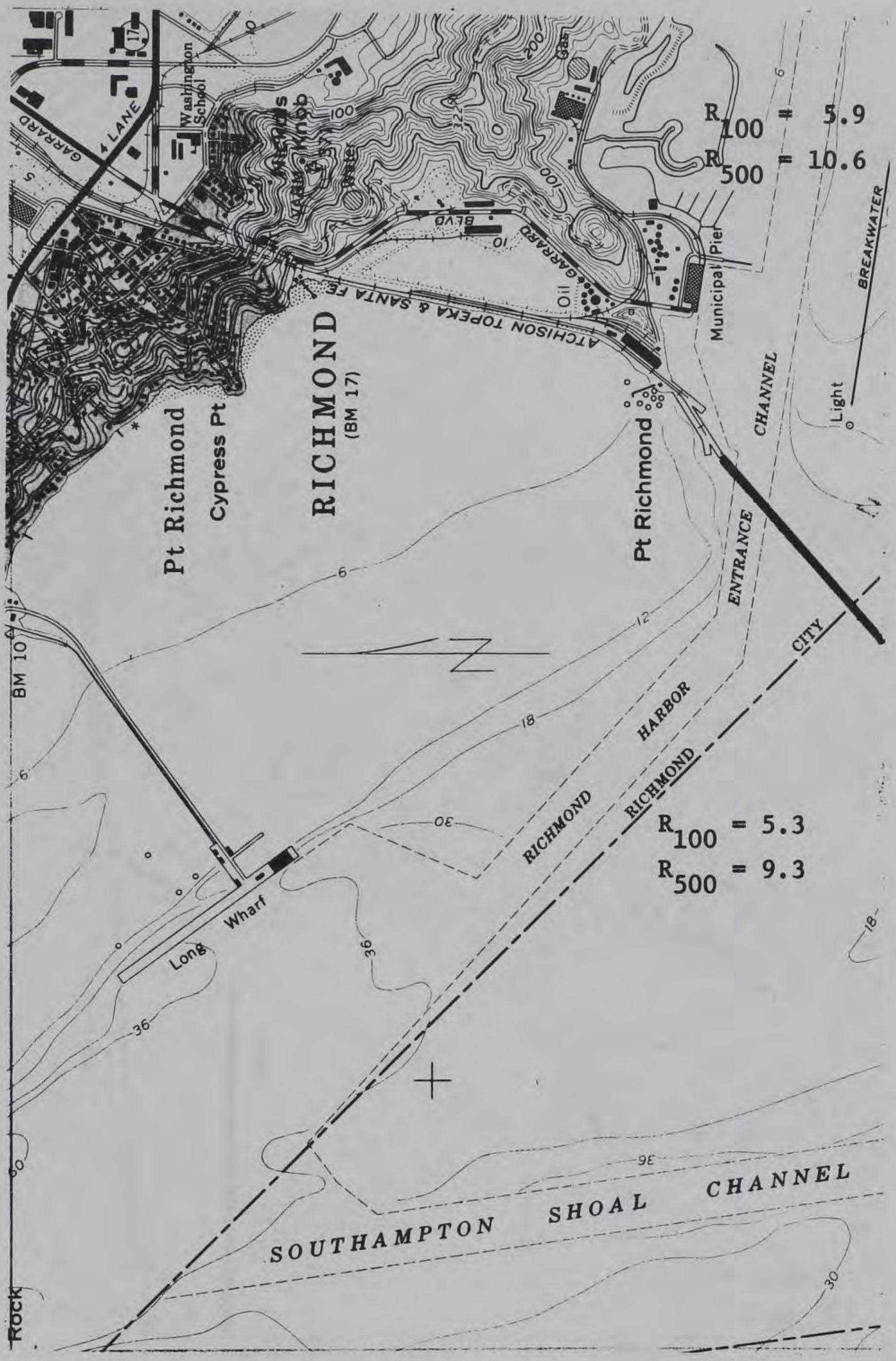

Figure 69. San Quentin, Calif., 95N to 98N, R

Figure 70. San Quentin, Calif., 98N to 01N, R

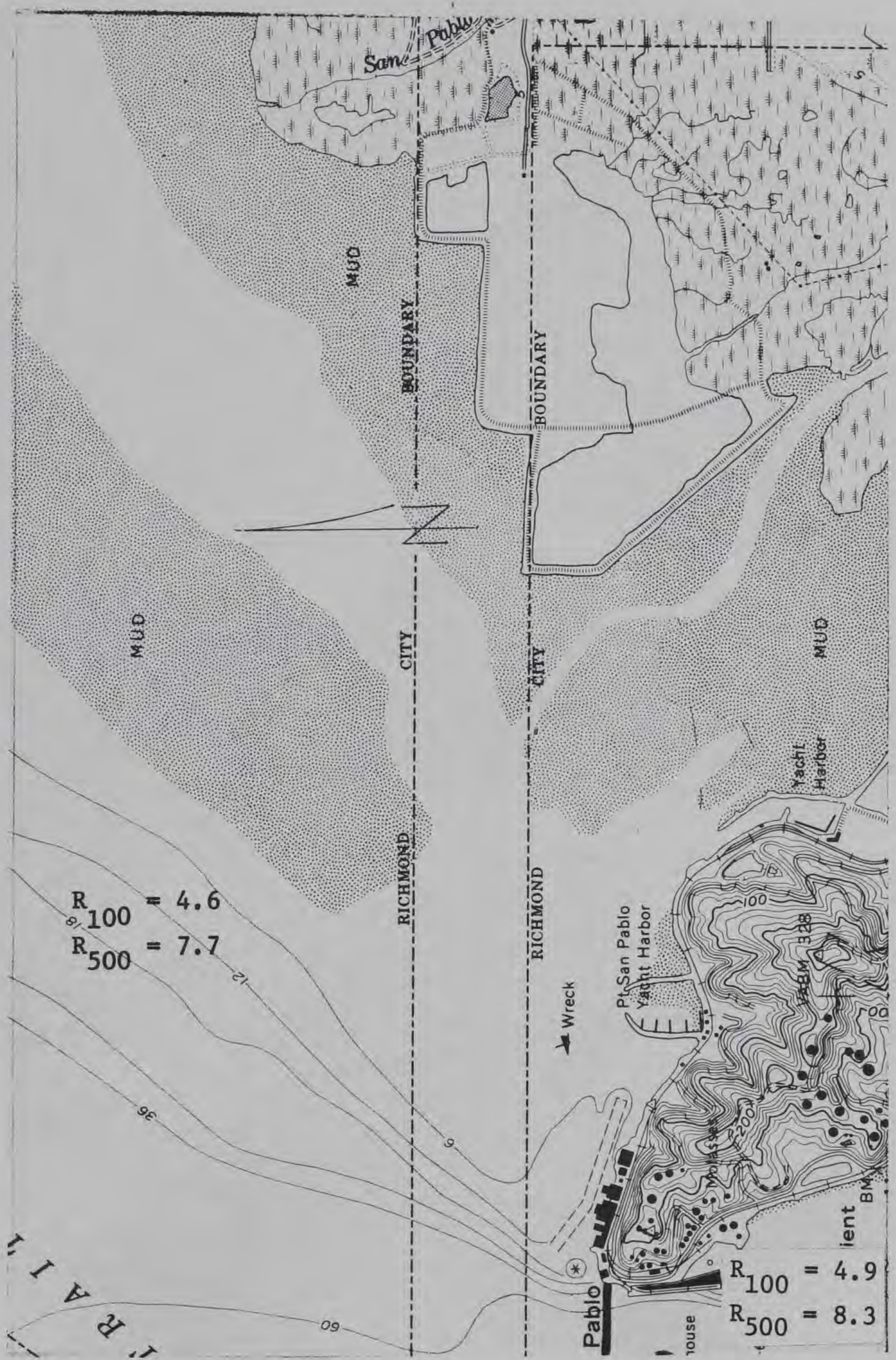

Figure 71. San Quentin, Calif., O1N to O4N, R

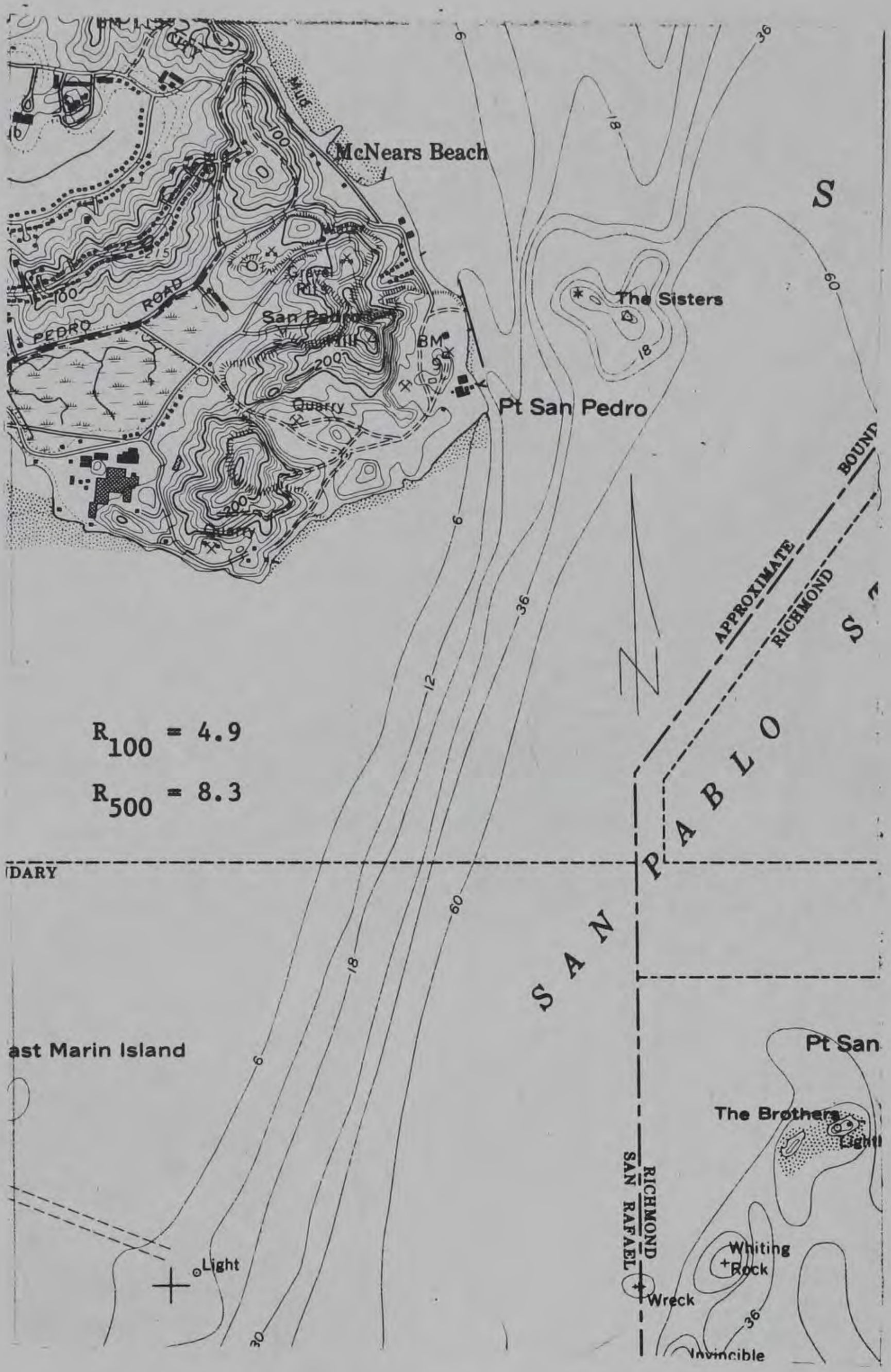

Figure 72. San Quentin, Calif., 47E to 50E, T

Figure 73. San Quentin, Calif., 44E to 47E, T

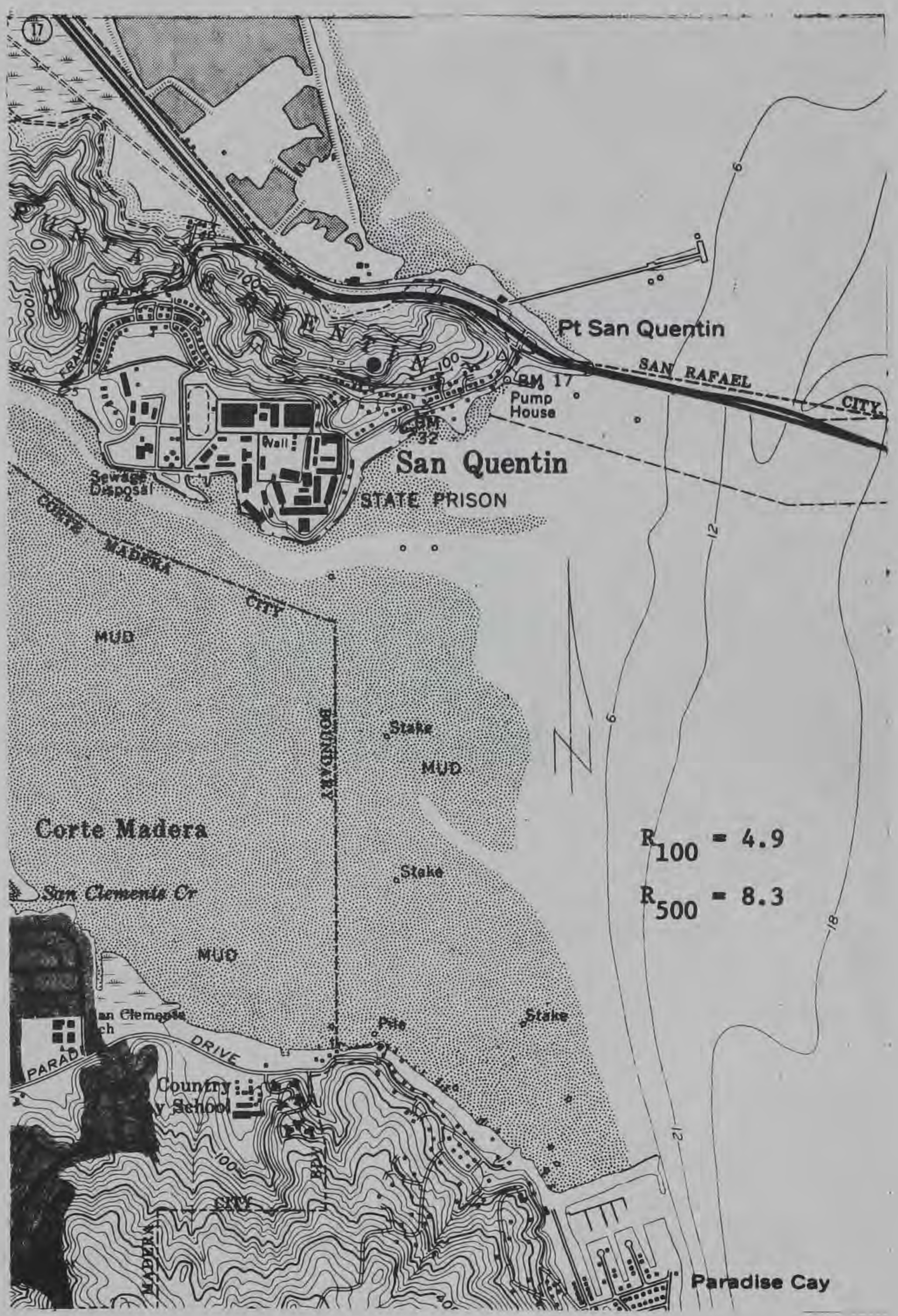

Figure 74. San Quentin, Calif., (41)96N to (42)00 N, L

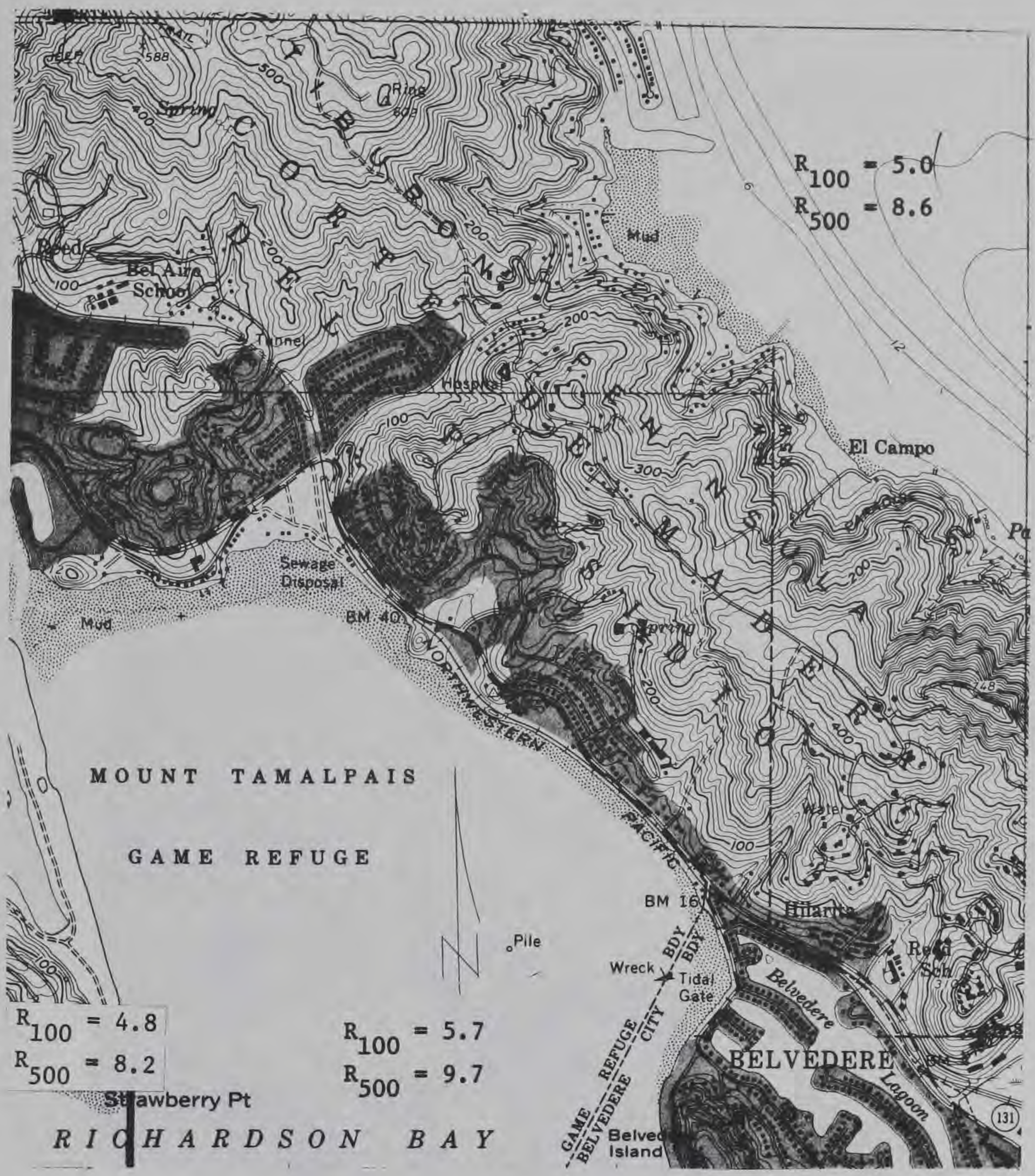

Figure 75. San Quentin, Calif., 94N to 96N, L

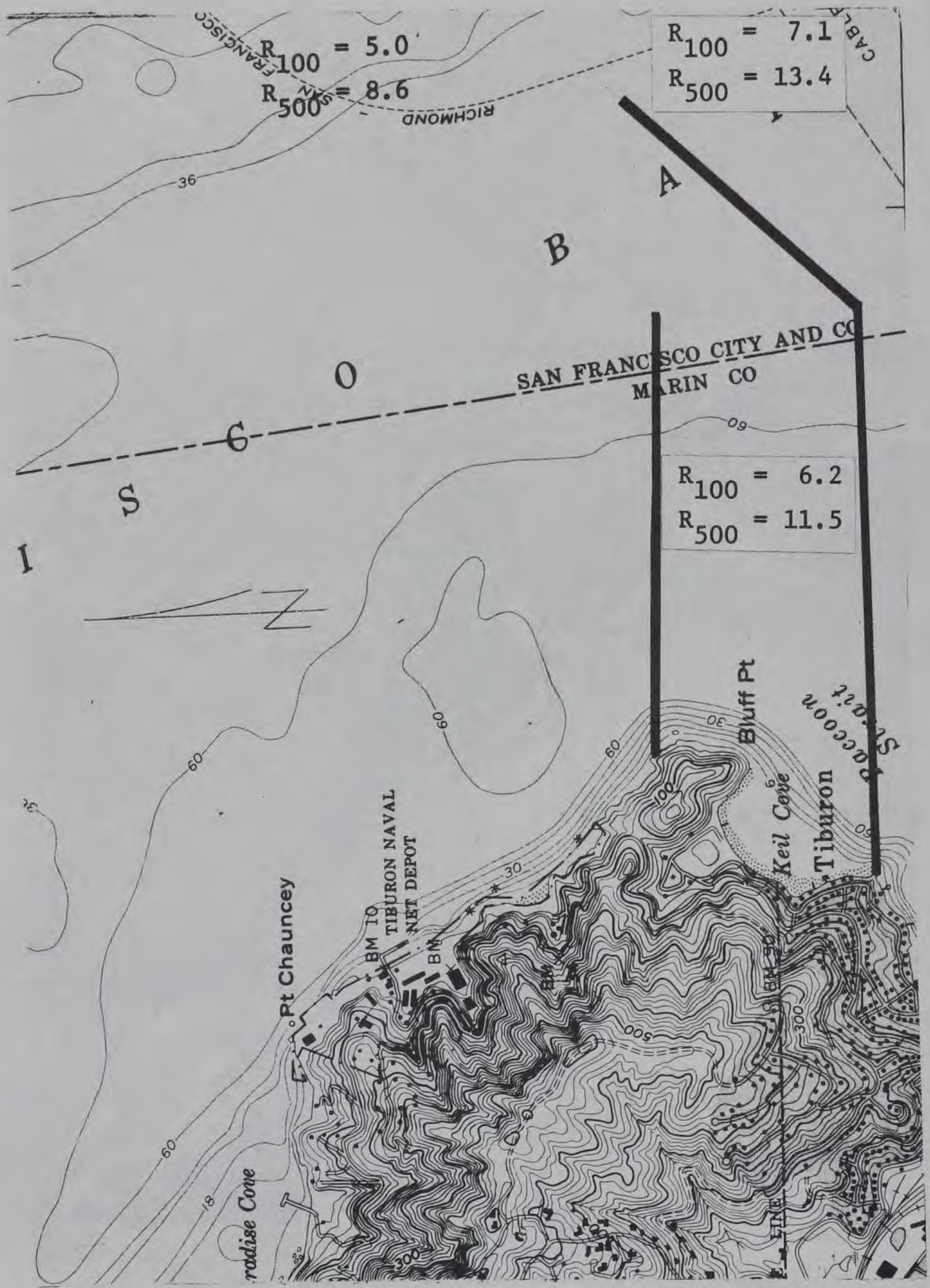

Figure 76. San Quentin, Calif., 91+N - 95N, R

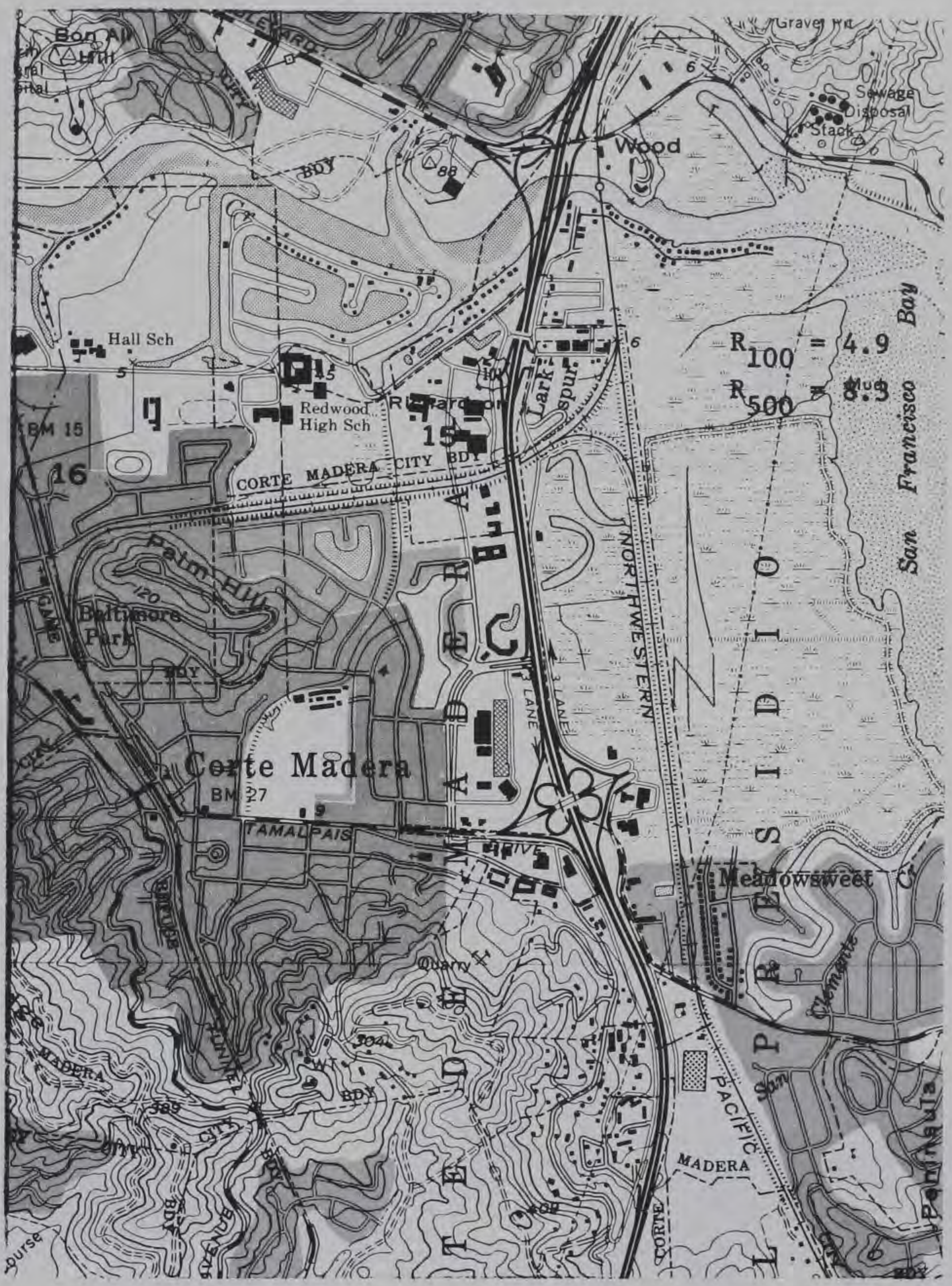

Figure 77. San Rafael, Calif. (41)96N to (42)00N, R

Figure 78. San Rafael, Calif., 92N to 95N, R

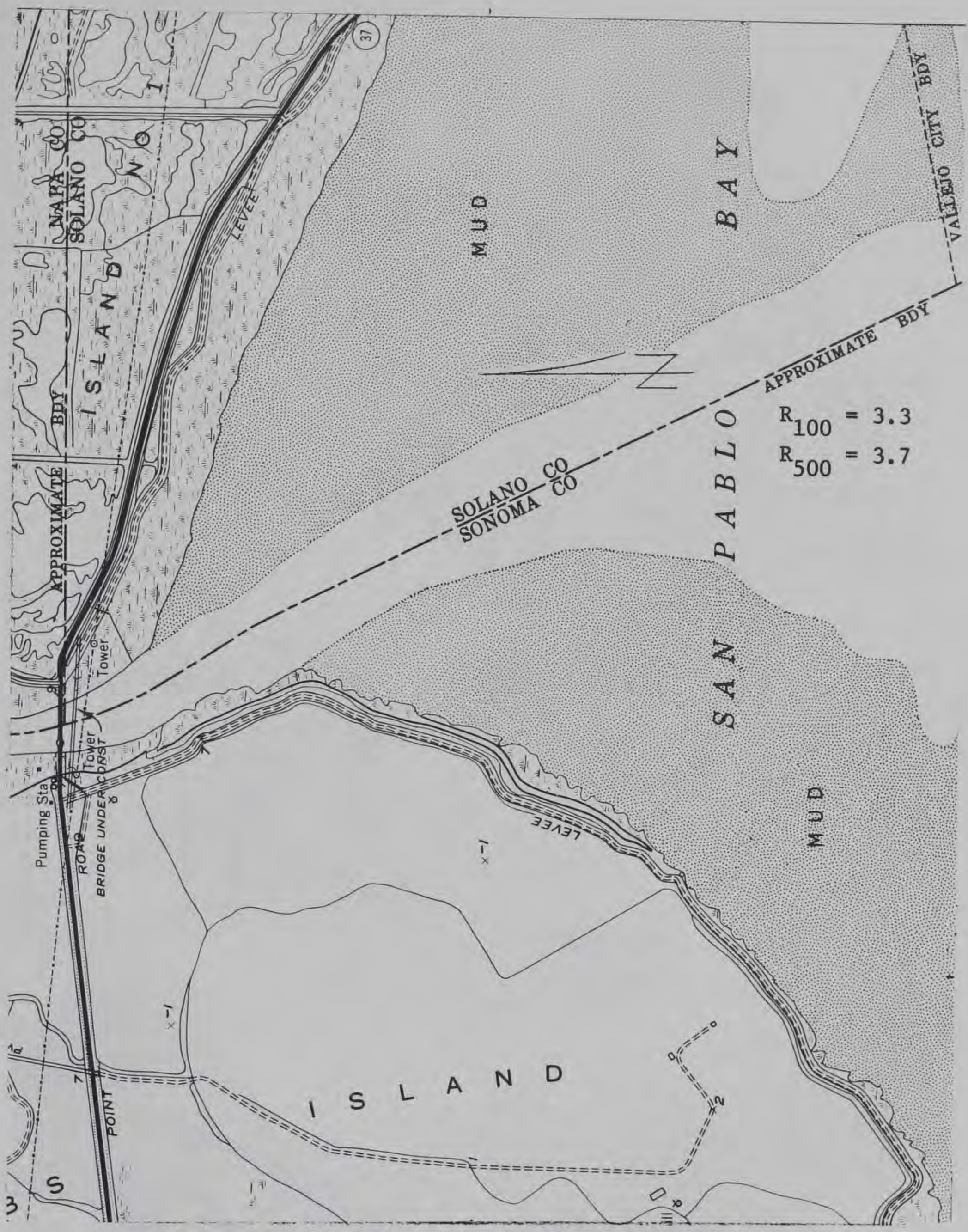

Figure 79. Sears Point, Calif., 50E to 54+E, B

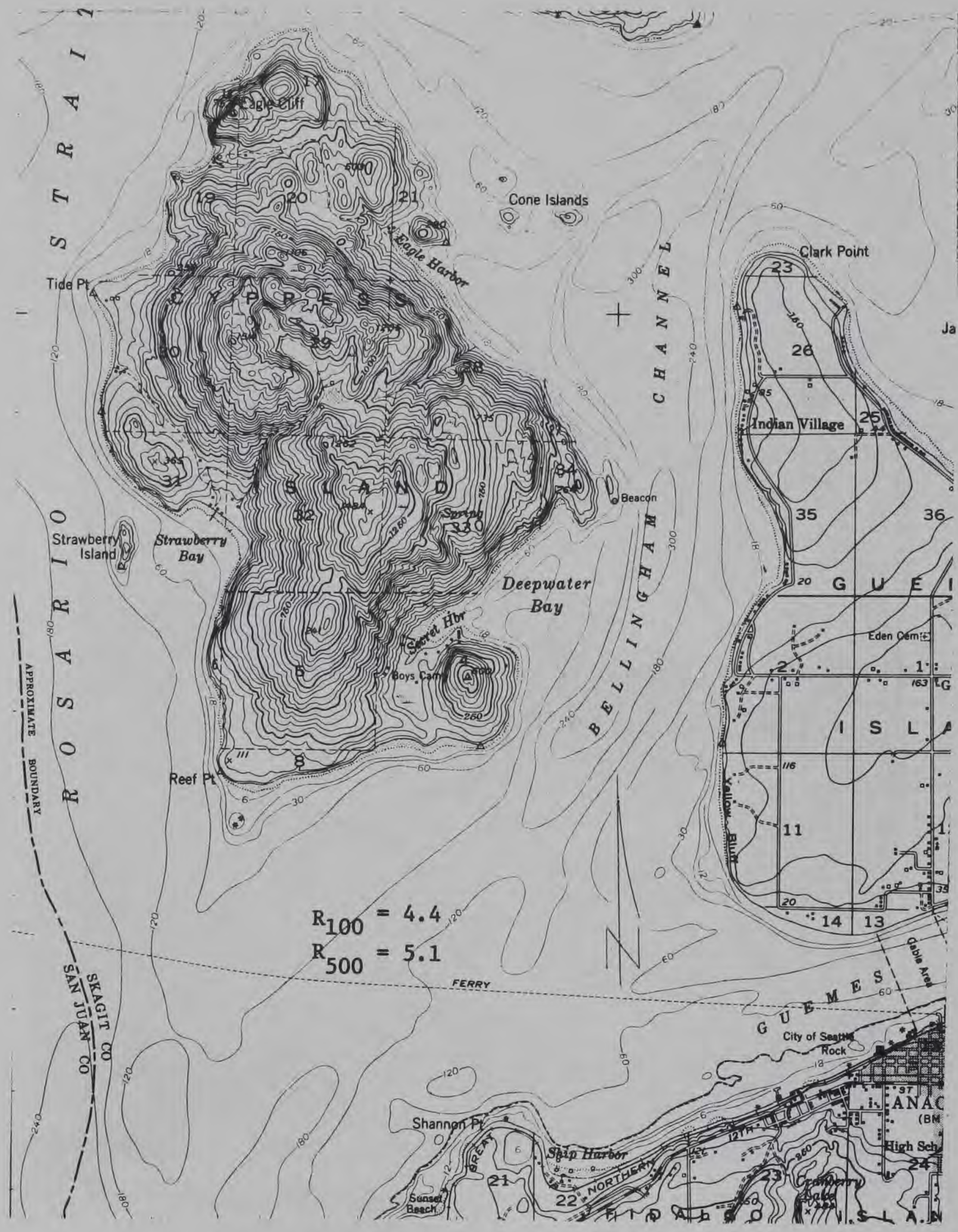

Figure 80. Anacortes, Wash., 71+N to 84N, L (1:62500)

Figure 81. Anacortes, Wash., 72+N to 84N, R (1:62500)

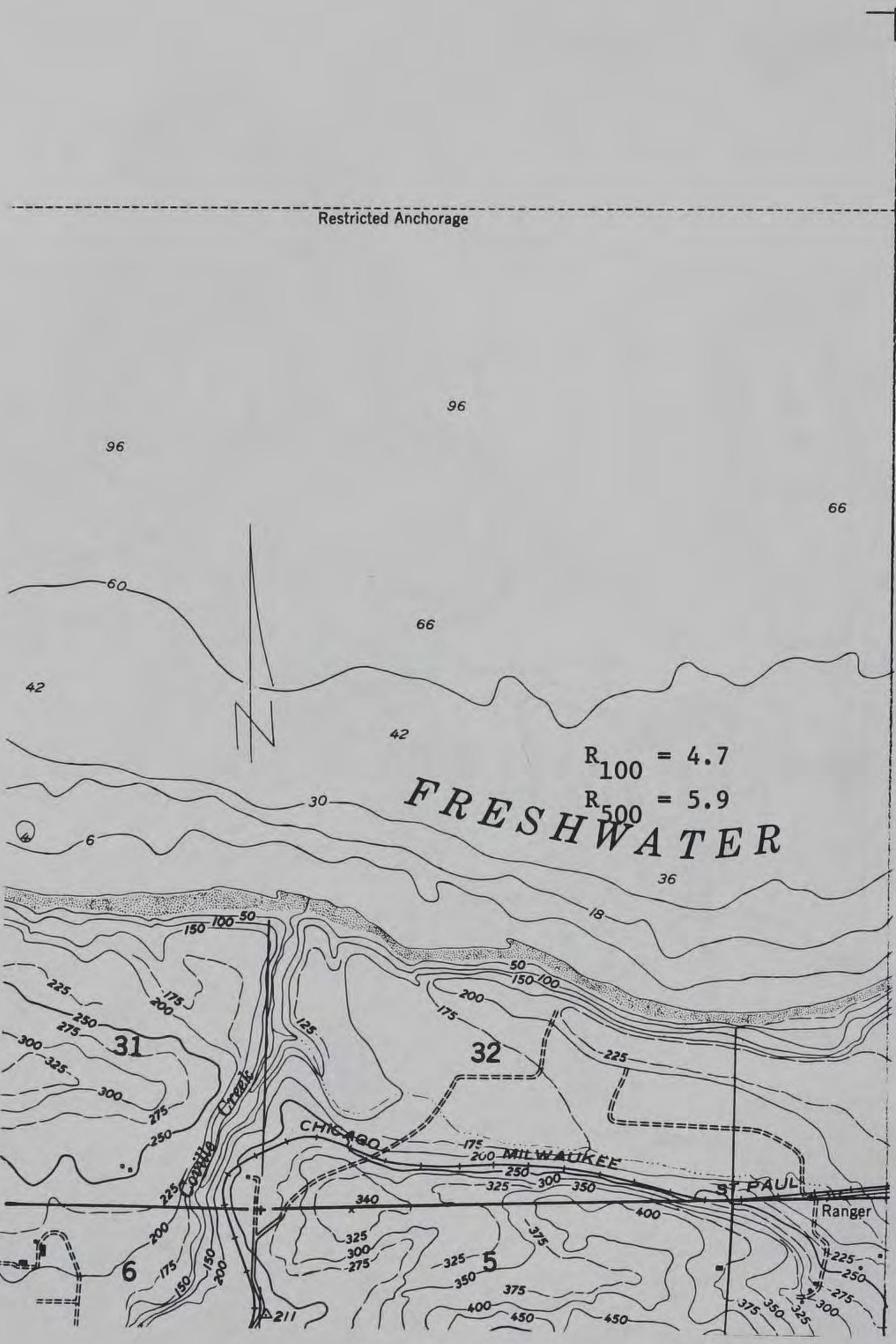

Figure 82. Angeles Point, Wash., 123°37'30" W to 123°37'55" W, B

Figure 83. Angeles Point, Wash., 123°35'00" W to 123°32'30" W, B

Figure 84. Angeles Point, Wash., 123°31'30" W to 123°30' W, B

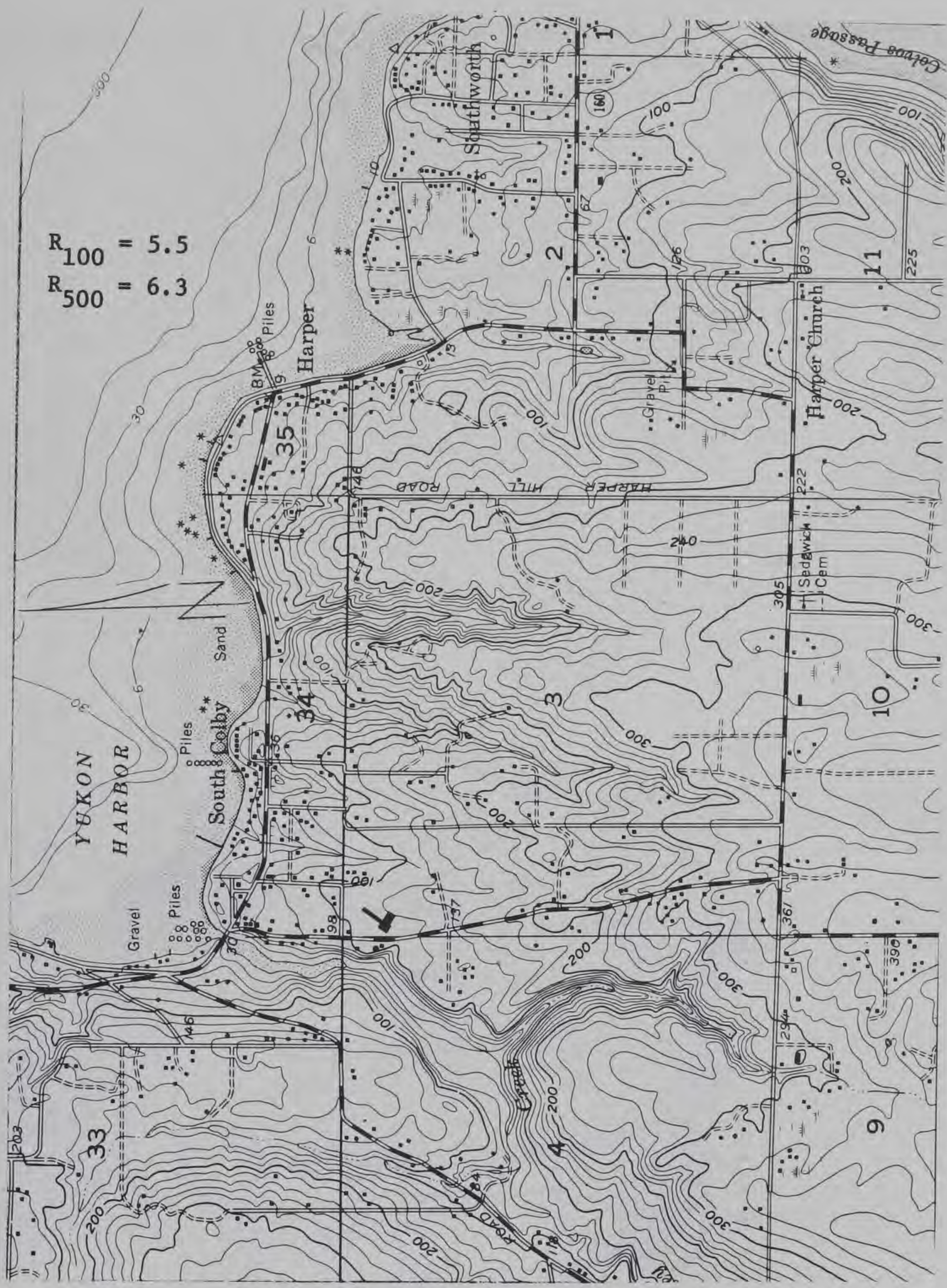

Figure 85. Bremerton East, Wash., 33E to 37+E, B

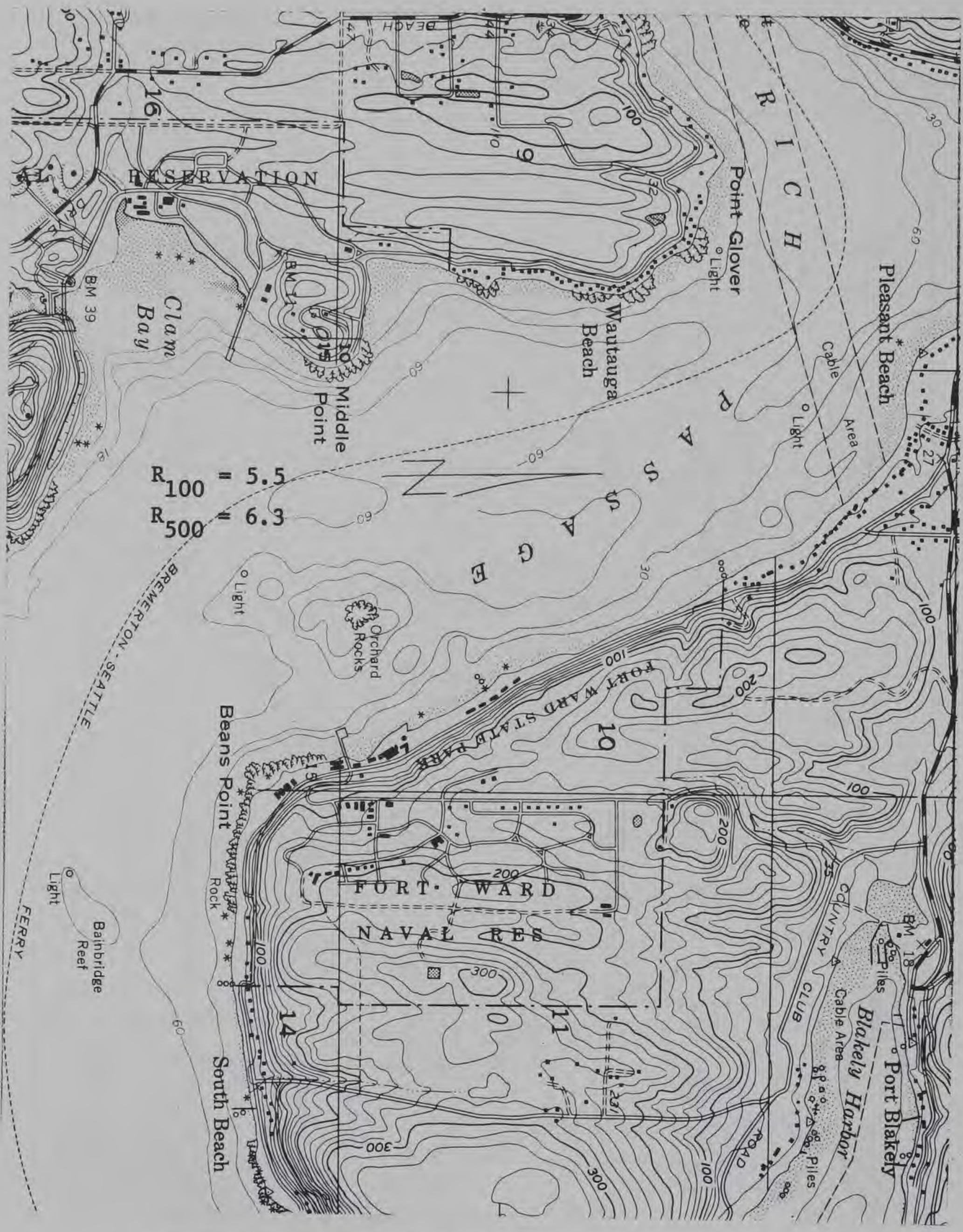

Figure 86. Bremerton East, Wash., 68N to 71+N, R

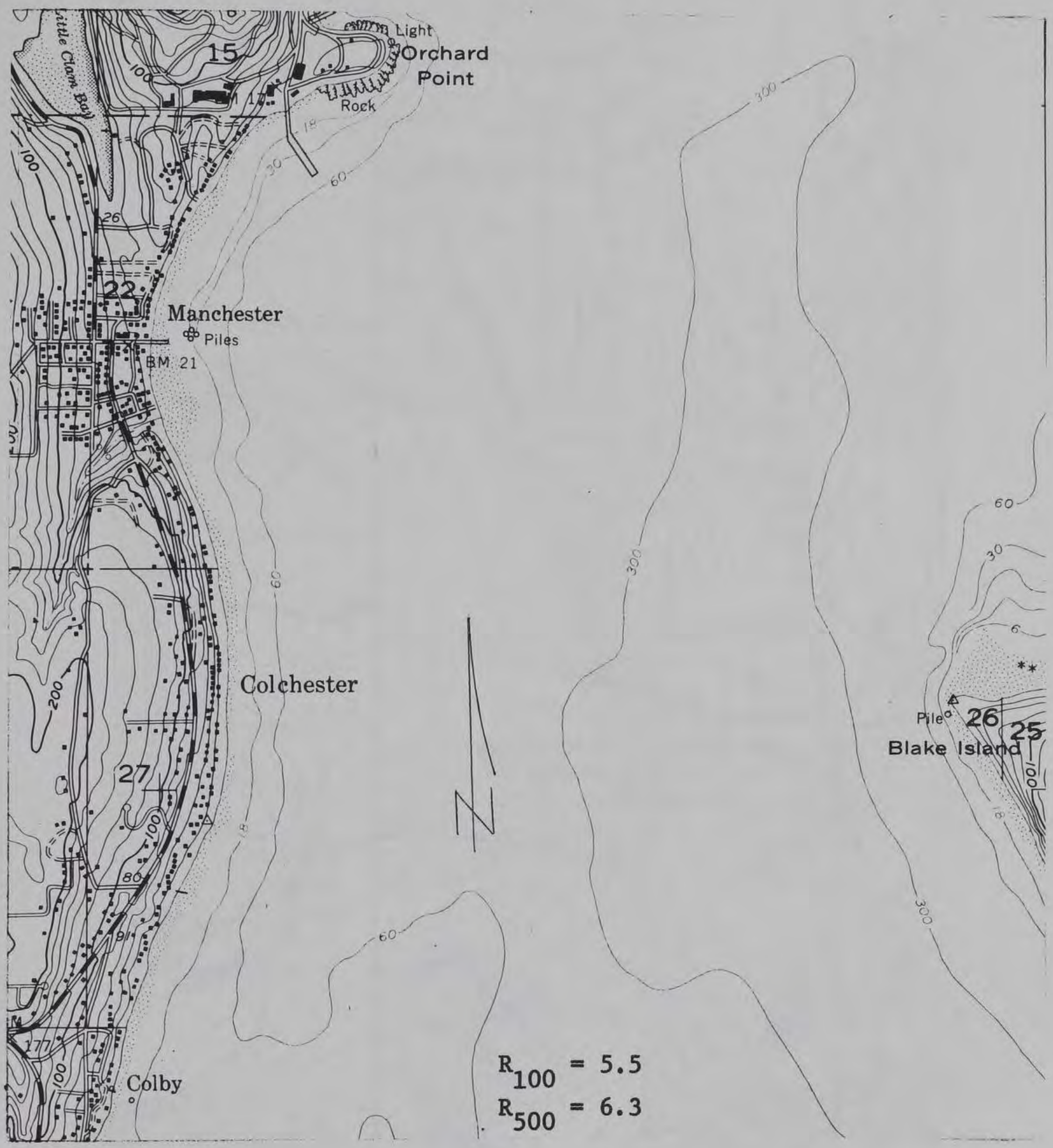

Figure 87. Bremerton East, Wash., 64N to 68N, R

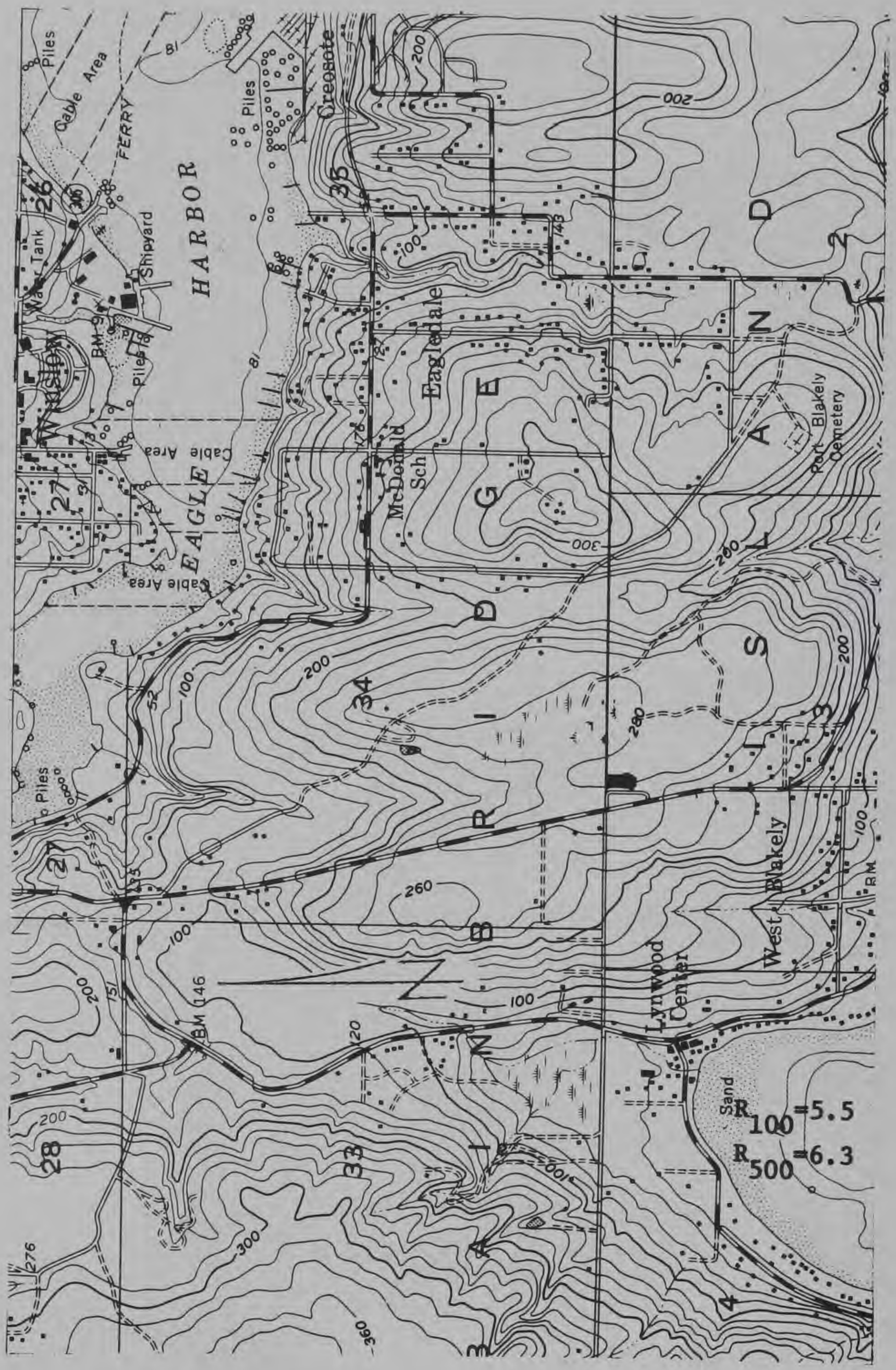

Figure 88. Bremerton East, Wash., 33E to 37+E, T

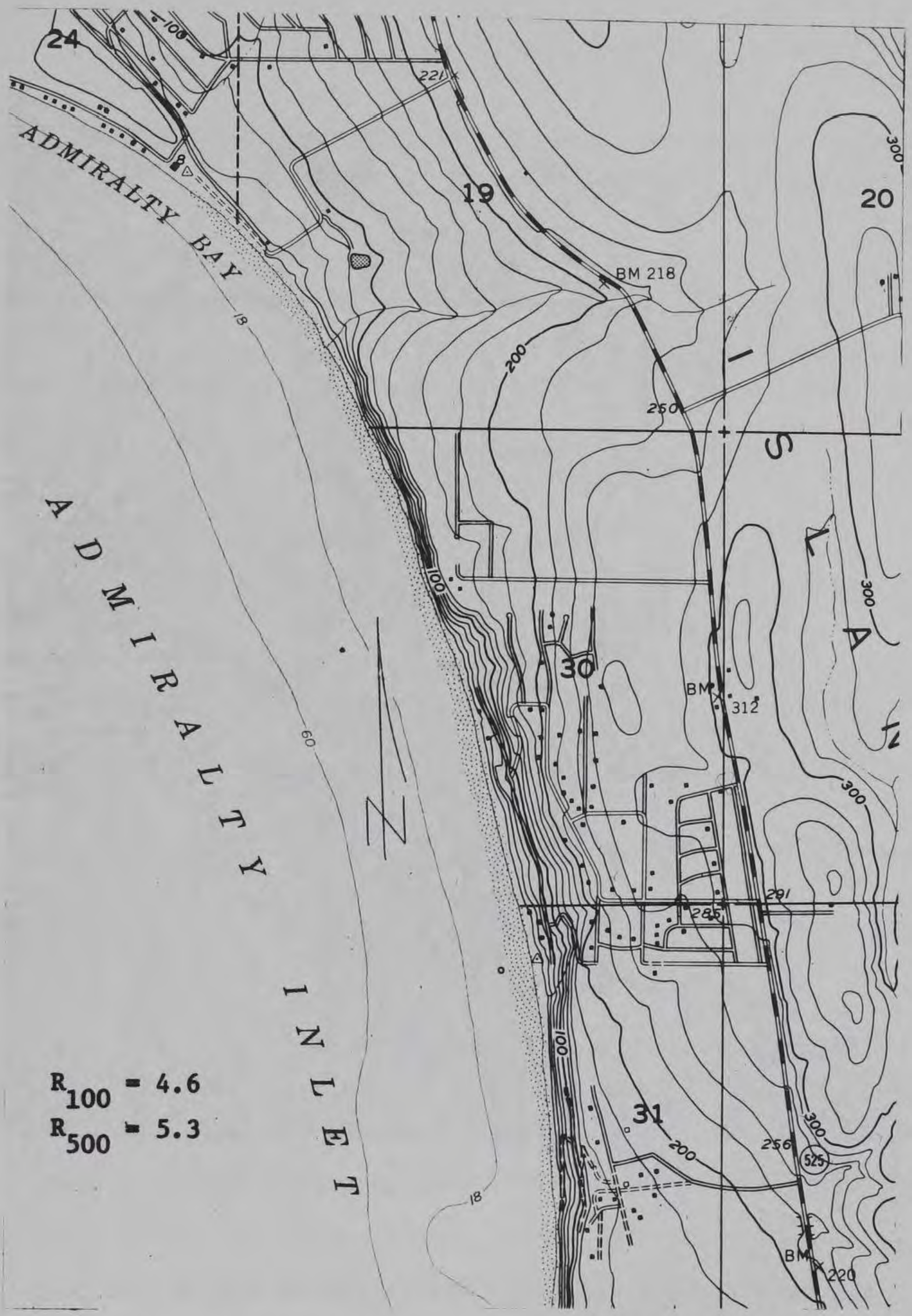

Figure 89. Camano, Wash., 27+E to 31E, B

Figure 90. Cape Flattery, Wash., 55N to 64N, L (1:62500)

Figure 91. Cape Flattery, Wash., 54+N to 63+N, R (1:62500)

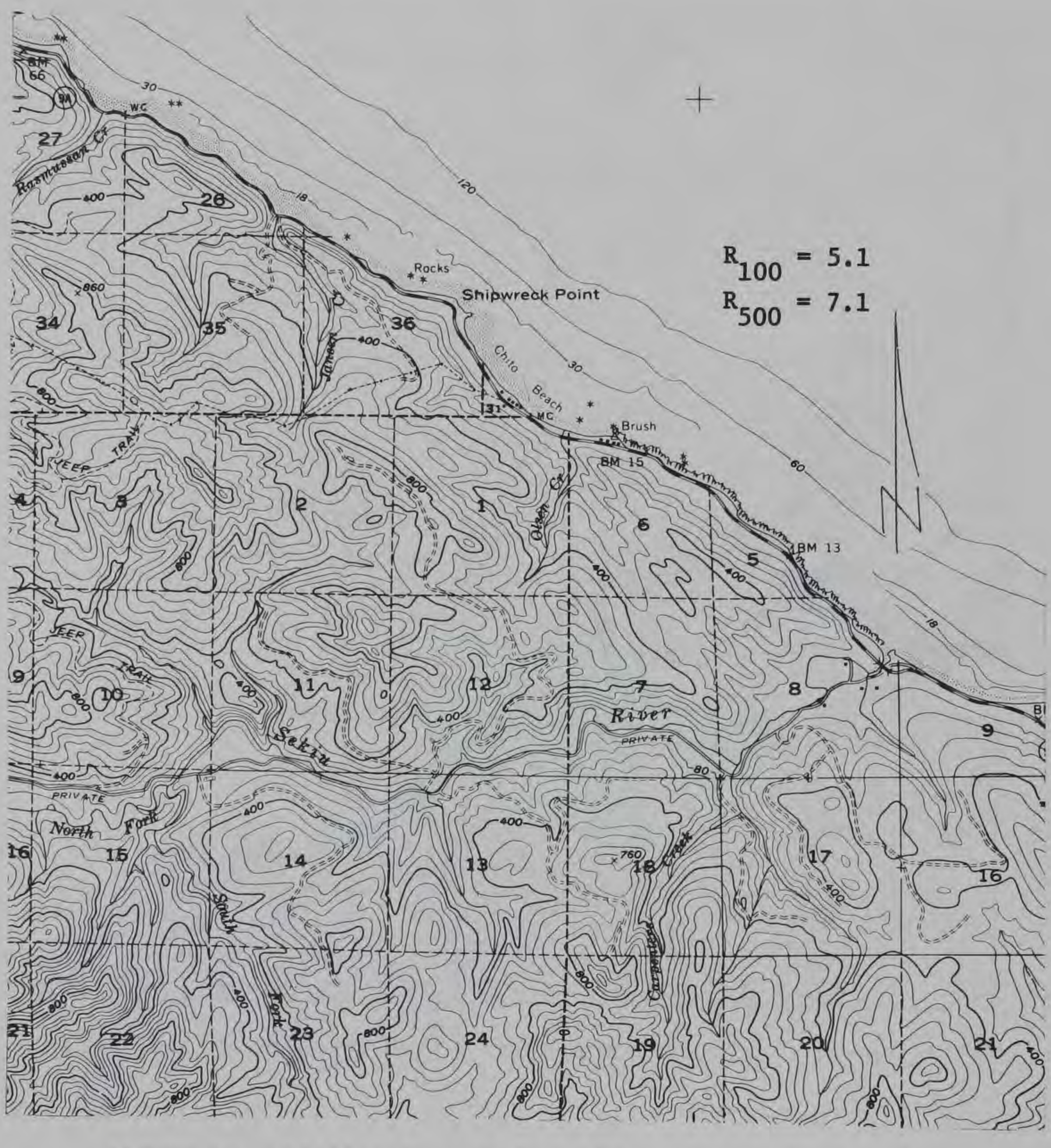

Figure 92. Clallam Bay, Wash., 45N to 55N, L (1:62500)

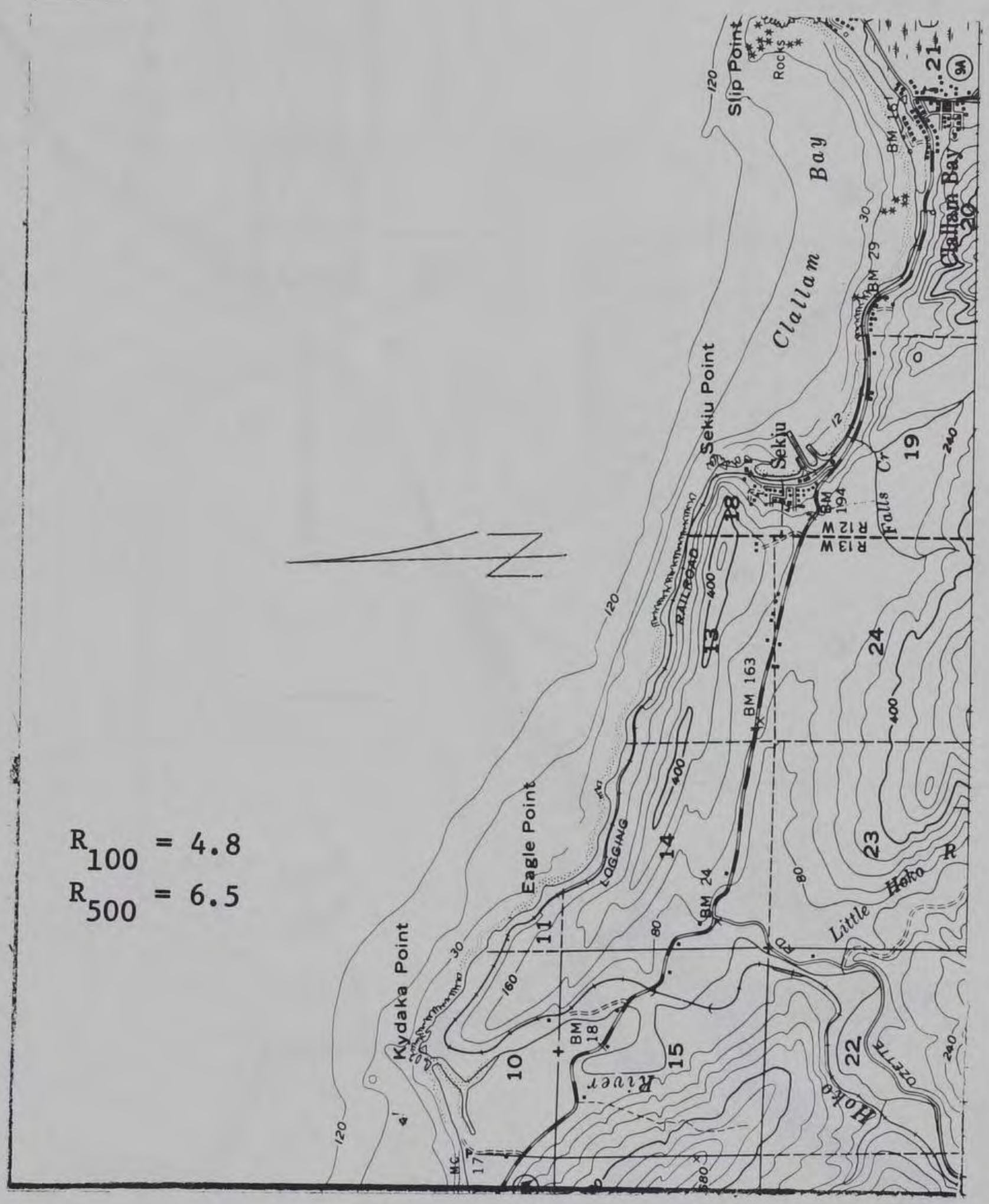

$R_{100} = 4.8$

$R_{500} = 6.5$

Figure 93. Clallam Bay, Wash., 44+N to 52N (1:62500)

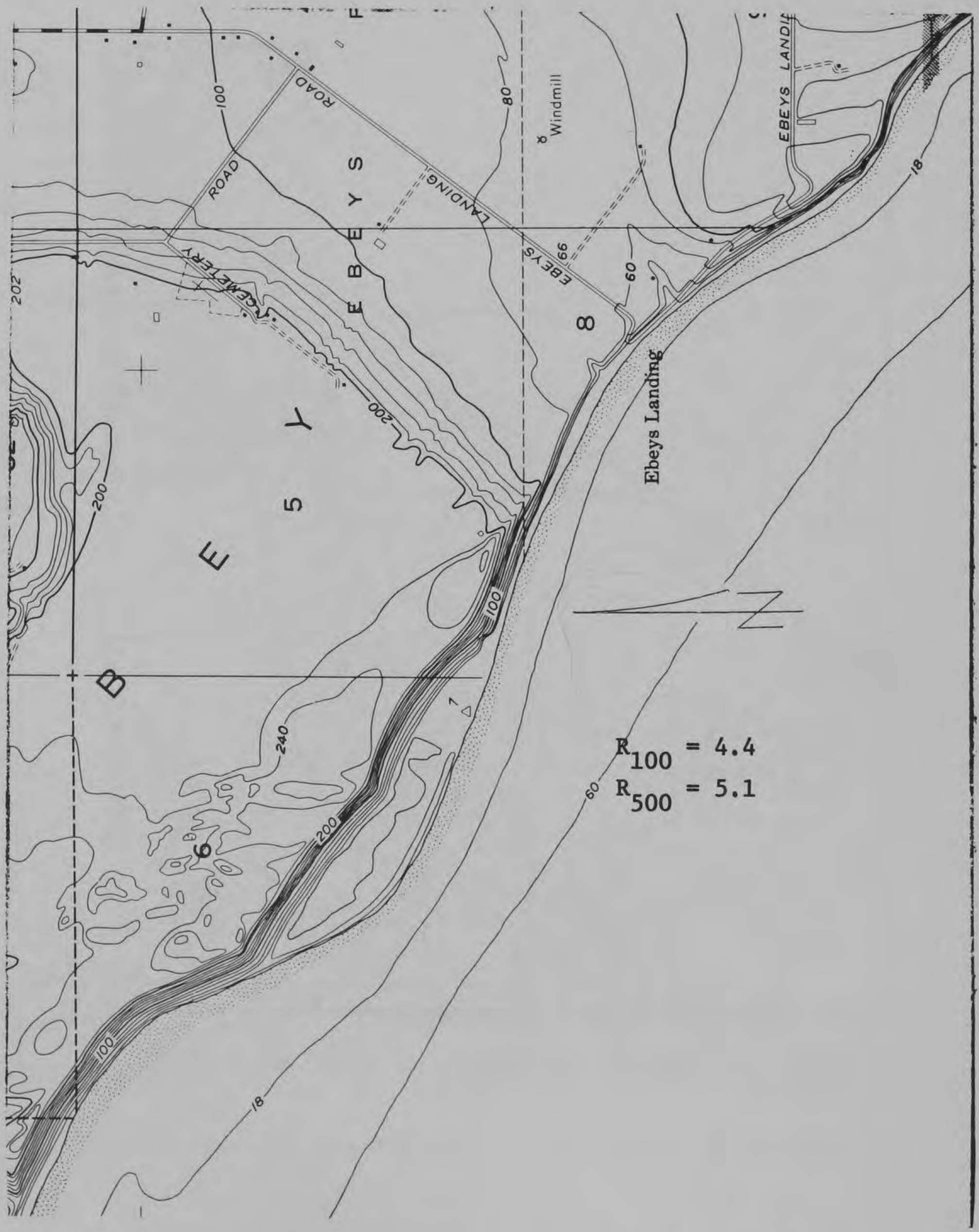

Figure 94. Coupeville, Wash., 18+E to 23E, B

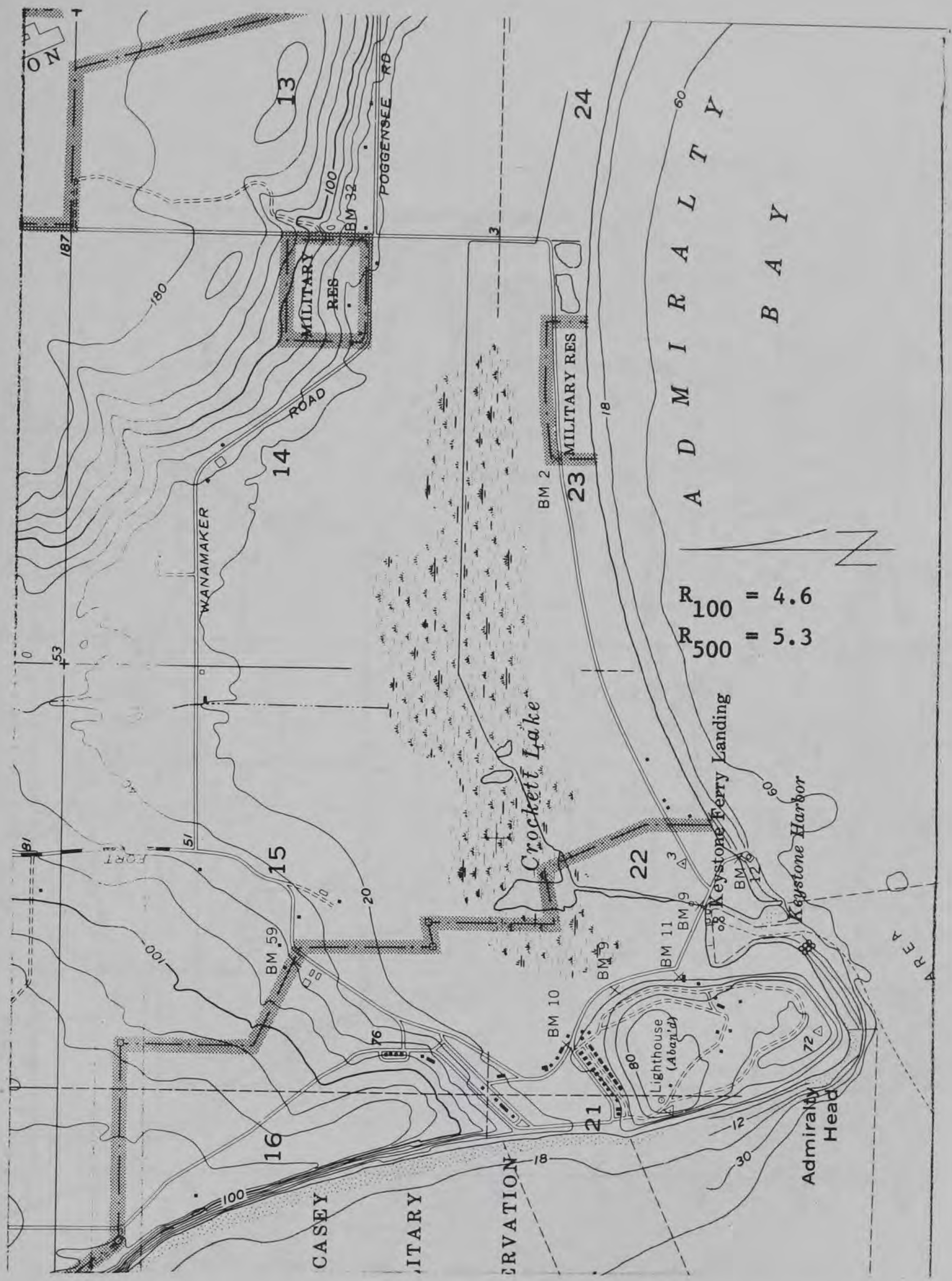

Figure 95. Coupeville, Wash., 33N to 36N, R

Figure 96. Deception Pass, Wash., 44N to 53+N, L (1:62500)

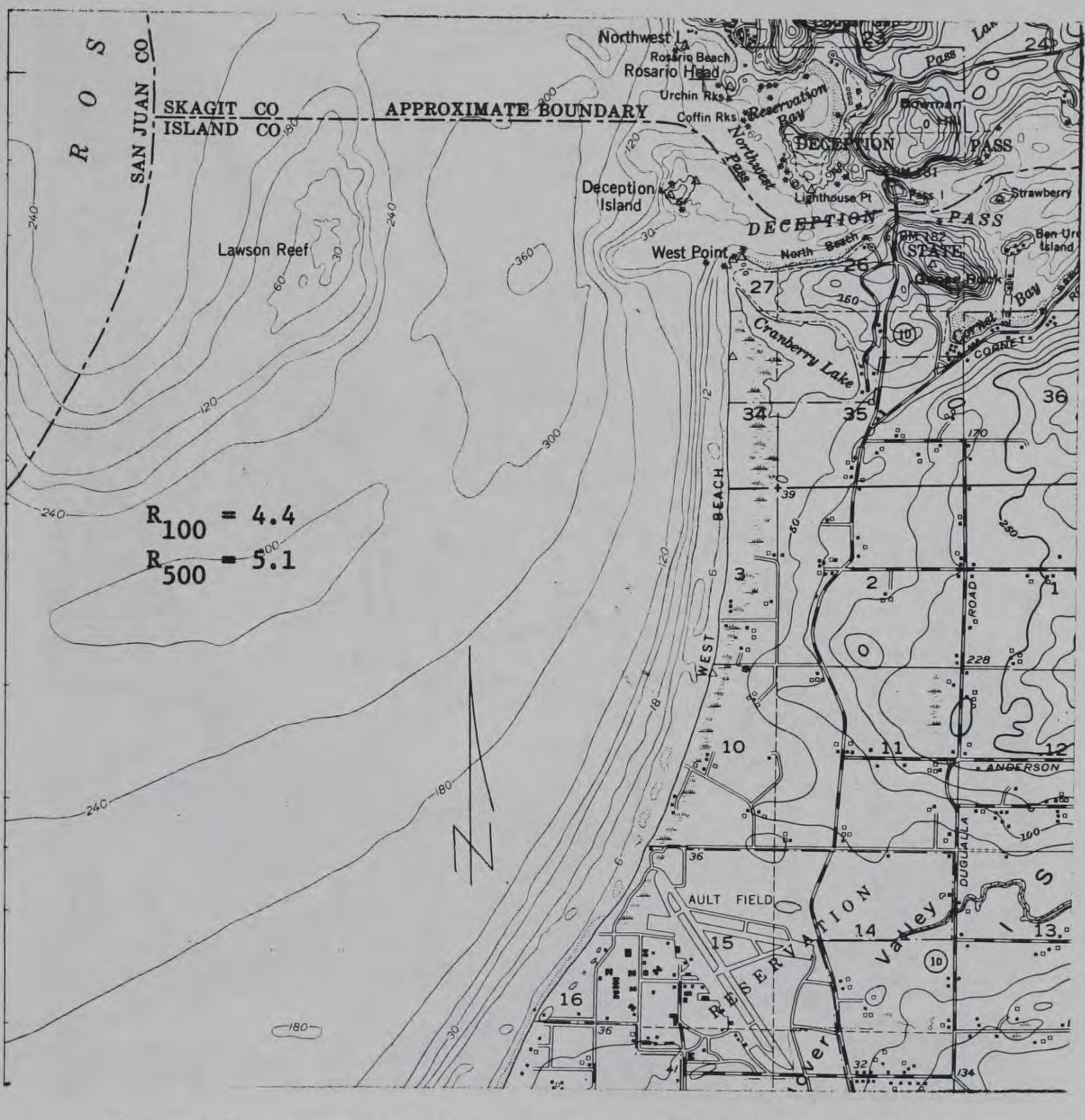

Figure 97. Deception Pass, Wash., 53+N to 63N, L (1:62500)

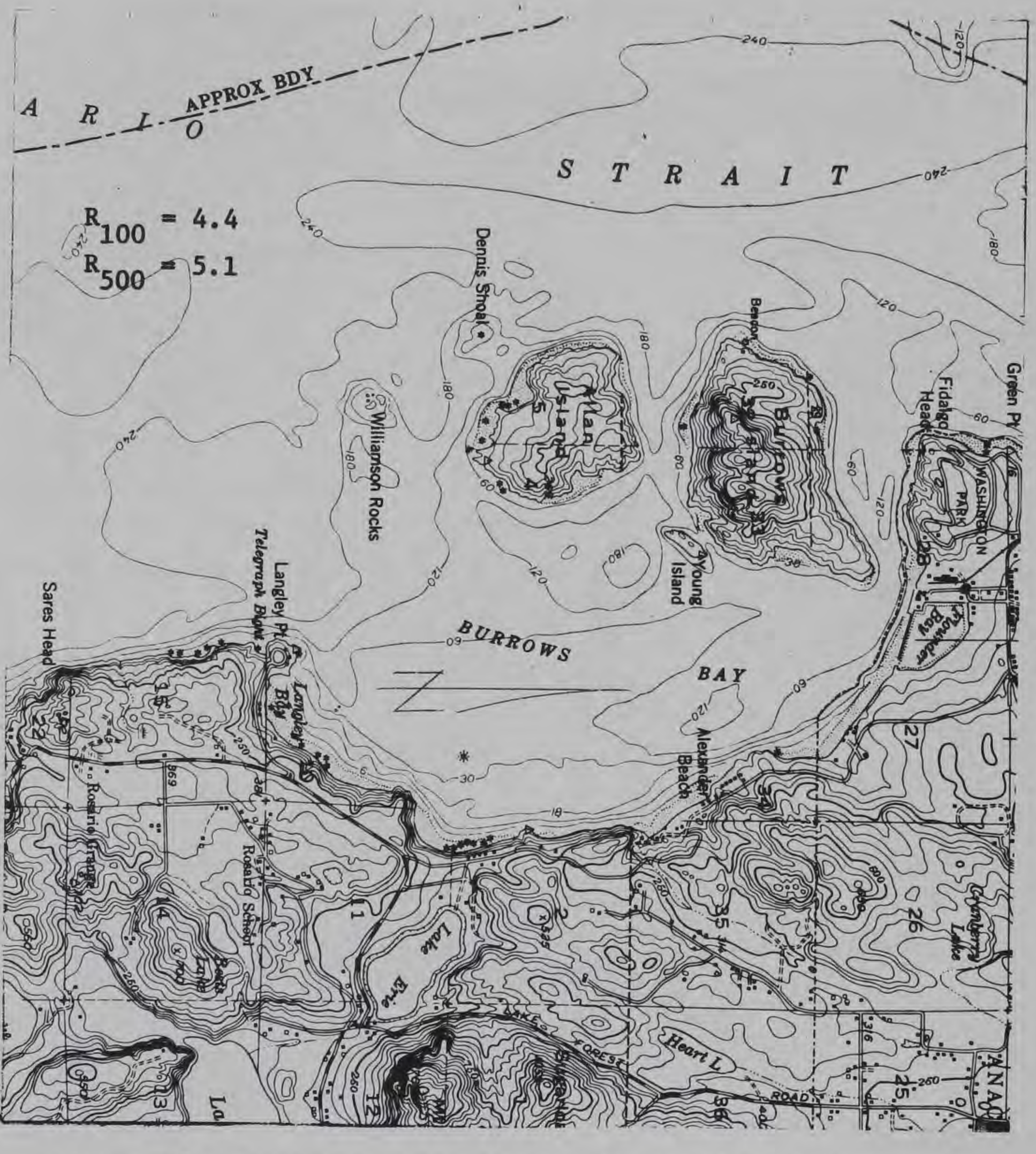

Figure 98. Deception Pass, Wash., 63N to 71+N, L (1:62500)

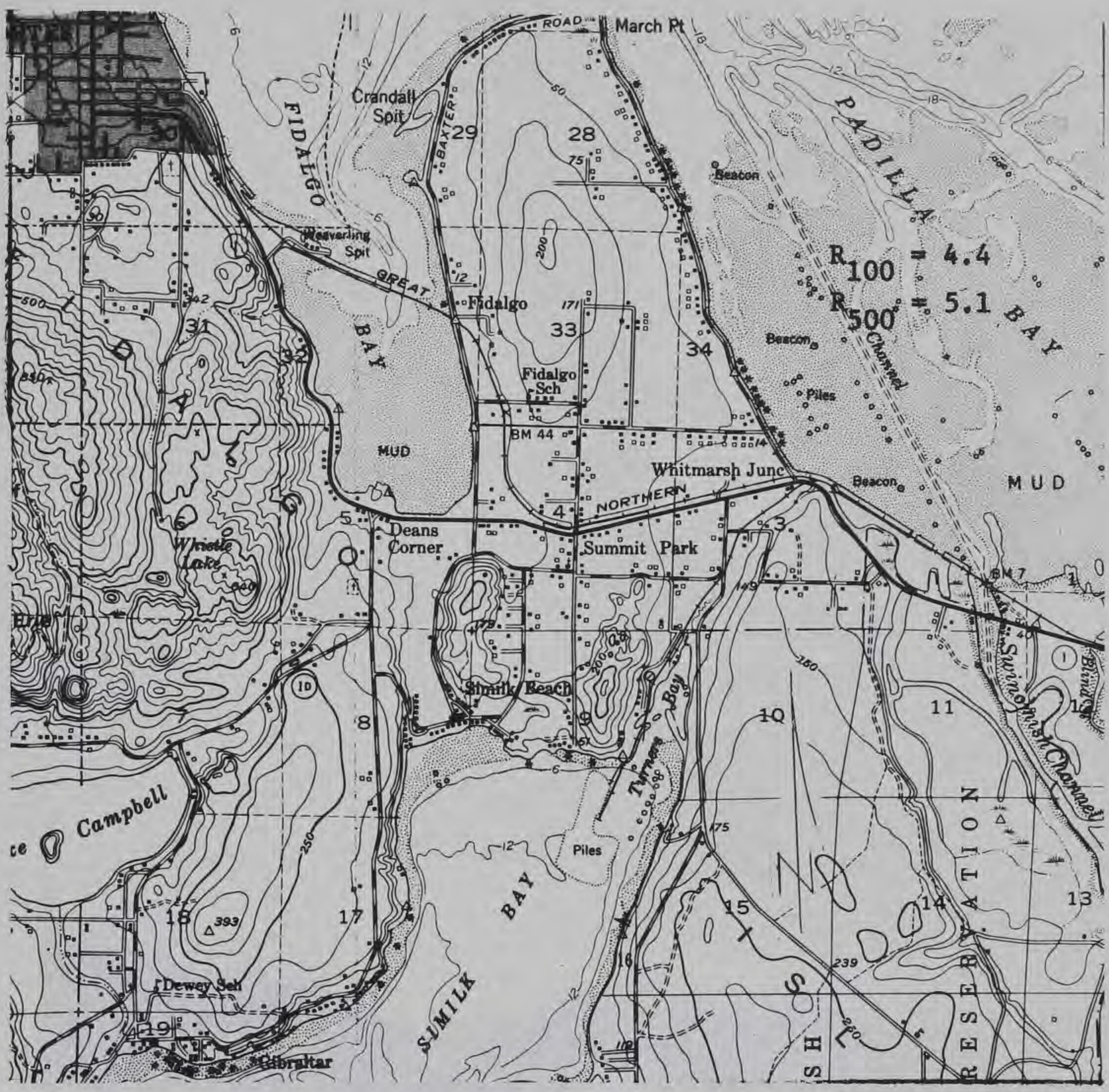

Figure 99. Deception Pass, Wash., 63N to 71+N, L (1:62500)

MAURY ISLAND

3: Robinson Point

$R_{100} = 5.7$

$R_{500} = 6.5$

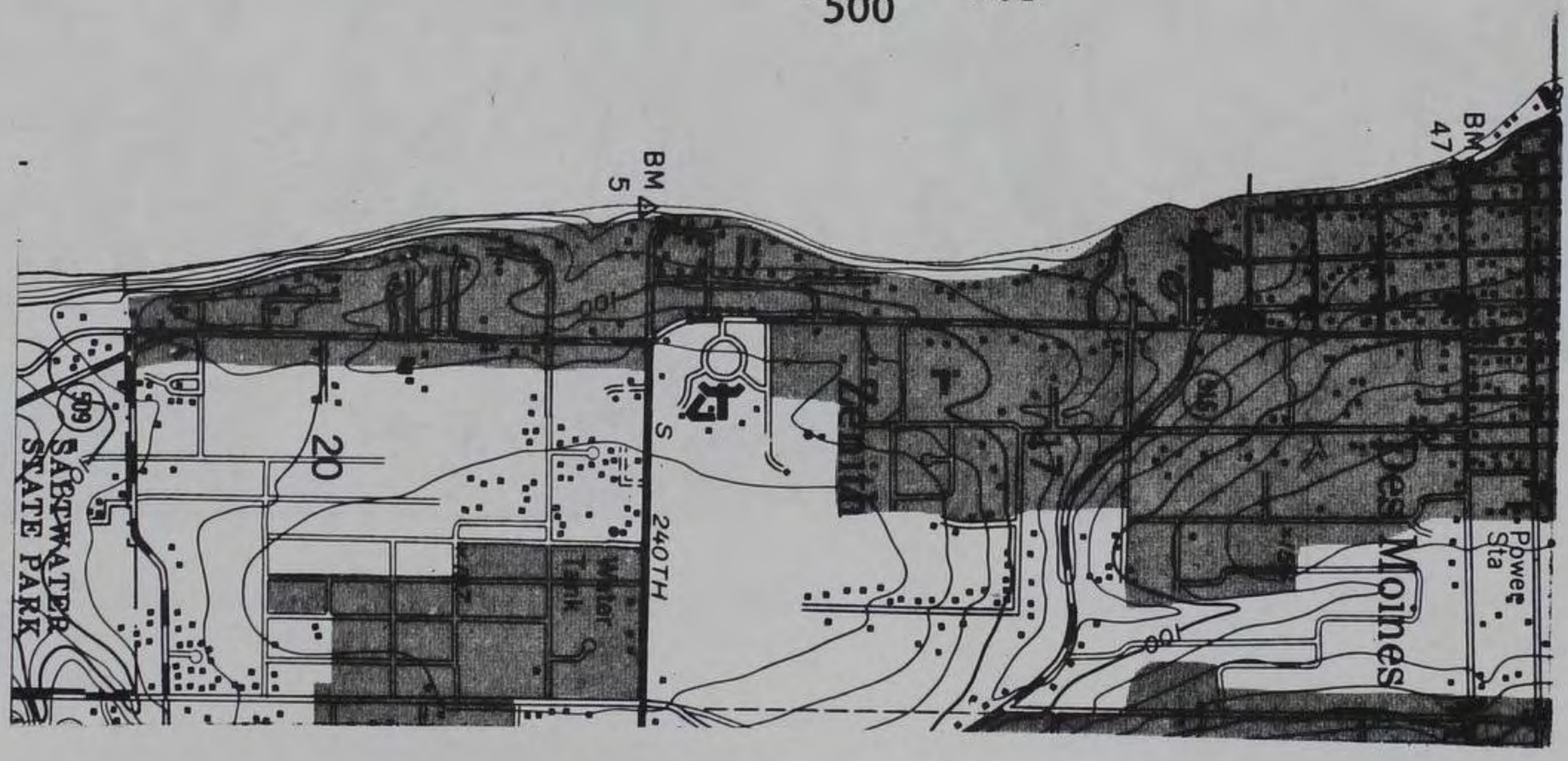

Figure 100. Des Moines, Wash., 47-N to 50N, L

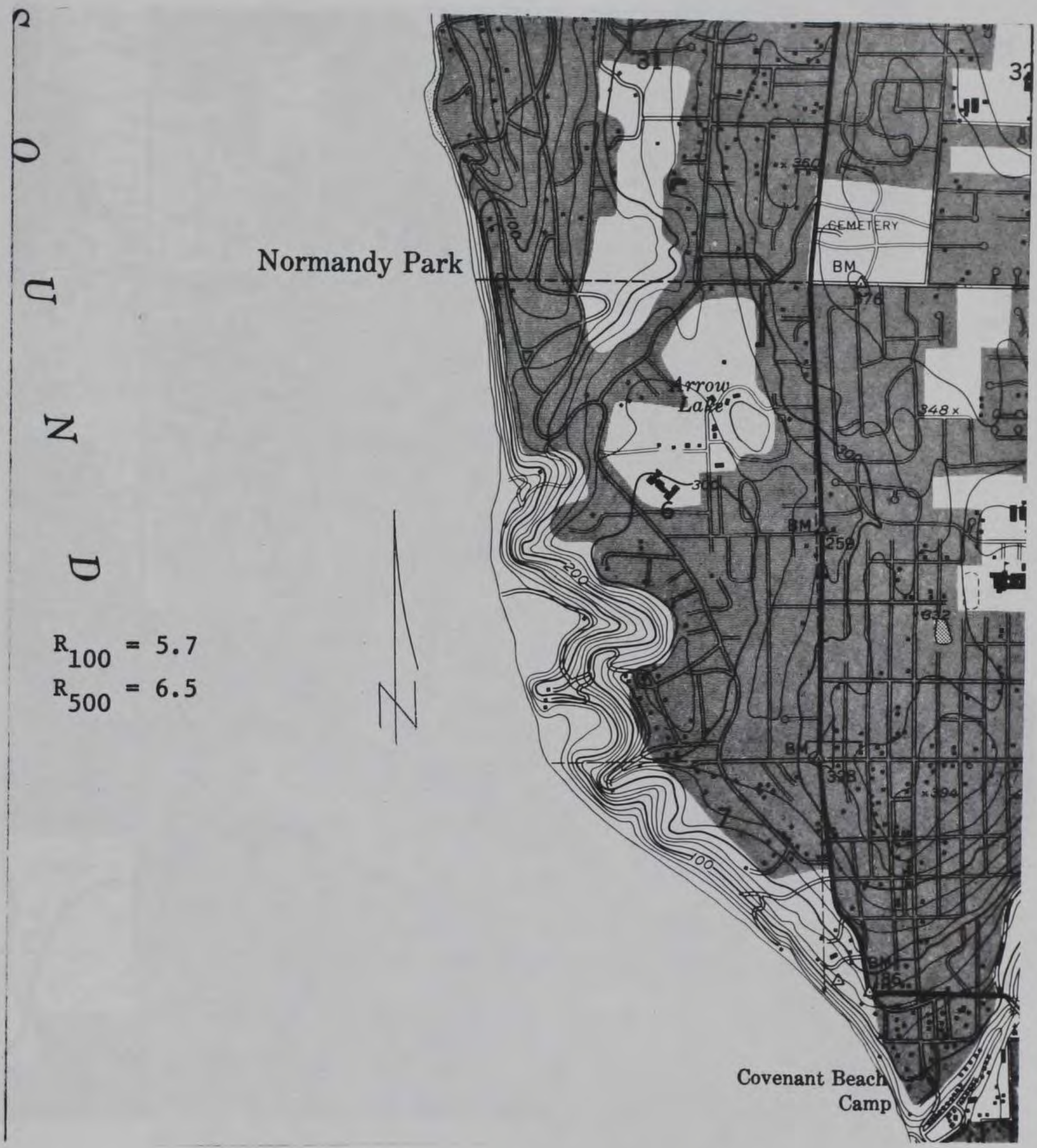

Figure 101. Des Moines, Wash., 50N to 54N, L

Figure 102. Des Moines, Wash., 54N to 58N, L

Figure 103. Des Moines, Wash., 58N to 60+N, L

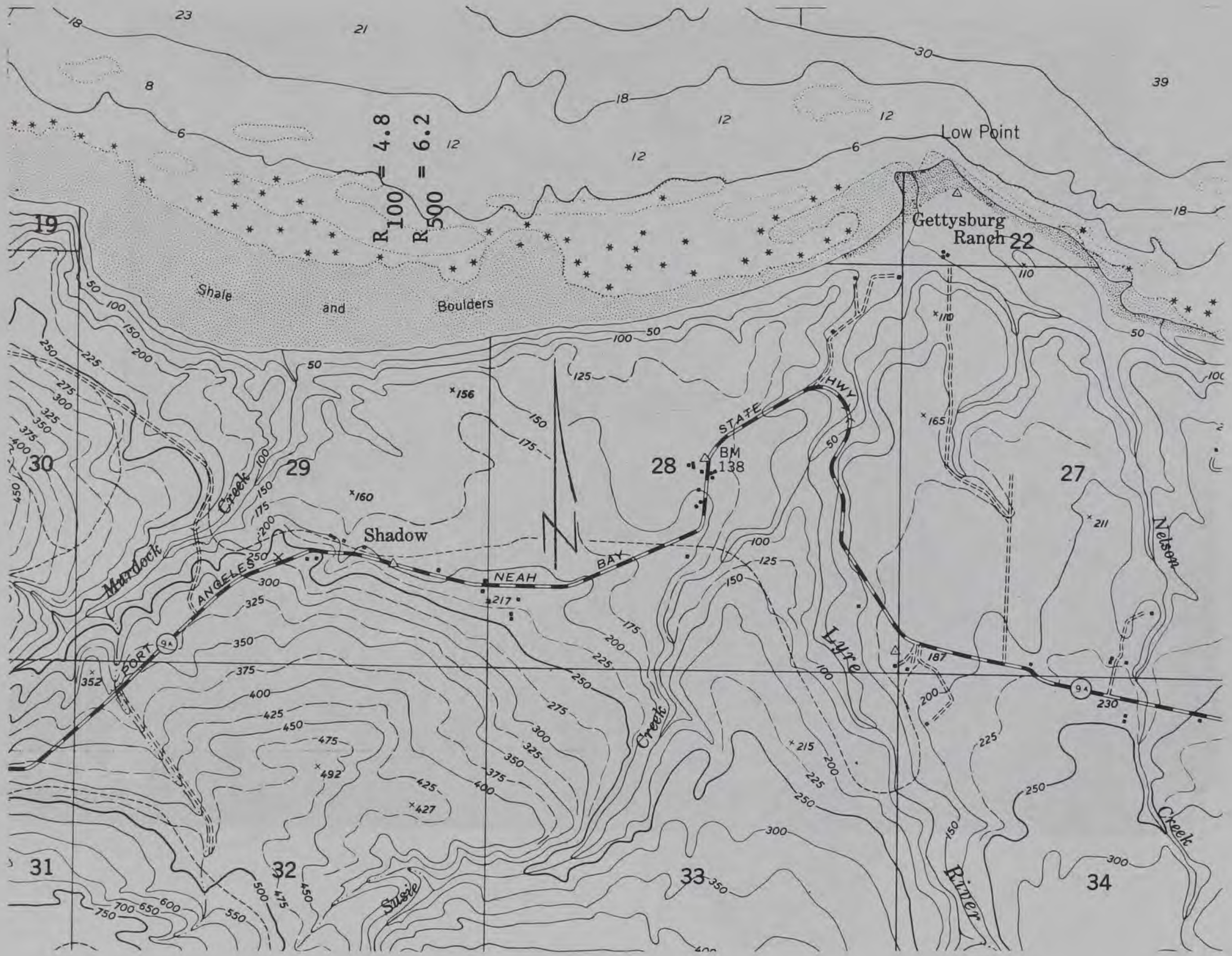

Figure 104. Disque, Wash., 48°08' N to 48°10'+N, L

Figure 105. Disque, Wash., 48°08'+N to 48°10' N, R

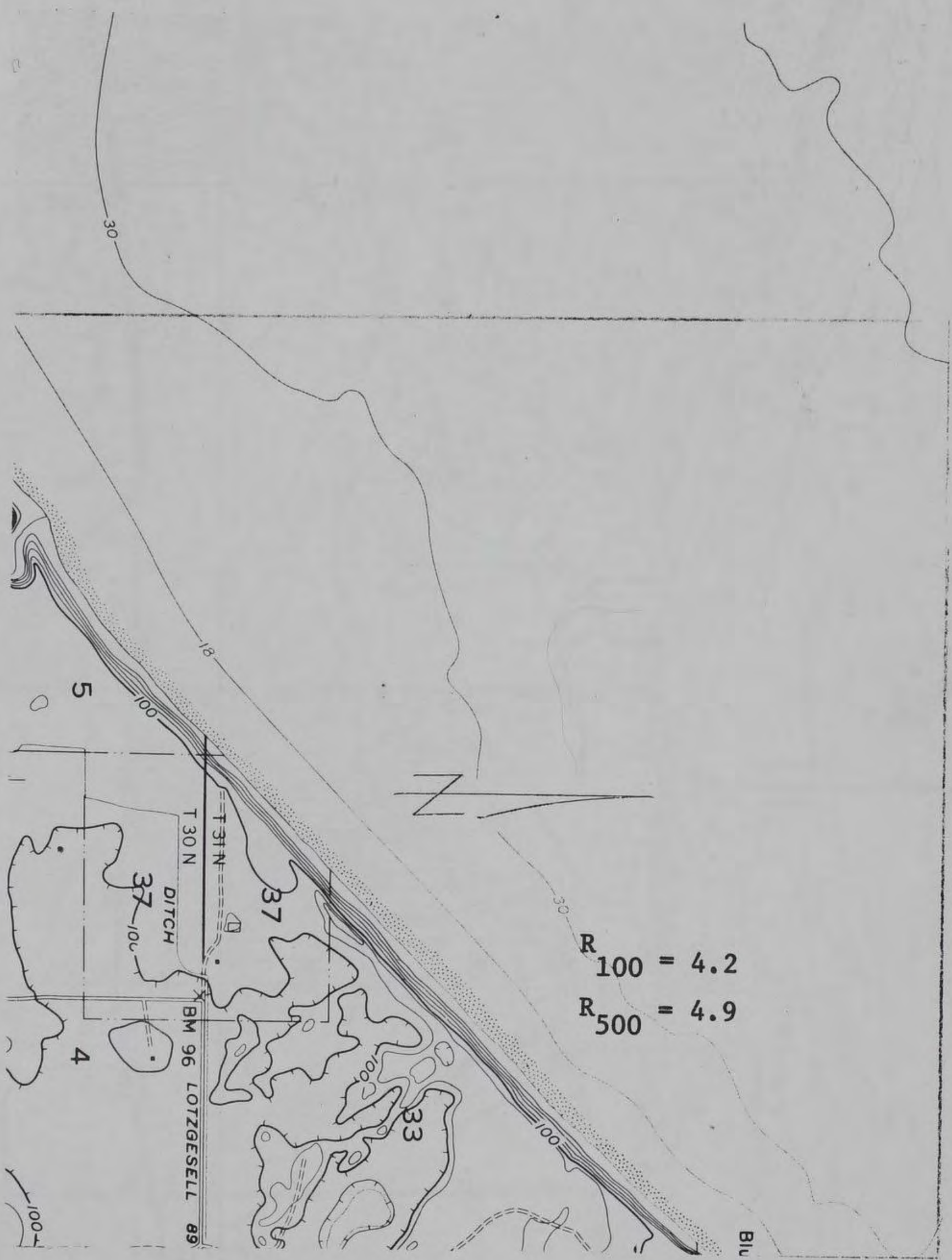

Figure 106. Dungeness, Wash., 30N to 33N, L

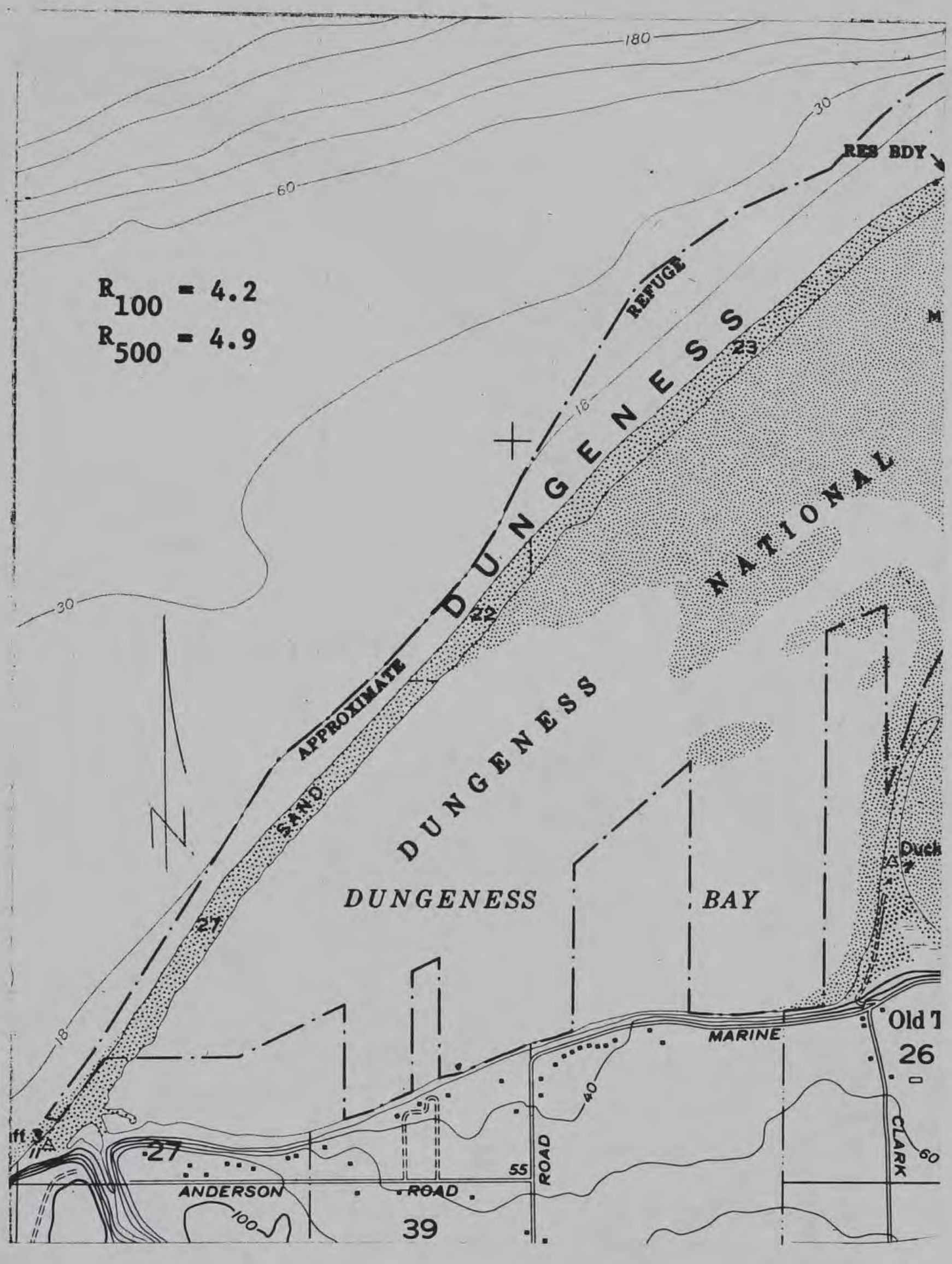

Figure 107. Dungeness, Wash., 32N to 36N, L

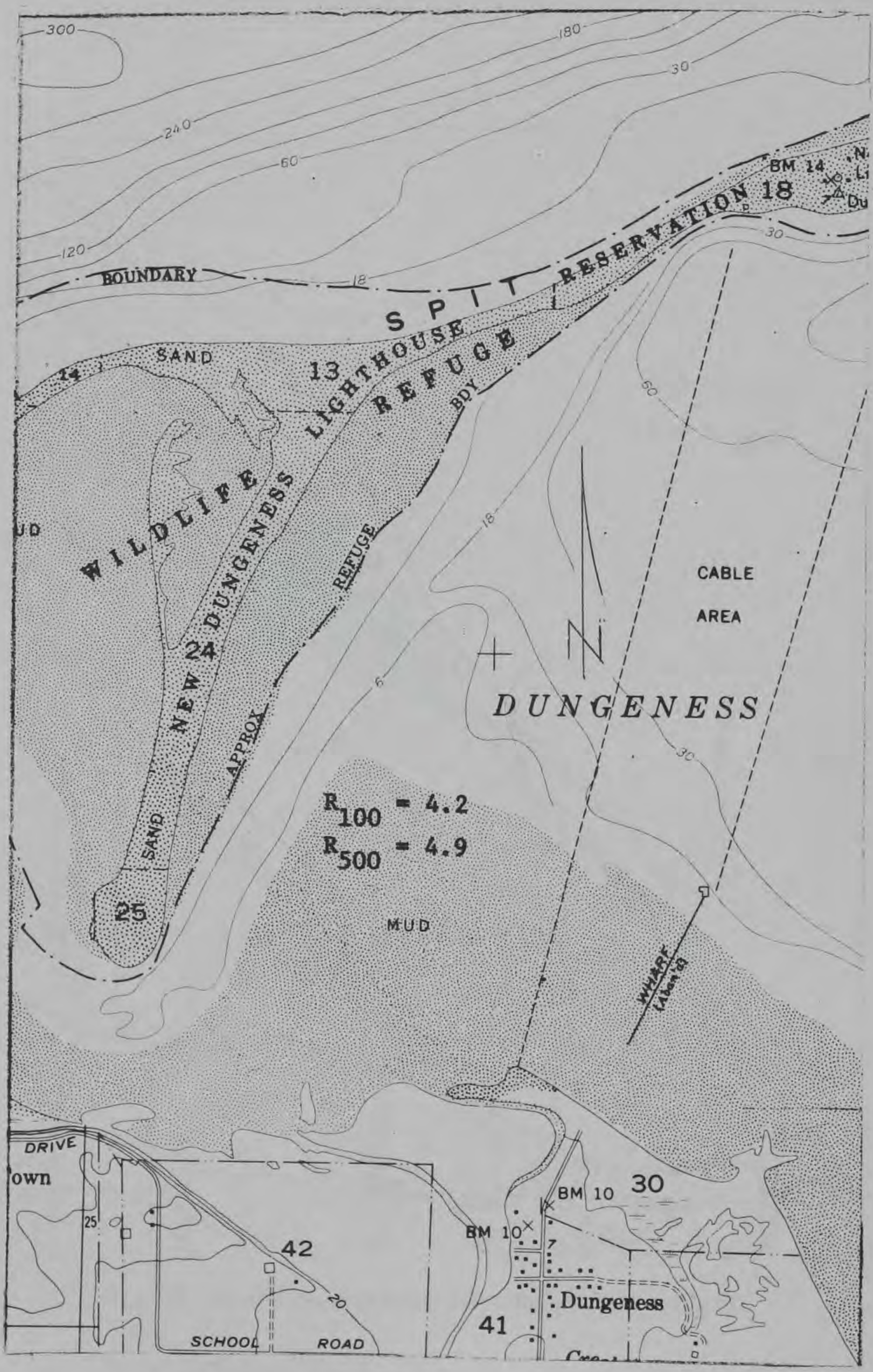

Figure 108. Dungeness, Wash., 89E to 92E, B

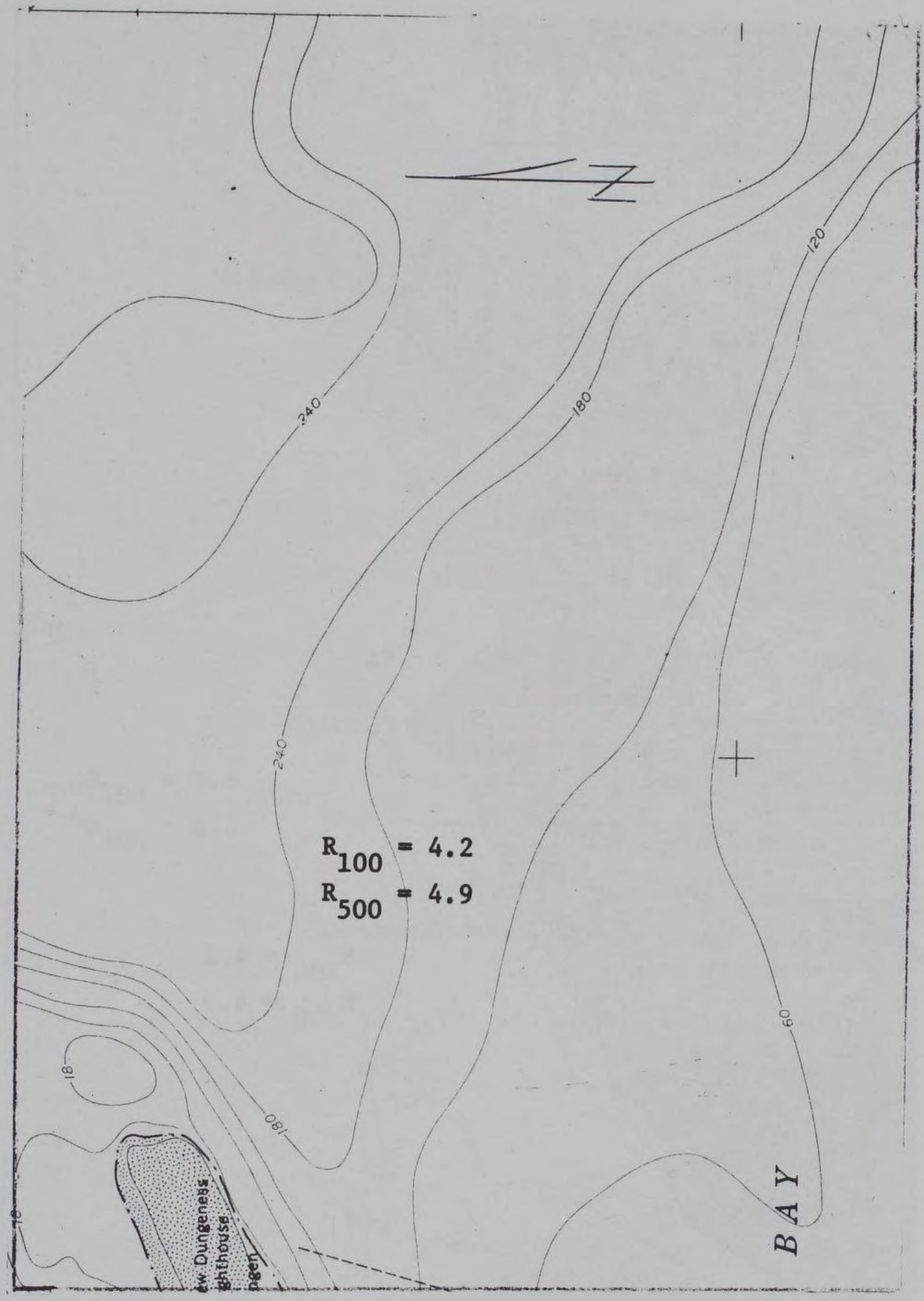

Figure 109. Dungeness, Wash., 34N to 37N, R

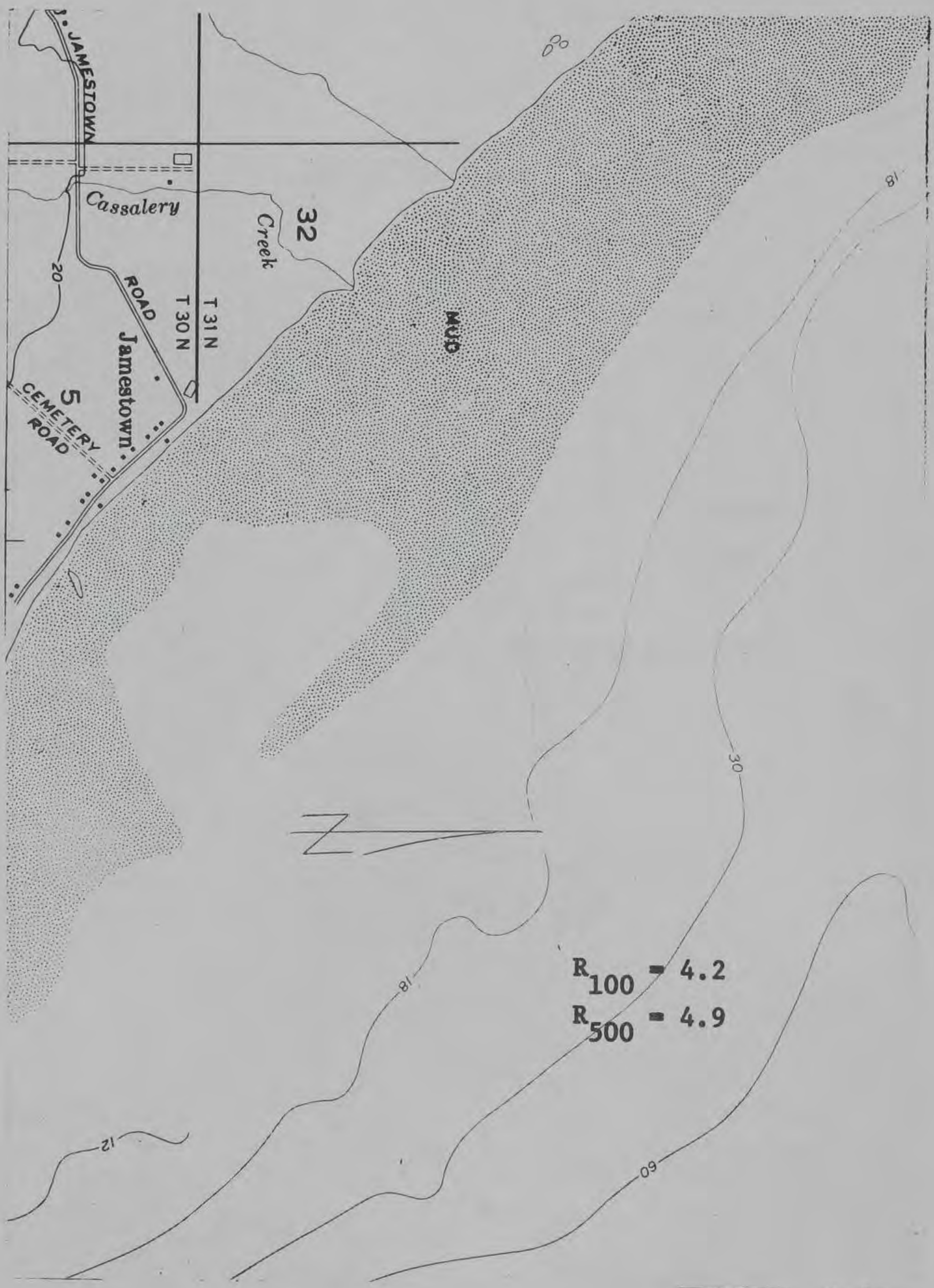

Figure 110. Dungeness, Wash., 30N to 33N, R

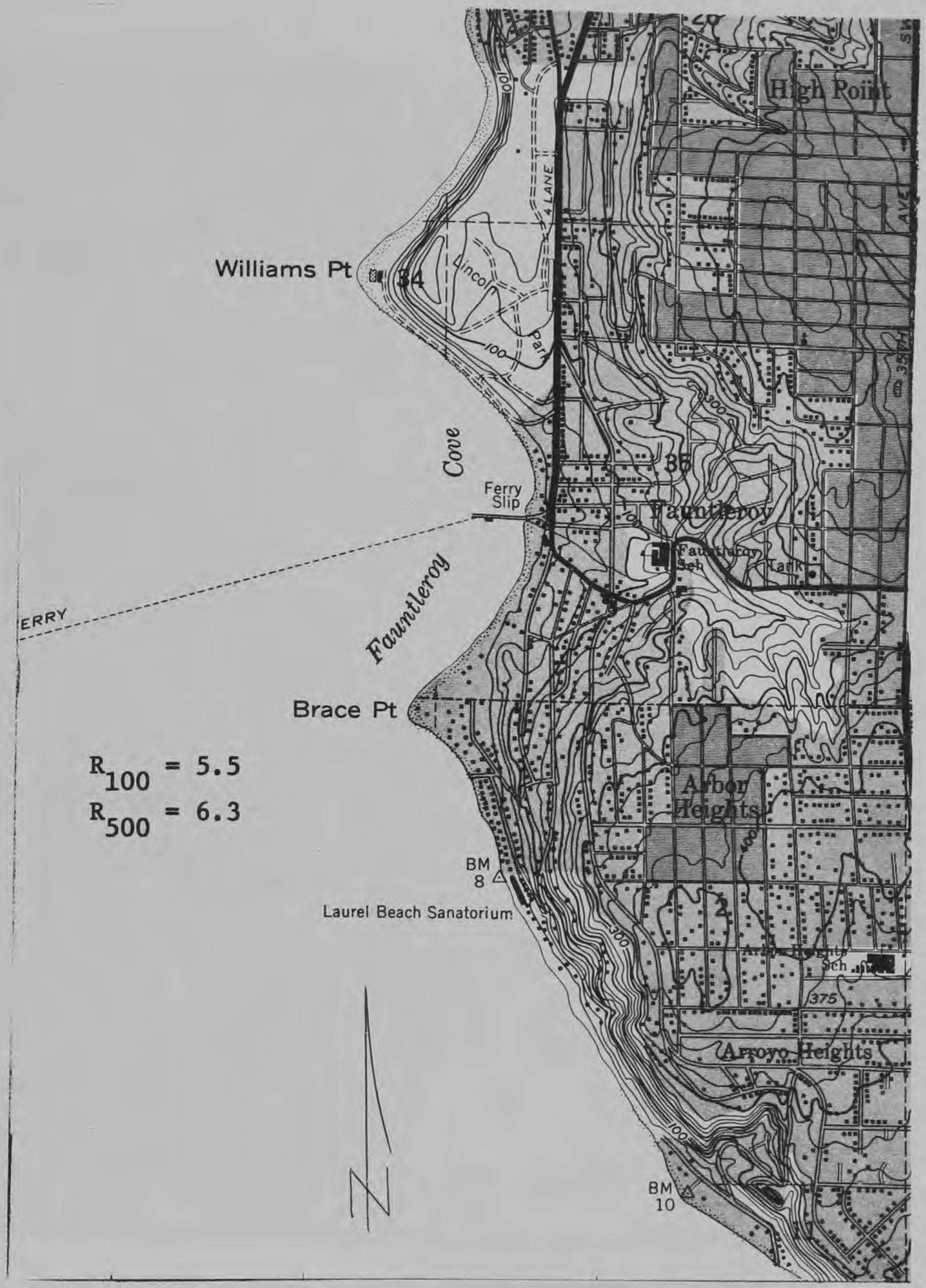

Figure 111. Duwamish Head, Wash., 61-N to 65N, R

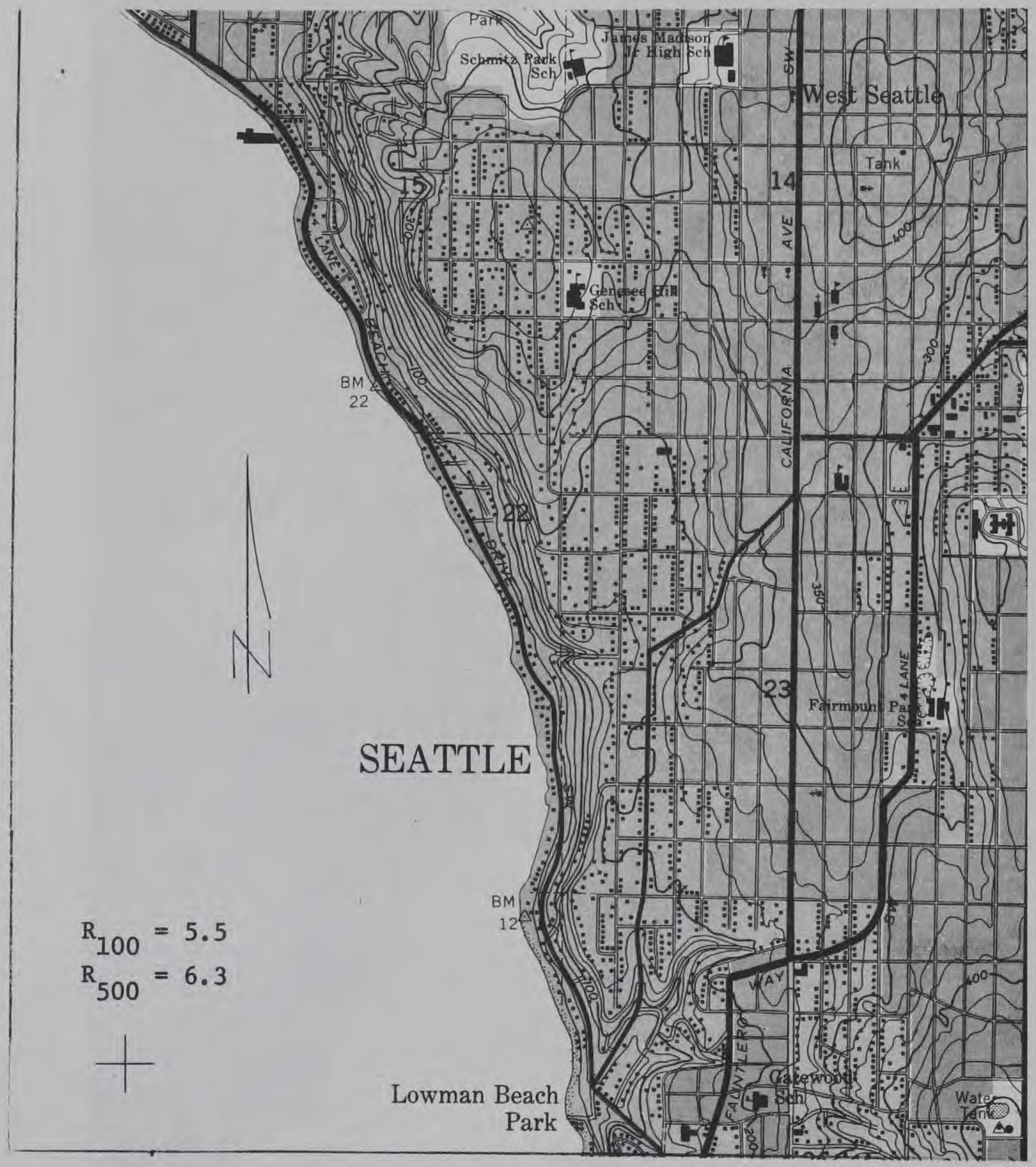

Figure 112. Duwamish Head, Wash., 65N to 69N, R

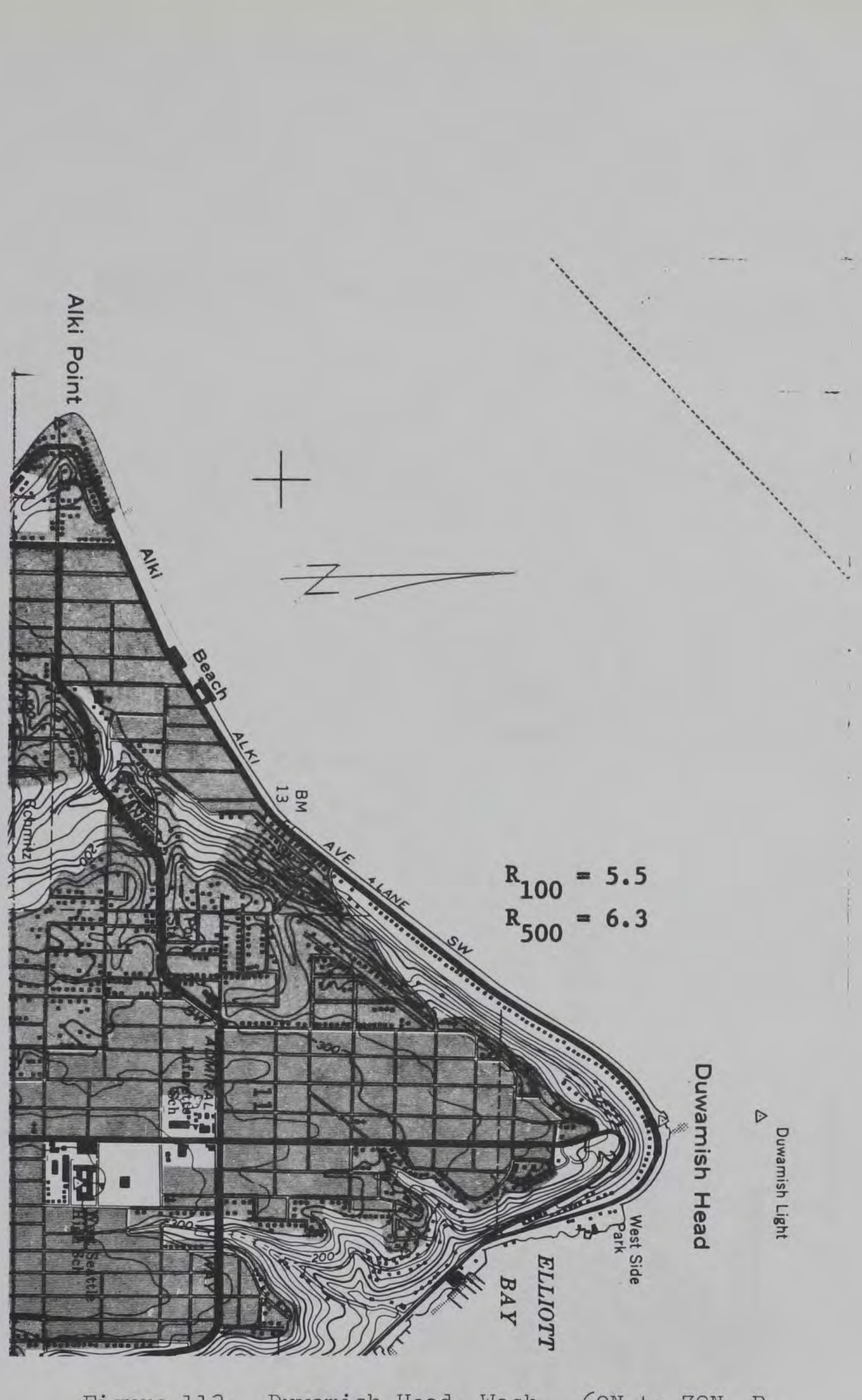

Figure 113. Duwamish Head, Wash., 69N to 72N, R

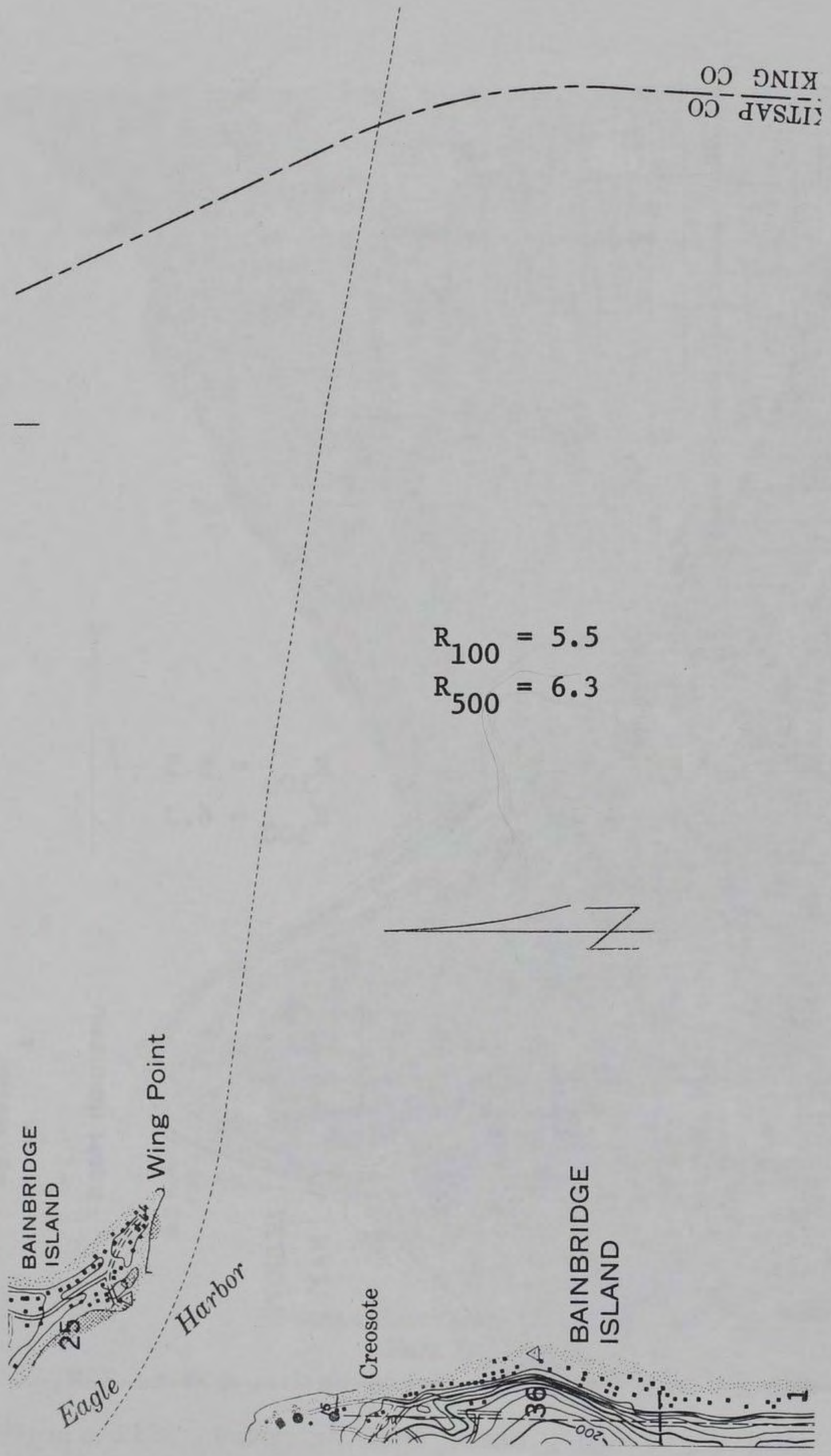

Figure 114. Duwamish Head, Wash., 72N to 74+N, L

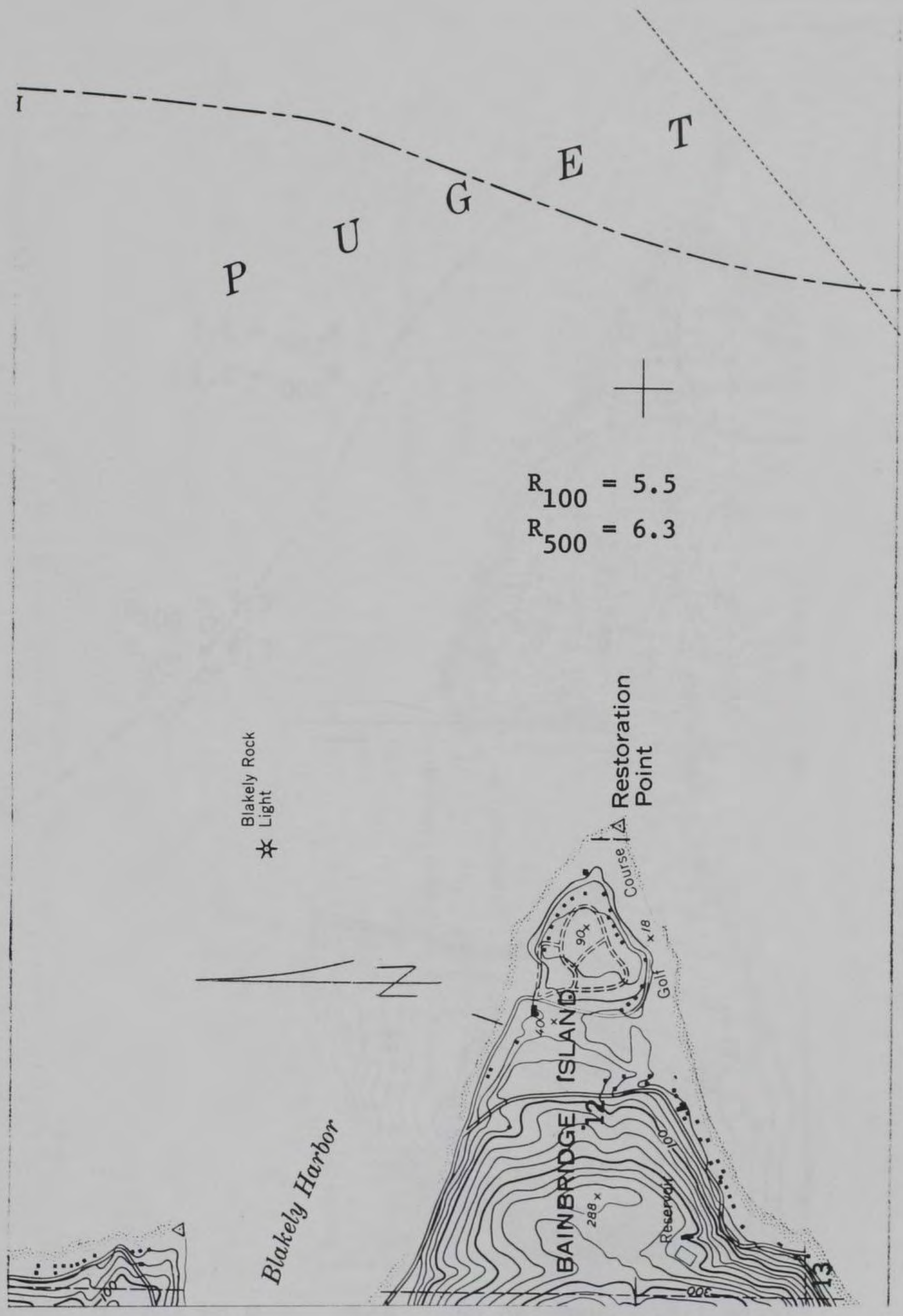

Figure 115. Duwamish Head, Wash., 69N to 72N, L

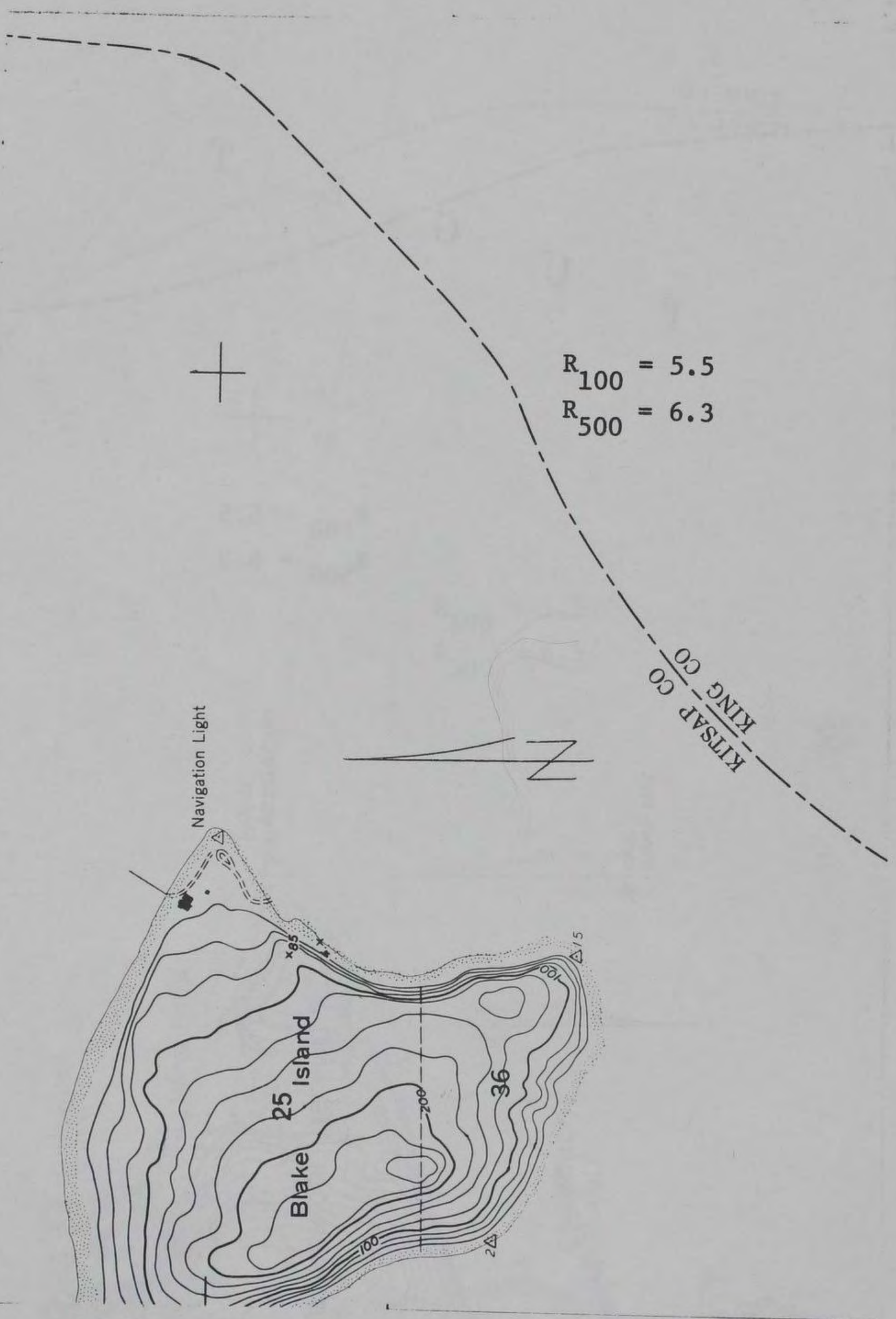

Figure 116. Duwamish Head, Wash., 63N to 66N, L

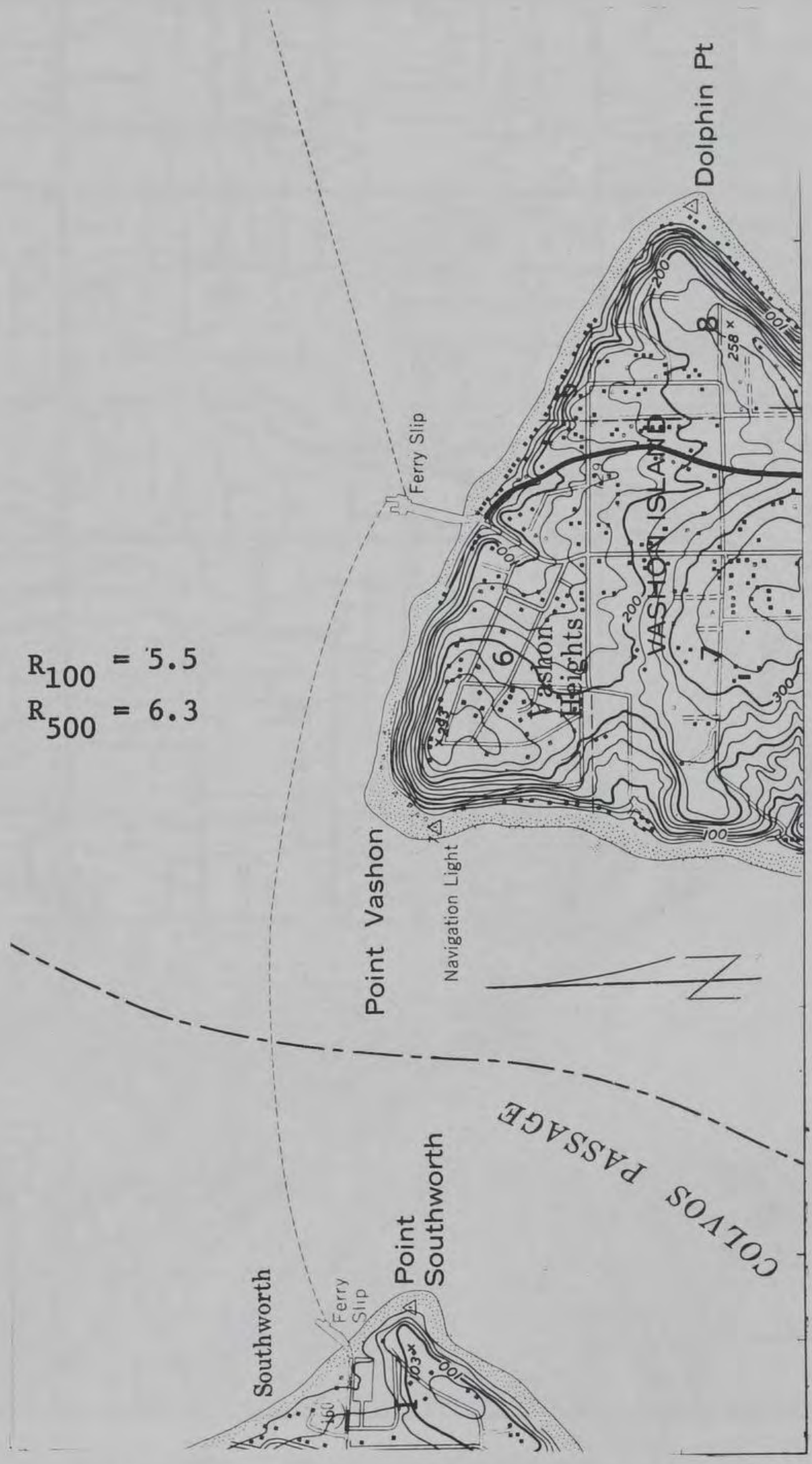

$R_{100} = 5.5$
$R_{500} = 6.3$

Figure 117. Duwamish Head, Wash., 38-E to 42E, B

Figure 118. Edmonds East, Wash., 96N to 99N, L

$R_{100} = 5.5$
$R_{500} = 6.3$

Figure 119. Edmonds East, Wash., 99N to 02+N, L

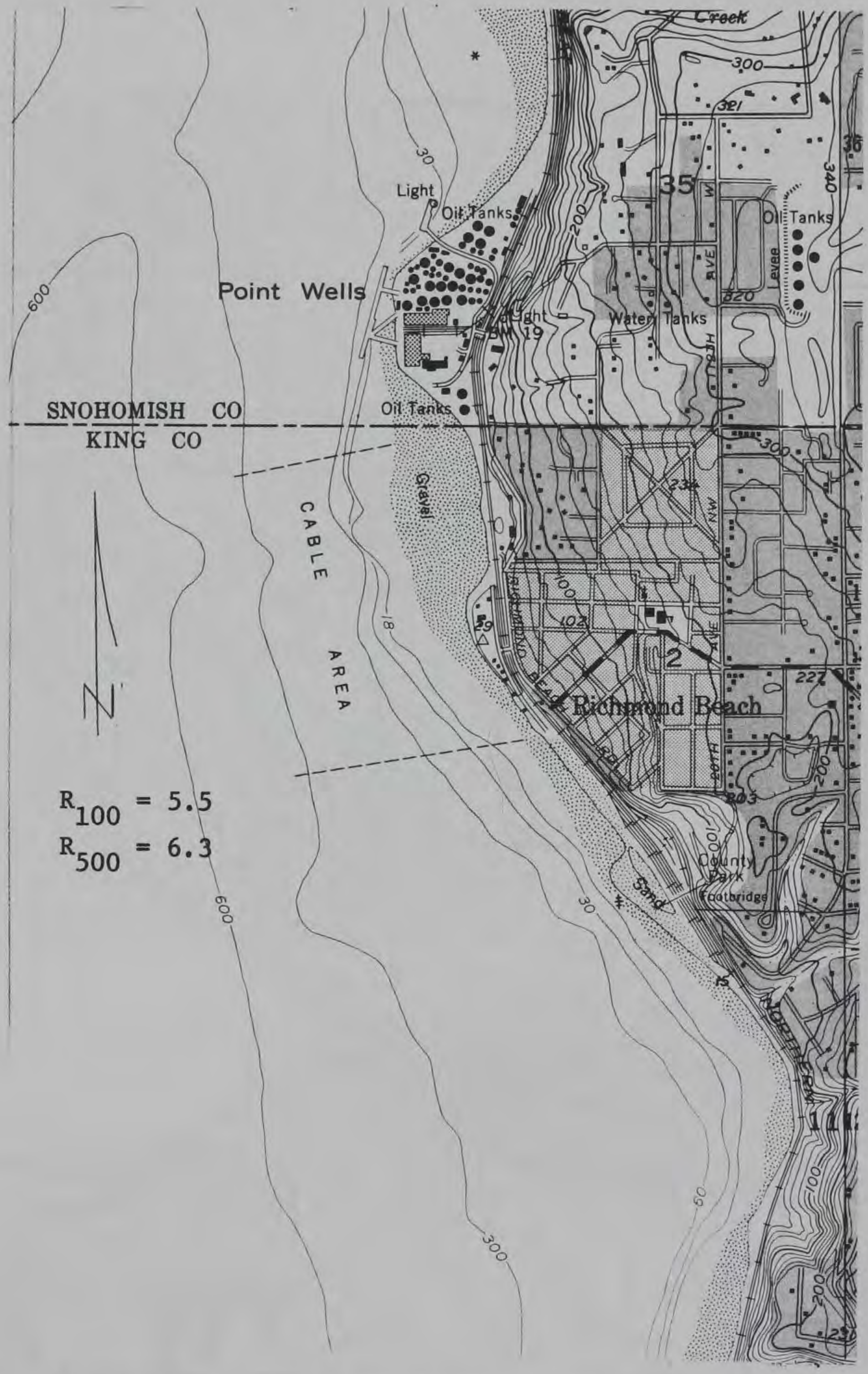

Figure 120. Edmonds West, Wash., 89-N to 93N, R

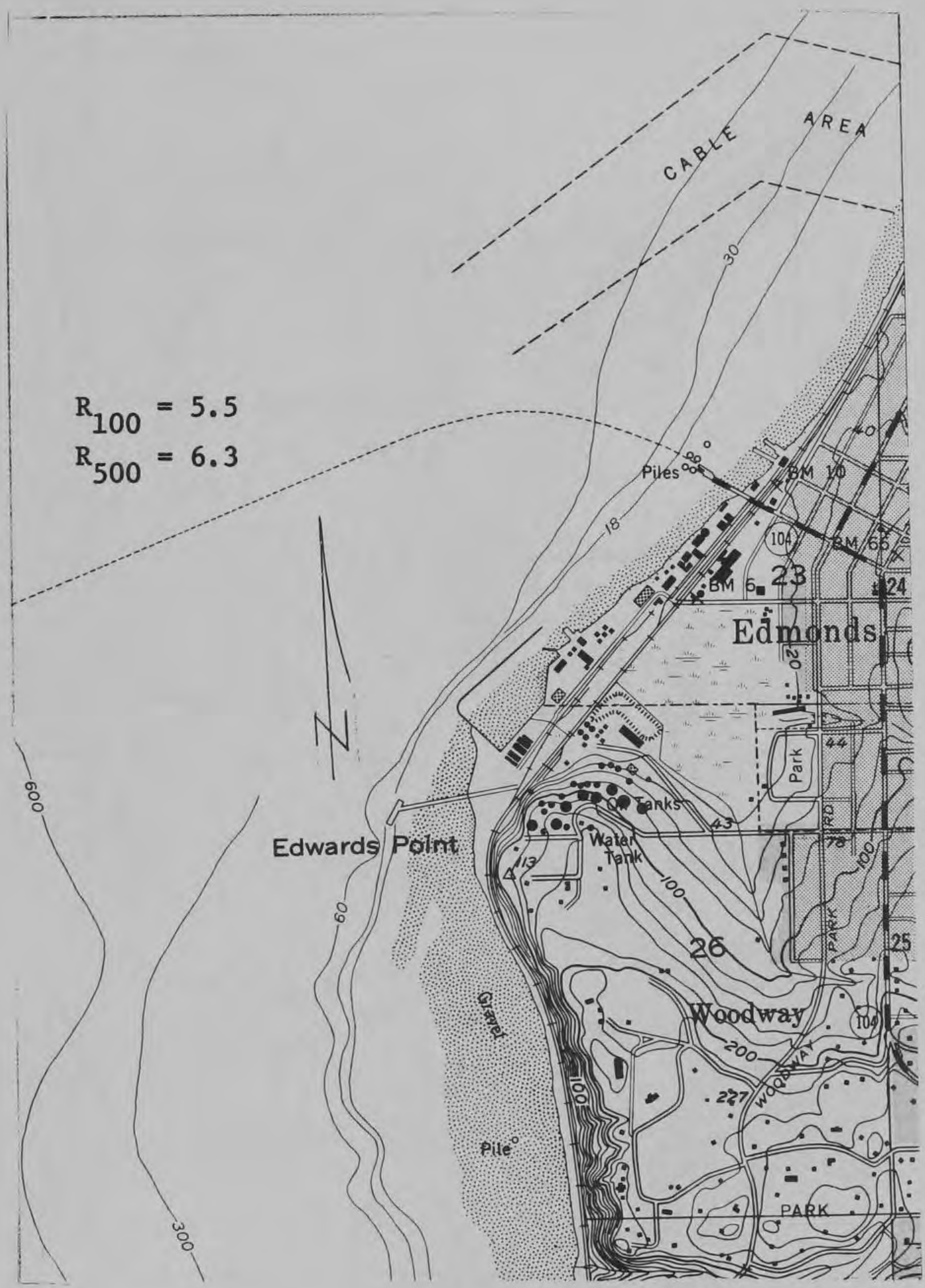

Figure 121. Edmonds West, Wash., 93N to 97N, R

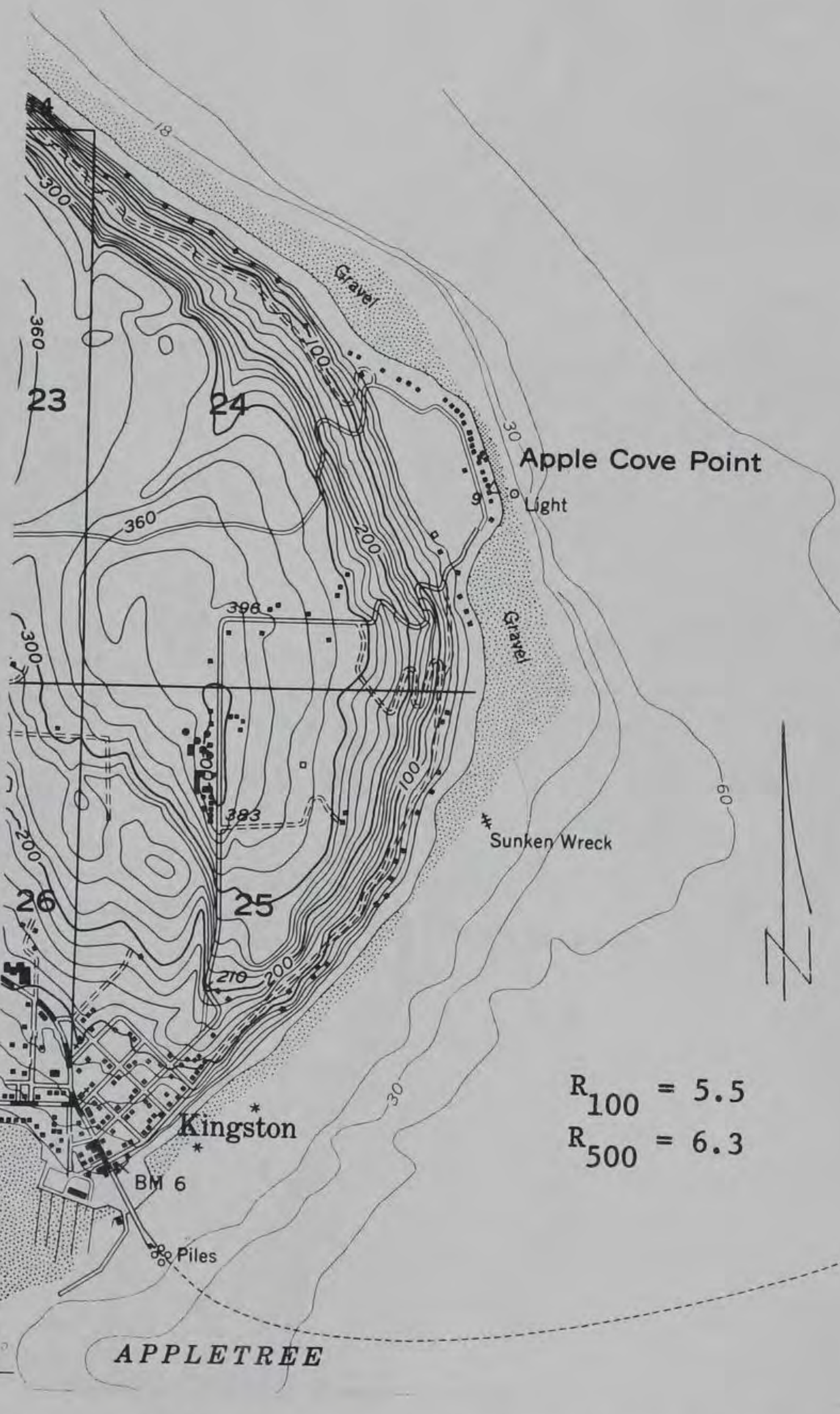

Figure 122. Edmonds West, Wash., 93N to 97N, L

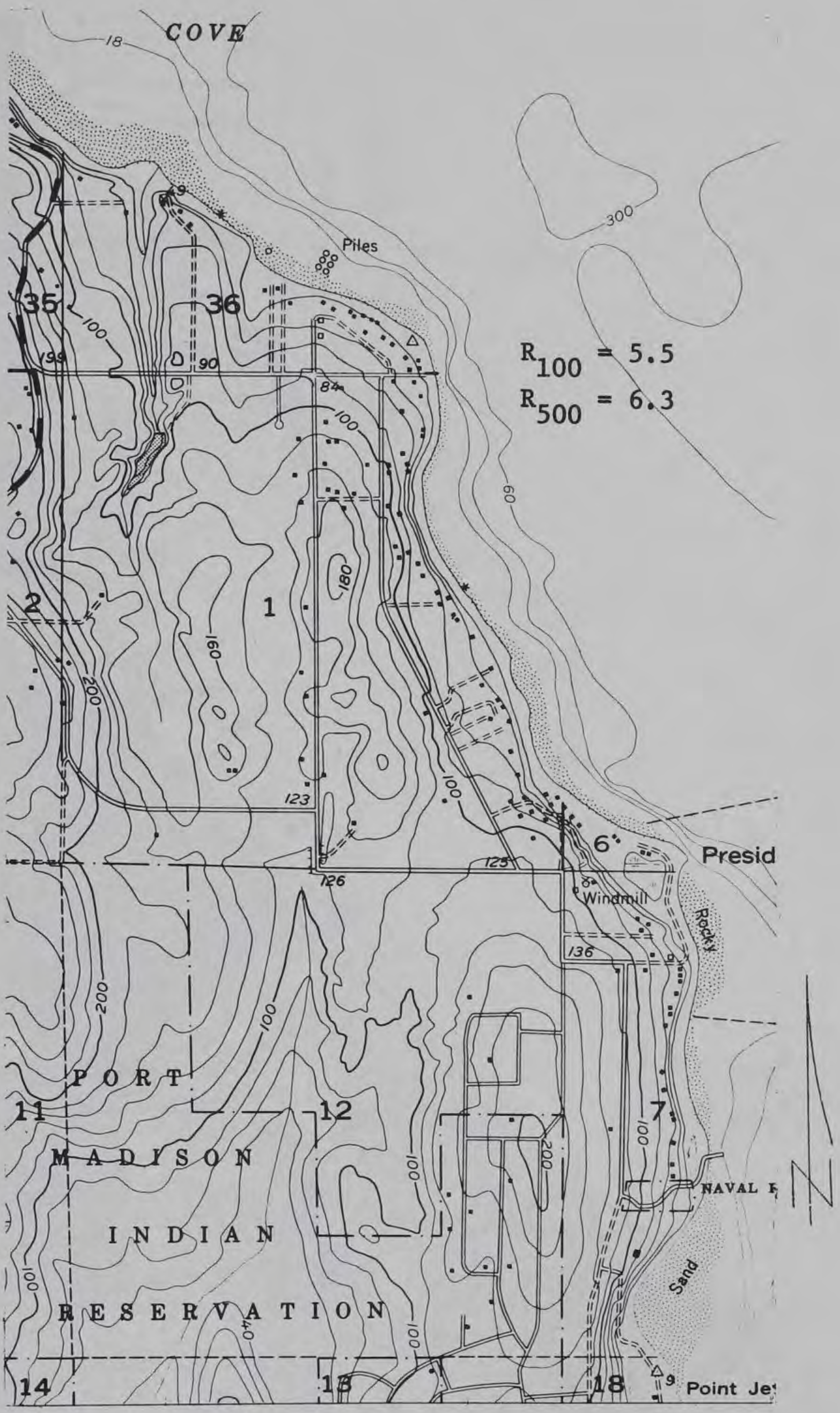

Figure 123. Edmonds West, Wash., 89-N to 93N, L

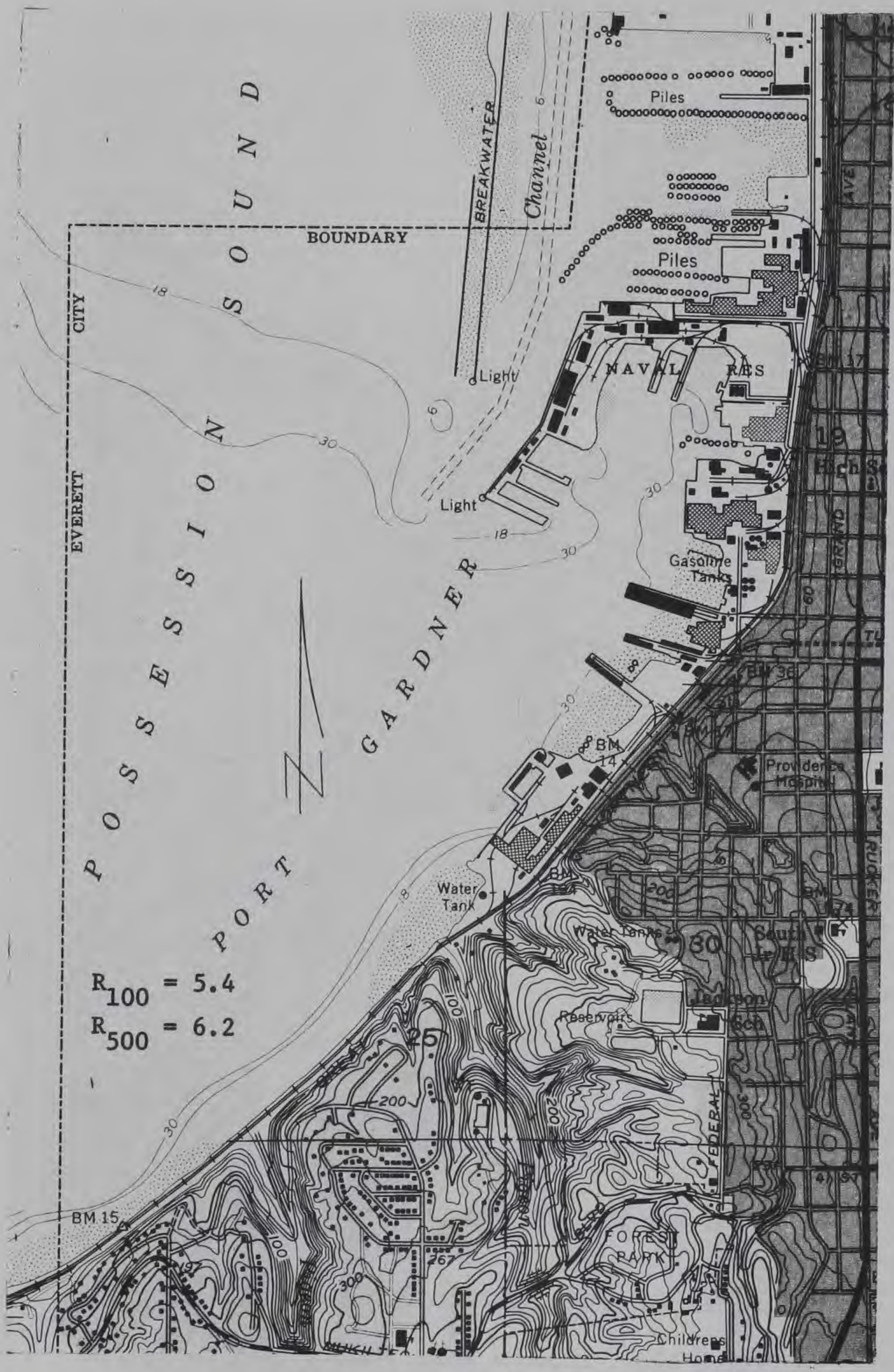

Figure 124. Everett, Wash., 56E to 59E, T

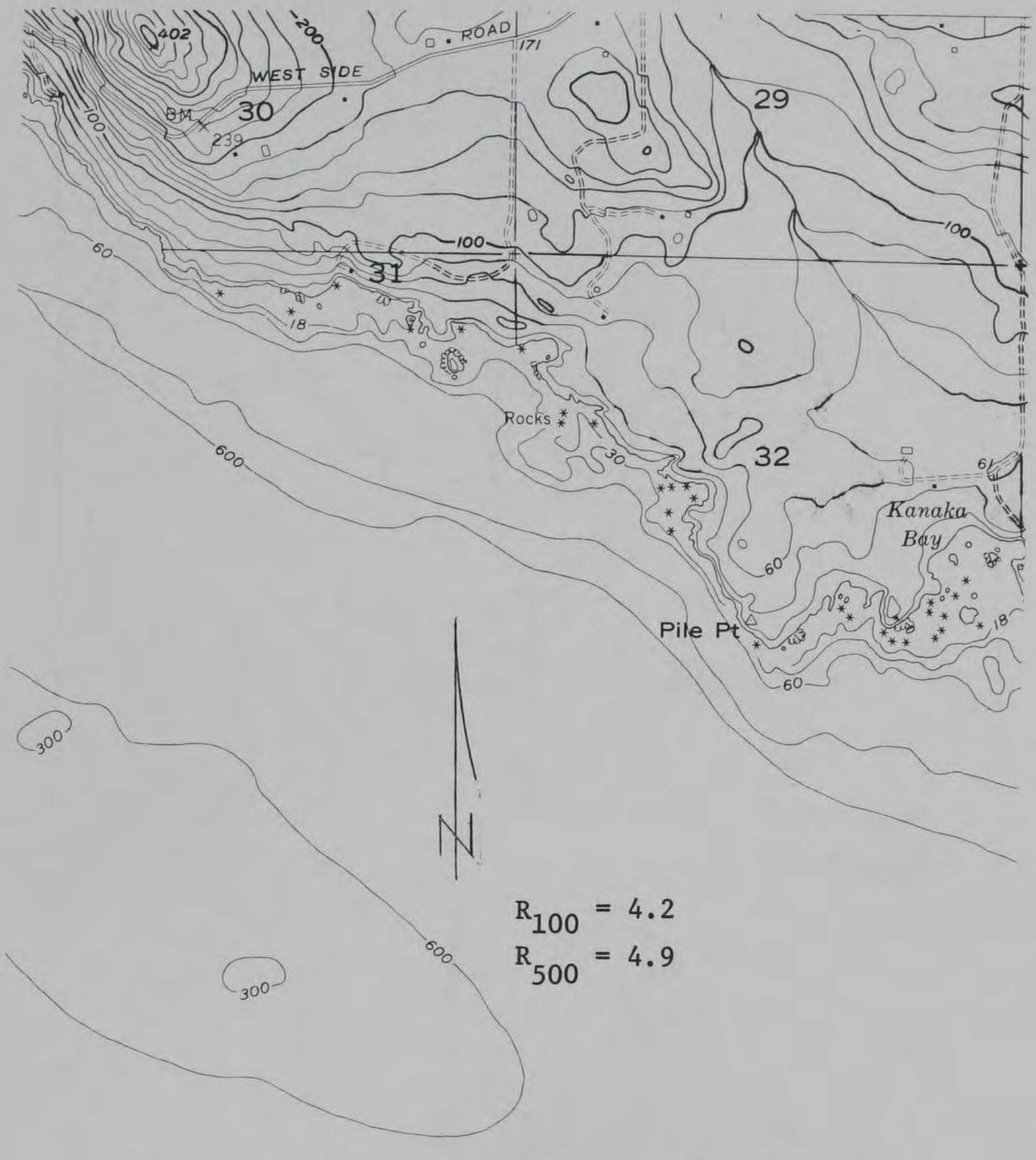

Figure 125. False Bay, Wash., 68N to 71+N, R

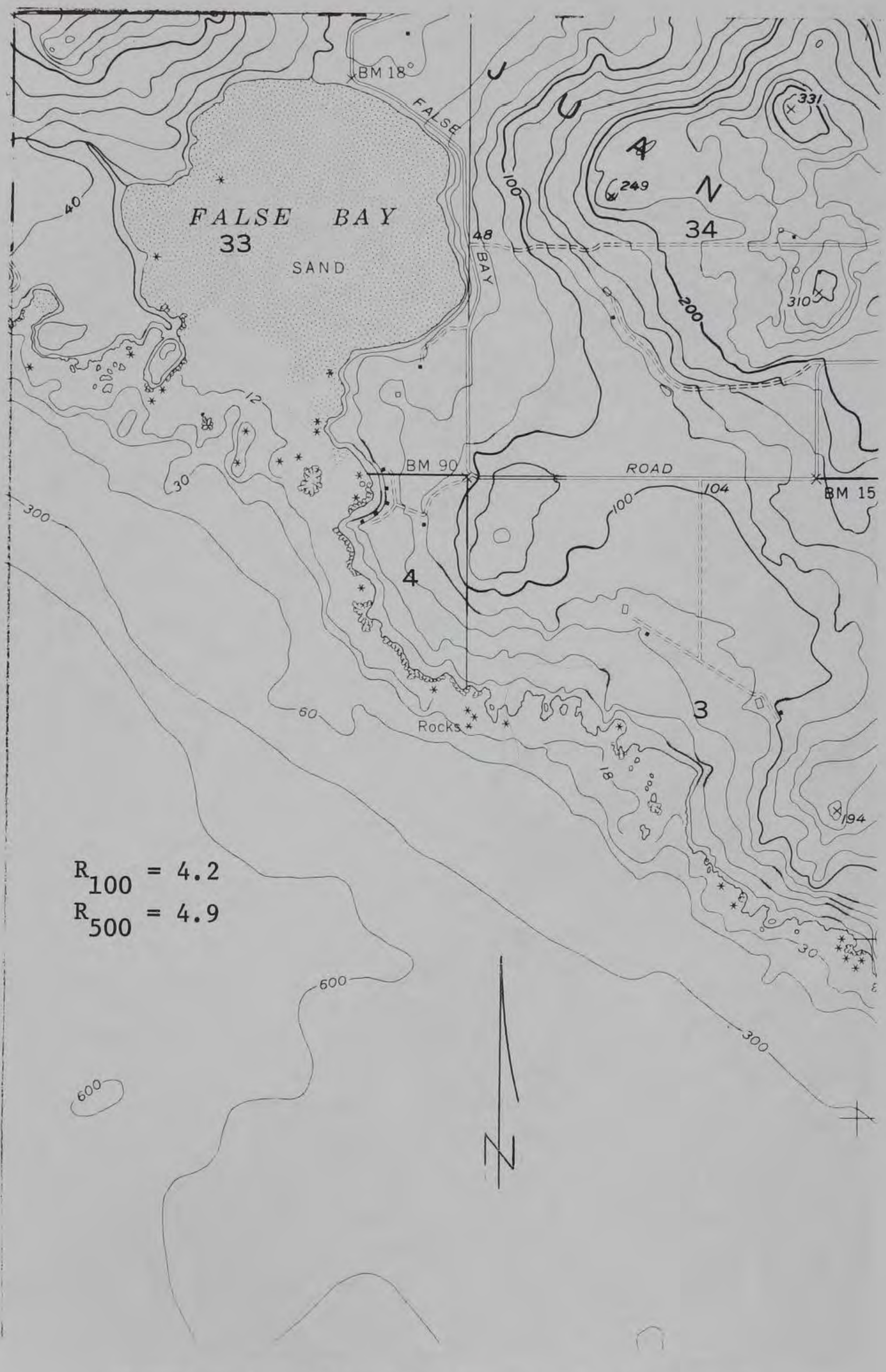

Figure 126. False Bay, Wash., 94E to 97E, T

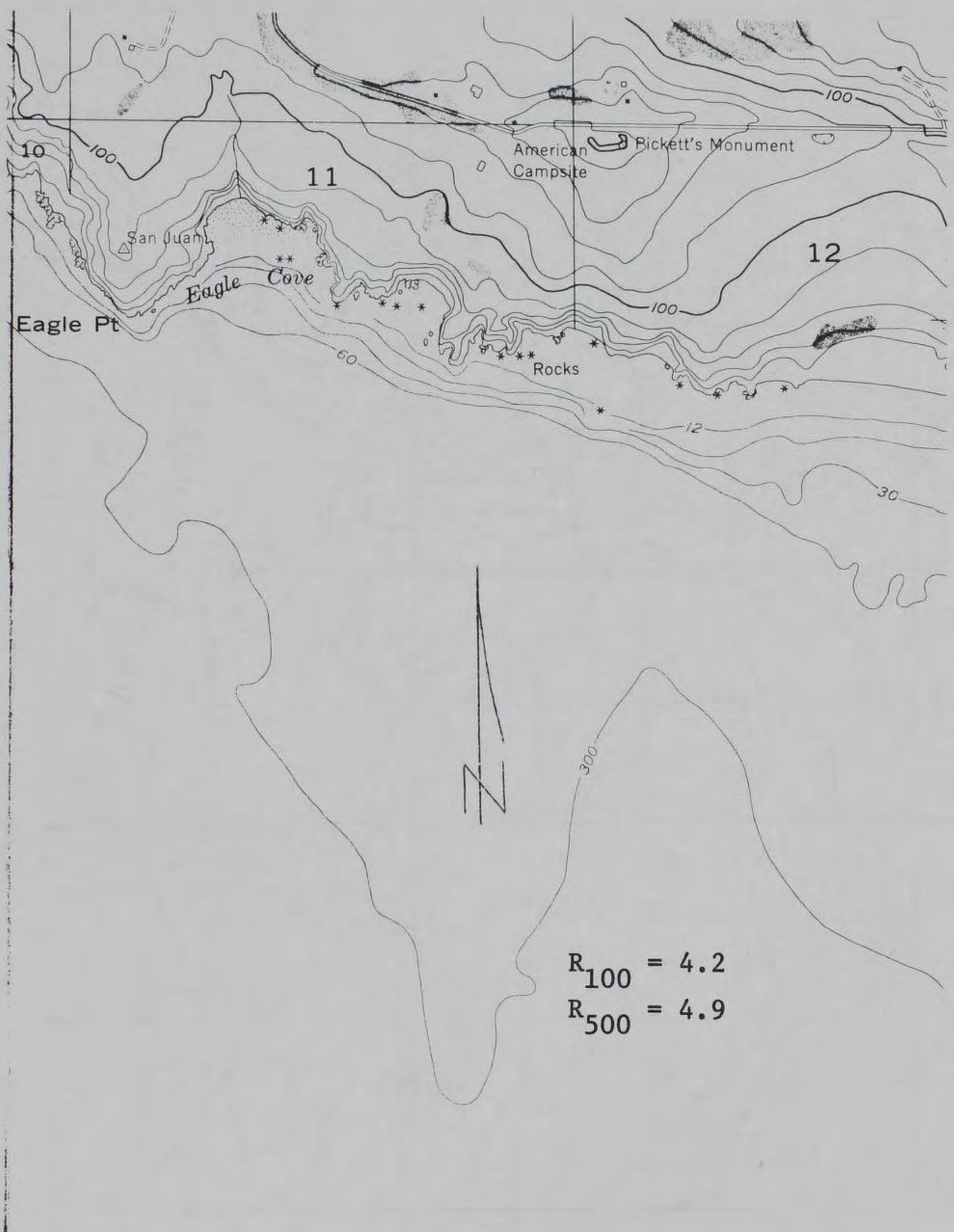

Figure 127. False Bay, Wash., 64N to 68N, R

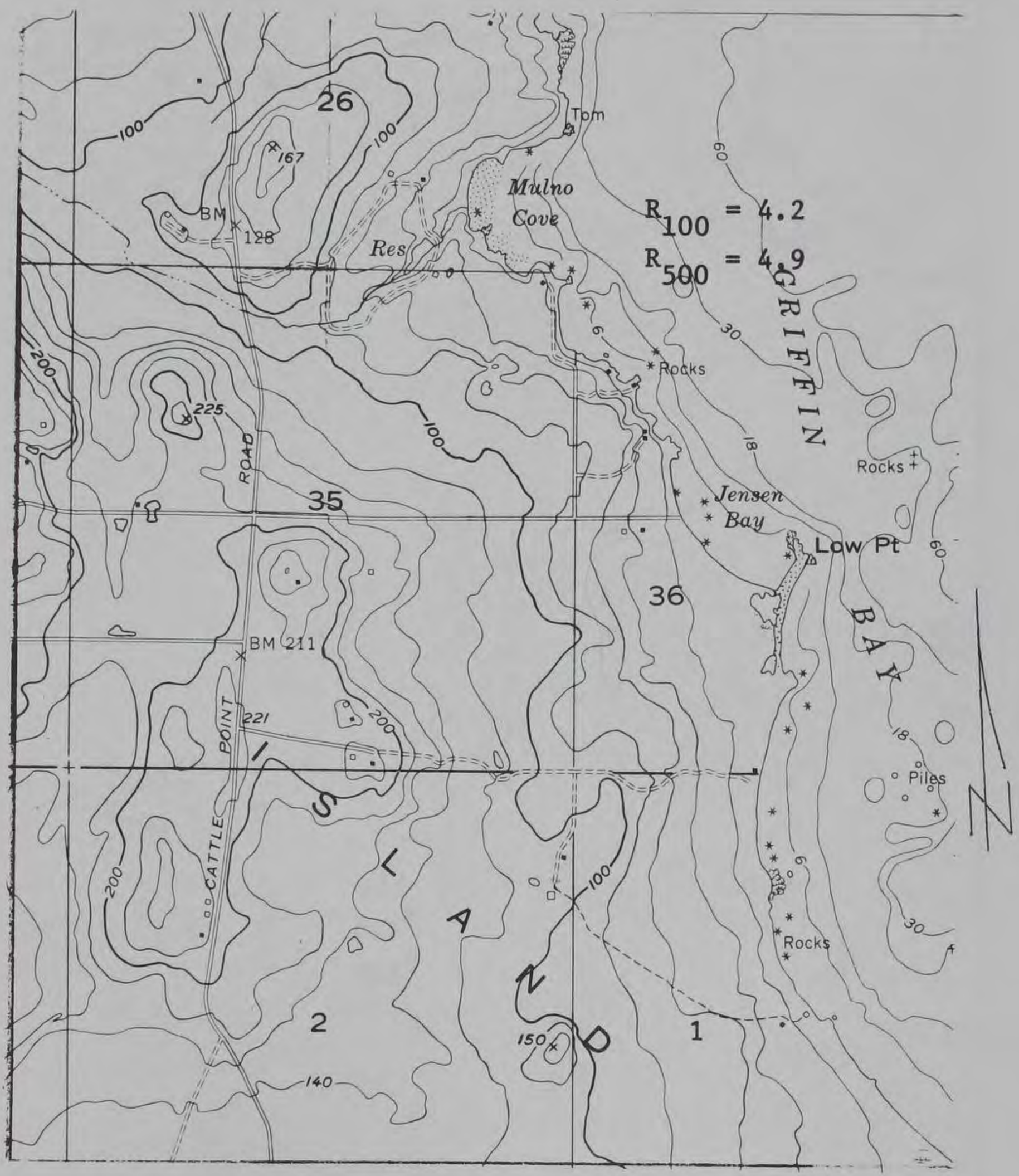

Figure 128. False Bay, Wash., 68N to 71+N, R

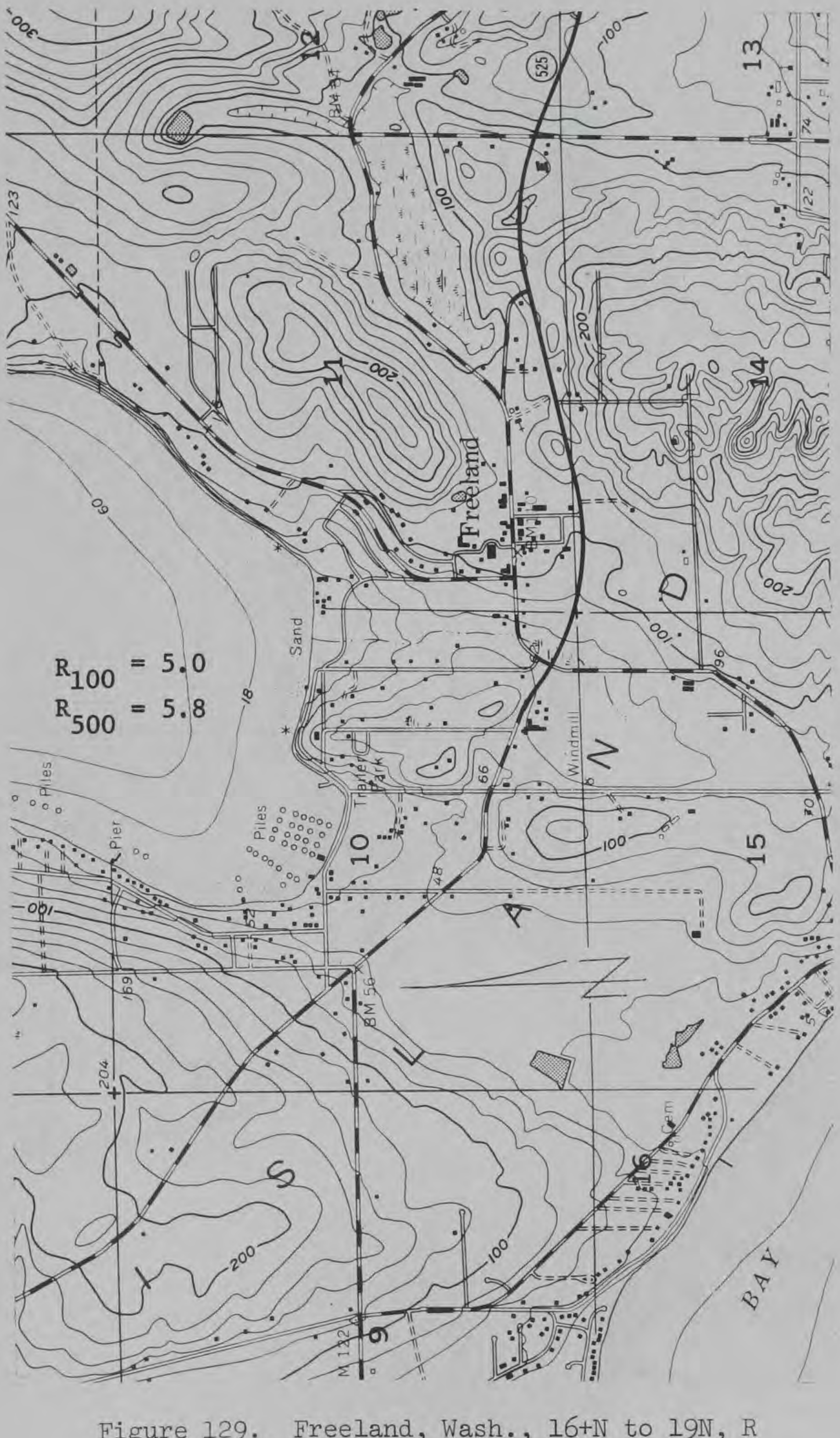

Figure 129. Freeland, Wash., 16+N to 19N, R

$R_{100} = 5.0$

$R_{500} = 5.8$

Figure 130. Freeland, Wash., 16+N to 21N, L

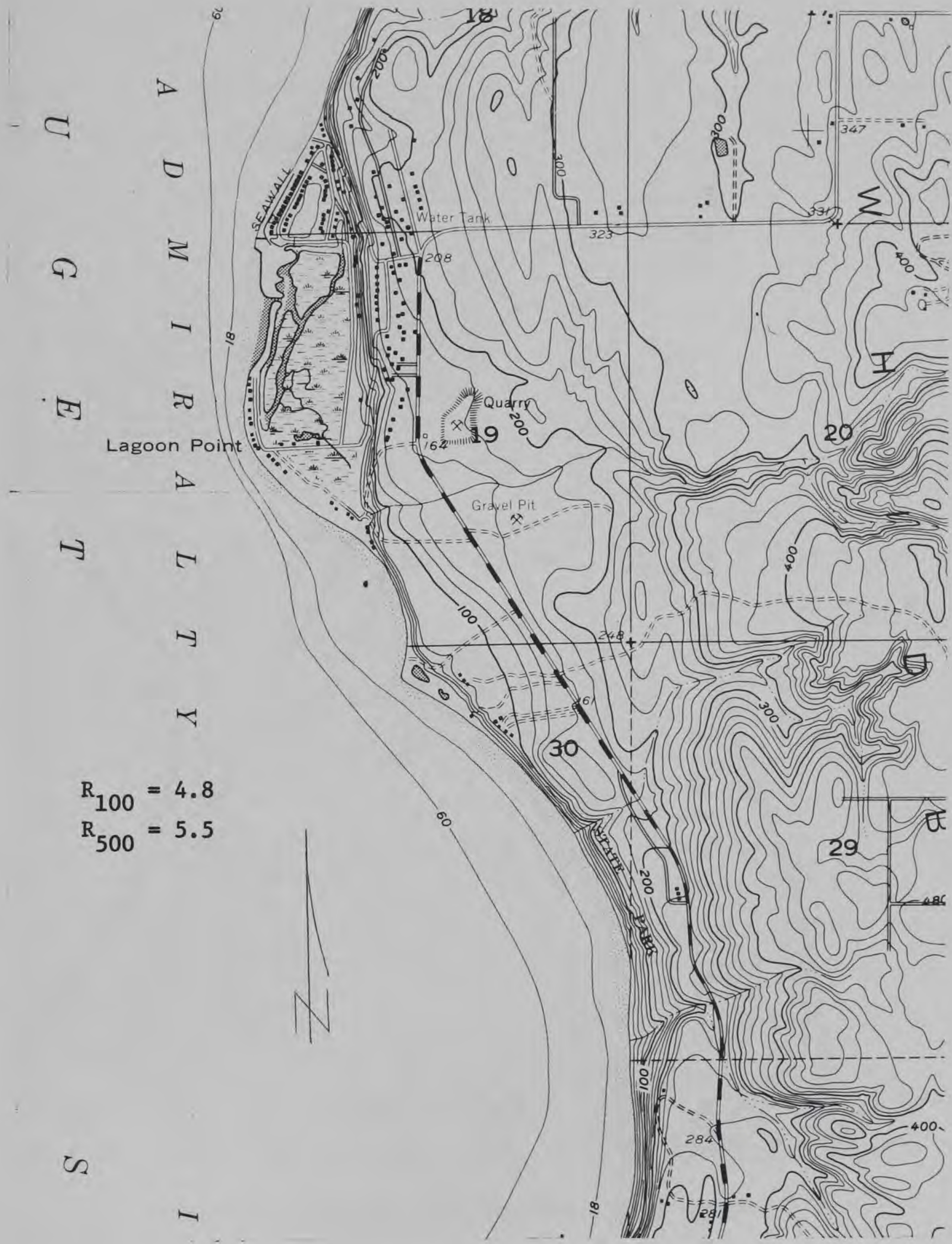

Figure 131. Freeland, Wash., 21N to 25+N, L

$R_{100} = 4.8$

$R_{500} = 5.5$

Figure 132. Freeland, Wash., 26N to 30N, L

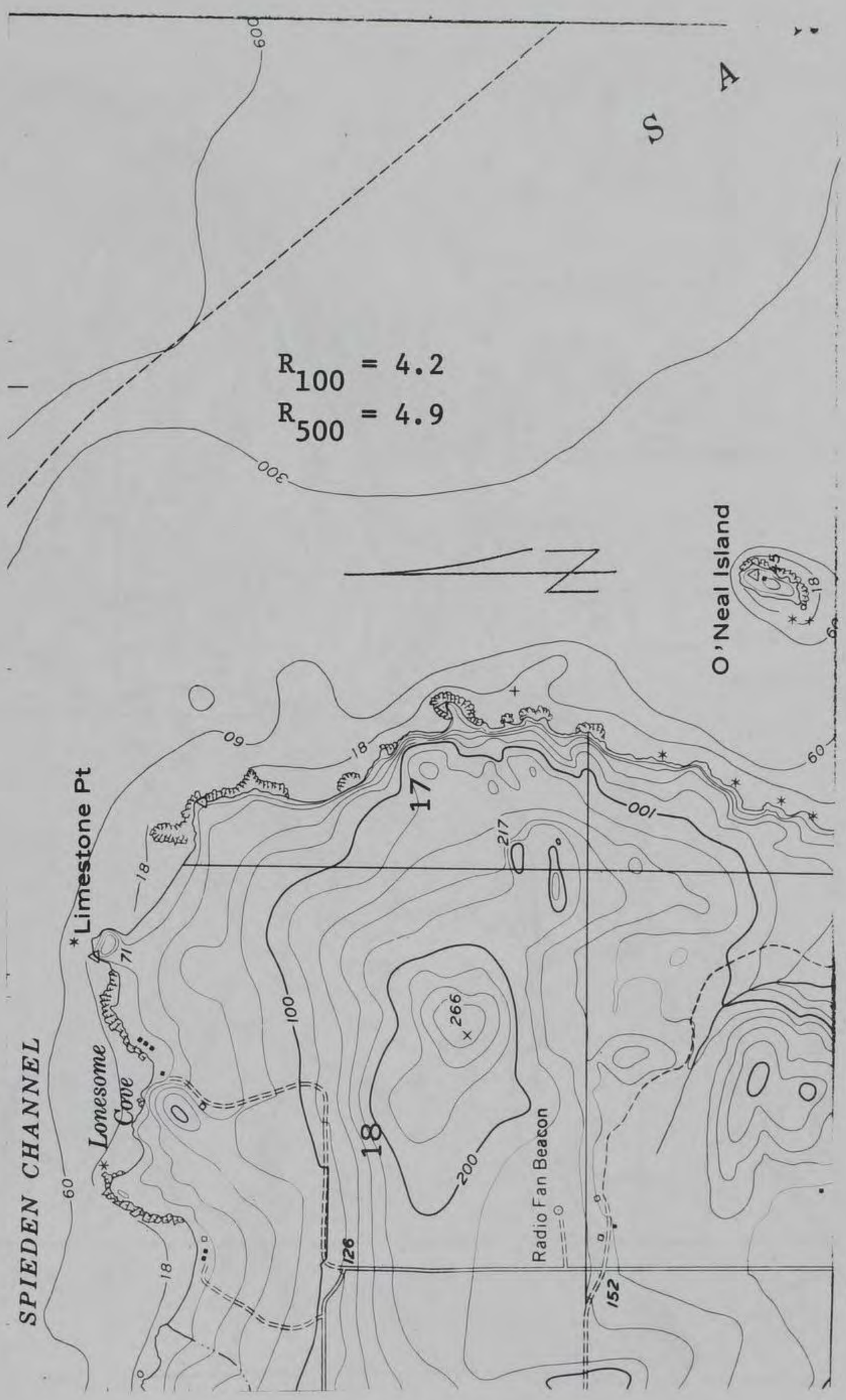

Figure 133. Friday Harbor, Wash., 90+E to 95E, T

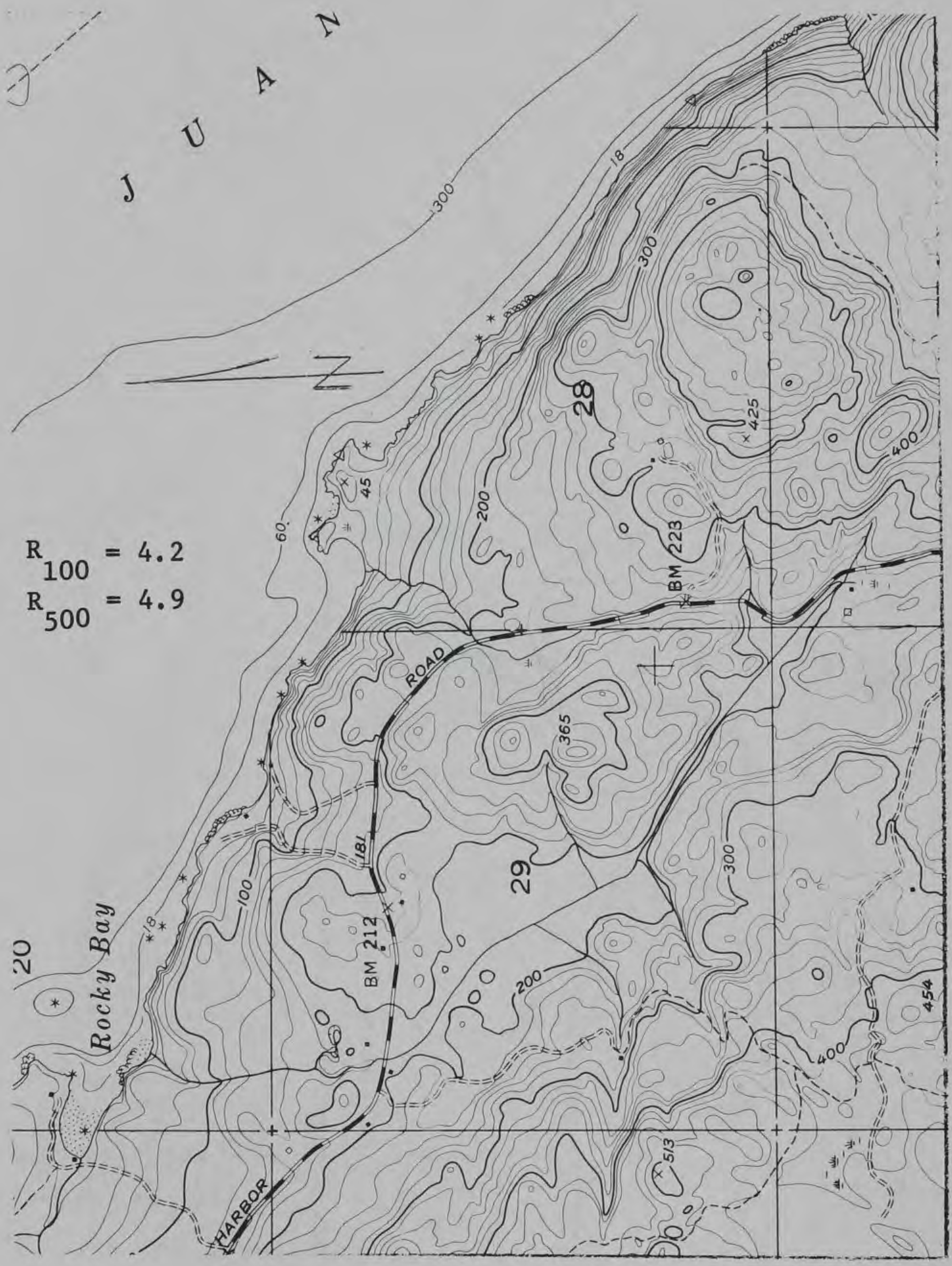

Figure 134. Friday Harbor, Wash., 80N to 83N, L

Figure 135. Friday Harbor, Wash., 80N to 83N, R

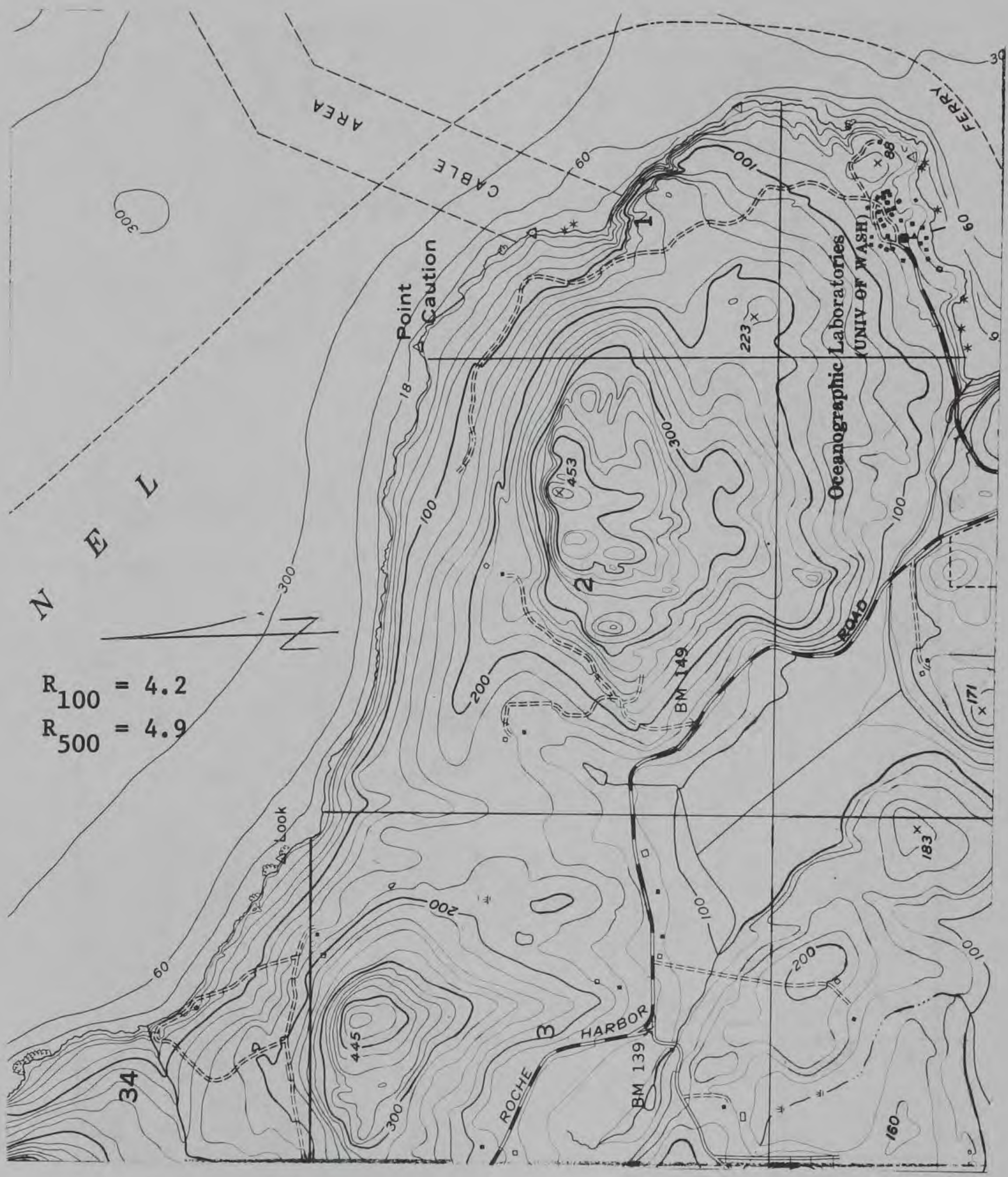

Figure 136. Friday Harbor, Wash., 76+N to 80N, R

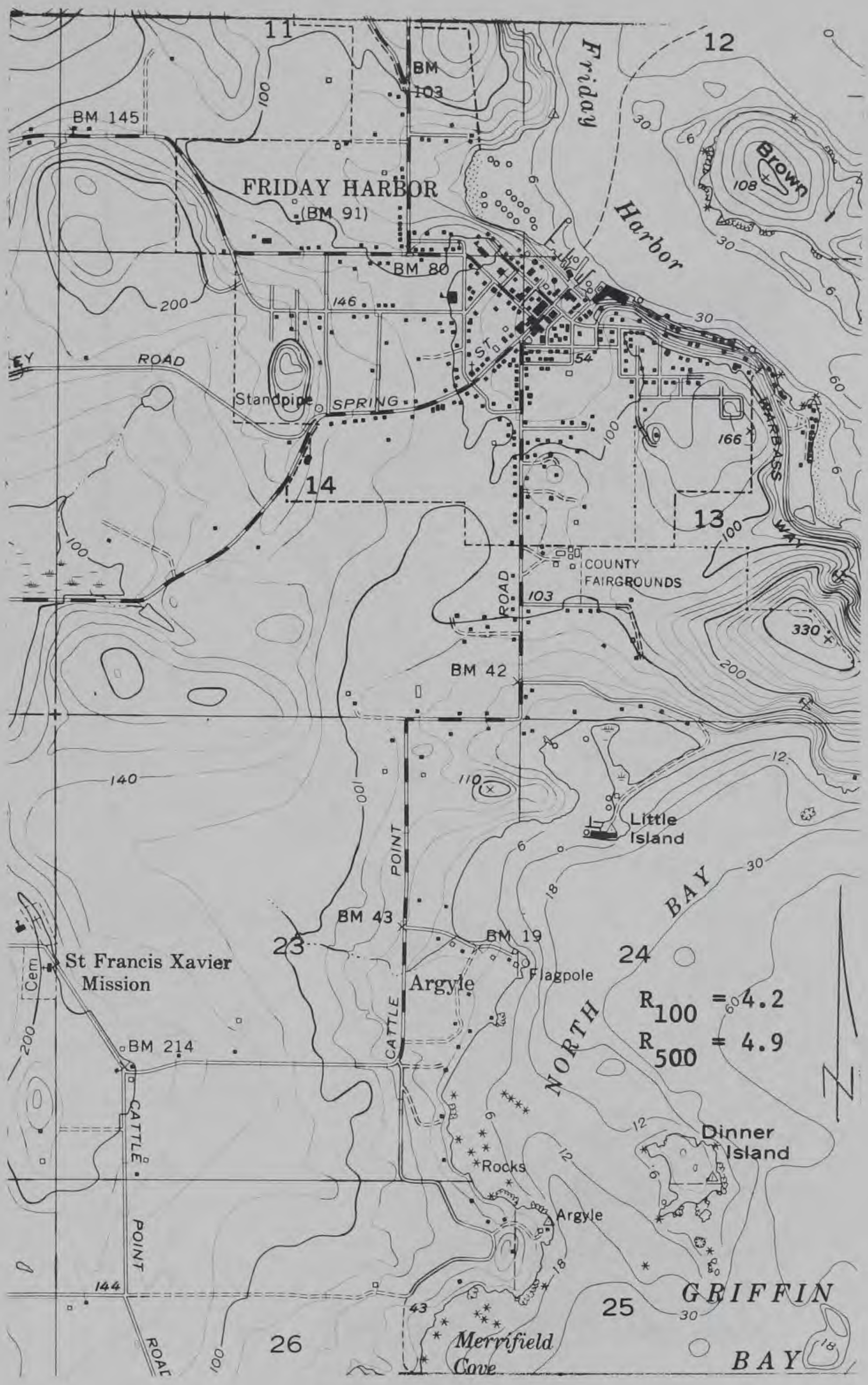

Figure 137. Friday Harbor, Wash., 97E to 00E, B

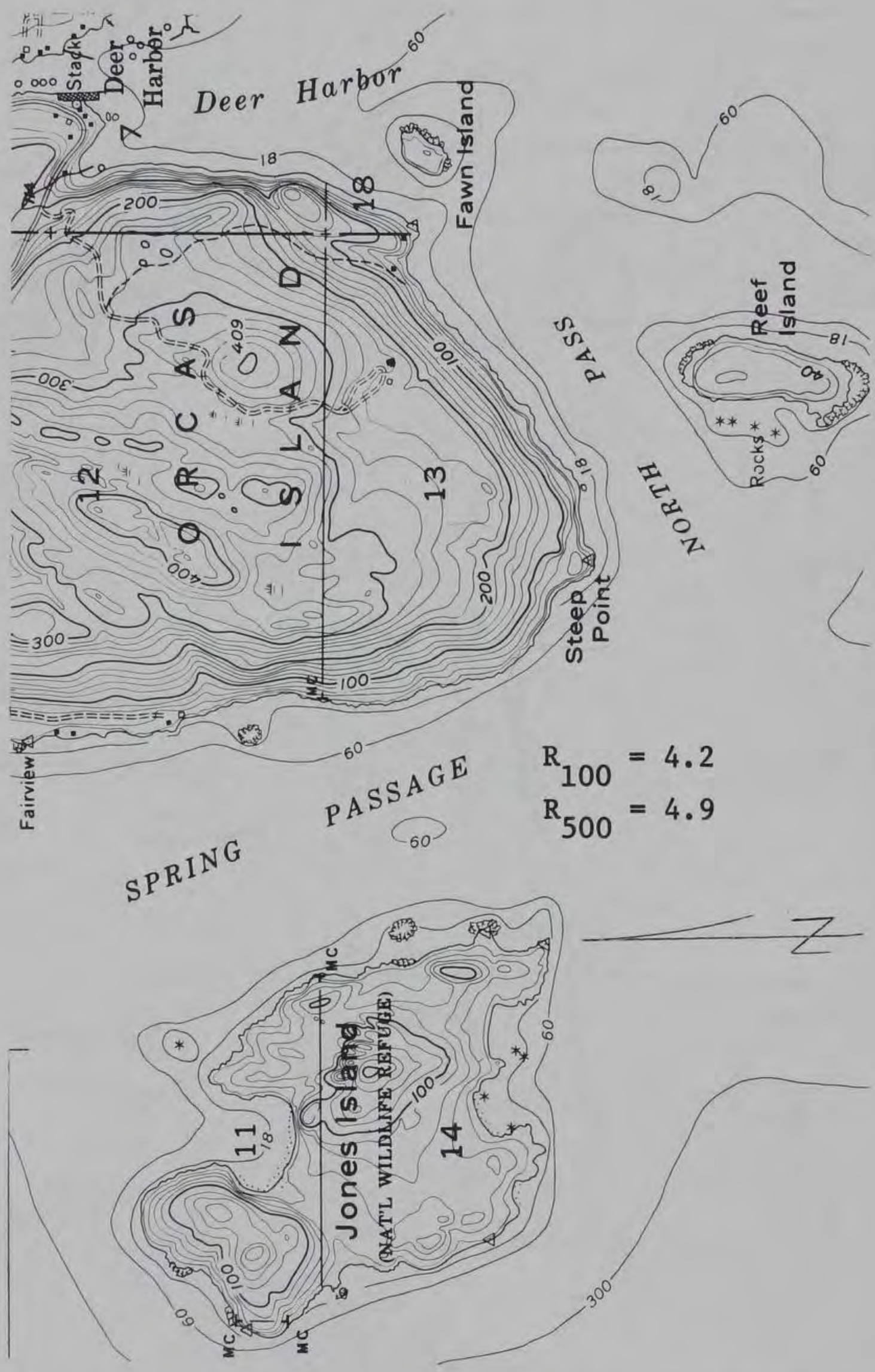

Figure 138. Friday Harbor, Wash., 83N to 85+N, R

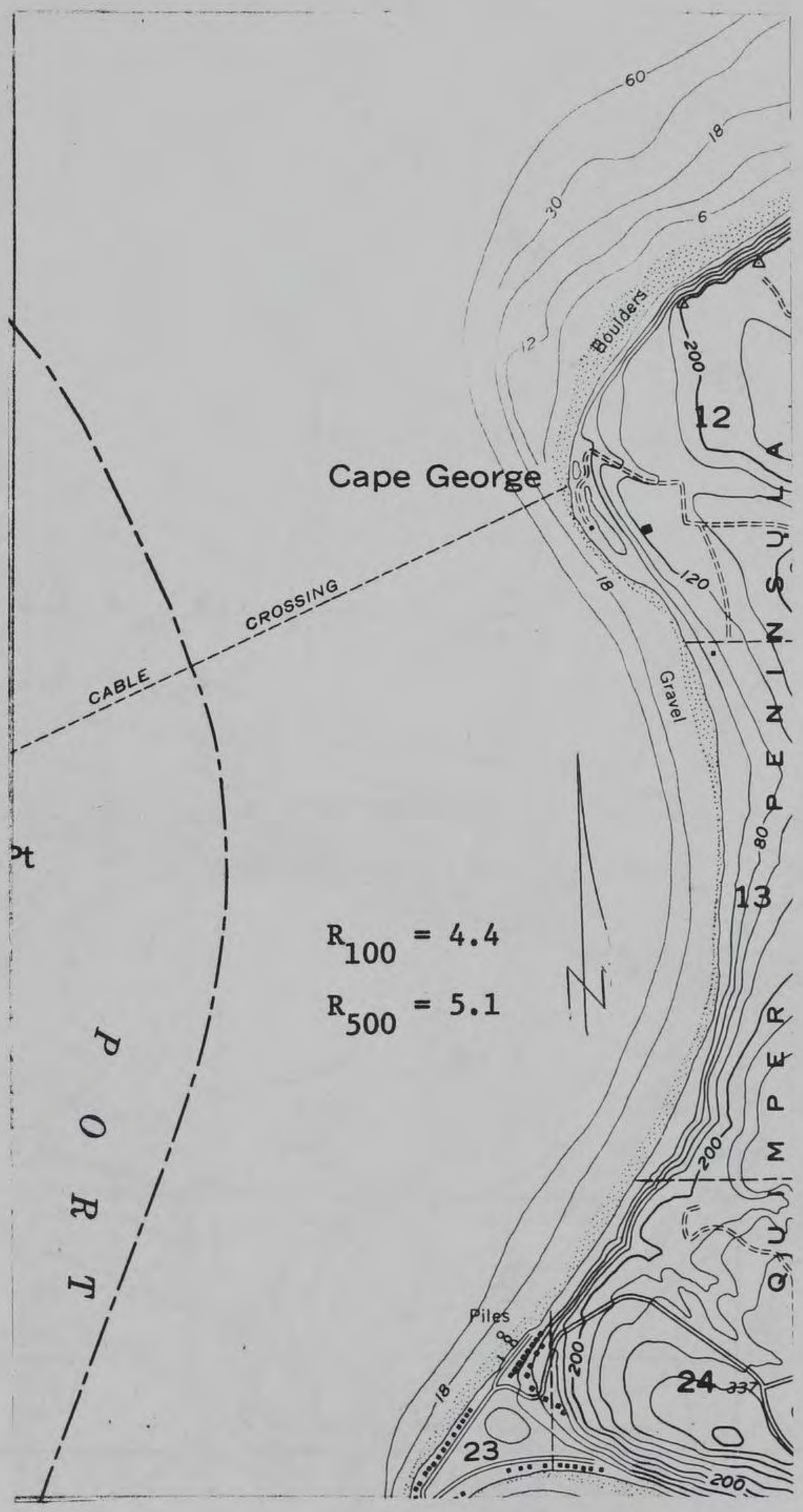

Figure 139. Gardiner, Wash., 24+N to 29N, R

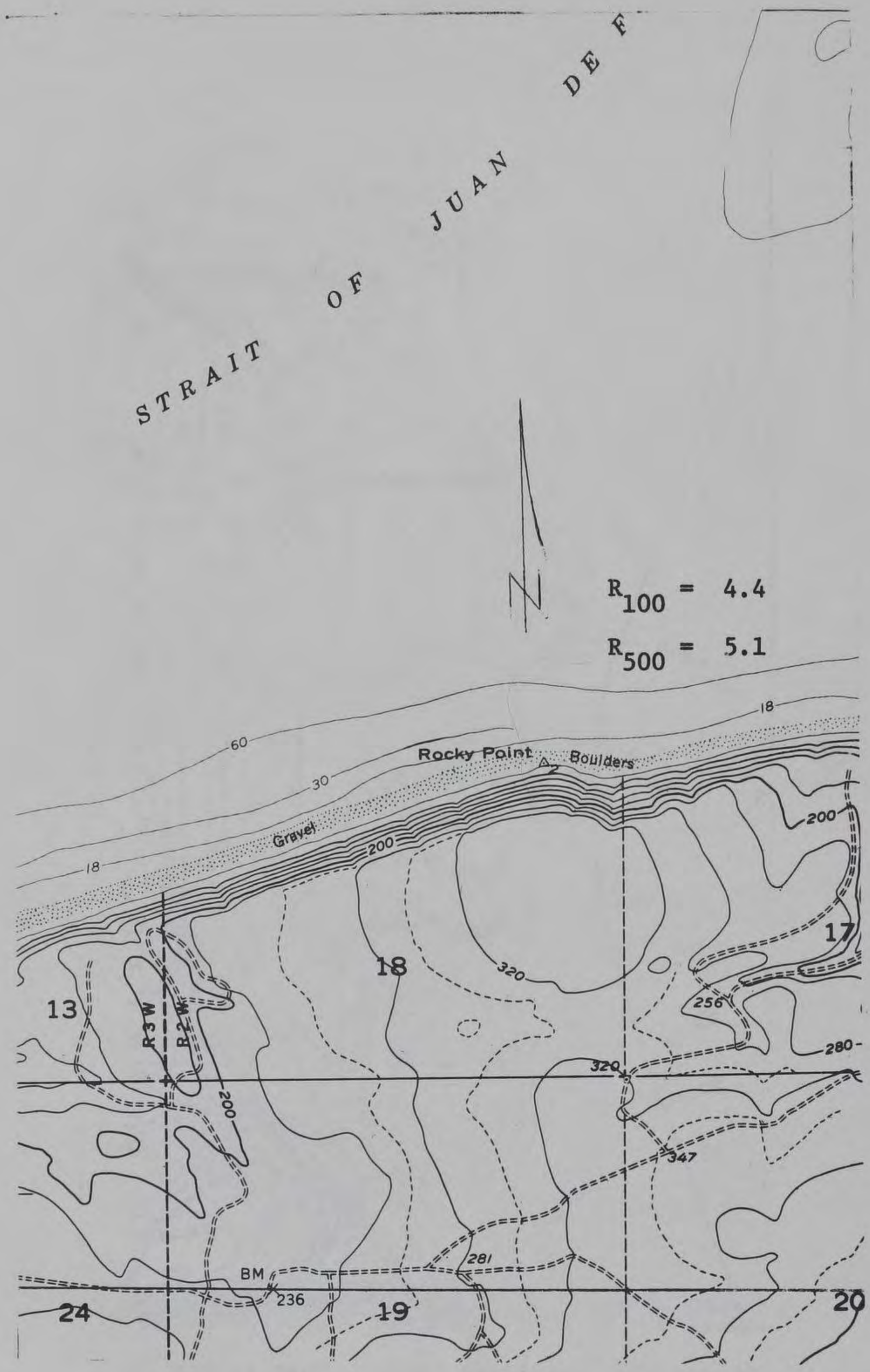

Figure 140. Gardiner, Wash., 25N to 29N, L

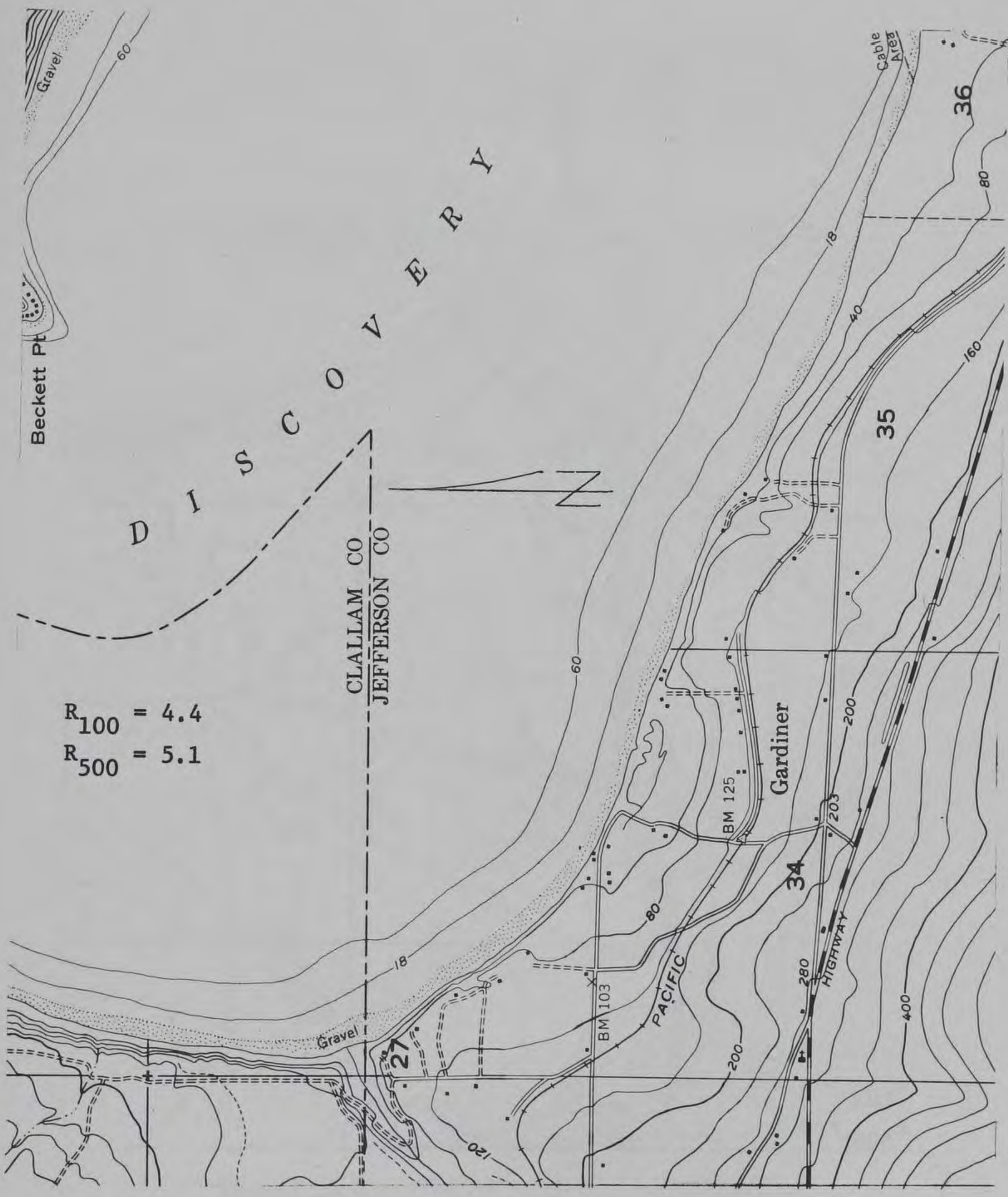

Figure 141. Gardiner, Wash., 21N to 24+N, R

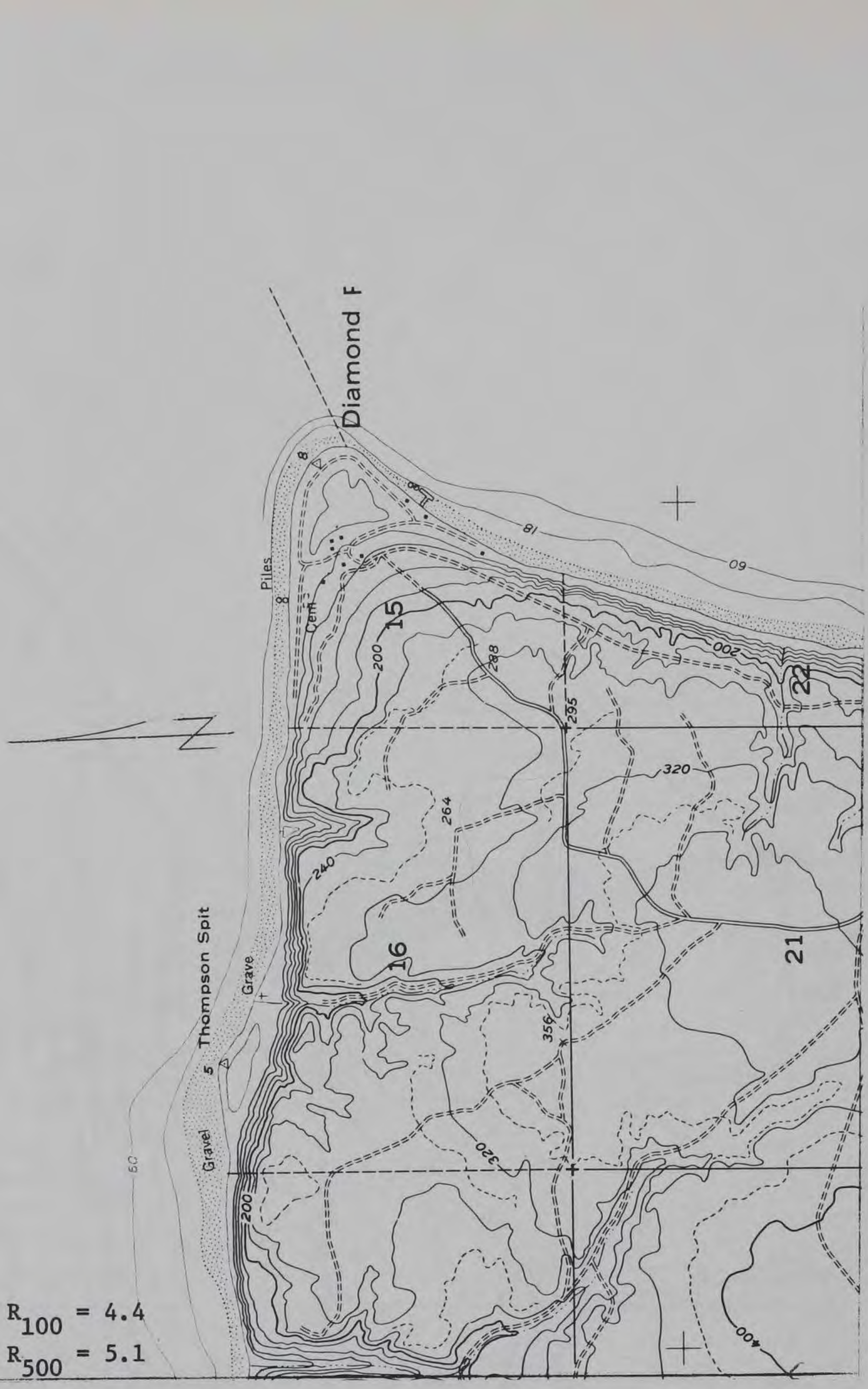

Figure 142. Gardiner, Wash., 03E to 07E, T

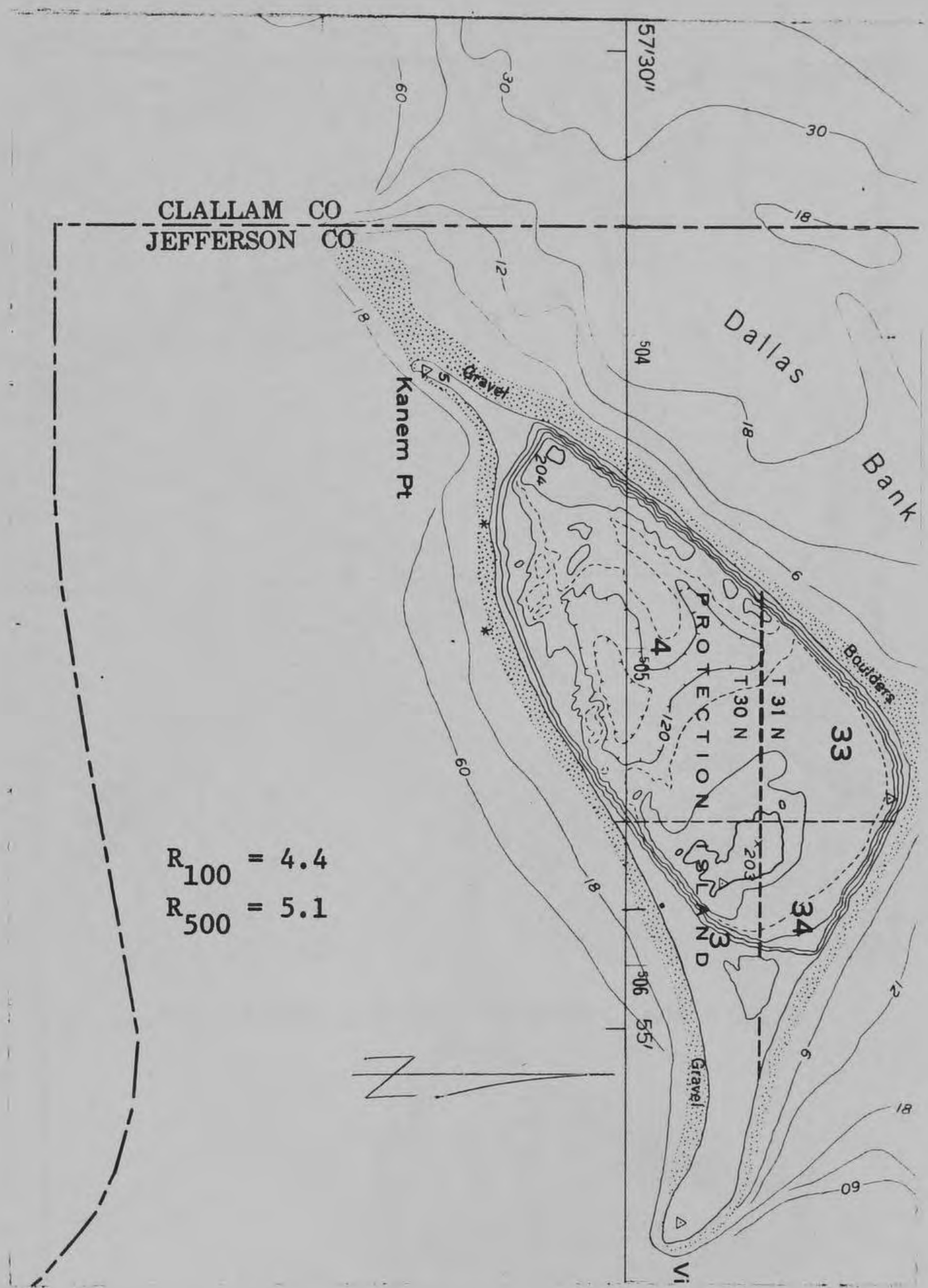

Figure 143. Gardiner, Wash., 03E to 07E, T

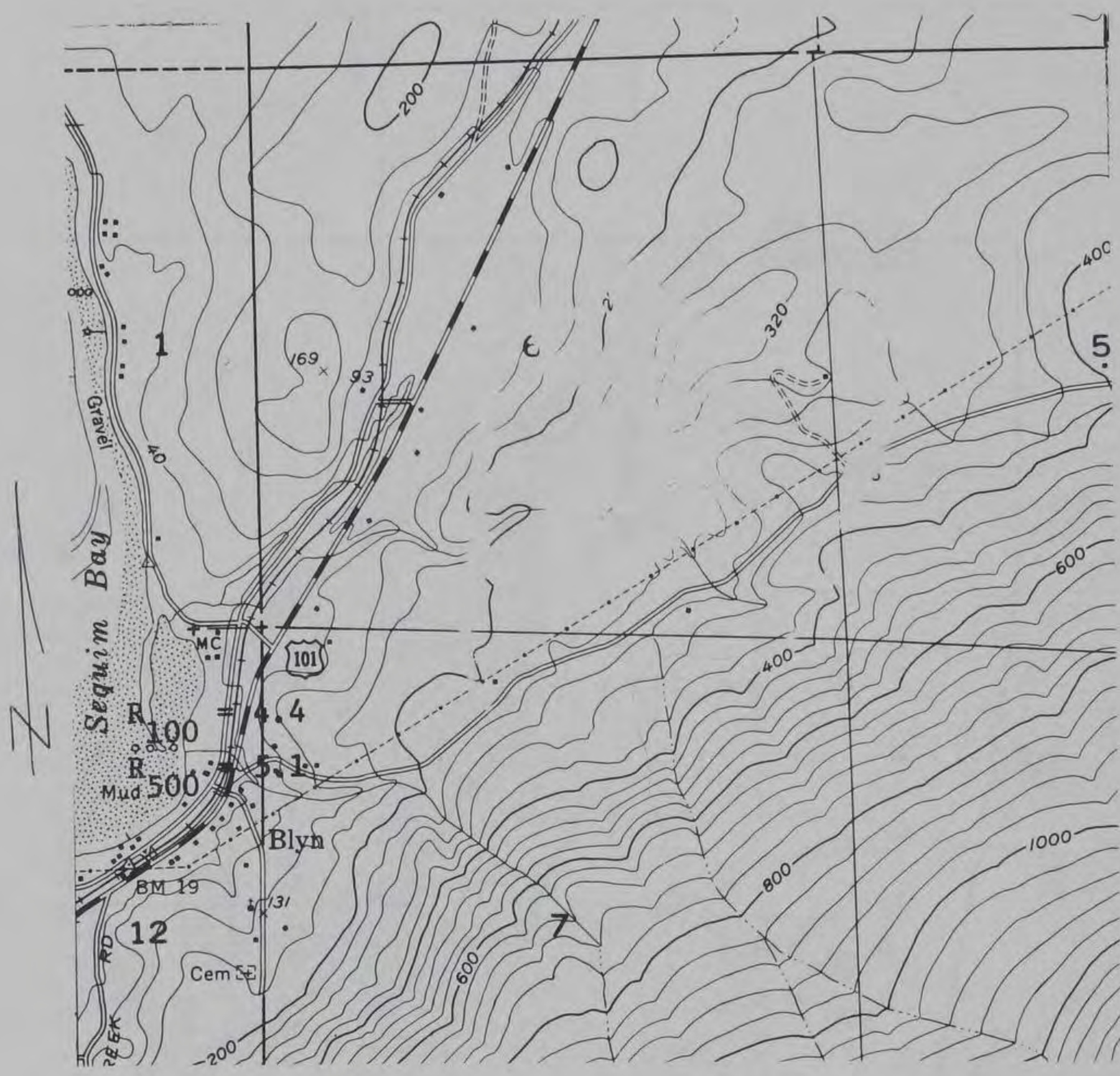

Figure 144. Gardiner, Wash., 18N to 21N, L

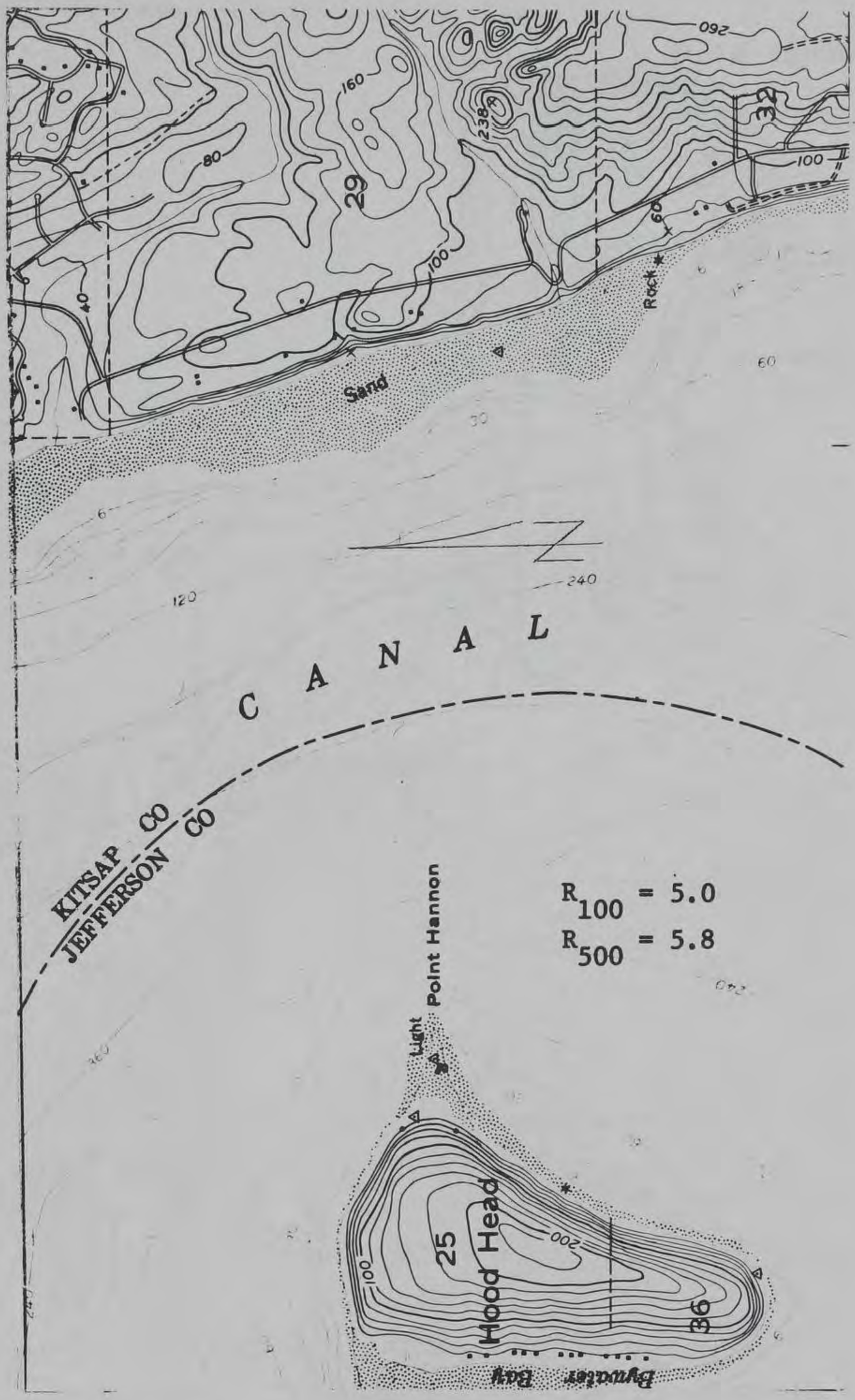

Figure 145. Hansville, Wash., 03-N to 05N, L

$R_{100} = 5.2$

$R_{500} = 6.0$

Figure 146. Hansville, Wash., 05N to 09+N, L

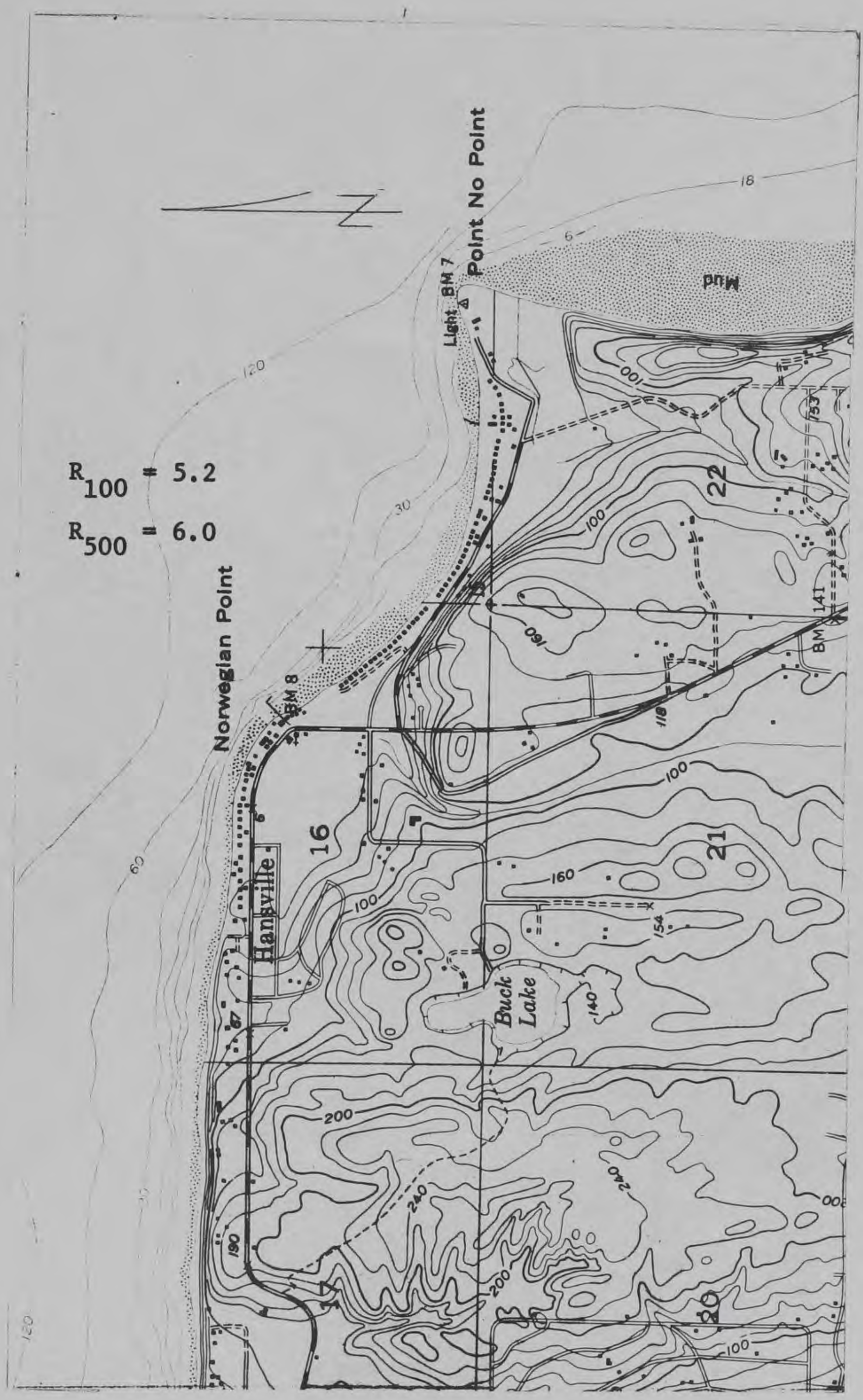

Figure 147. Hansville, Wash., 05+N to 08N, R

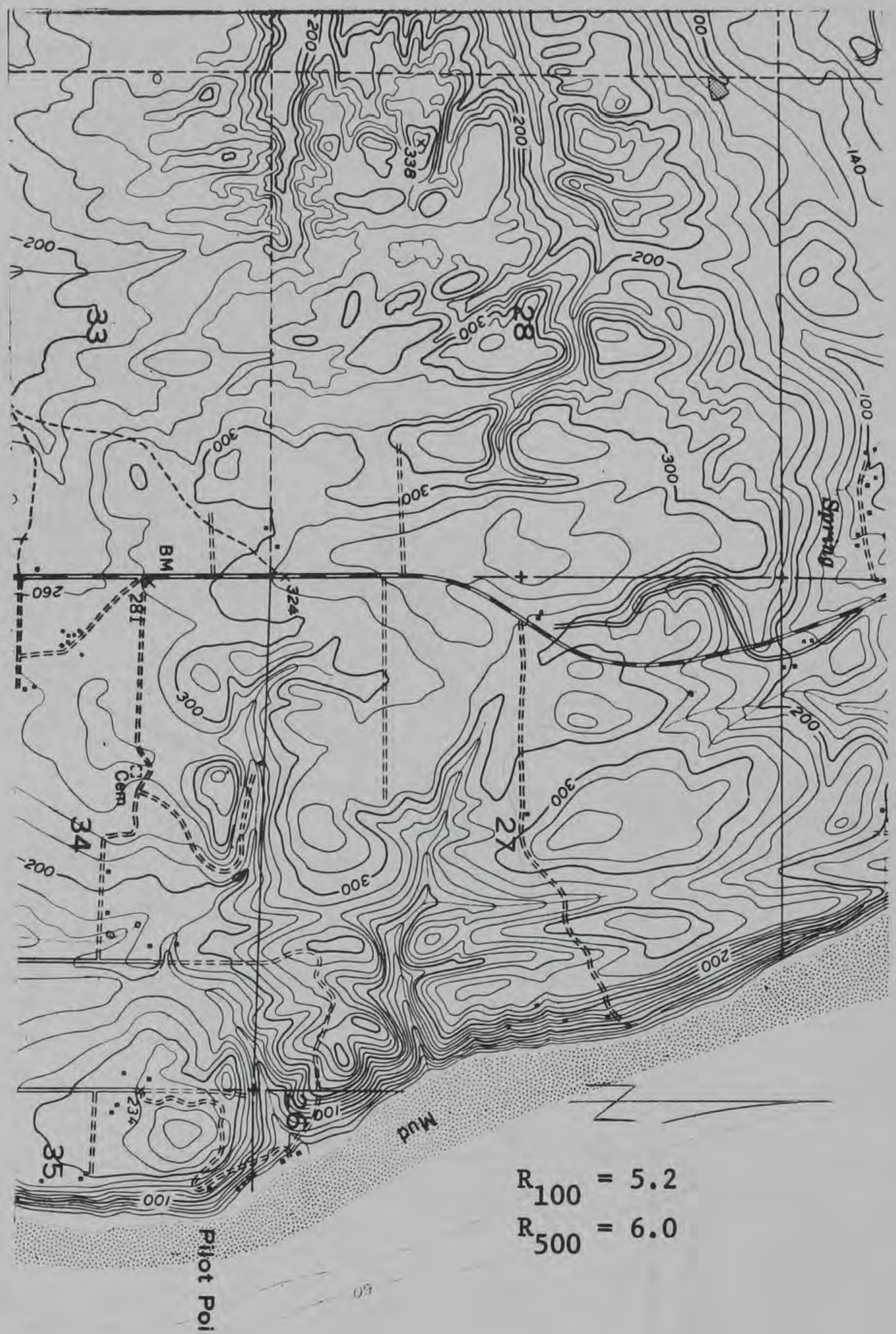

$R_{100} = 5.2$
$R_{500} = 6.0$

Figure 148. Hansville, Wash., 03N to 05+N, R

Figure 149. Hansville, Wash., 33E to 37+E, T

Figure 150. Joyce, Wash., 48°07'48"+N to 48°10'01" N, R

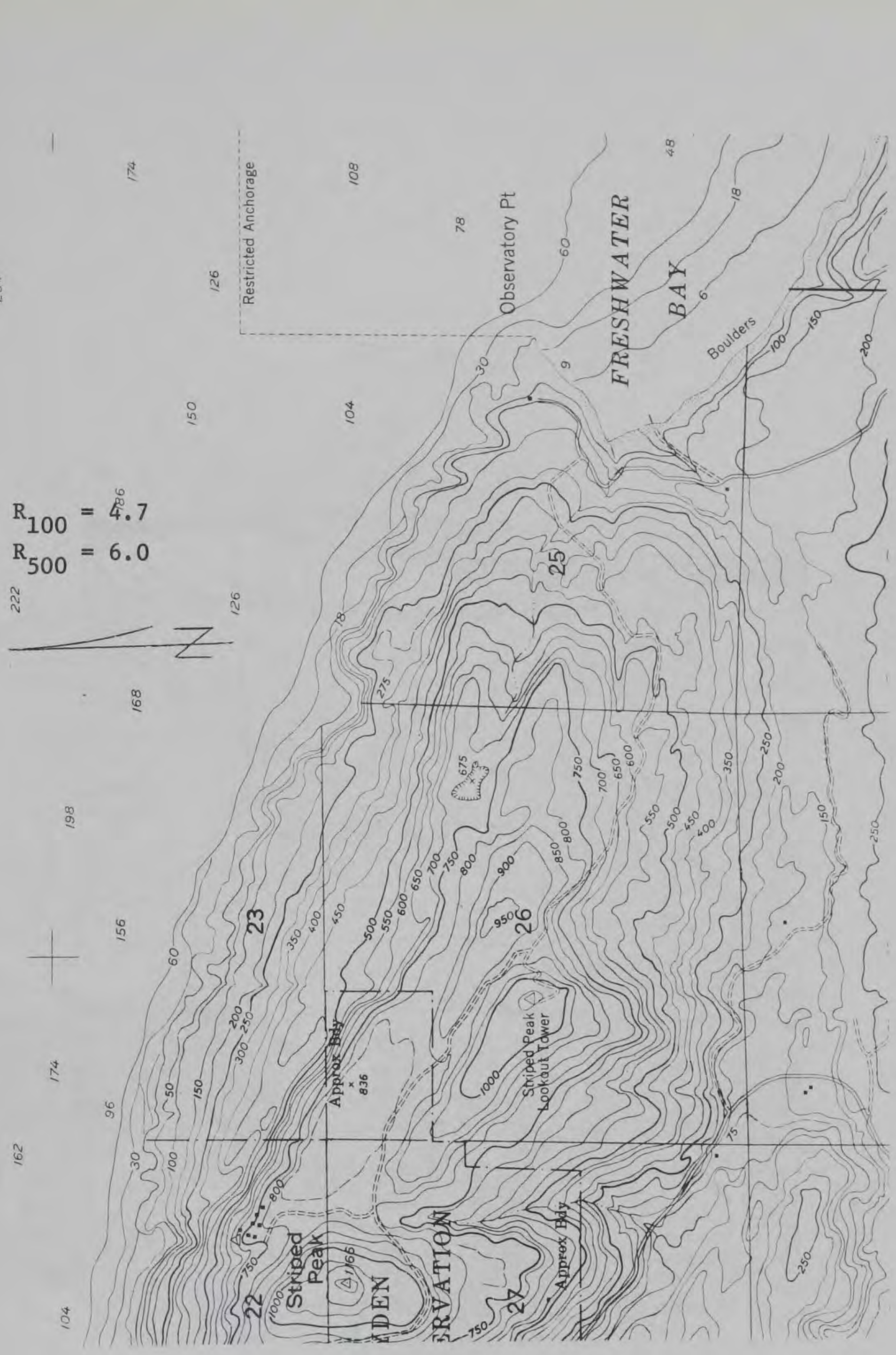

Figure 151. Joyce, Wash., 48°07'48" to 48°10'01" N, R

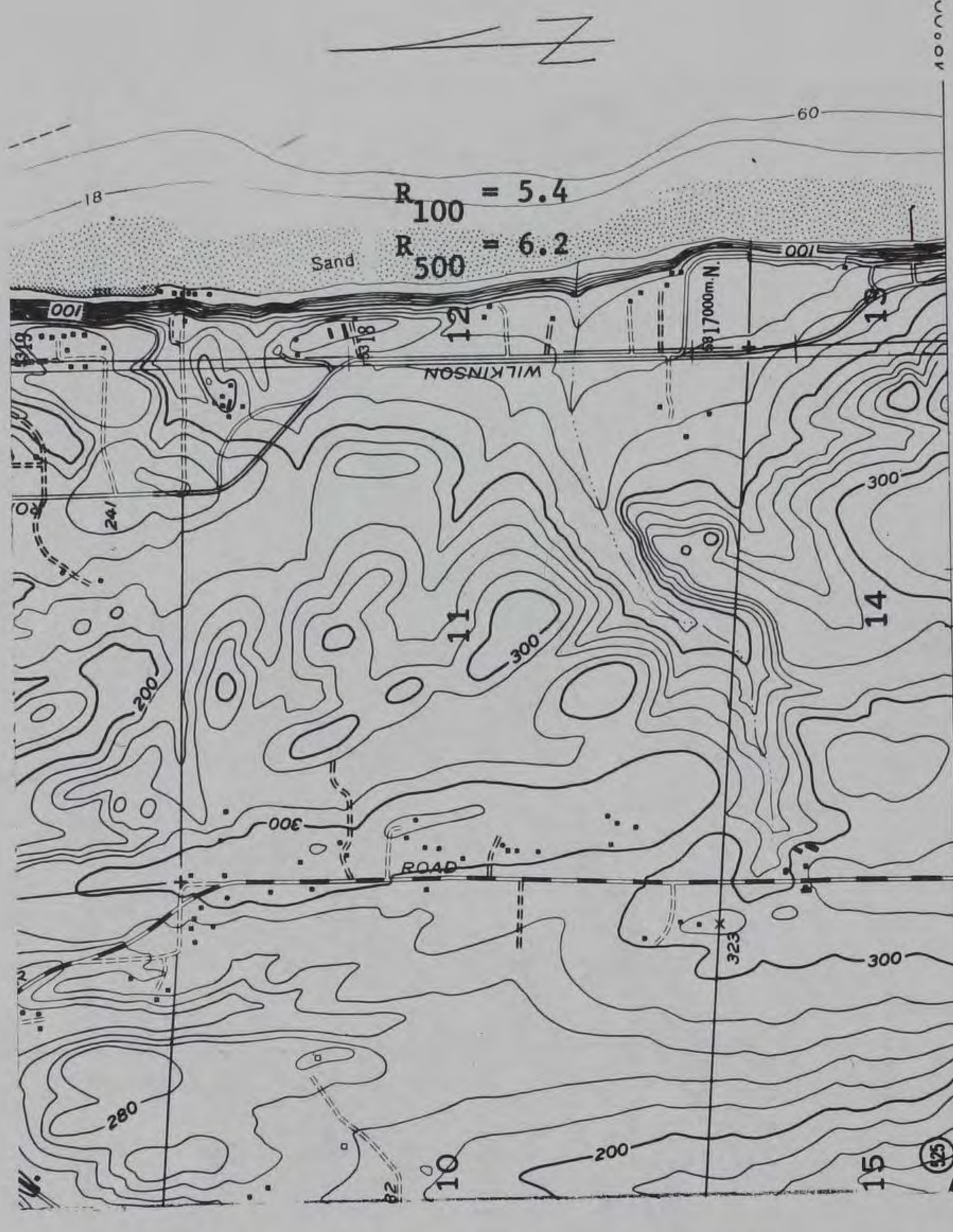

Figure 152. Langley, Wash., 16+N to 19N, R

Figure 153. Marysville, Wash., 17-N to 20N, L

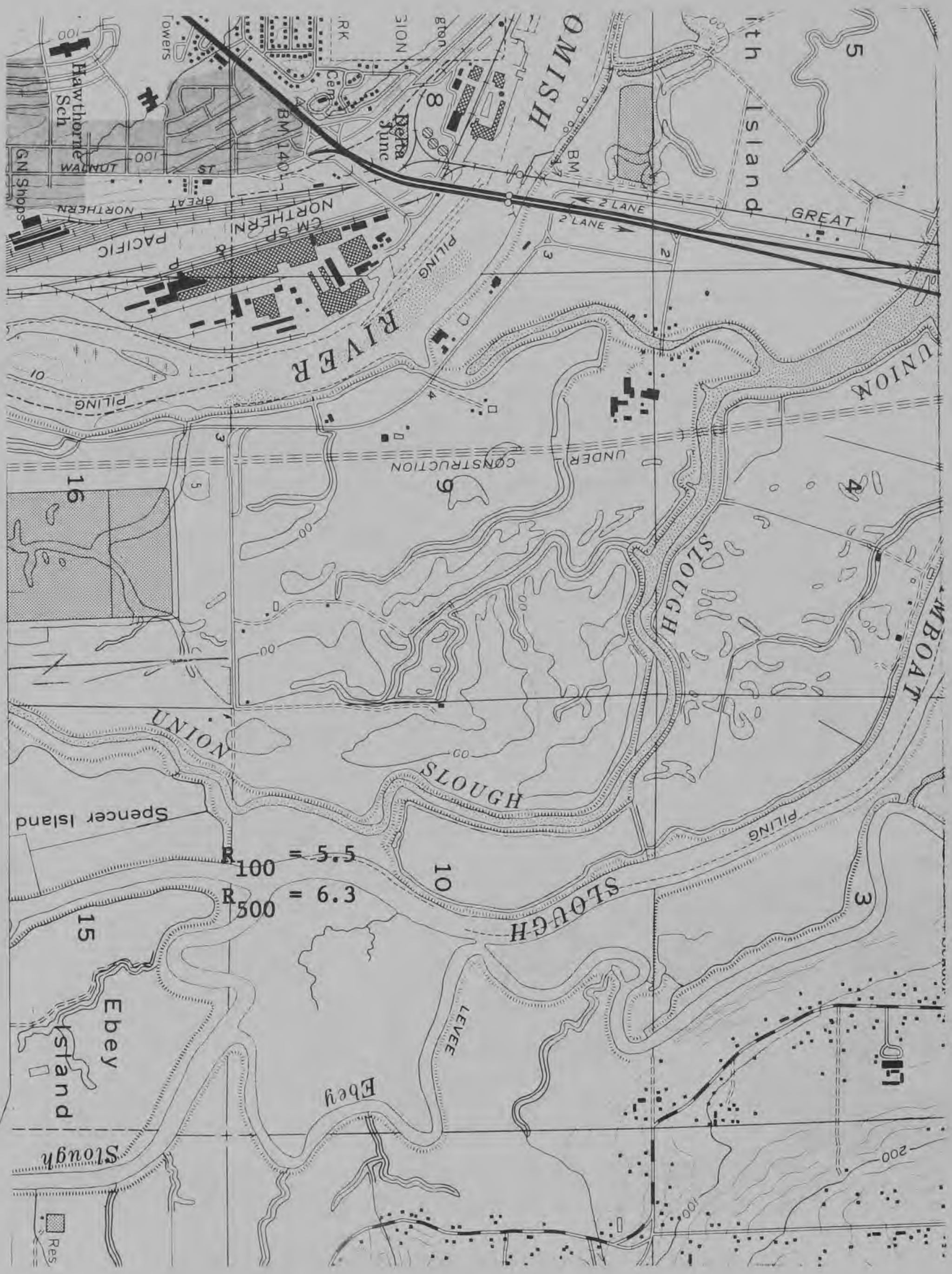

Figure 154. Marysville, Wash., 17-N to 20N, R

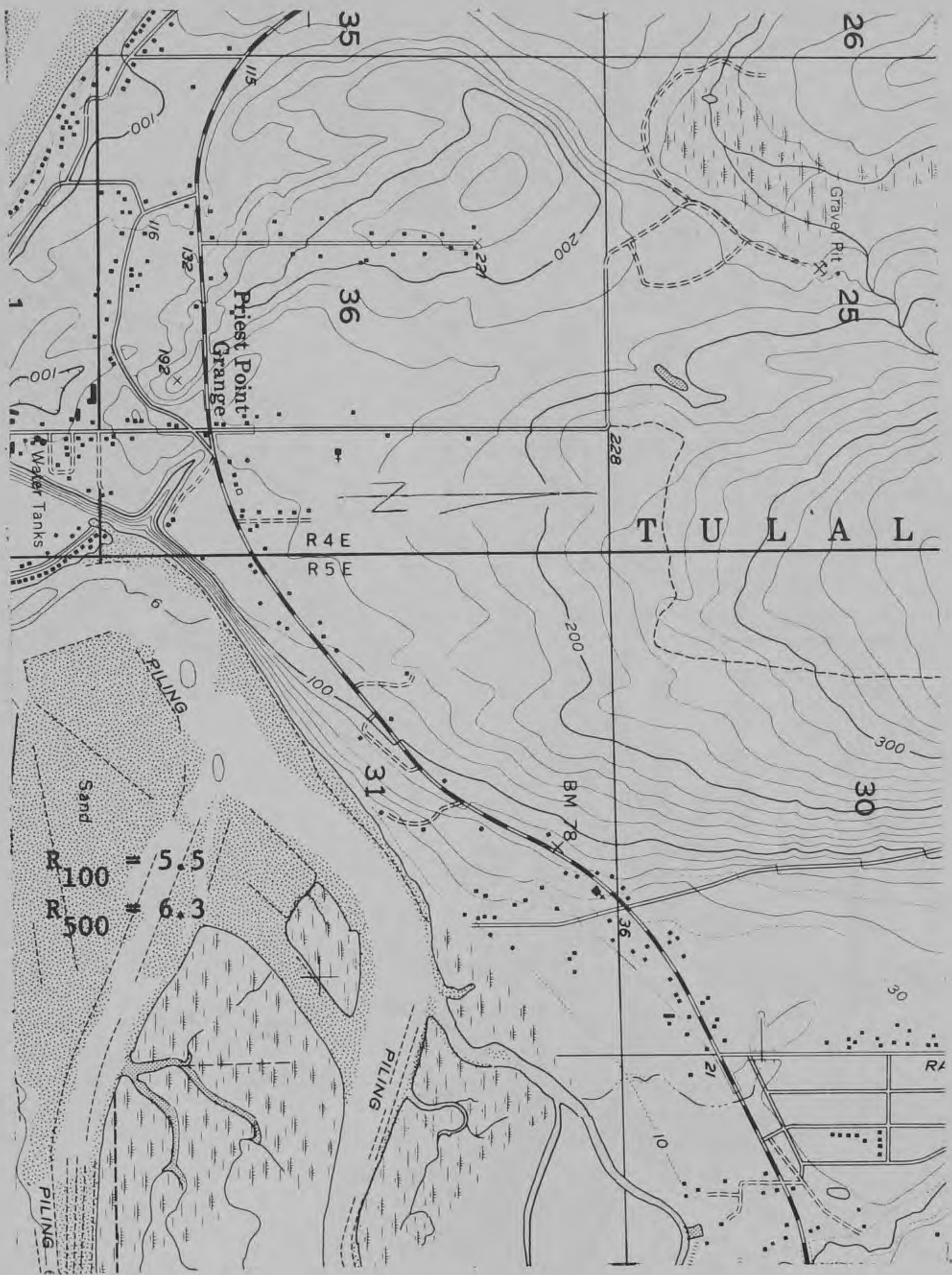

Figure 155. Marysville, Wash., 20N to 23N, L

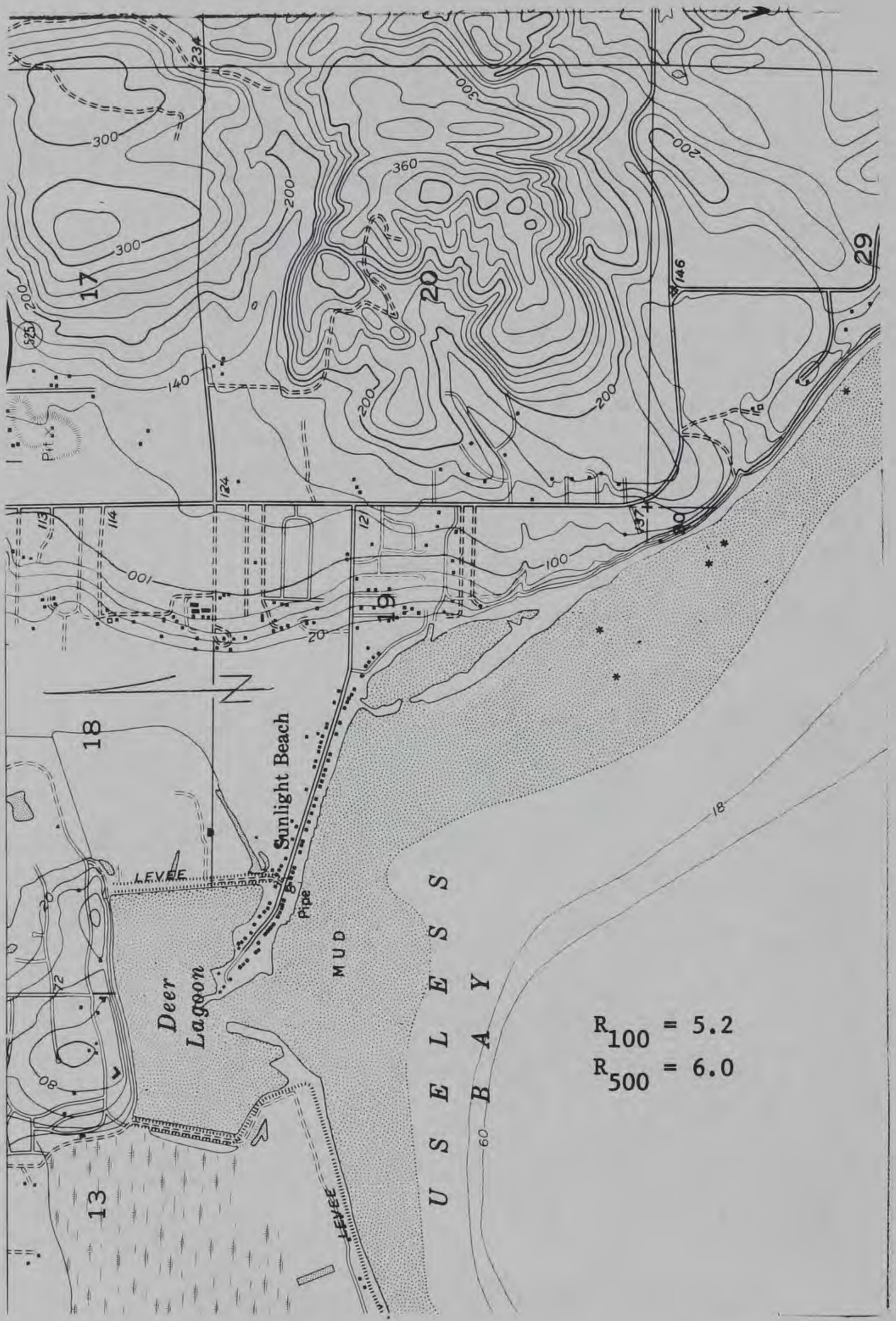

Figure 156. Maxwelton, Wash., 13N to 16+N, L

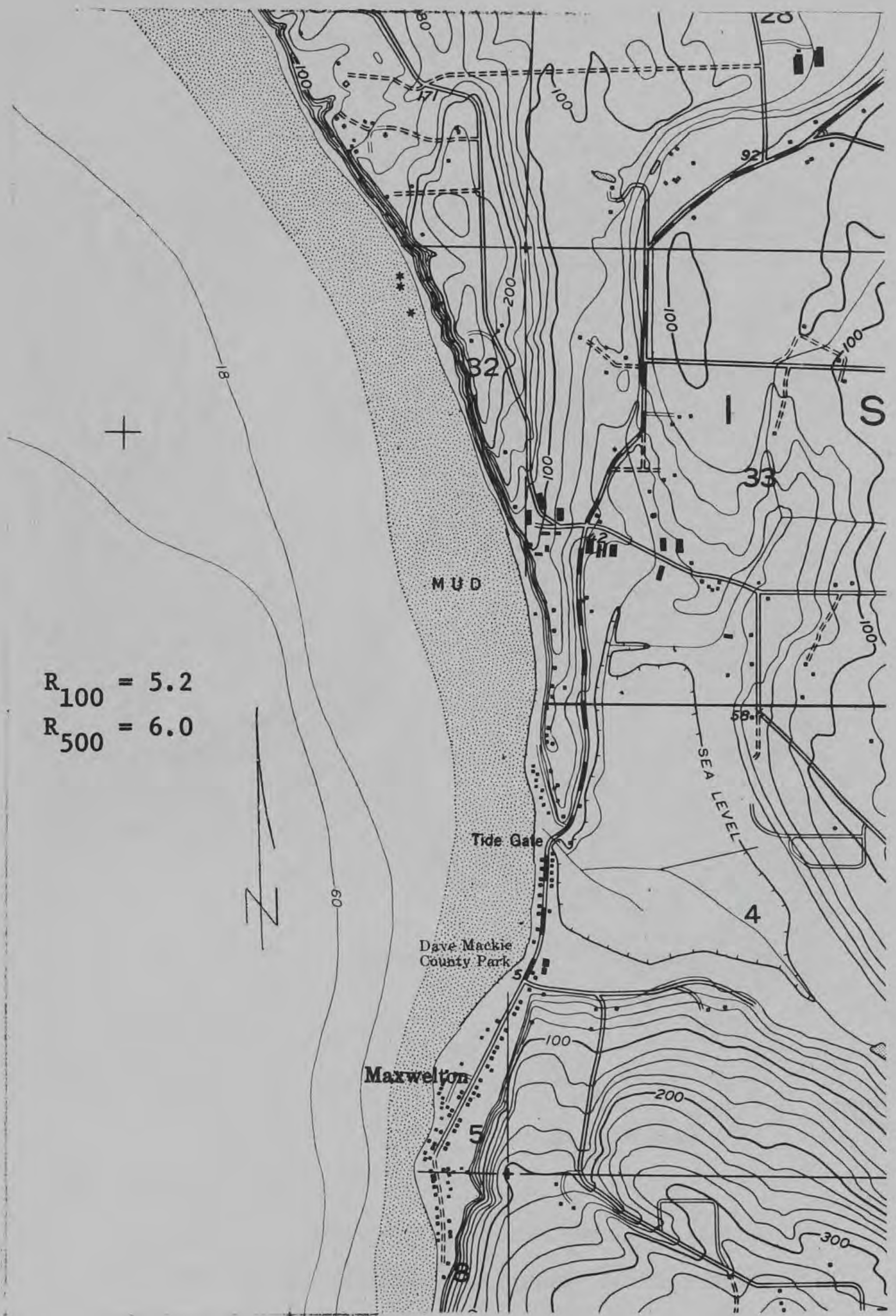

Figure 157. Maxwelton, Wash., 08+N to 13N, L

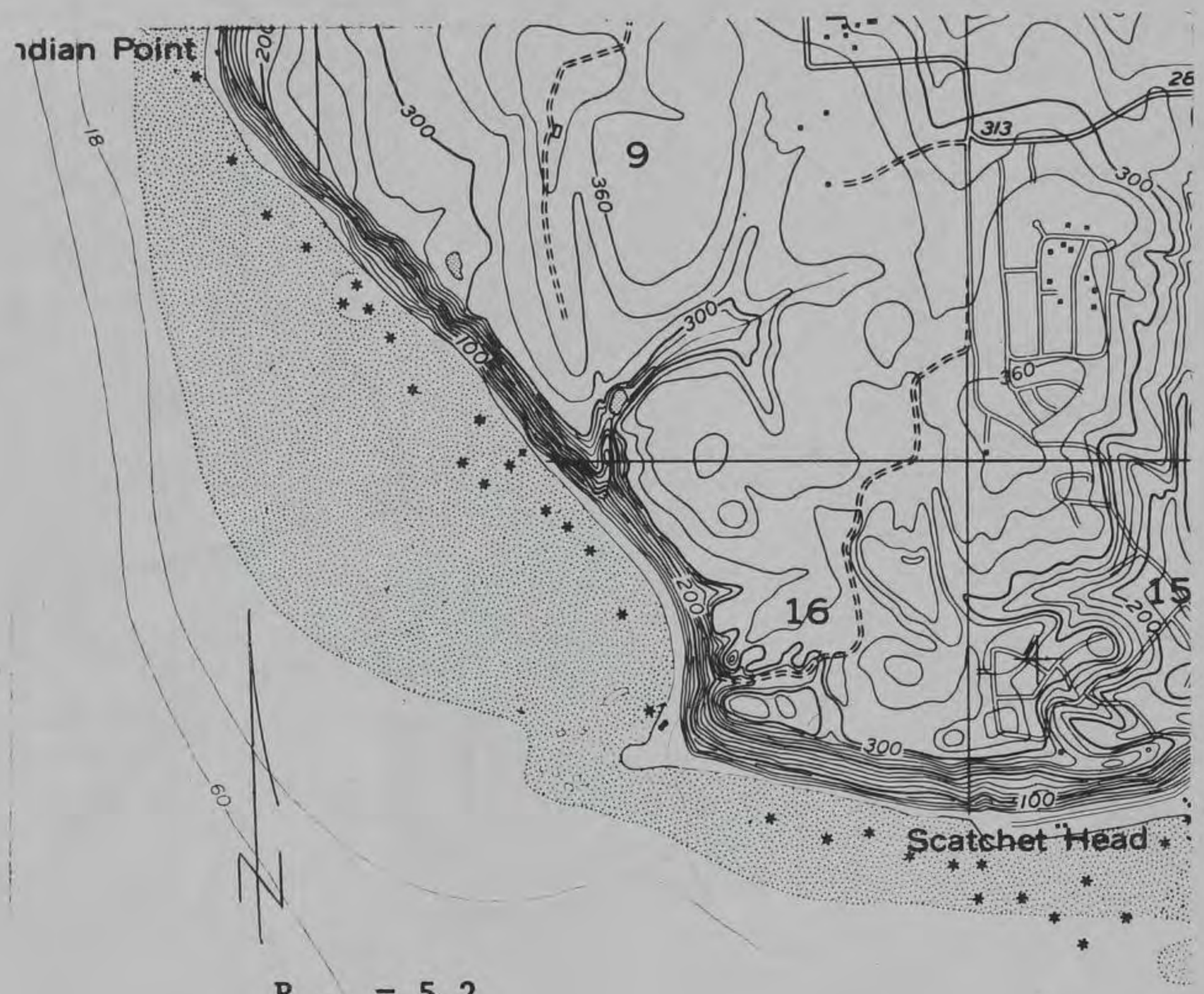

$R_{100} = 5.2$

$R_{500} = 6.0$

Figure 158. Maxwelton, Wash., 41E to 44E, B

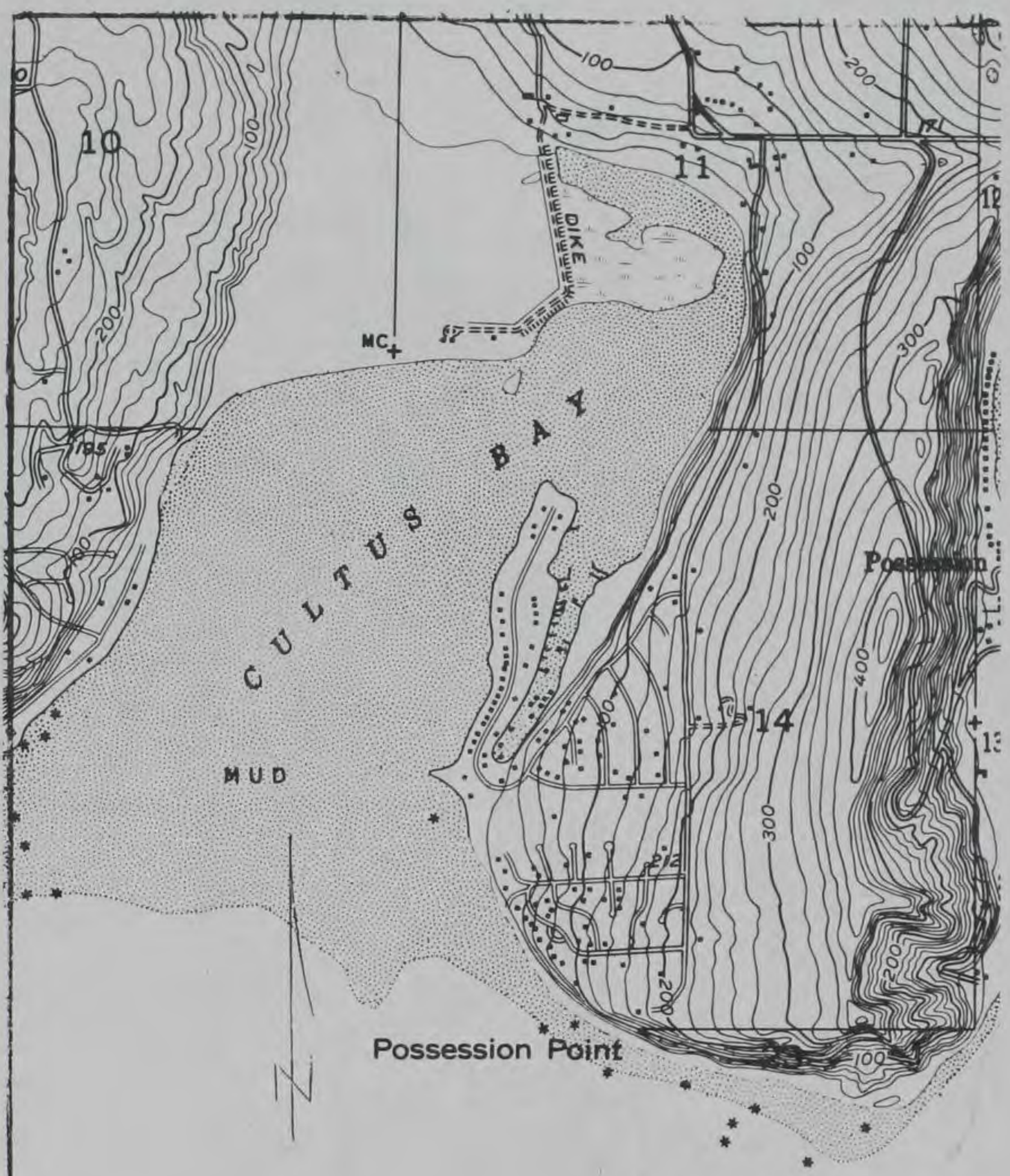

Figure 159. Maxwelton, Wash., 44E to 46E, B

$R_{100} = 5.4$

$R_{500} = 6.2$

Figure 160. Mukilteo, Wash., 49E to 52E, B

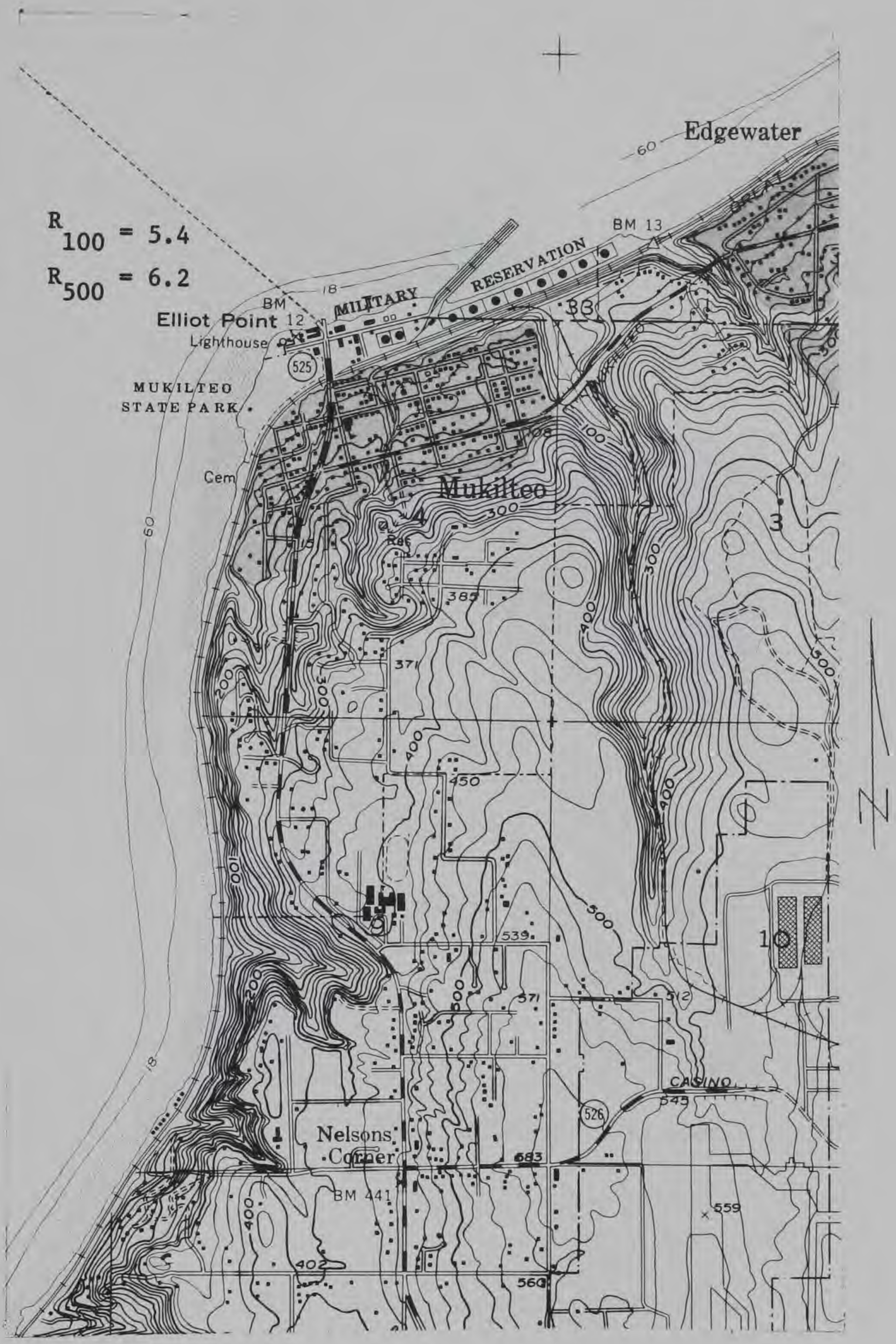

Figure 161. Mukilteo, Wash., 51E to 54E, B

$R_{100} = 5.4$
$R_{500} = 6.2$

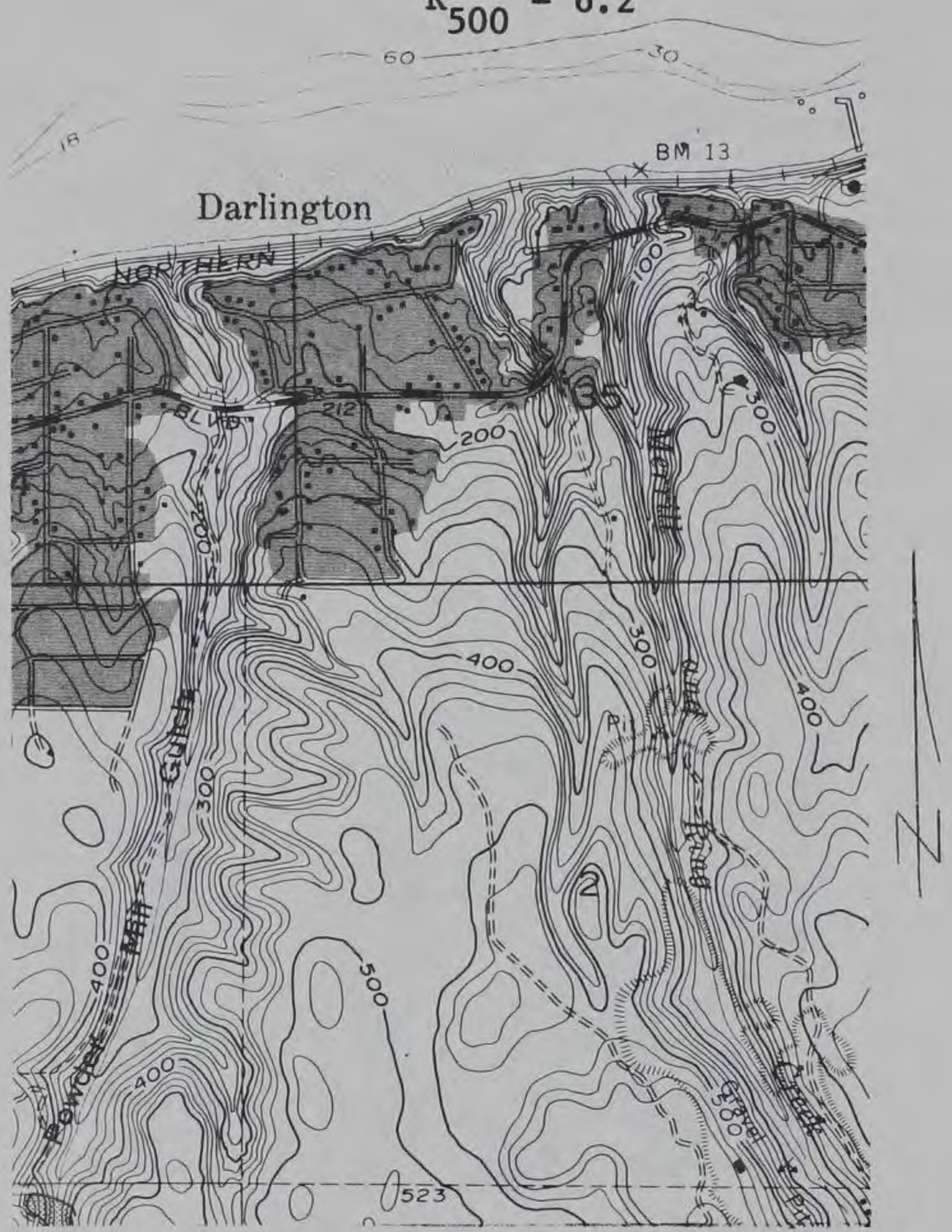

Figure 162. Mukilteo, Wash., 09N to 14N, R

Figure 163. Mukilteo, Wash., 06N to 10N, L

$R_{100} = 5.4$
$R_{500} = 6.2$

Figure 164. Mukilteo, Wash., 10N to 13N, L

Figure 165. Mukilteo, Wash., 13N to 16+N, L

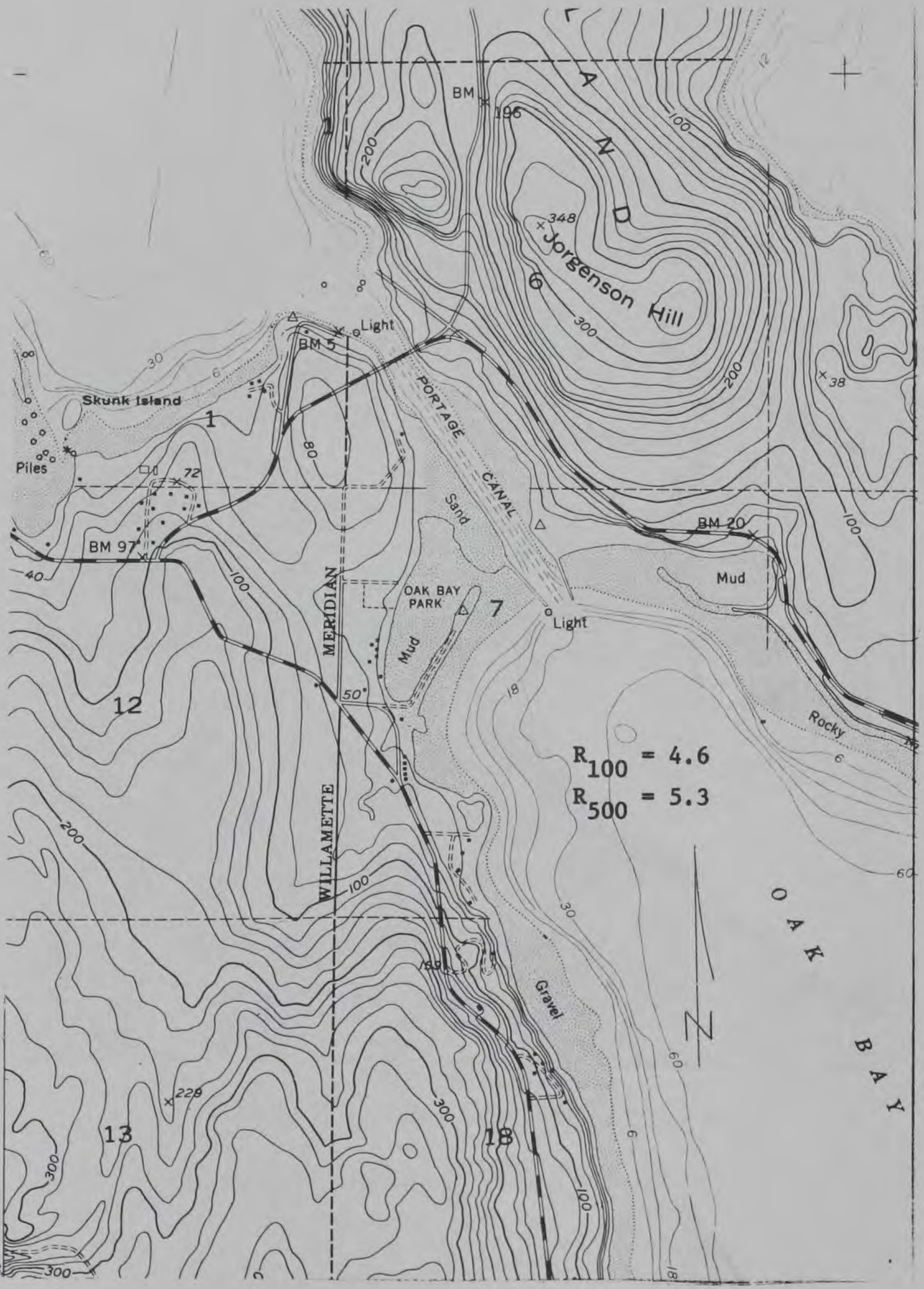

$R_{100} = 4.6$

$R_{500} = 5.3$

Figure 166. Nordland, Wash., 16+N to 21N, L

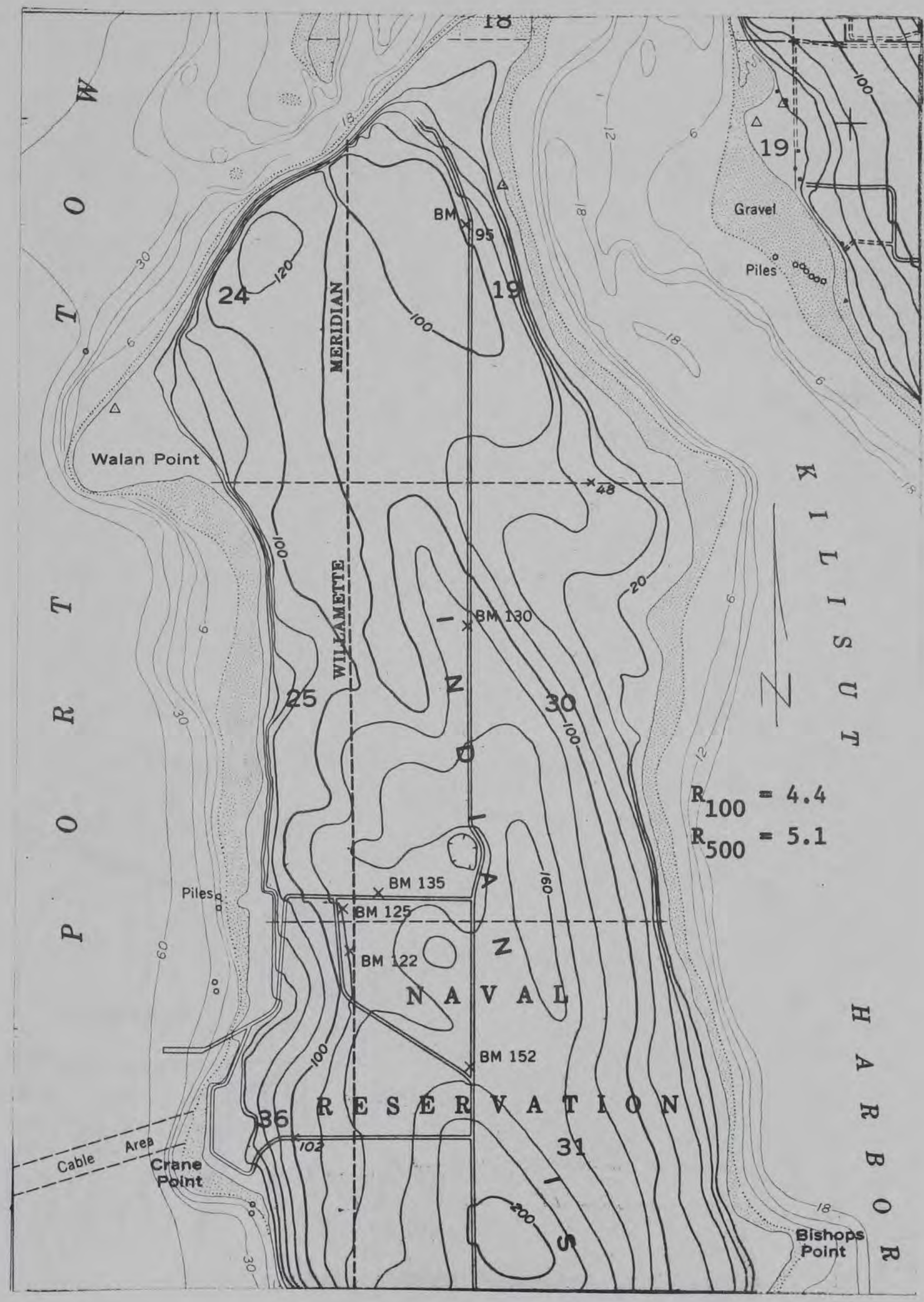

Figure 167. Nordland, Wash., 21N to 25+N, L

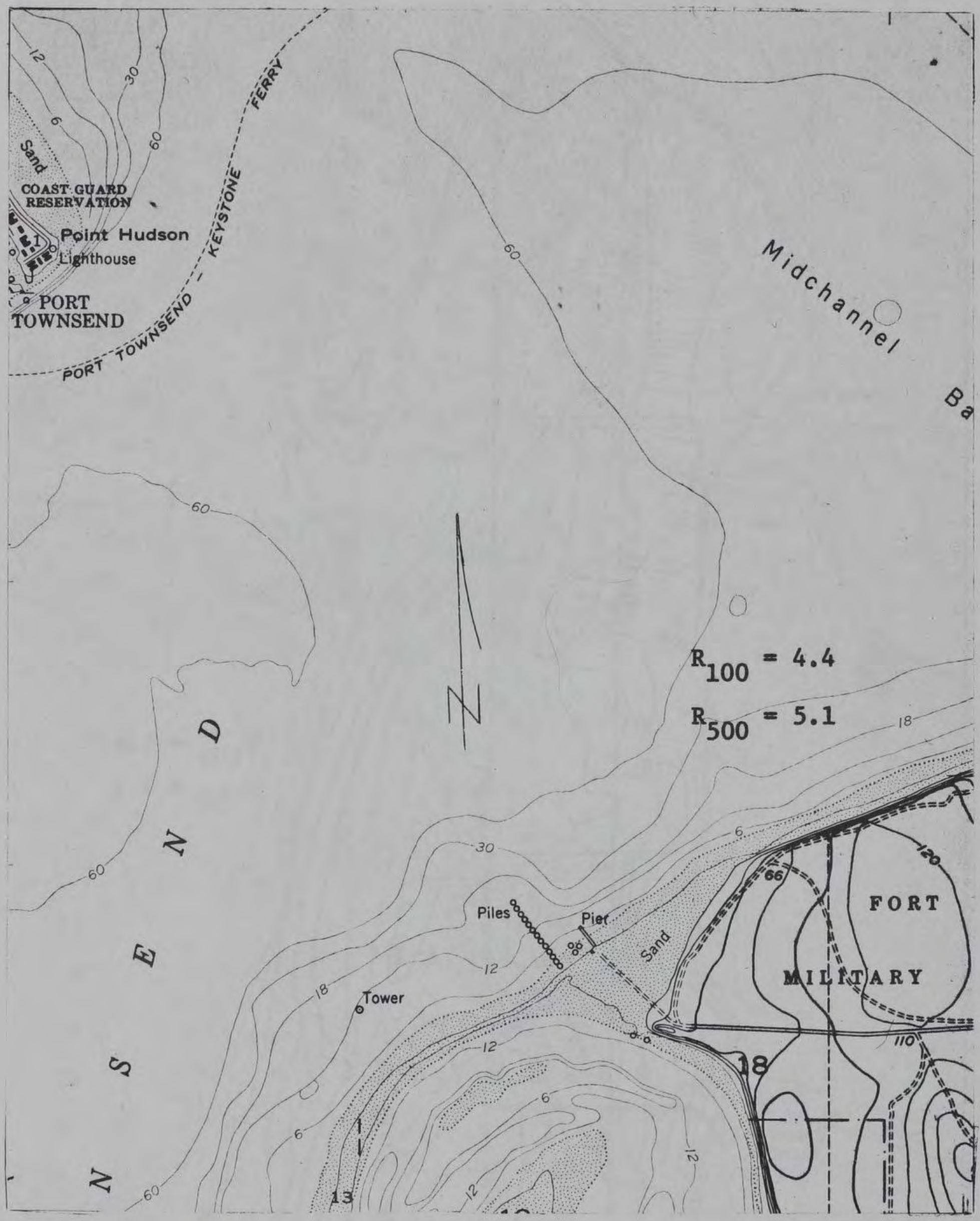

Figure 168. Nordland, Wash., 18+E to 22E, T

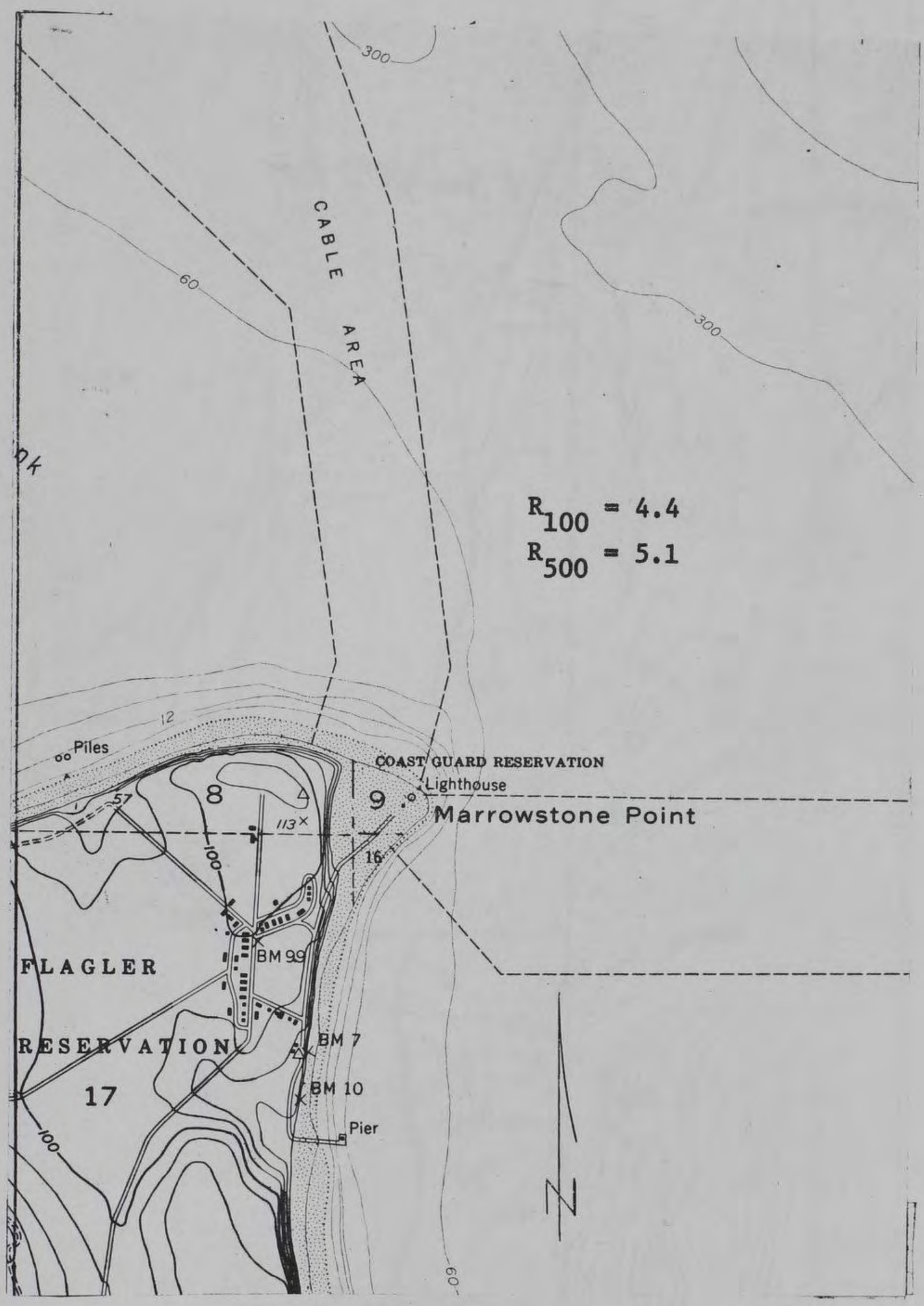

Figure 169. Nordland, Wash., 22E to 25E, T

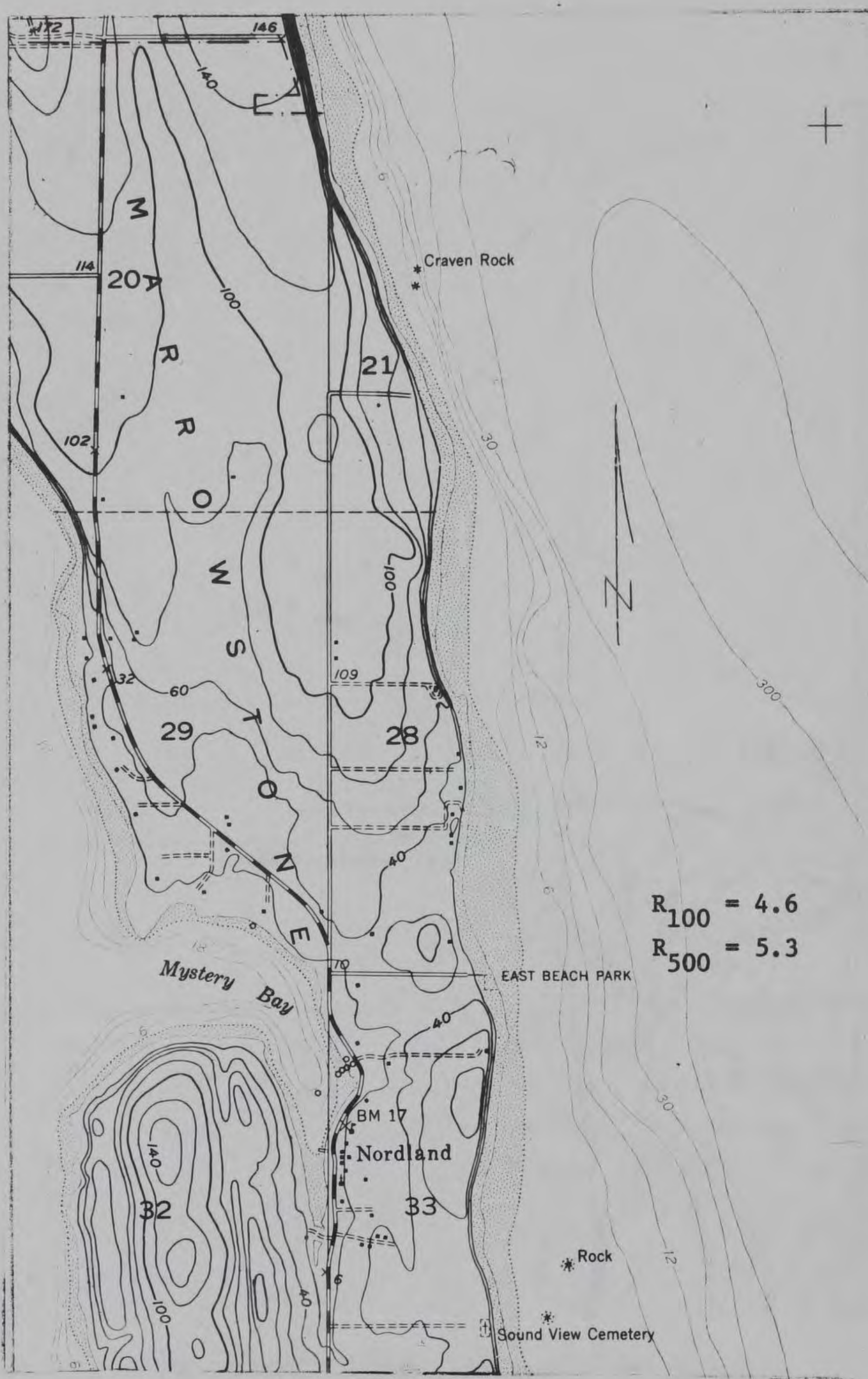

Figure 170. Nordland, Wash., 21N to 25+N, R

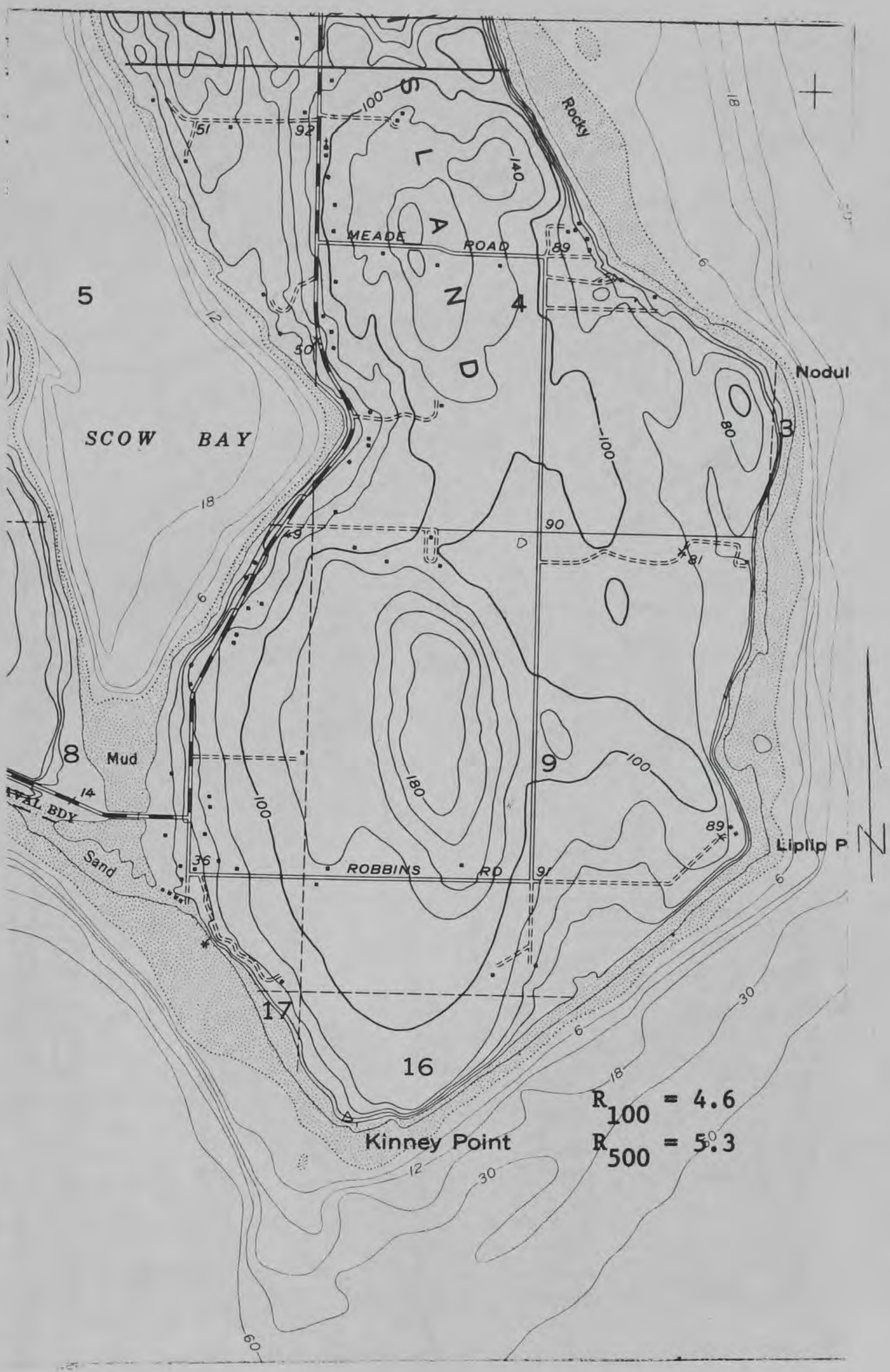

Figure 171. Nordland, Wash., 22E to 25E, B

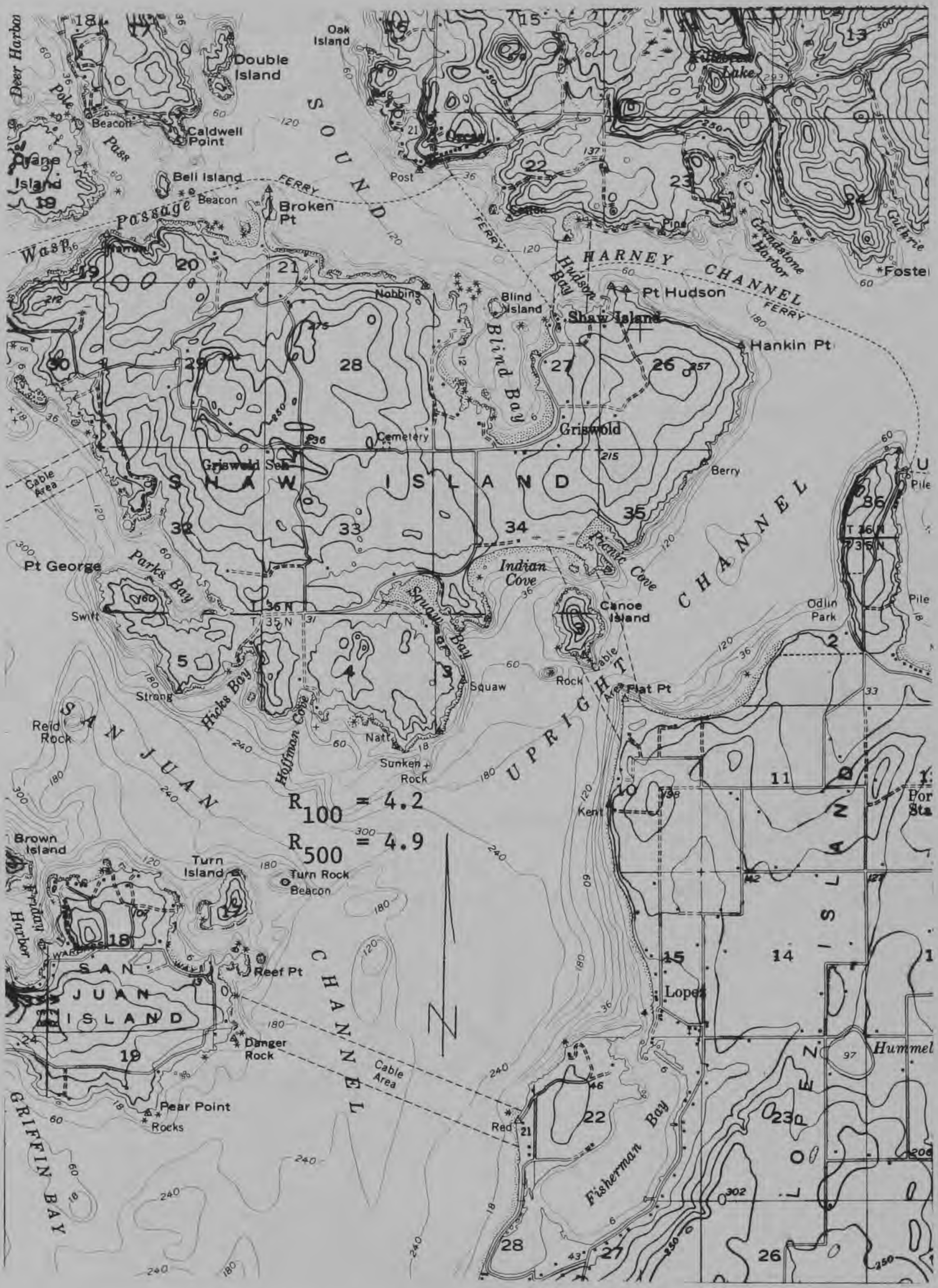

Figure 172. Orcas Island, Wash., 71+N to 84N, L (1:62500)

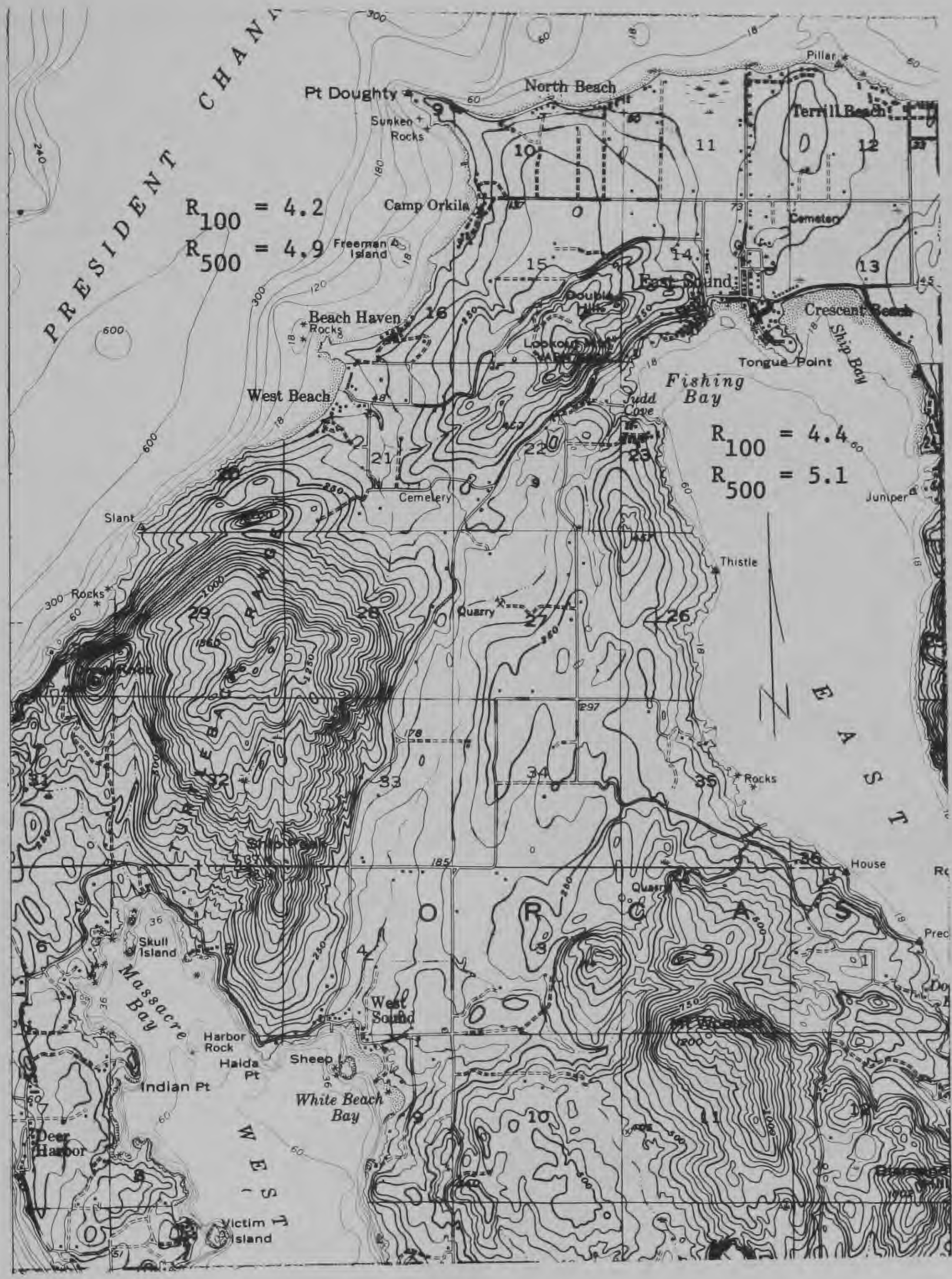

Figure 173. Orcas Island, Wash., 84N to 96N, L

Figure 174. Orcas Island, Wash., 84N to 96N, R (1:62500)

Figure 175. Orcas Island, Wash., 71+N to 84N, L (1:62500)

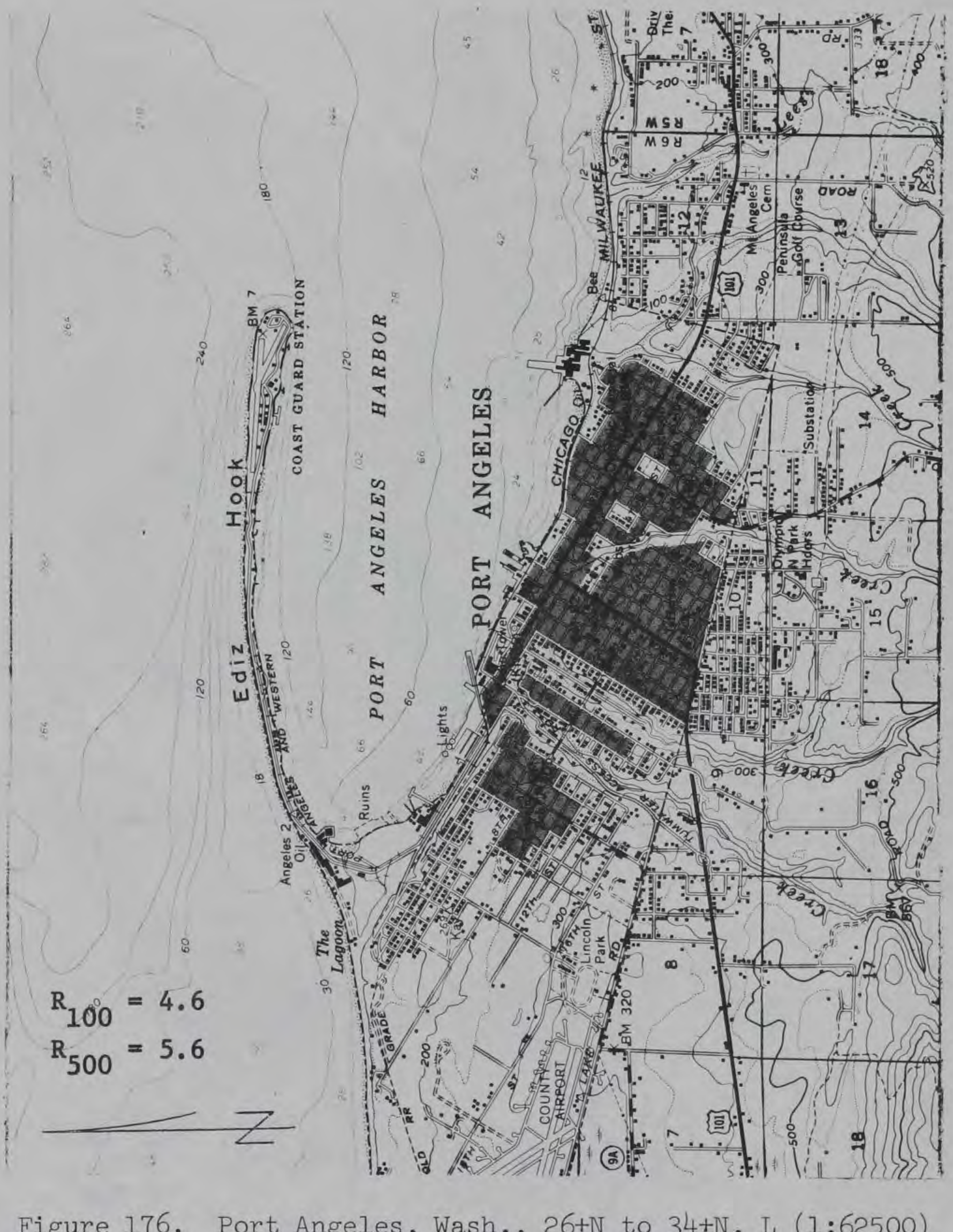

Figure 176. Port Angeles, Wash., 26+N to 34+N, L (1:62500)

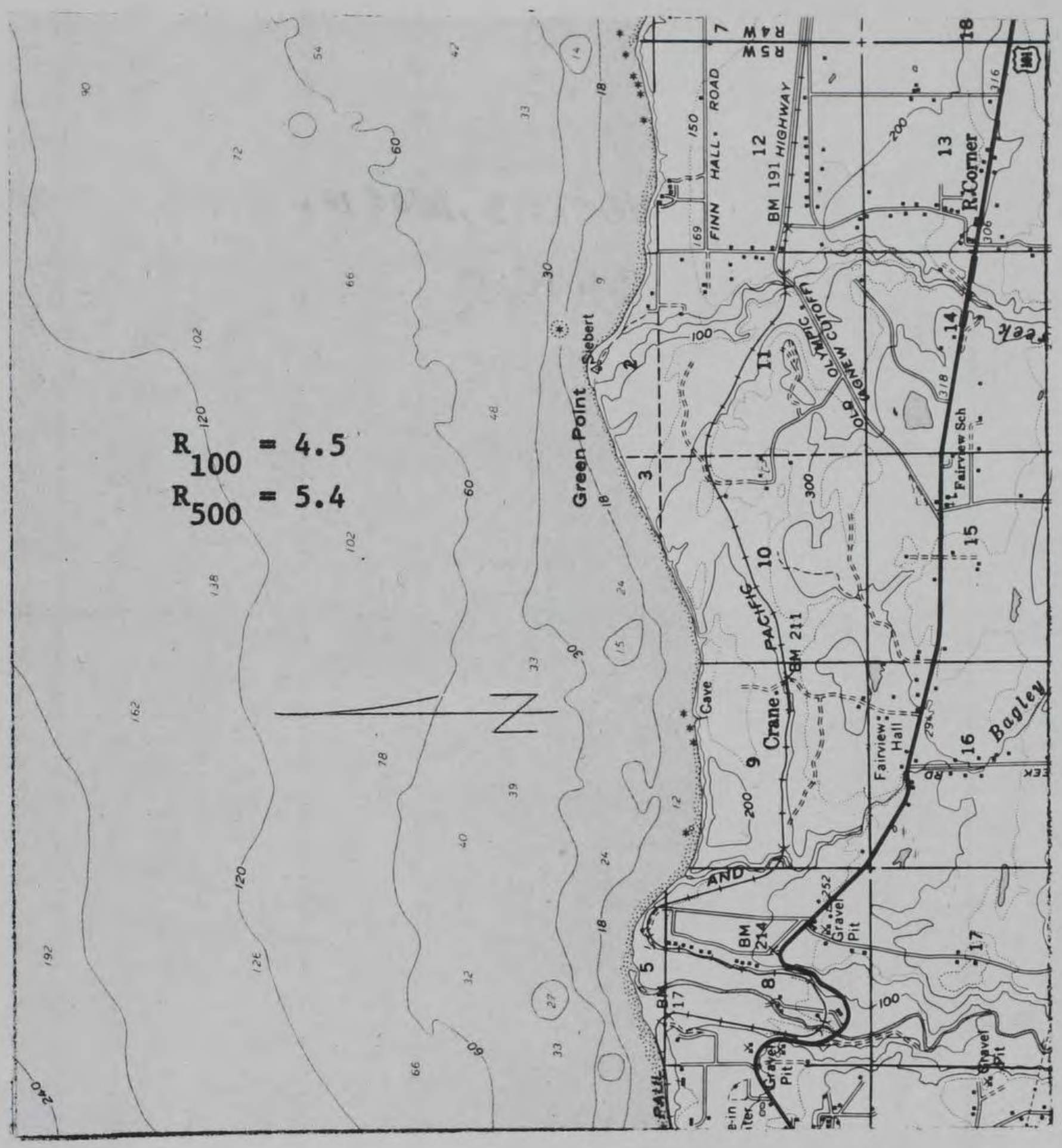

Figure 177. Port Angeles, Wash., 26N to 34N, R (1:62500)

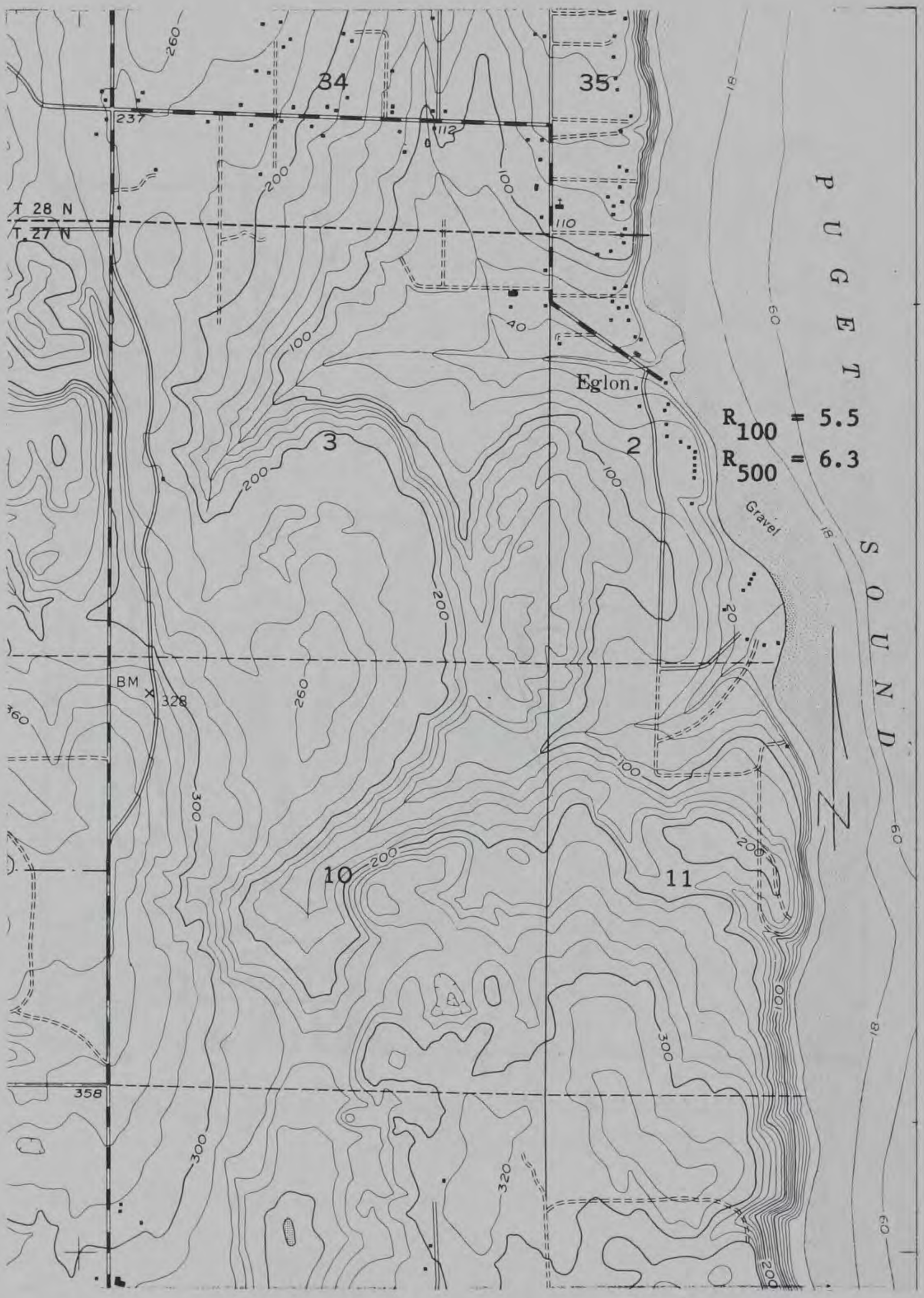

Figure 178. Port Gamble, Wash., 34E to 37+E, T

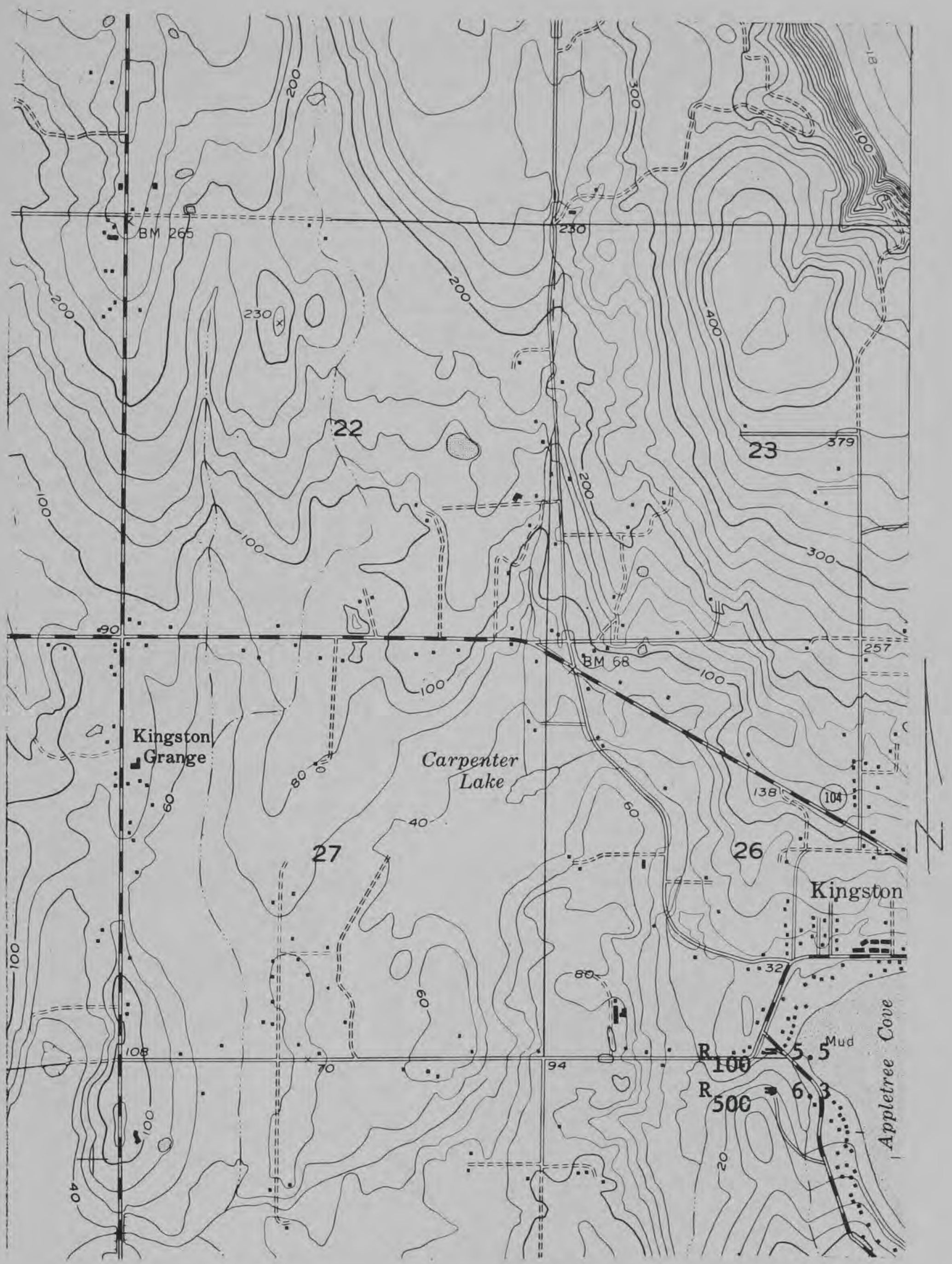

Figure 179. Port Gamble, Wash., 34E to 37+E, B

Figure 180. Port Gamble, Wash. (52)99N to (53)02+N, L

Figure 181. Port Gamble, Wash., 96-N to 99N, L

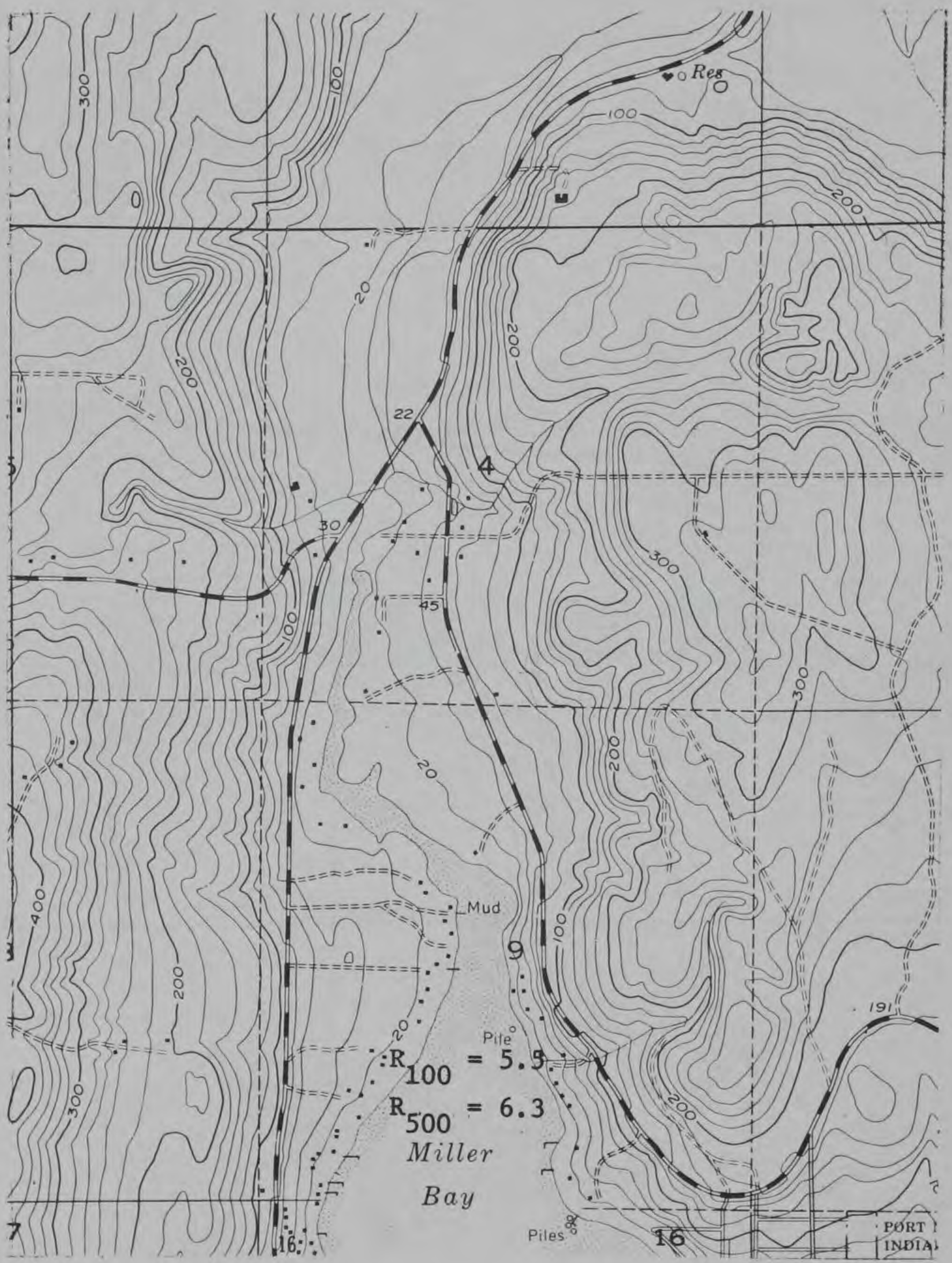

Figure 182. Port Gamble, Wash., 32E to 35E, B

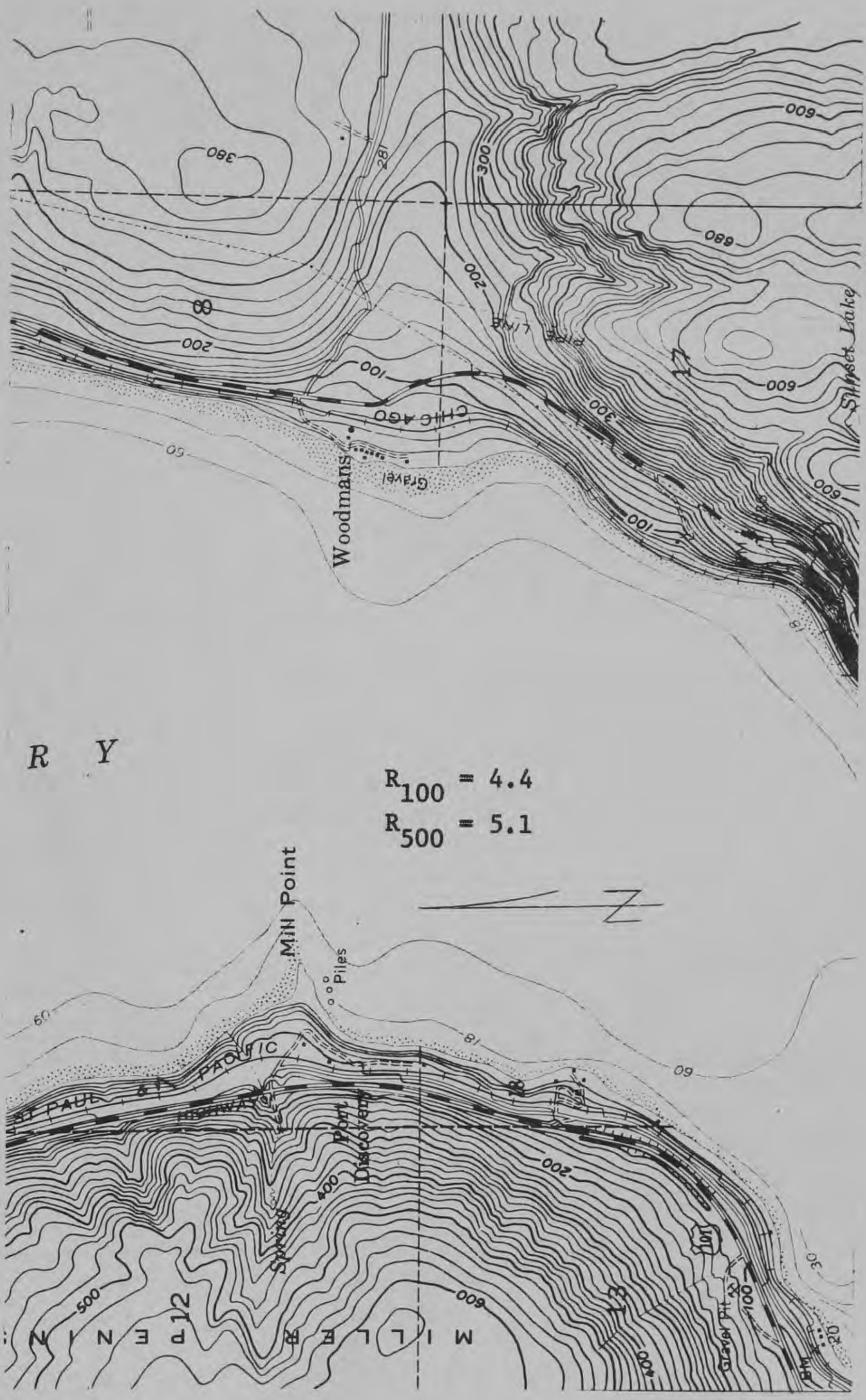

Figure 183. Port Townsend, Wash., 16+N to 19N, L

Figure 184. Port Townsend, Wash., 19N to 22N, L

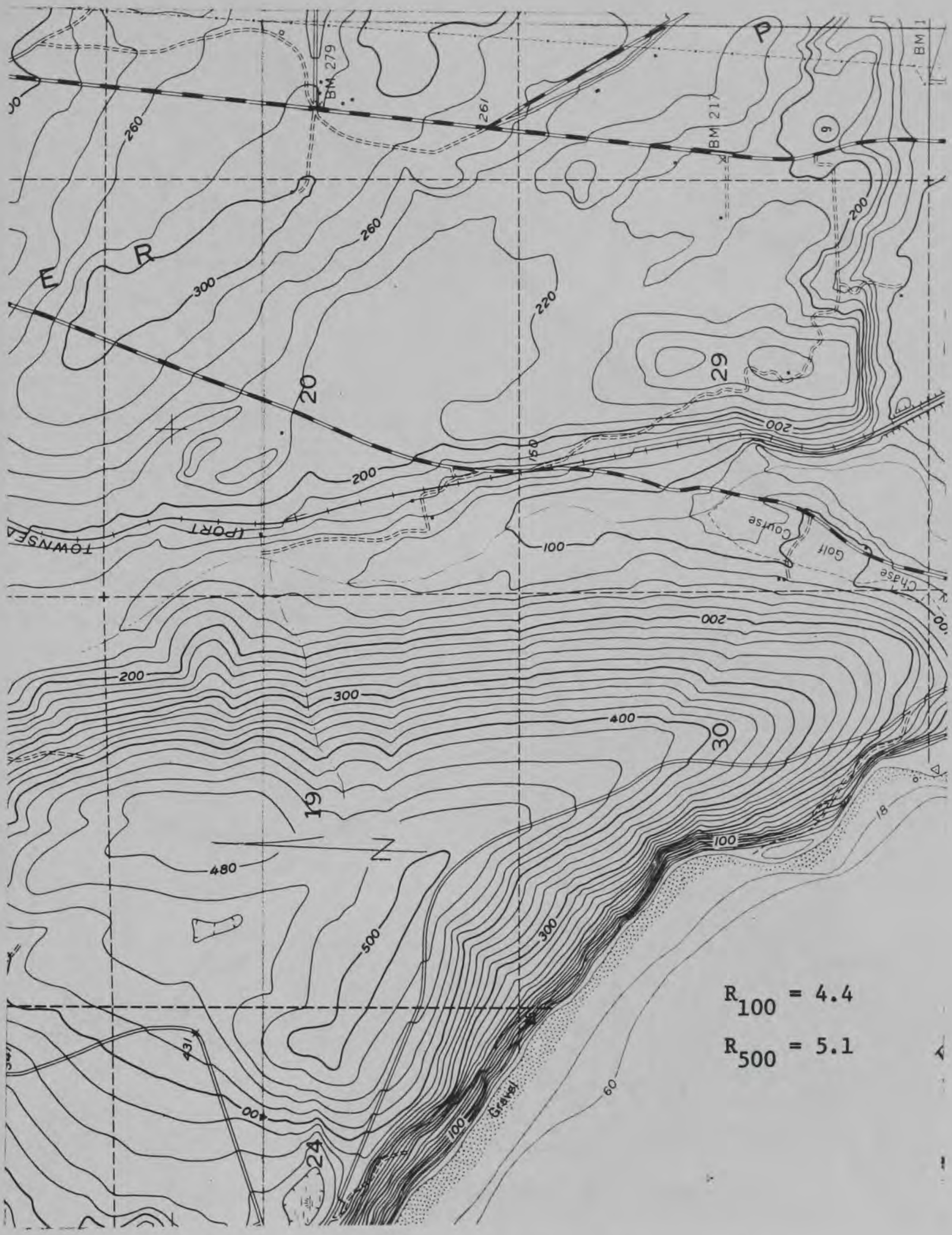

Figure 185. Port Townsend, Wash., 22N to 25N, L

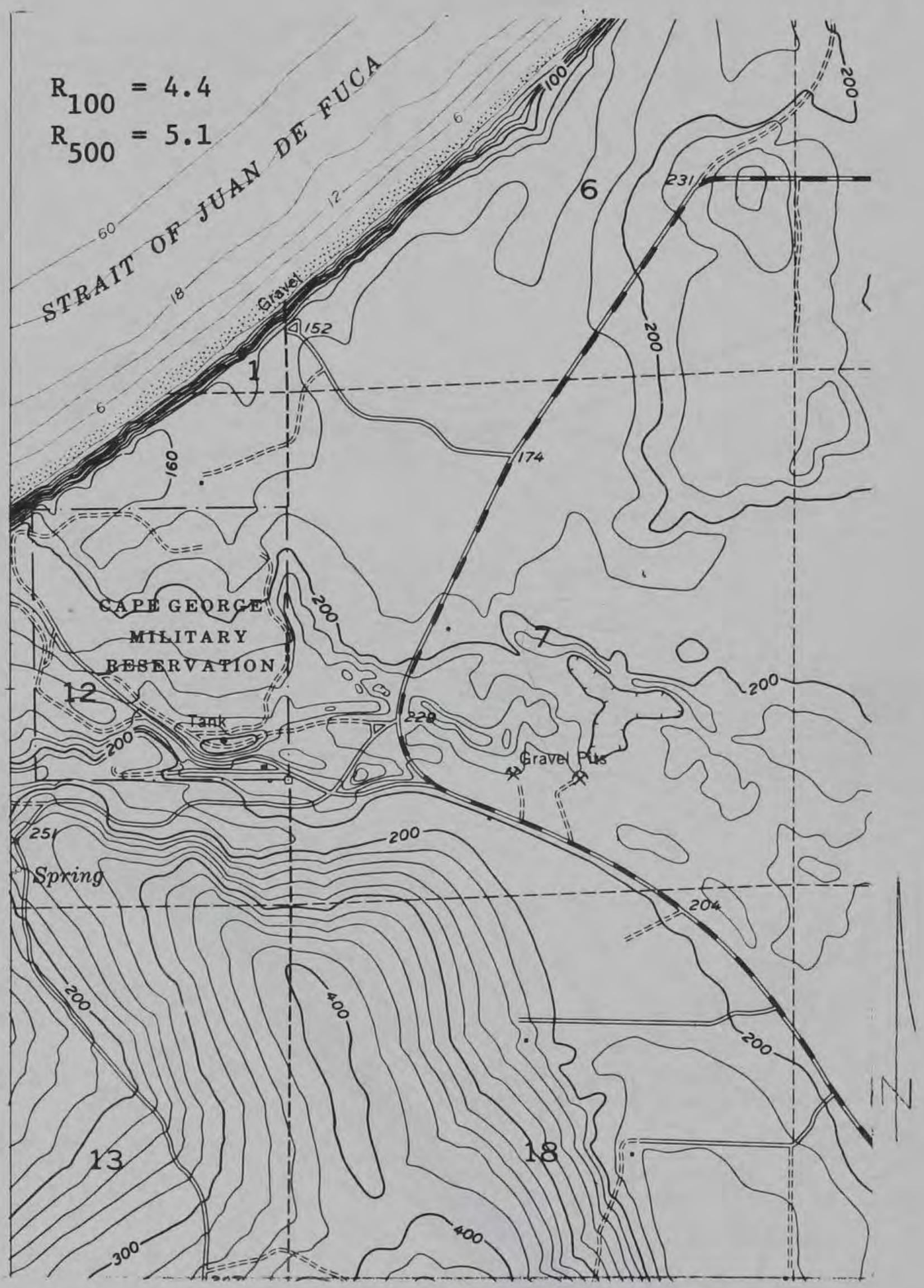

Figure 186. Port Townsend, Wash., 26N to 29+N, L

Figure 187. Port Townsend, Wash., 19N to 24N, R

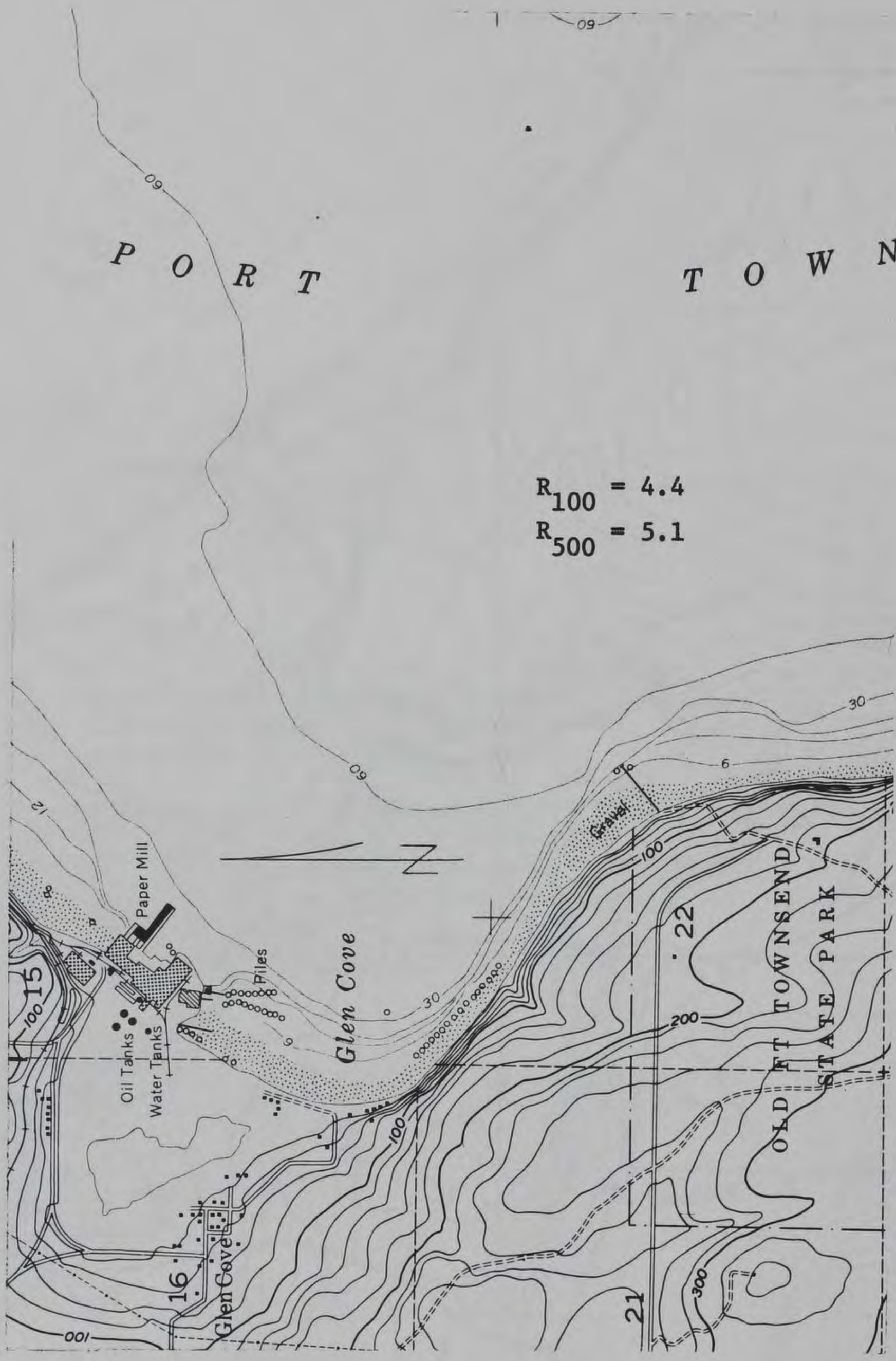

Figure 188. Port Townsend South, Wash., 24N to 27N, R

Figure 189. Port Townsend South, Wash., 27N to 30N, R

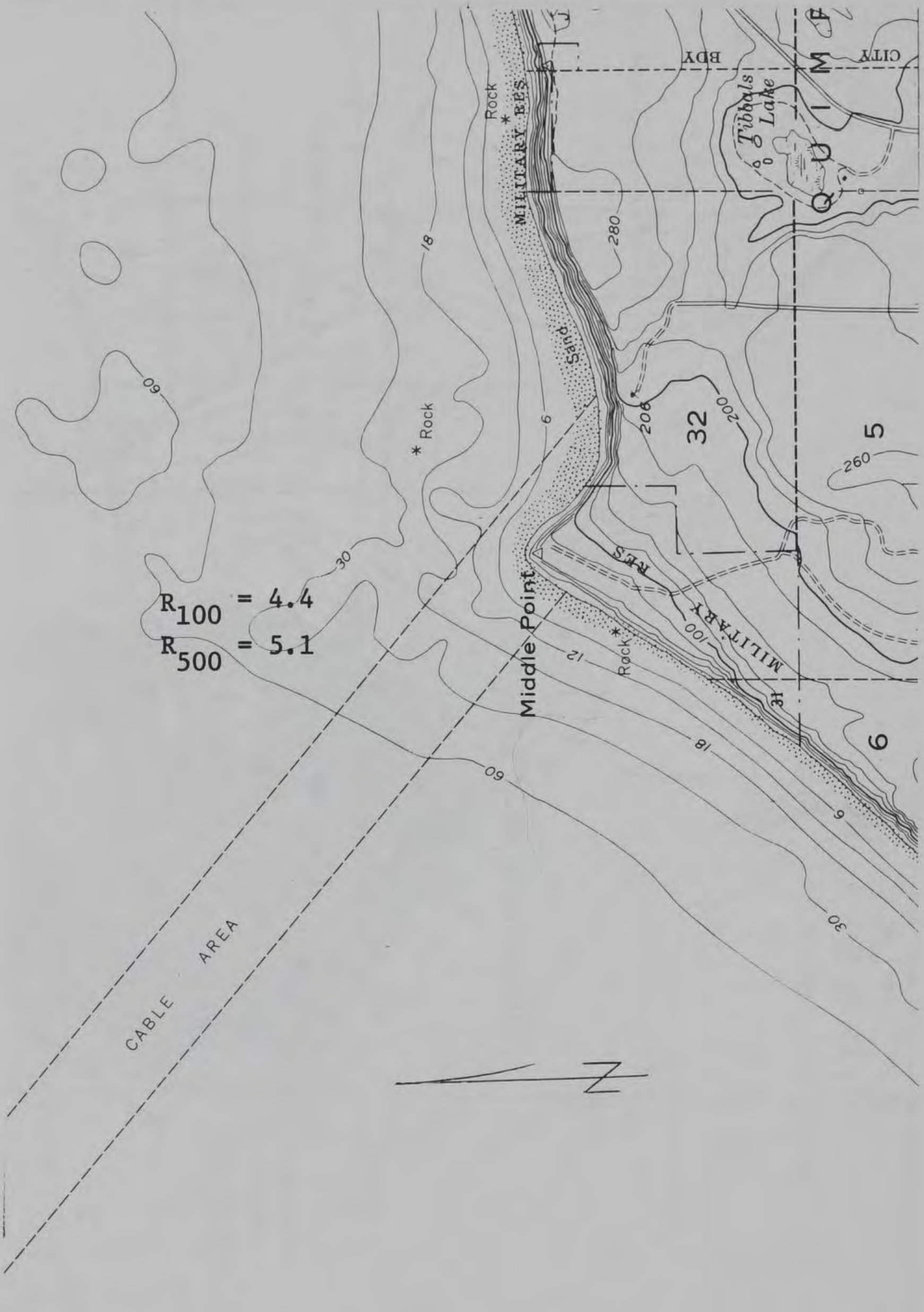

Figure 190. Port Townsend North, Wash., 9+E to 14E, B

Figure 191. Port Townsend North, Wash., 30N to 33N, R

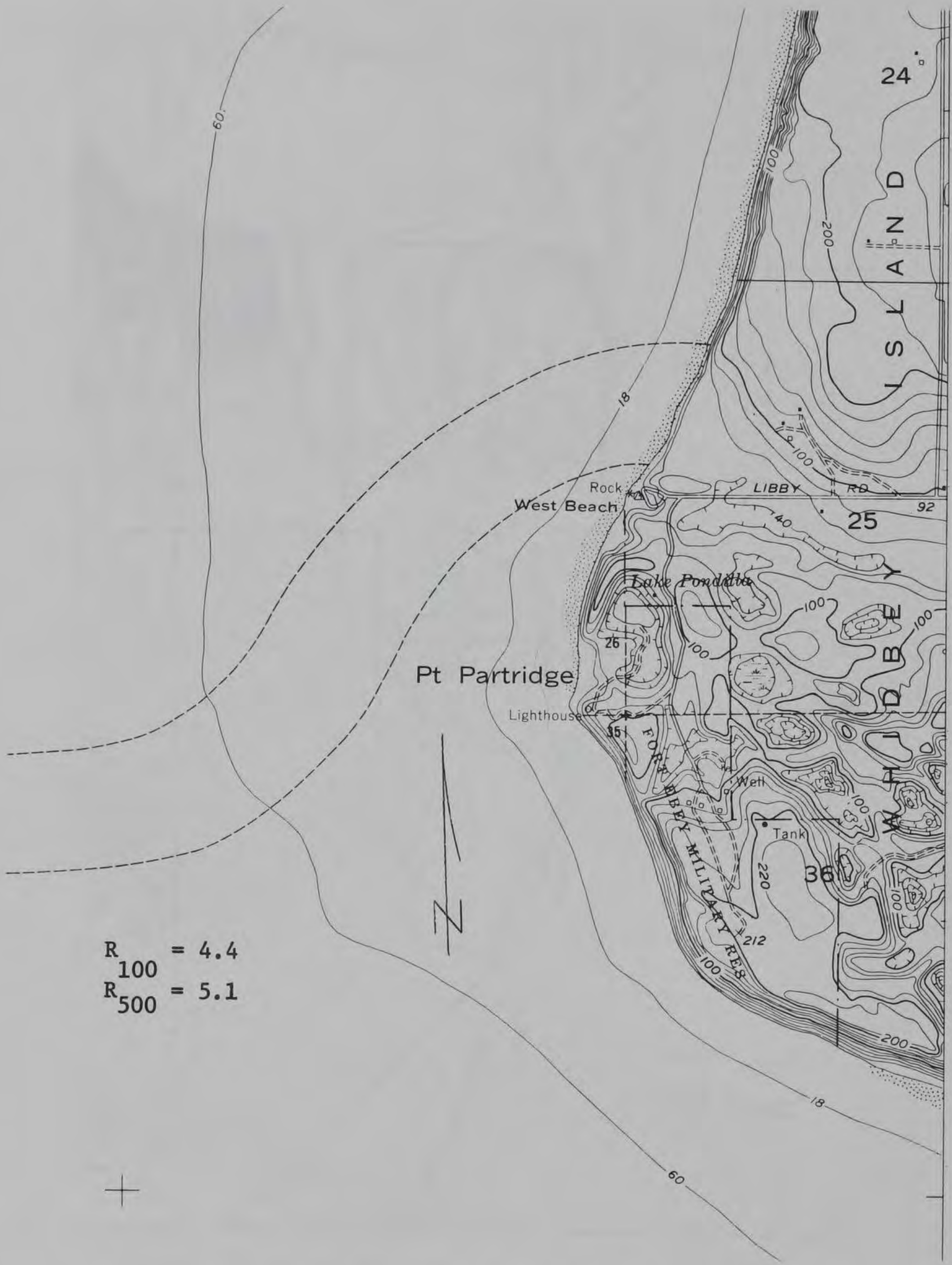

Figure 192. Port Townsend North, Wash., 39N to 43+N, R

$R_{100} = 5.8$

$R_{500} = 6.6$

Figure 193. Poverty Bay, Wash., 41N to 44N, L

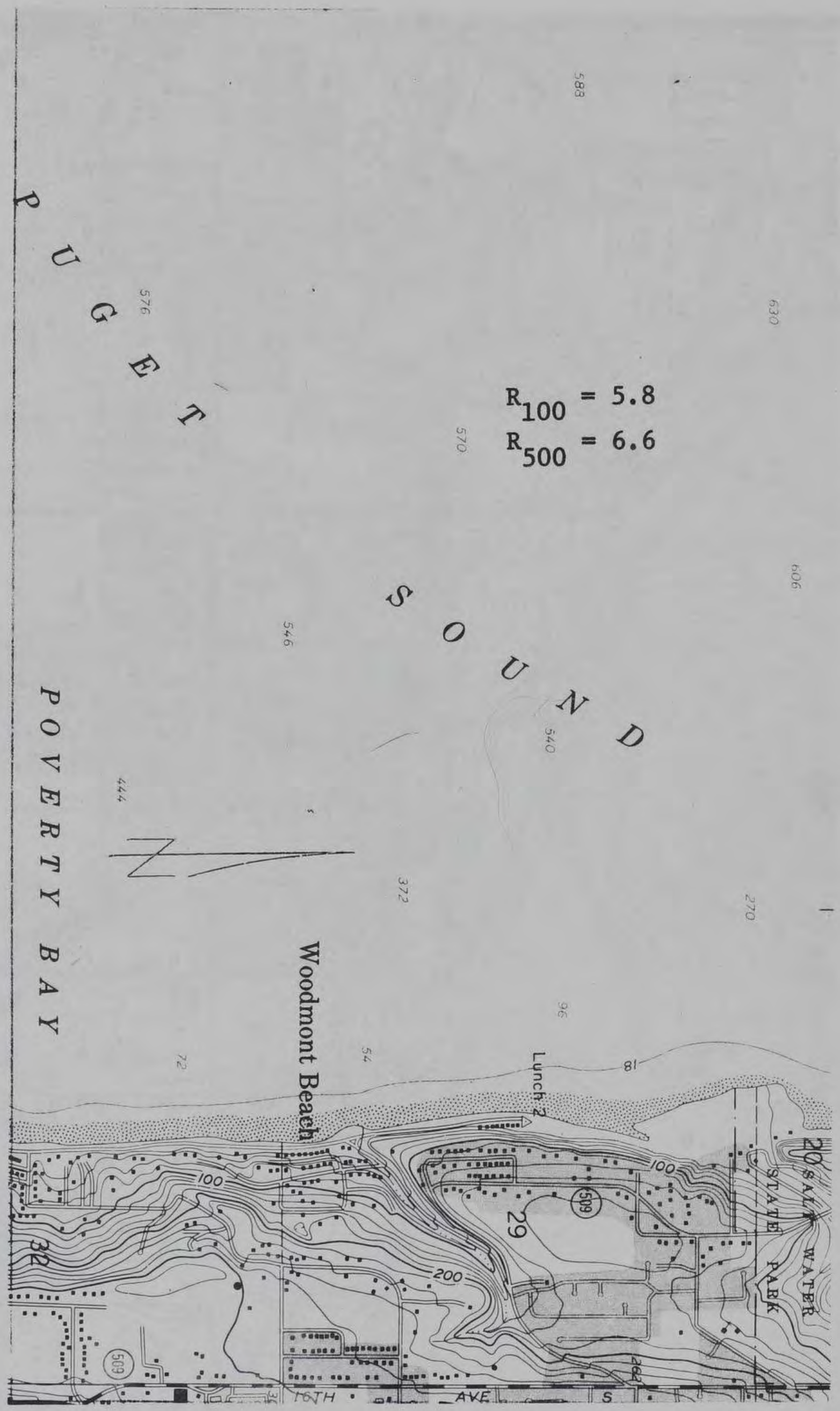

Figure 194. Poverty Bay, Wash., 44N to 46+N, L

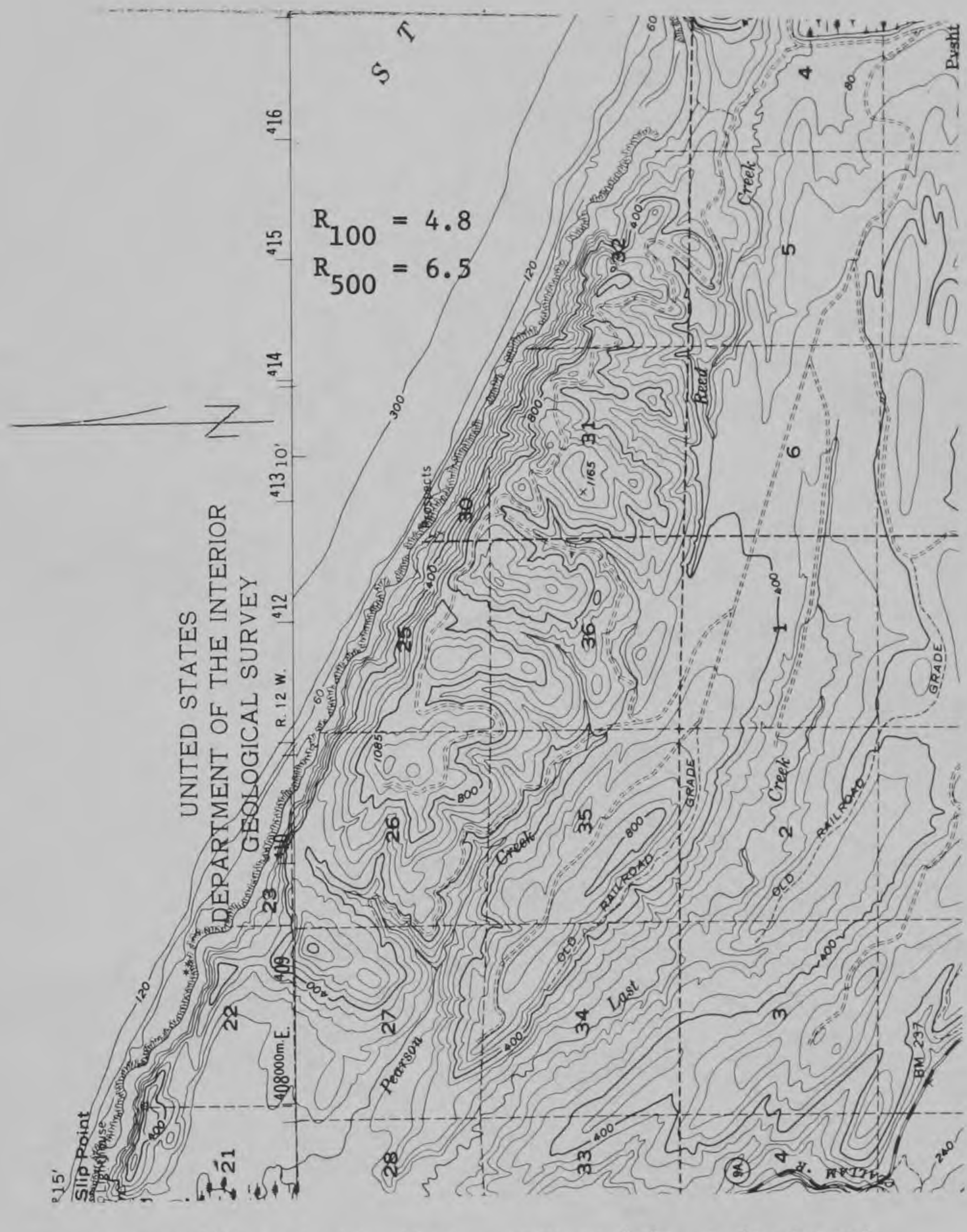

Figure 195. Pysht, Wash., 39N to 46N, L (1:62500)

Figure 196. Pysht, Wash., 33N to 44+N, R (1:62500)

Figure 197. Richardson, Wash., 62N to 71+N, L

Figure 198. Richardson, Wash., 62+N to 75+N, R

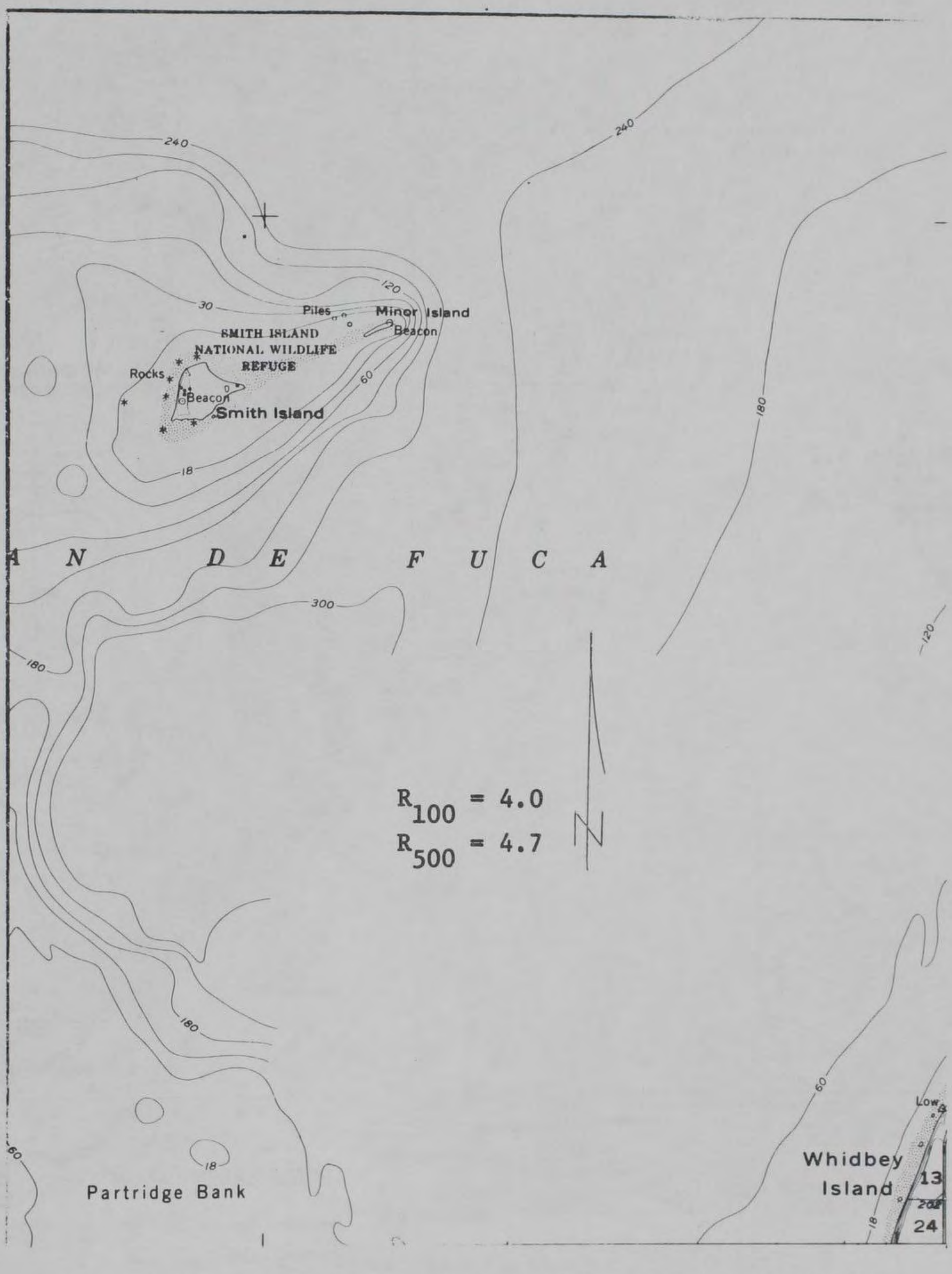

Figure 199. Richardson, Wash., 43+N to 55N, R (1:62500)

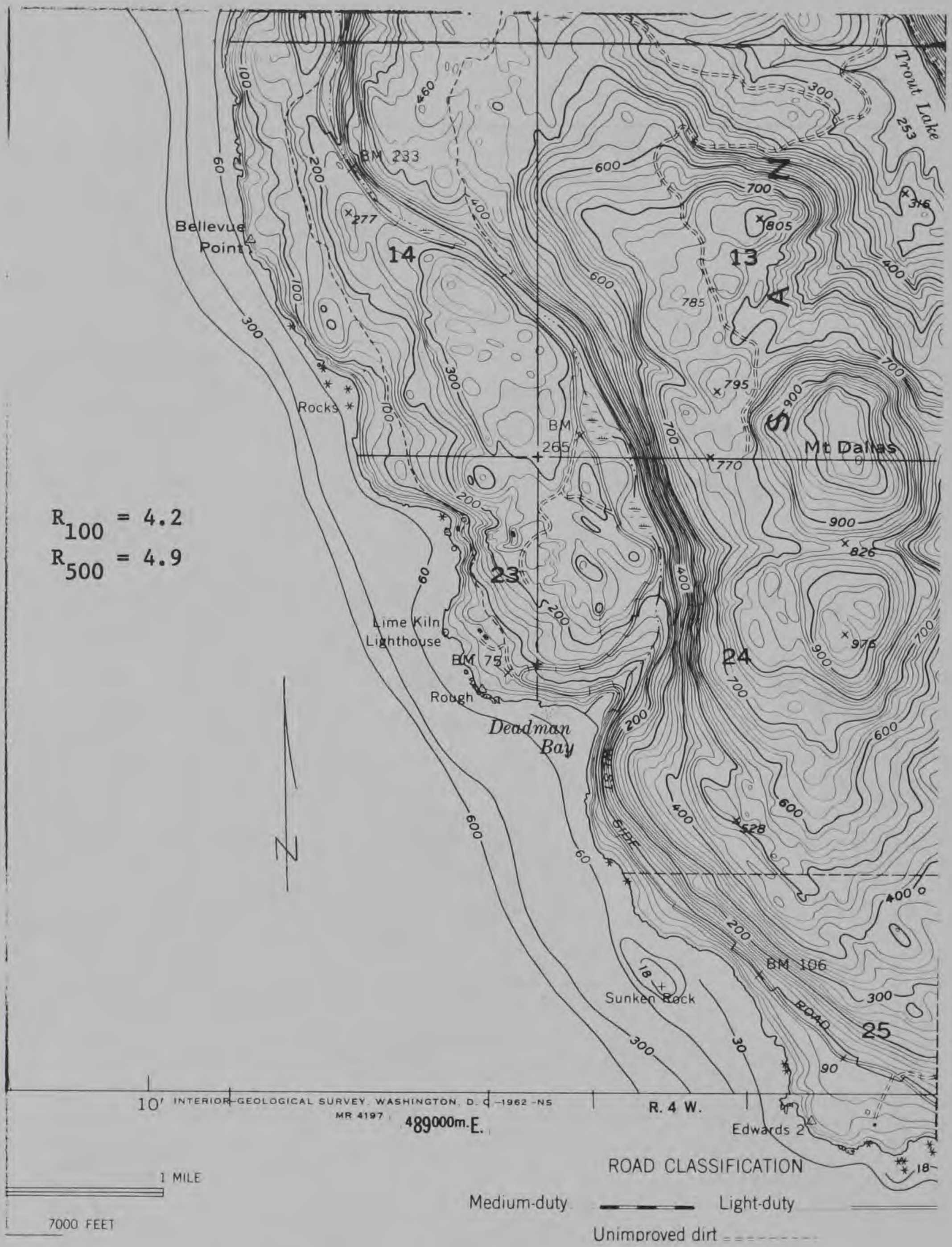

Figure 200. Roche Harbor, Wash., 52+N to 57N, R

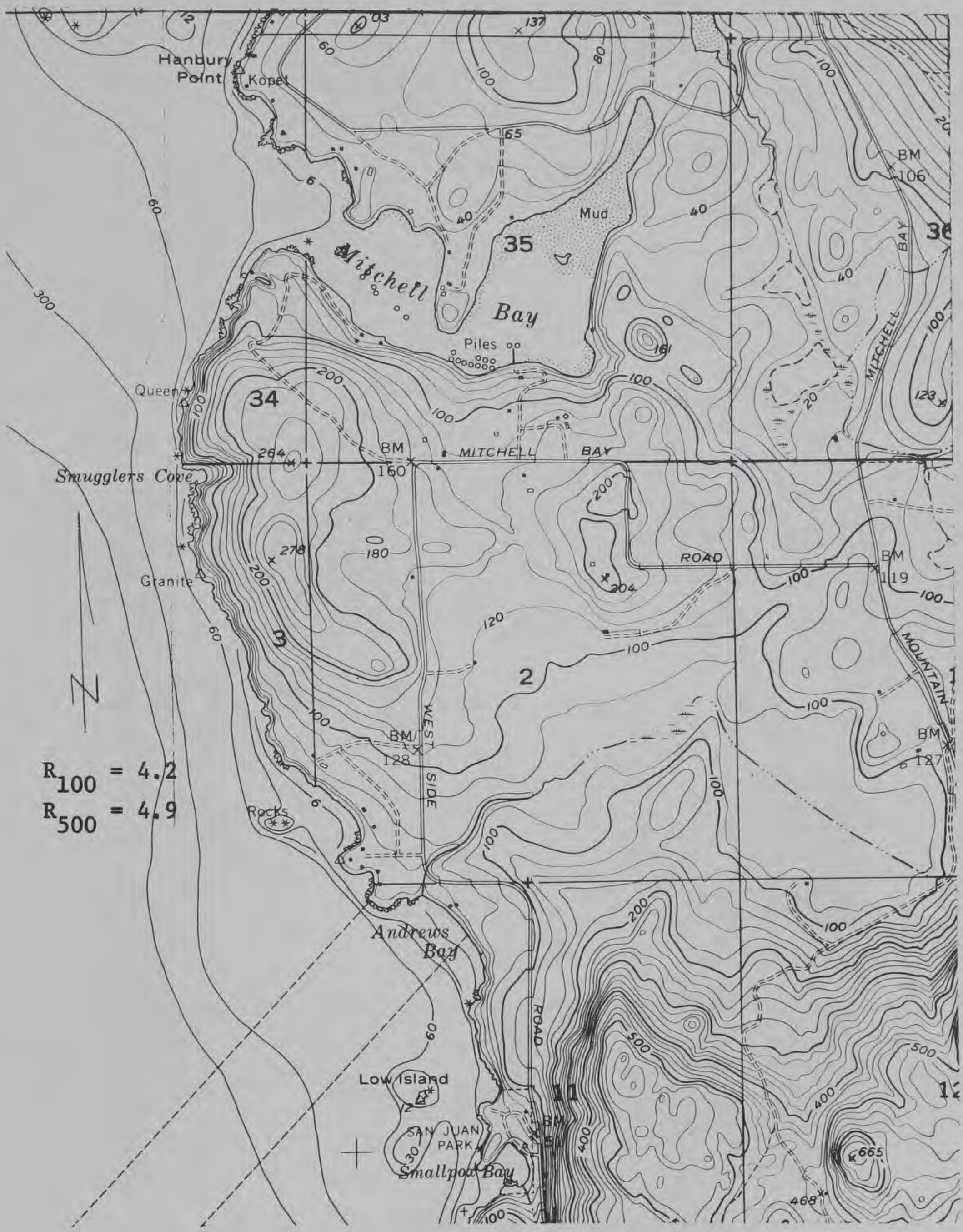

Figure 201. Roche Harbor, Wash., 57N to 61+N, R

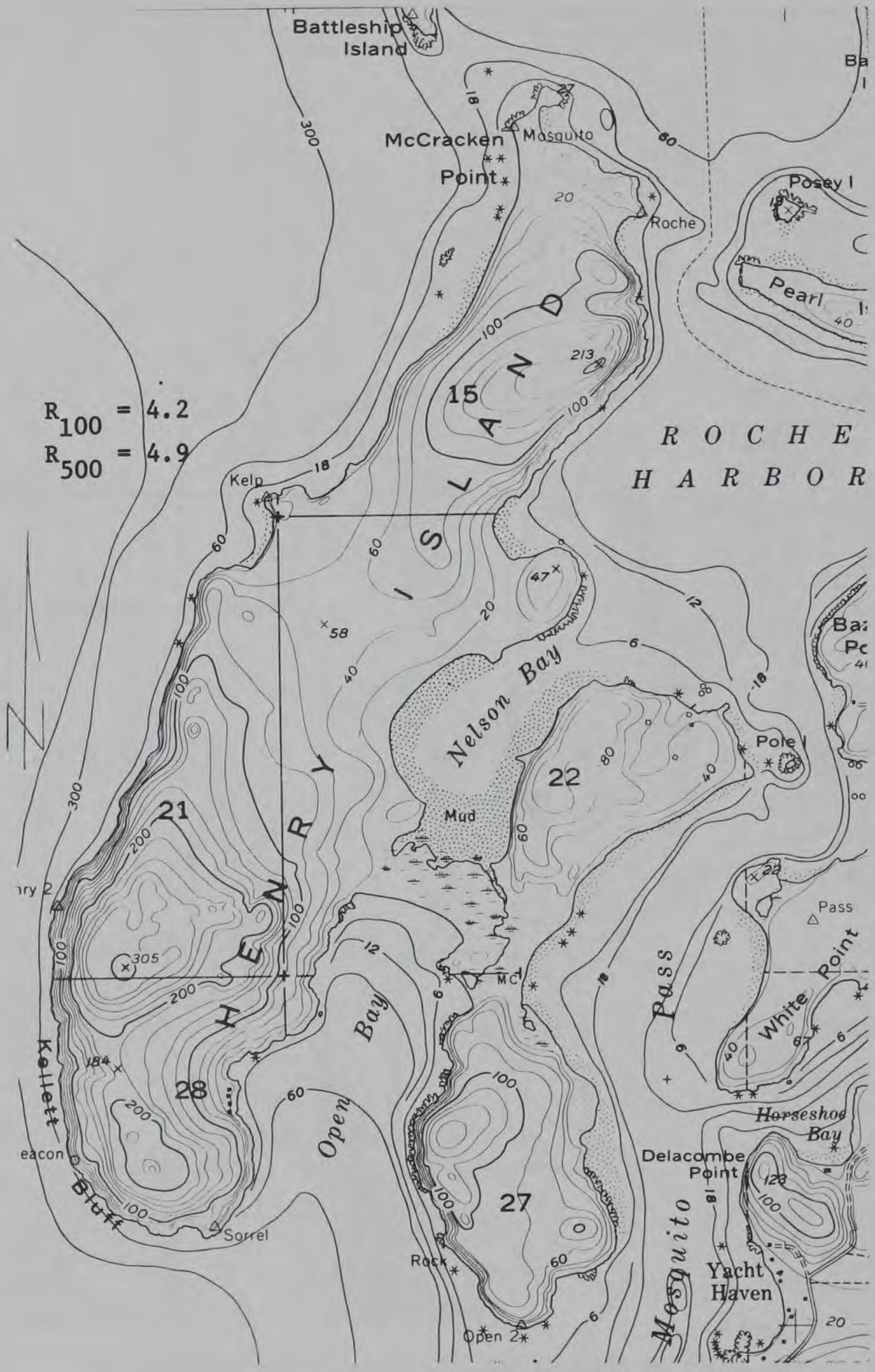

Figure 202. Roche Harbor, Wash., 85E to 88E, T

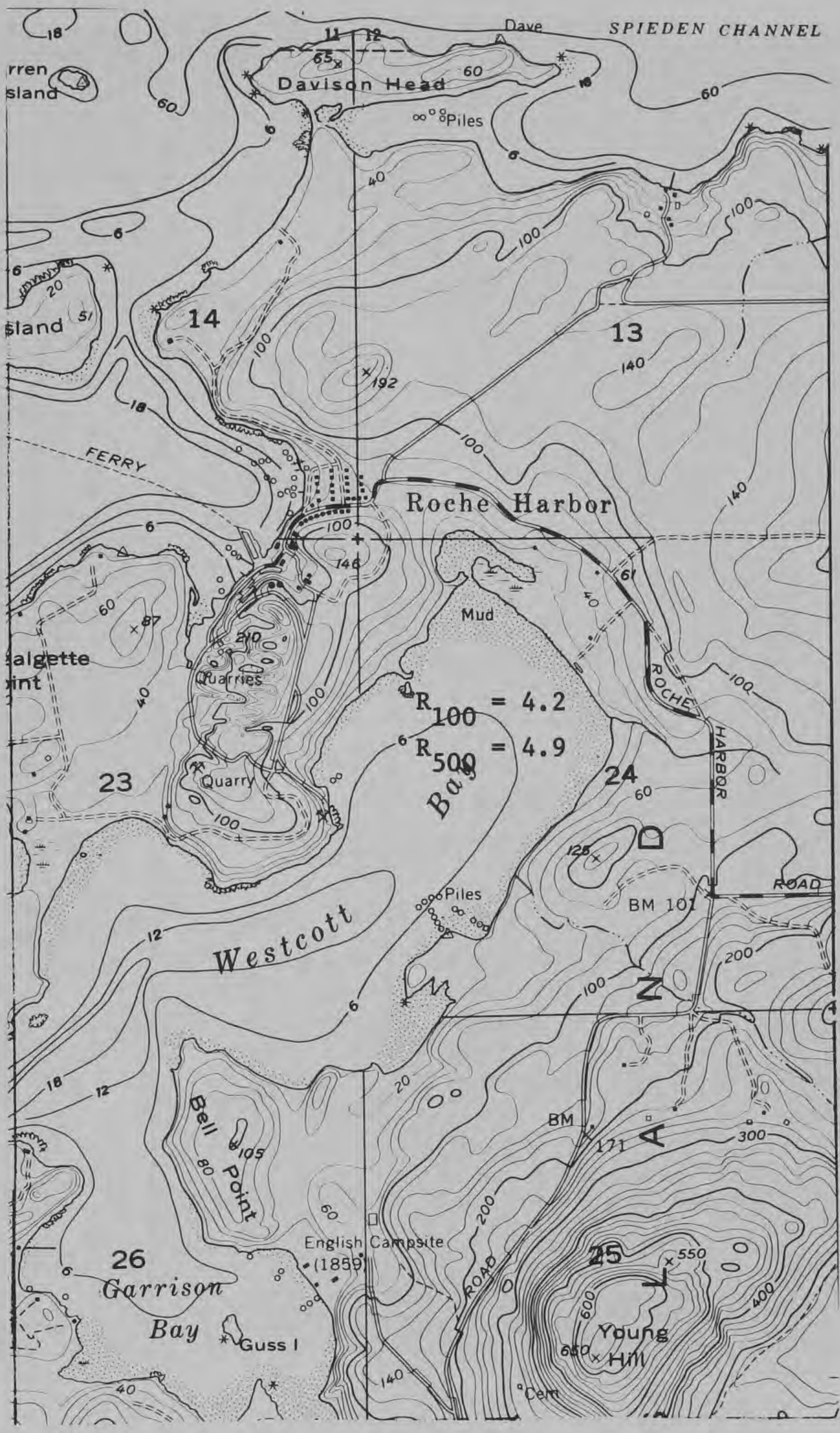

Figure 203. Roche Harbor, Wash., 61+N to 66+N, R

Figure 204. Seattle North, Wash., 84N to 88+N, L

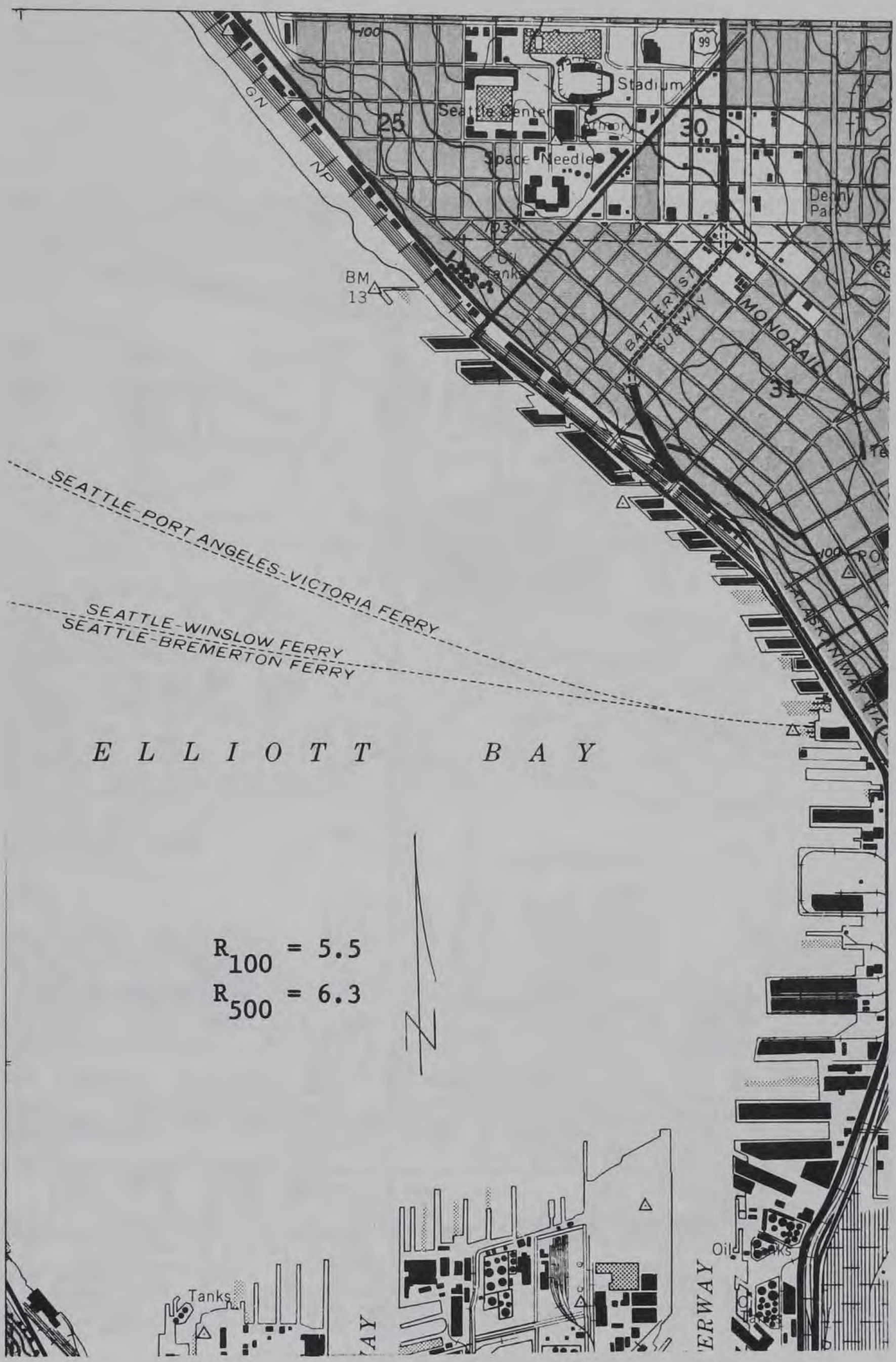

Figure 205. Seattle South, Wash., 70N to 74N, L

Figure 206. Seattle South, Wash., 67N to 70N, L

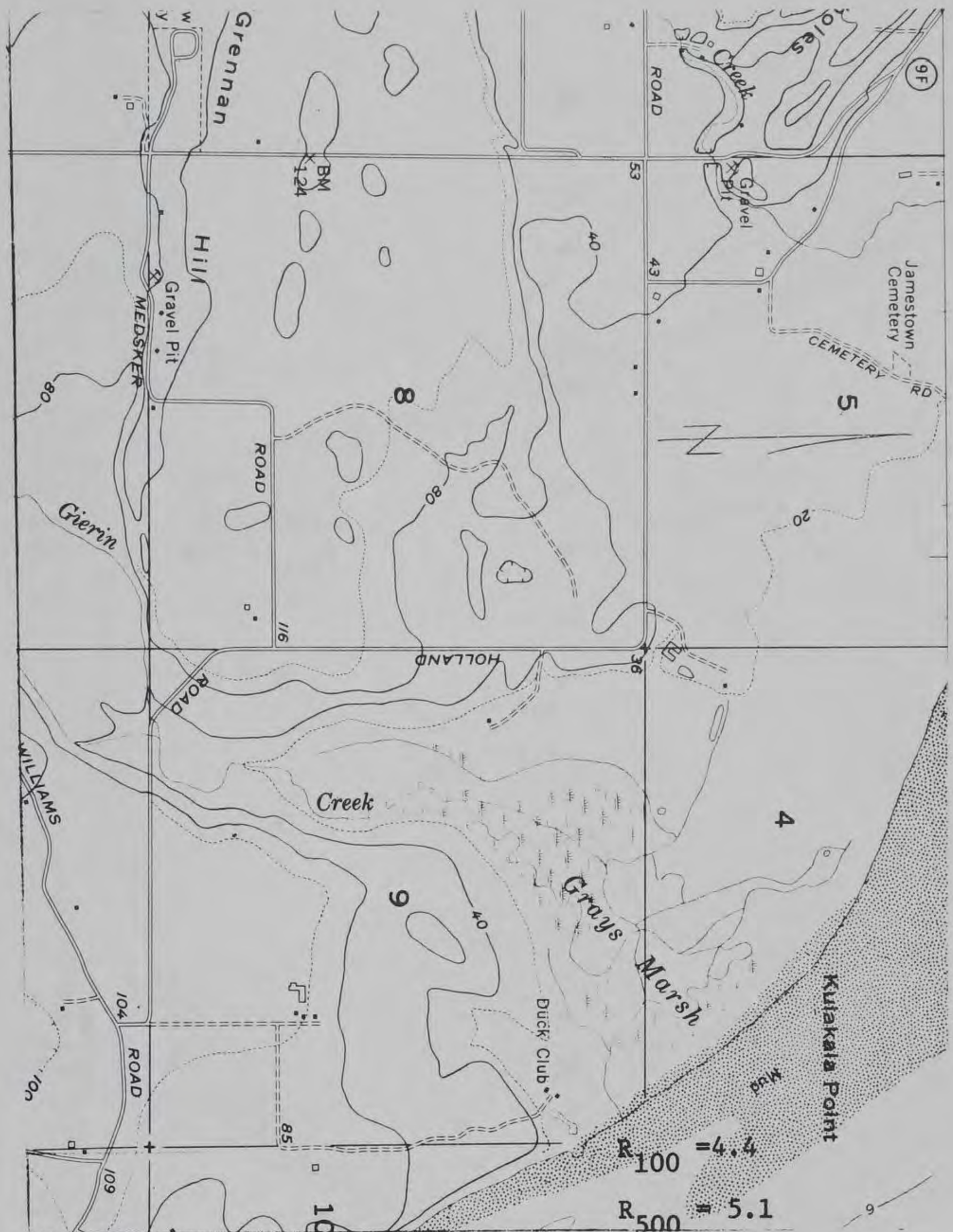

Figure 207. Sequim, Wash., 92E to 96E, T

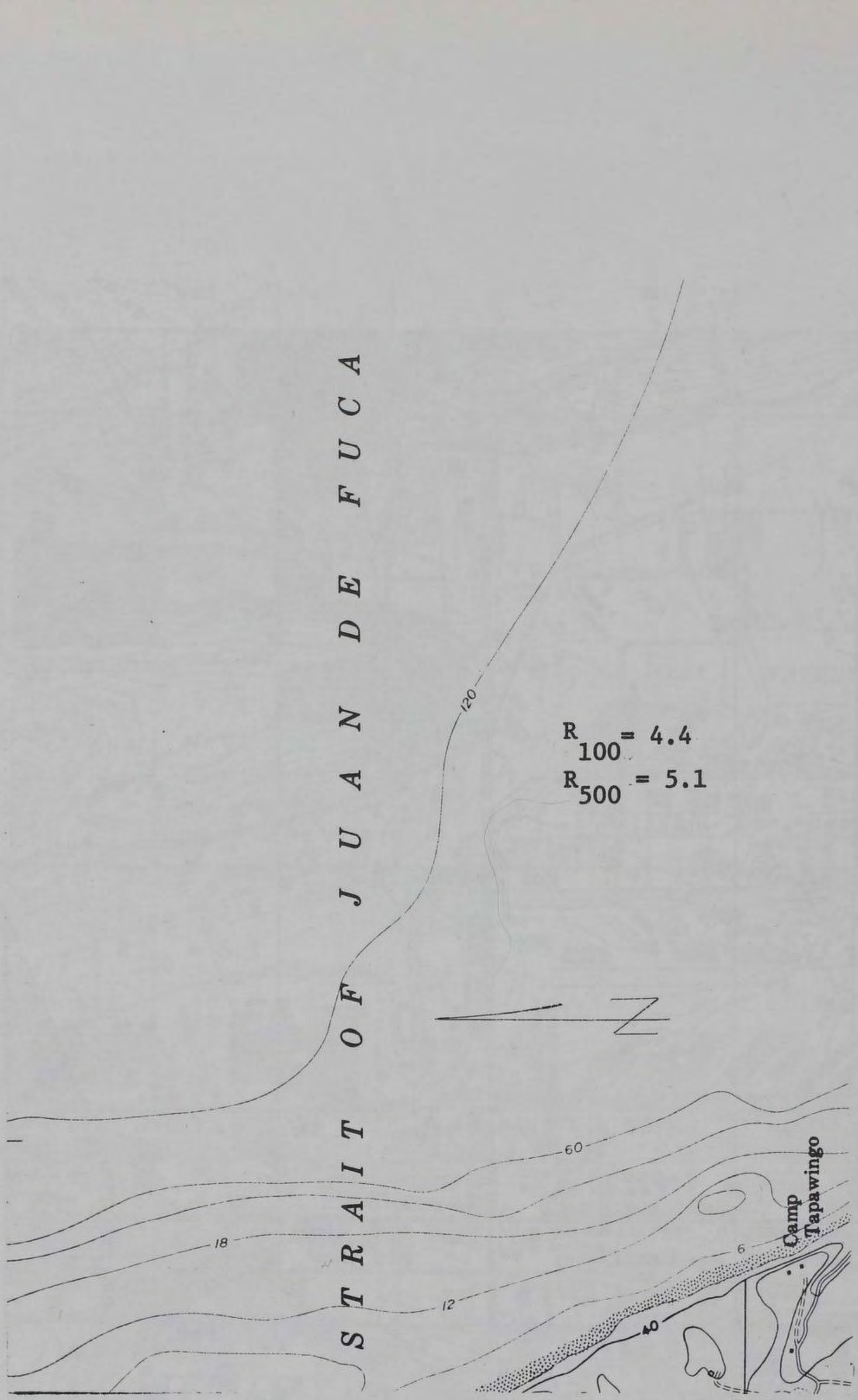

Figure 208. Sequim, Wash. (4)96E to (5)00E, T

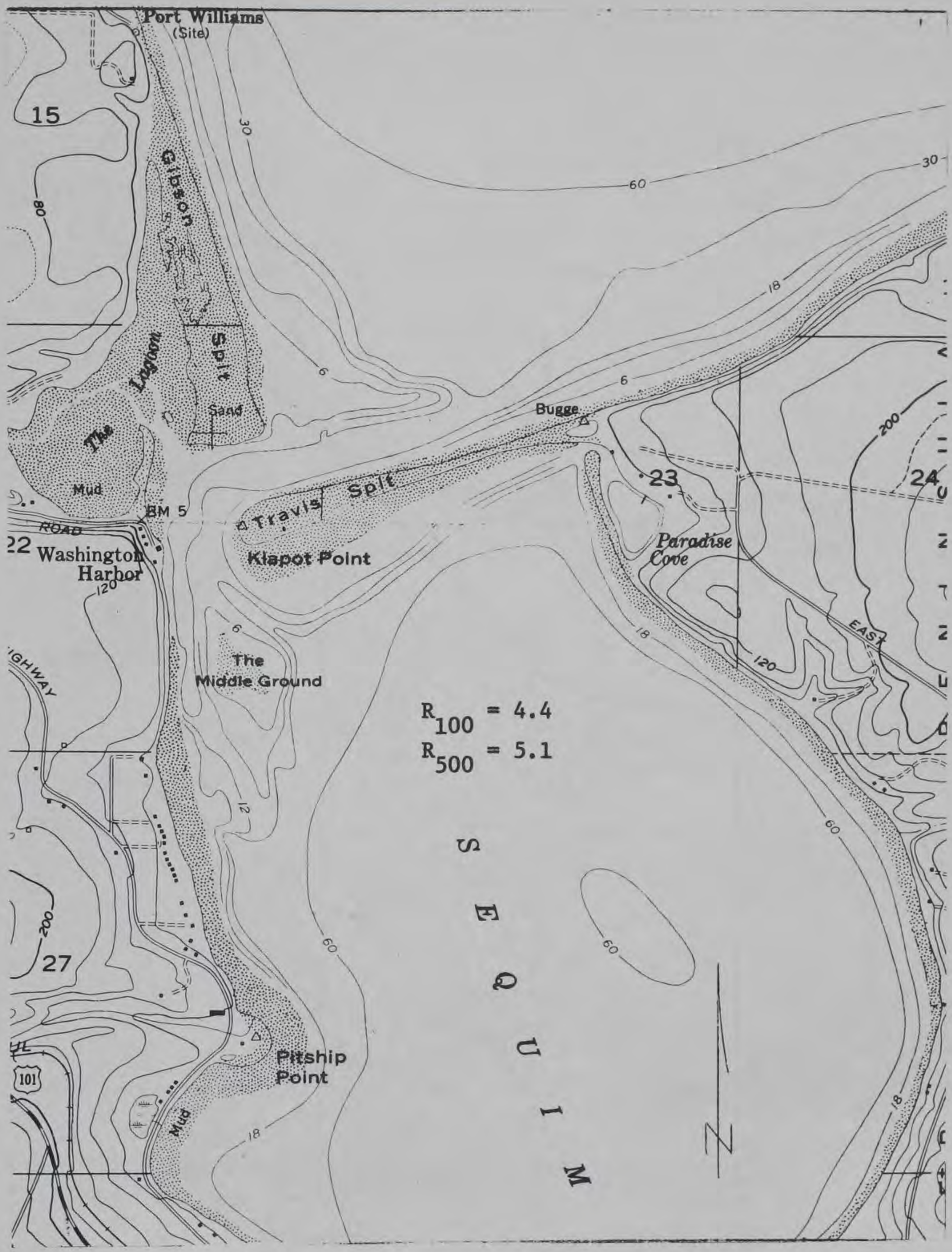

Figure 209. Sequim, Wash., 22N to 27N, R

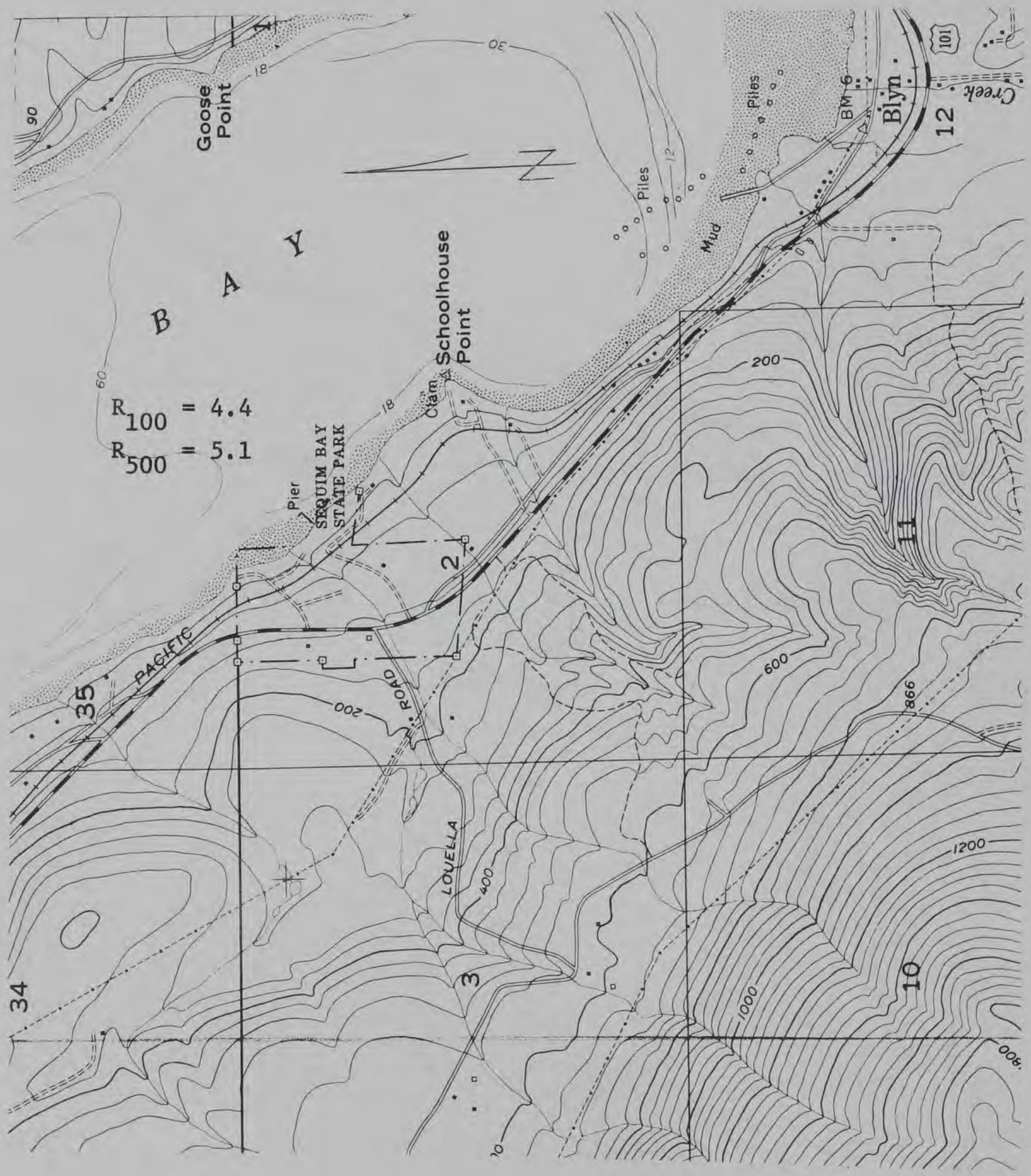

B A Y

$R_{100} = 4.4$

$R_{500} = 5.1$

Figure 210. Sequim, Wash., 18N to 22N, R

$R_{100} = 5.5$
$R_{500} = 6.3$

Figure 211. Shilshole Bay, Wash., 85N to 88+N, R

Figure 212. Shilshole Bay, Wash., 81N to 85N, R

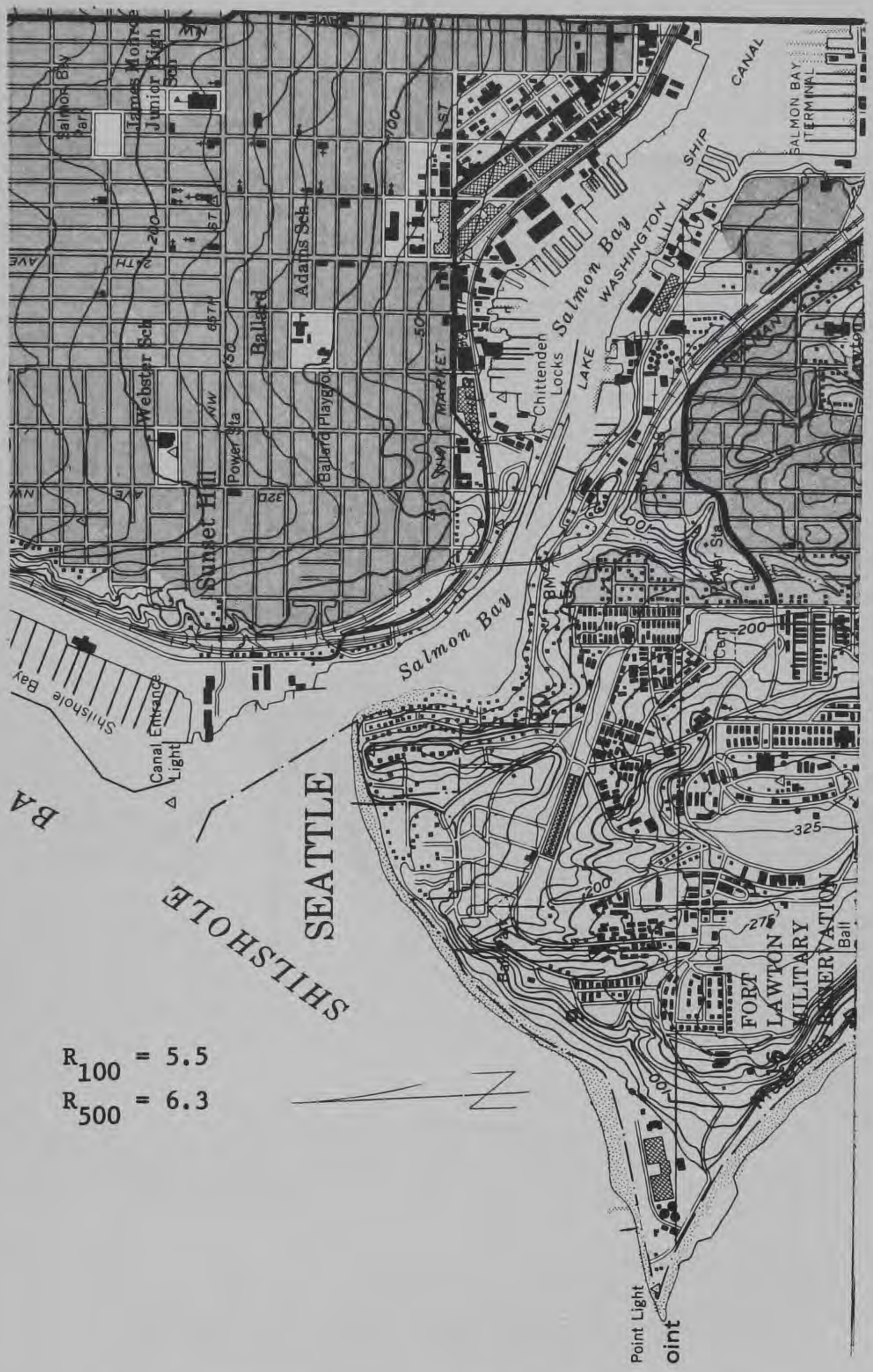

Figure 213. Shilshole Bay, Wash., 78N to 81N, R

Figure 214. Shilshole Bay, Wash., 74-N to 78N, R

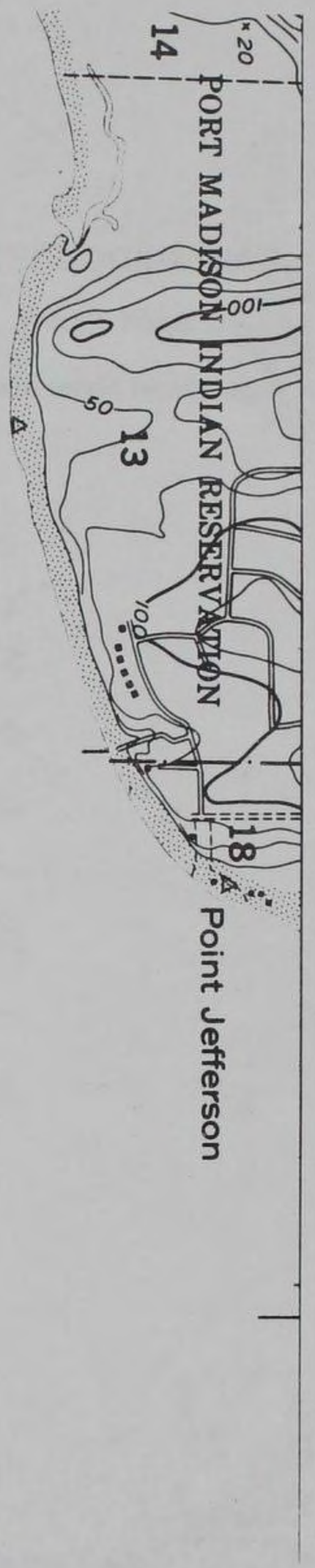

$R_{100} = 5.5$
$R_{500} = 6.3$

Angeles-Victoria Ferry

Figure 215. Shilshole Bay, Wash., 85N to 88+N, L

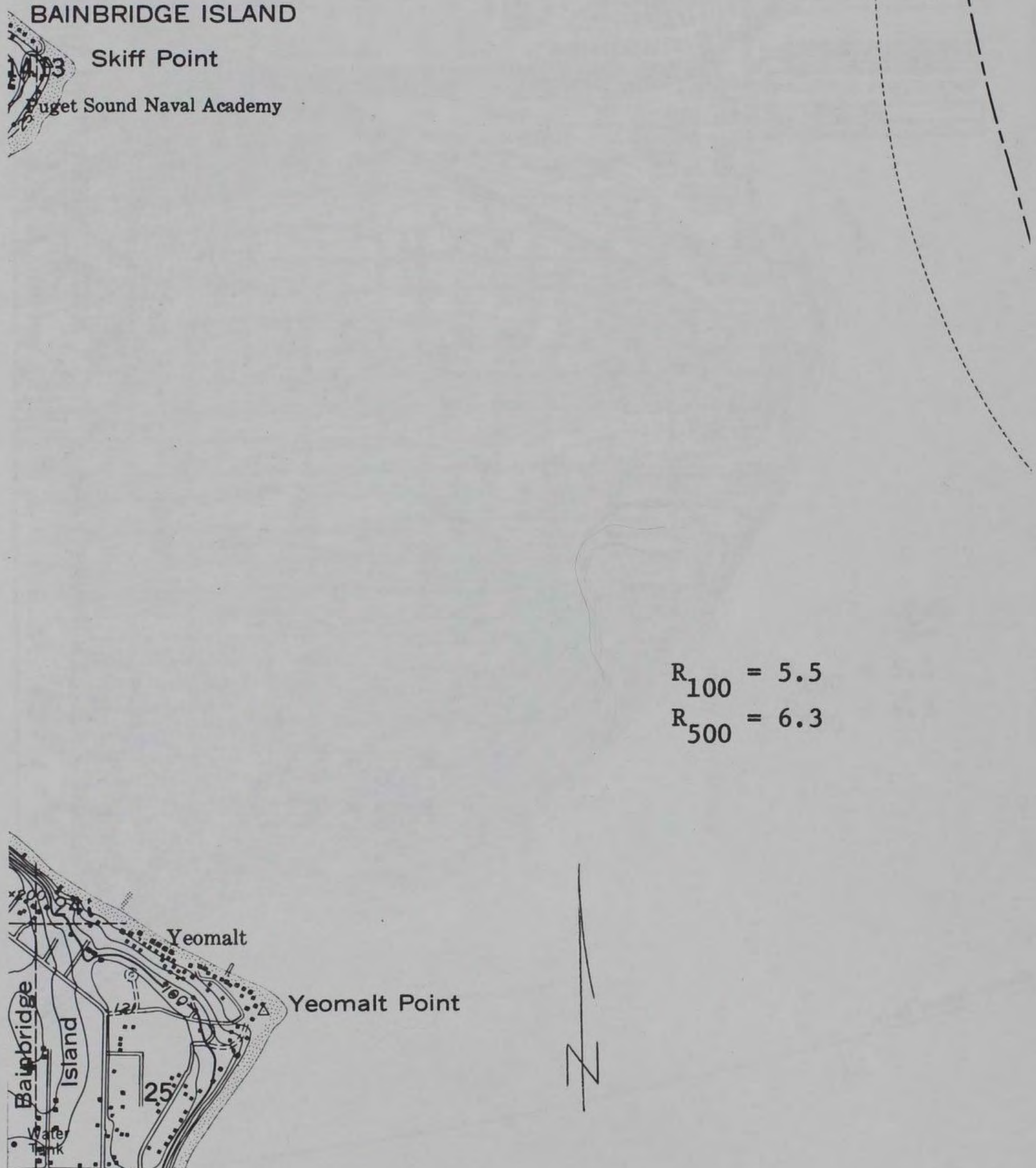

Figure 216. Shilshole Bay, Wash., 38-E to 41E, B

Figure 217. Suquamish, Wash., 85N to 88+N, R

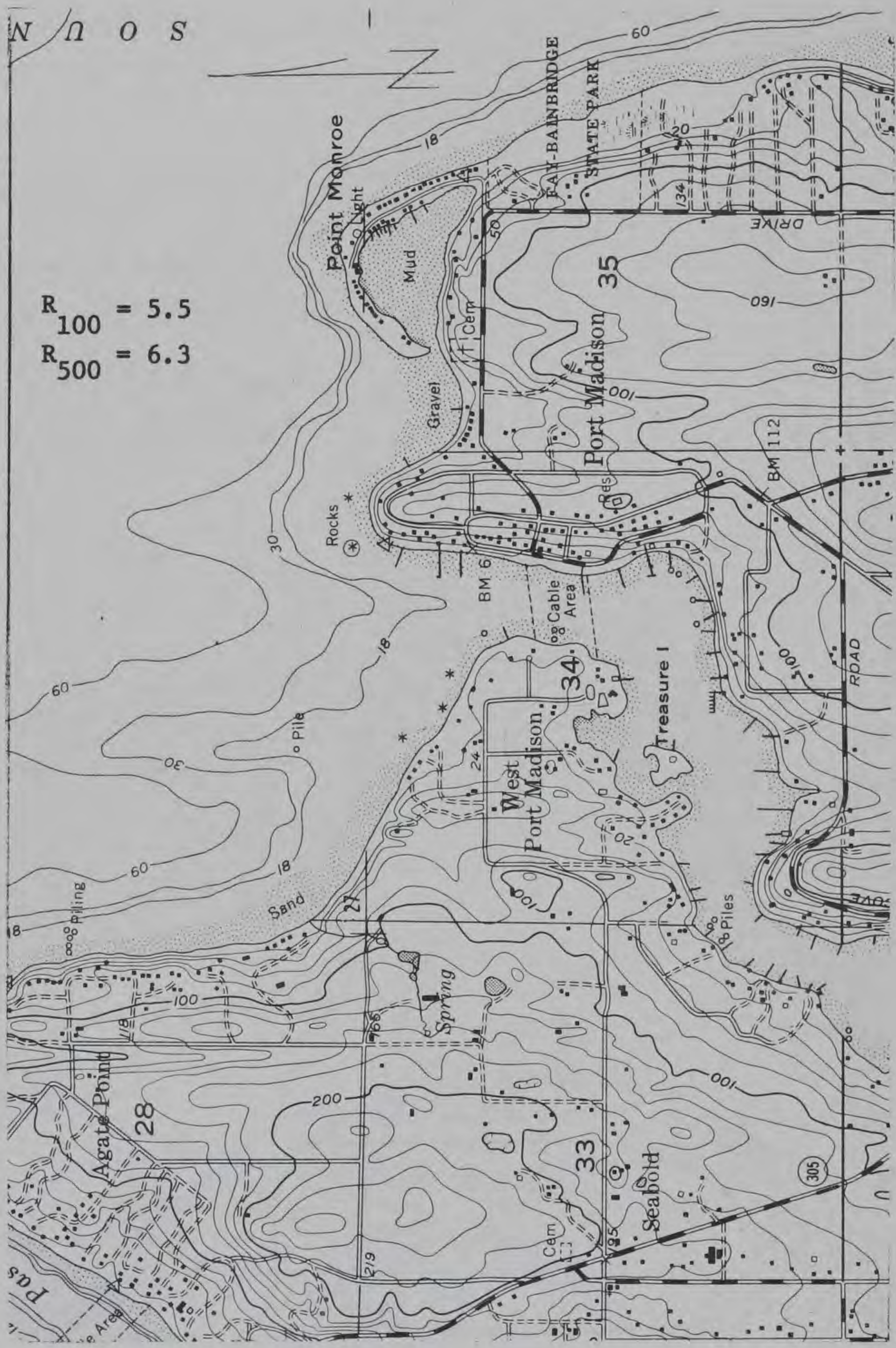

Figure 218. Suquamish, Wash., 82N to 85N, R

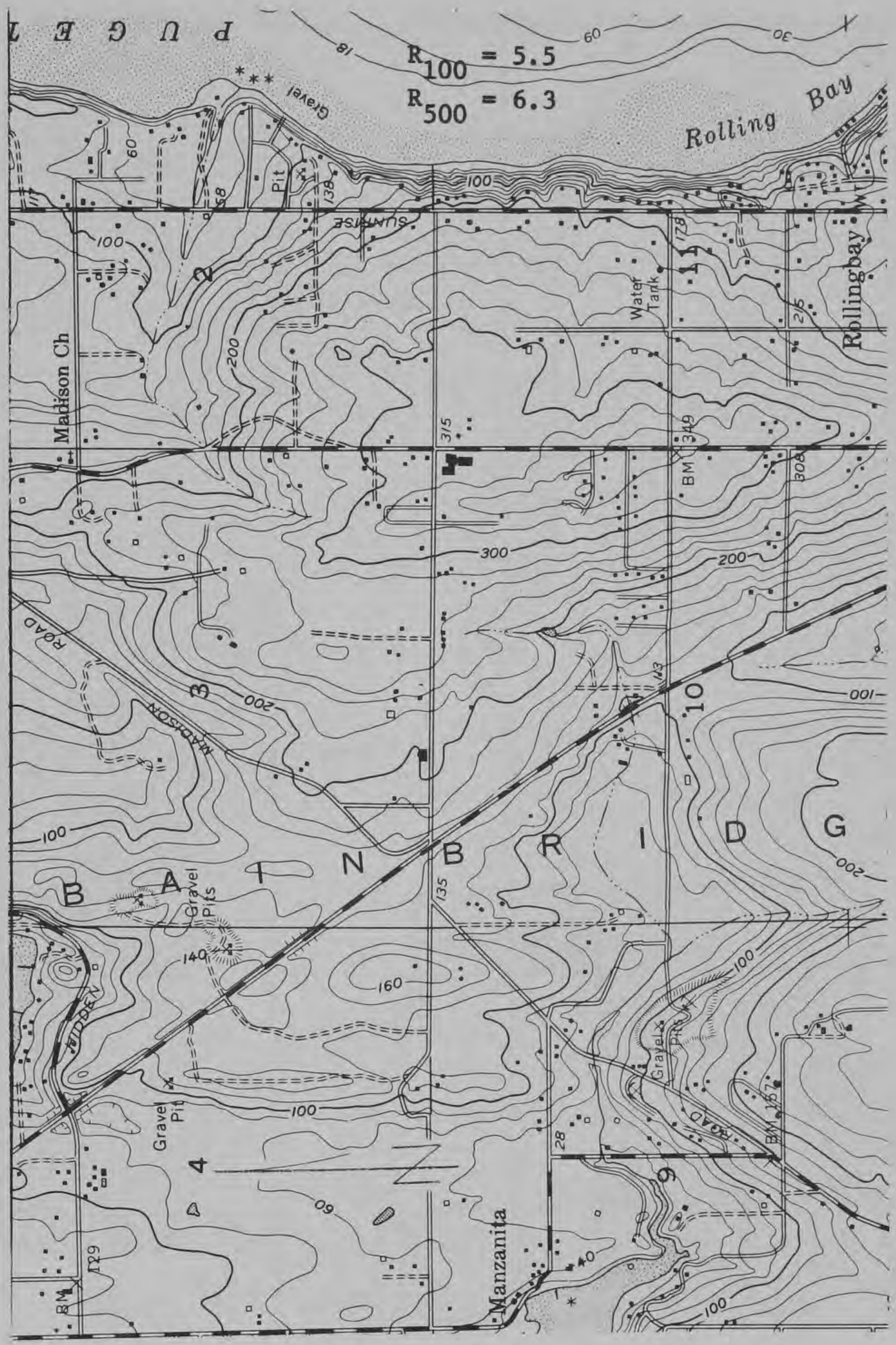

Figure 219. Suquamish, Wash., 79N to 82N, R

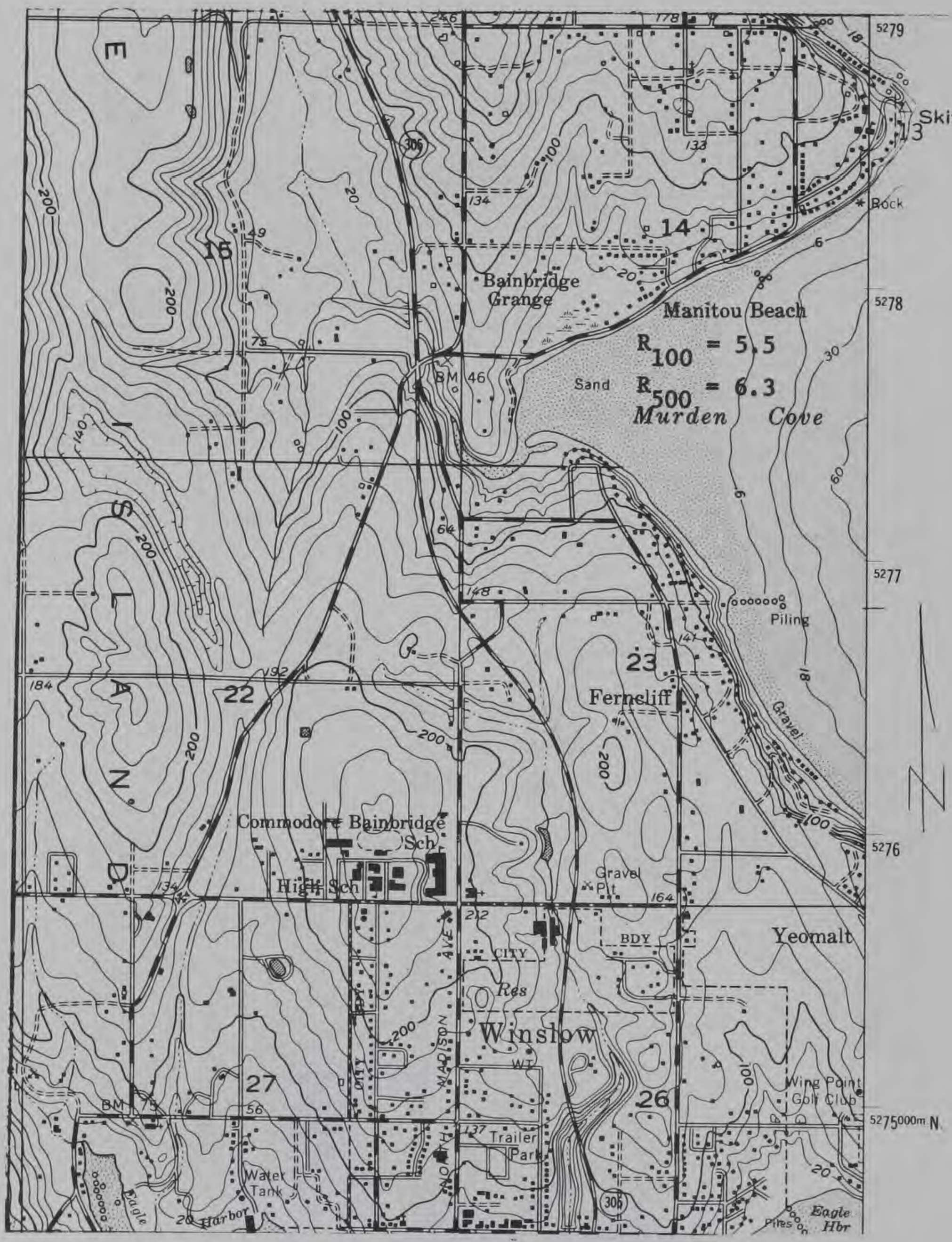

Figure 220. Suquamish, Wash., 75-N to 79N, R

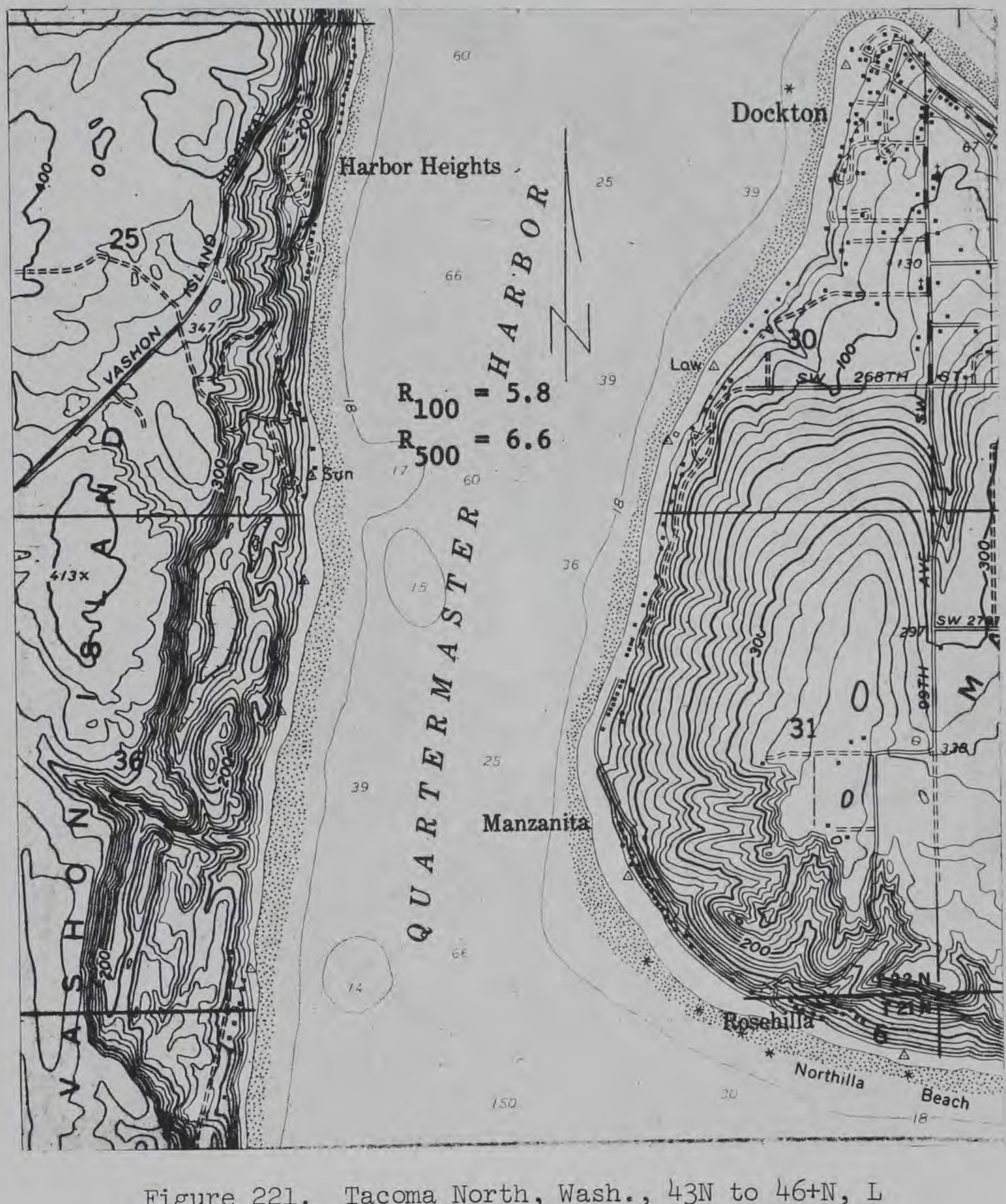

Figure 221. Tacoma North, Wash., 43N to 46+N, L

Figure 222. Tacoma North, Wash., 41E to 44+E, T

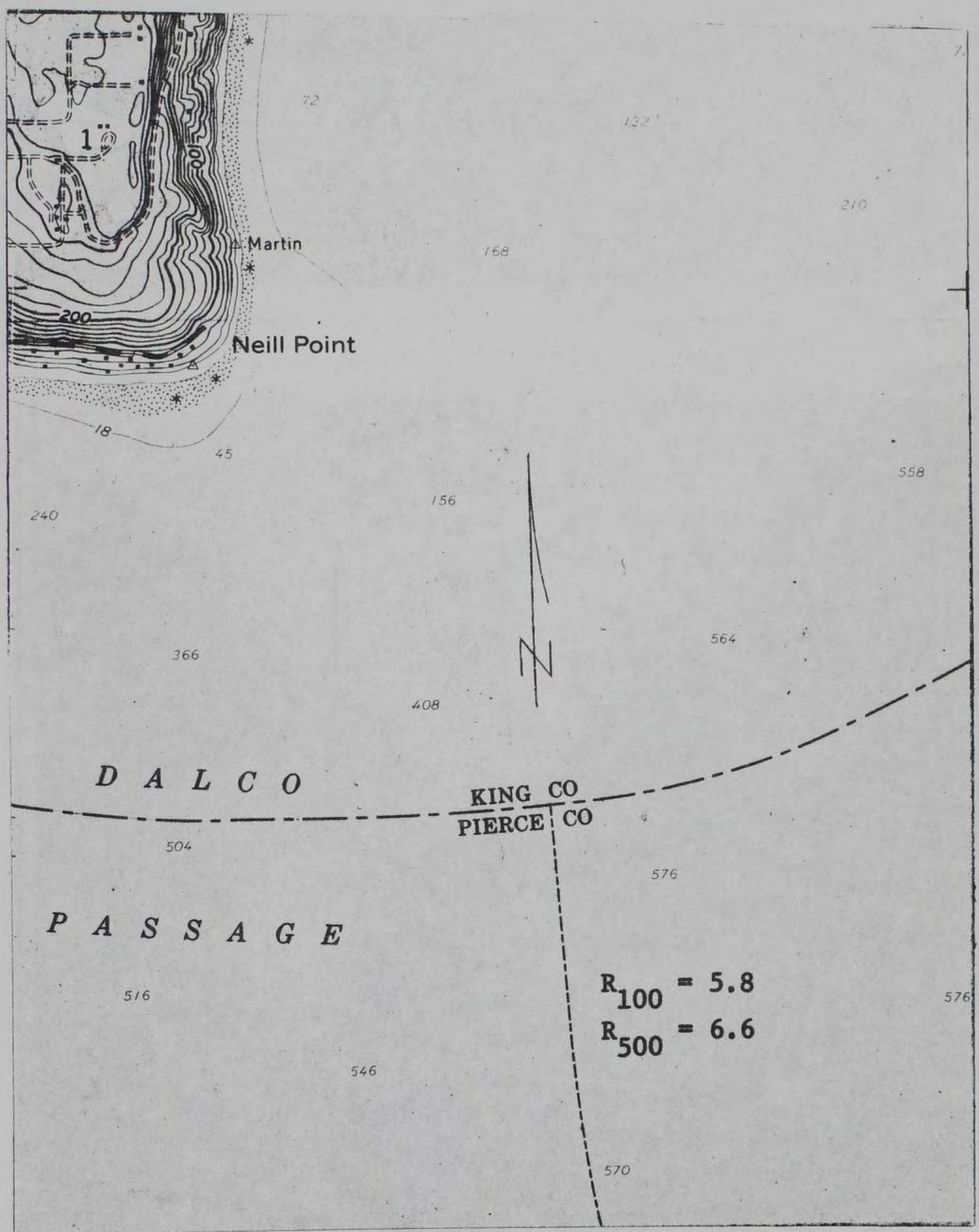

Figure 223. Tacoma North, Wash., 37-E to 41E, T

Figure 224. Tacoma North, Wash., 38-E to 41E, B

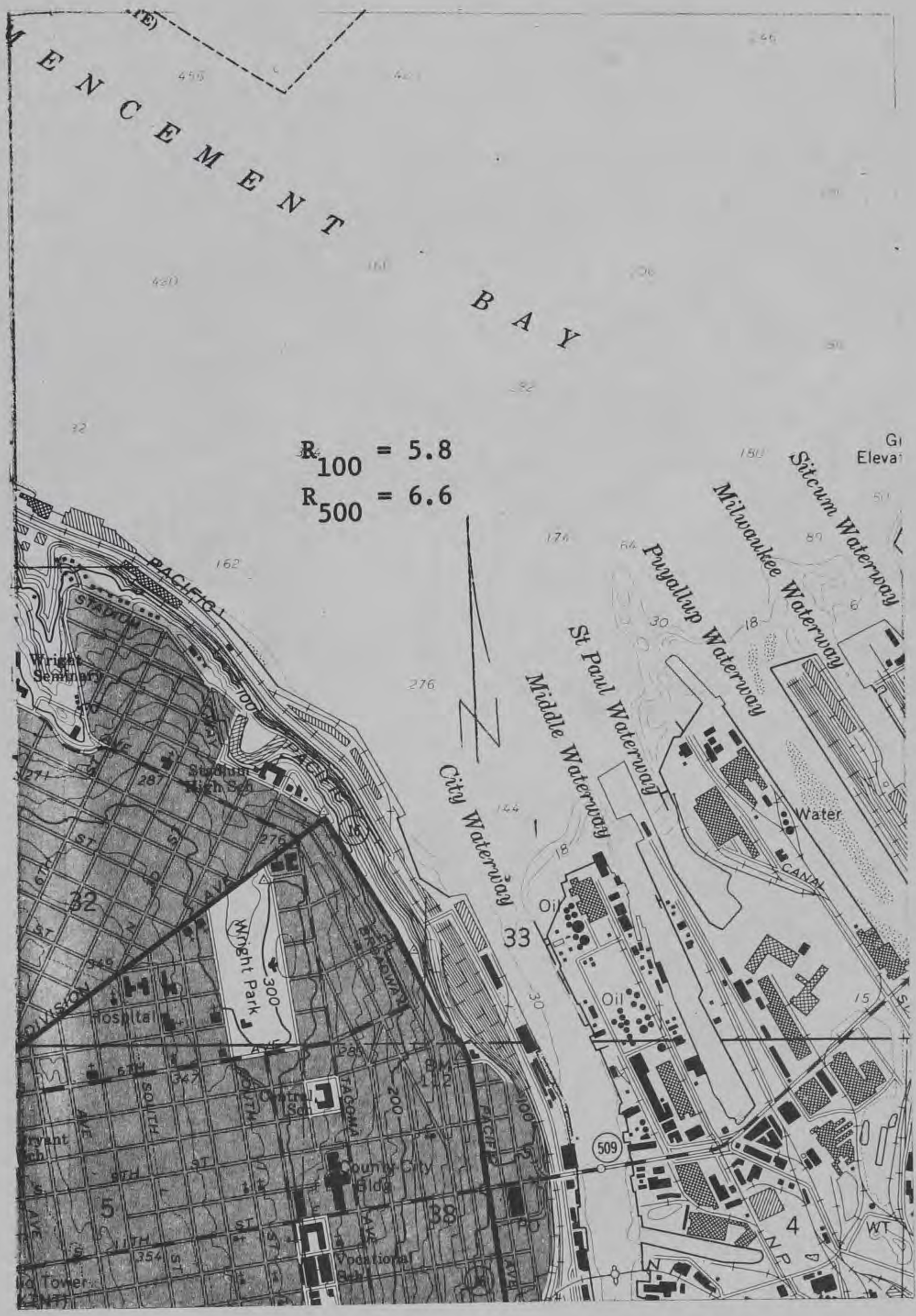

Figure 225. Tacoma North, Wash., 41E to 44E, B

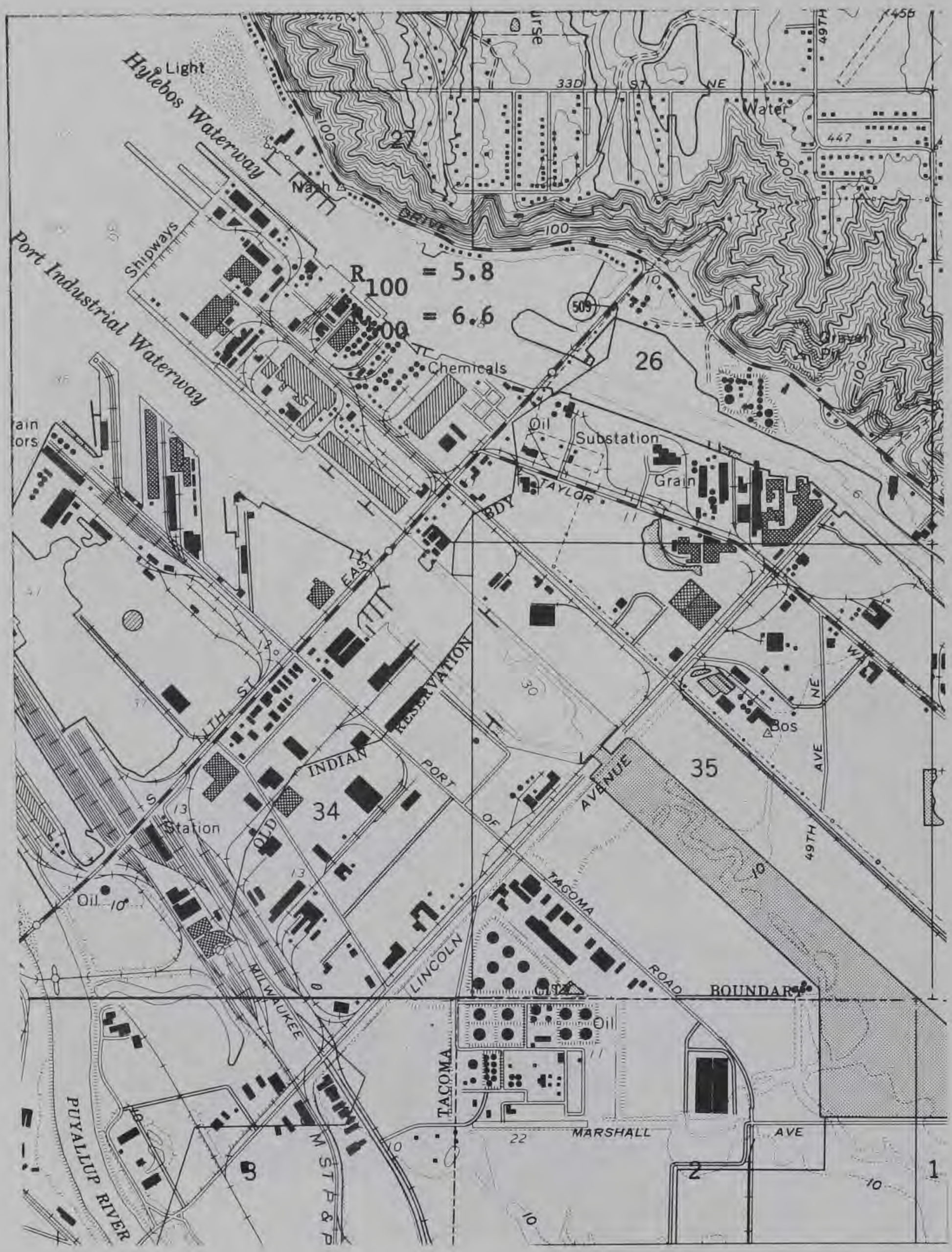

Figure 226. Tacoma North, Wash., 44E to 47+E, B

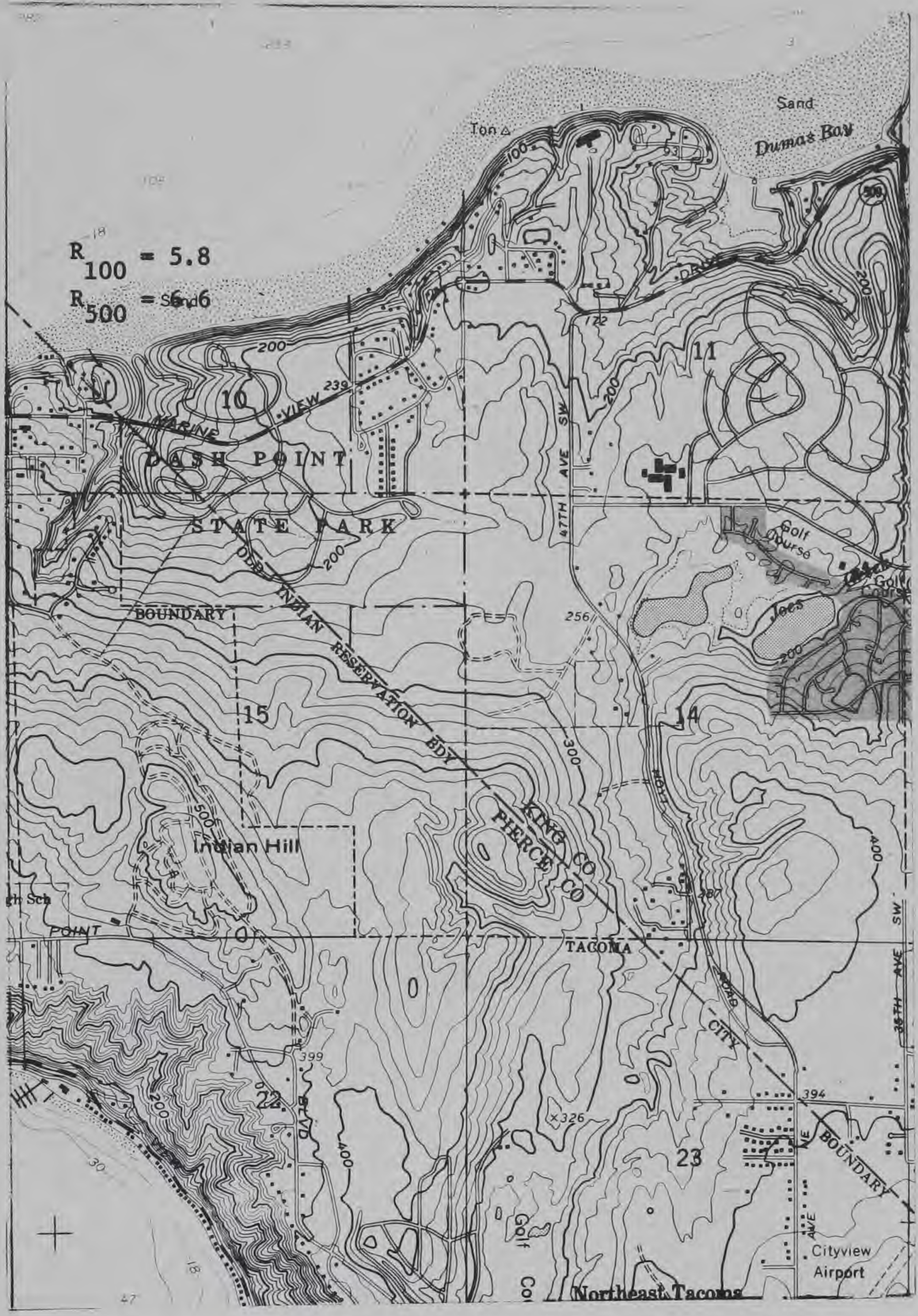

Figure 227. Tacoma North, Wash., 37+N to 42N, R

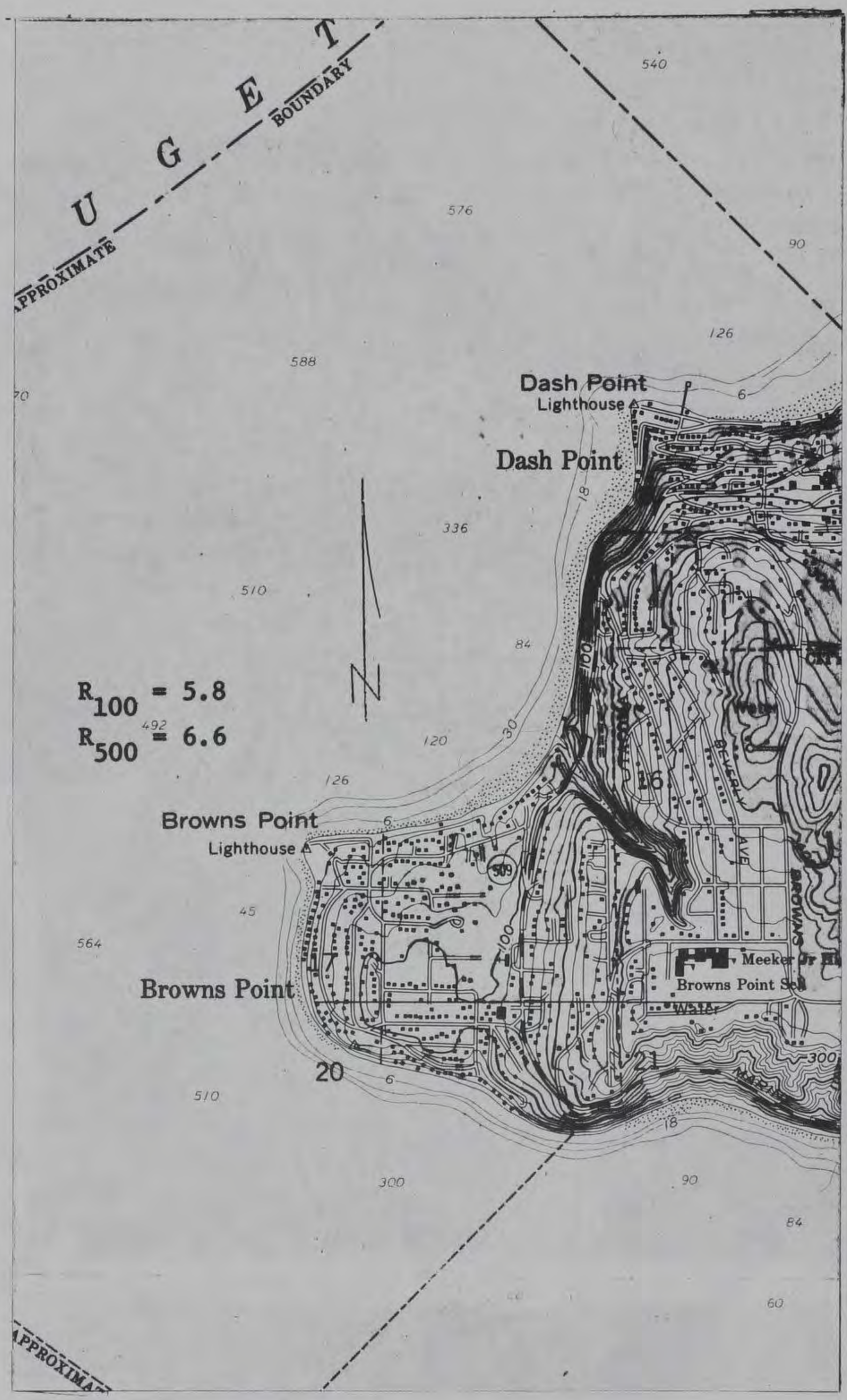

Figure 228. Tacoma North, Wash., 37+N to 42N, R

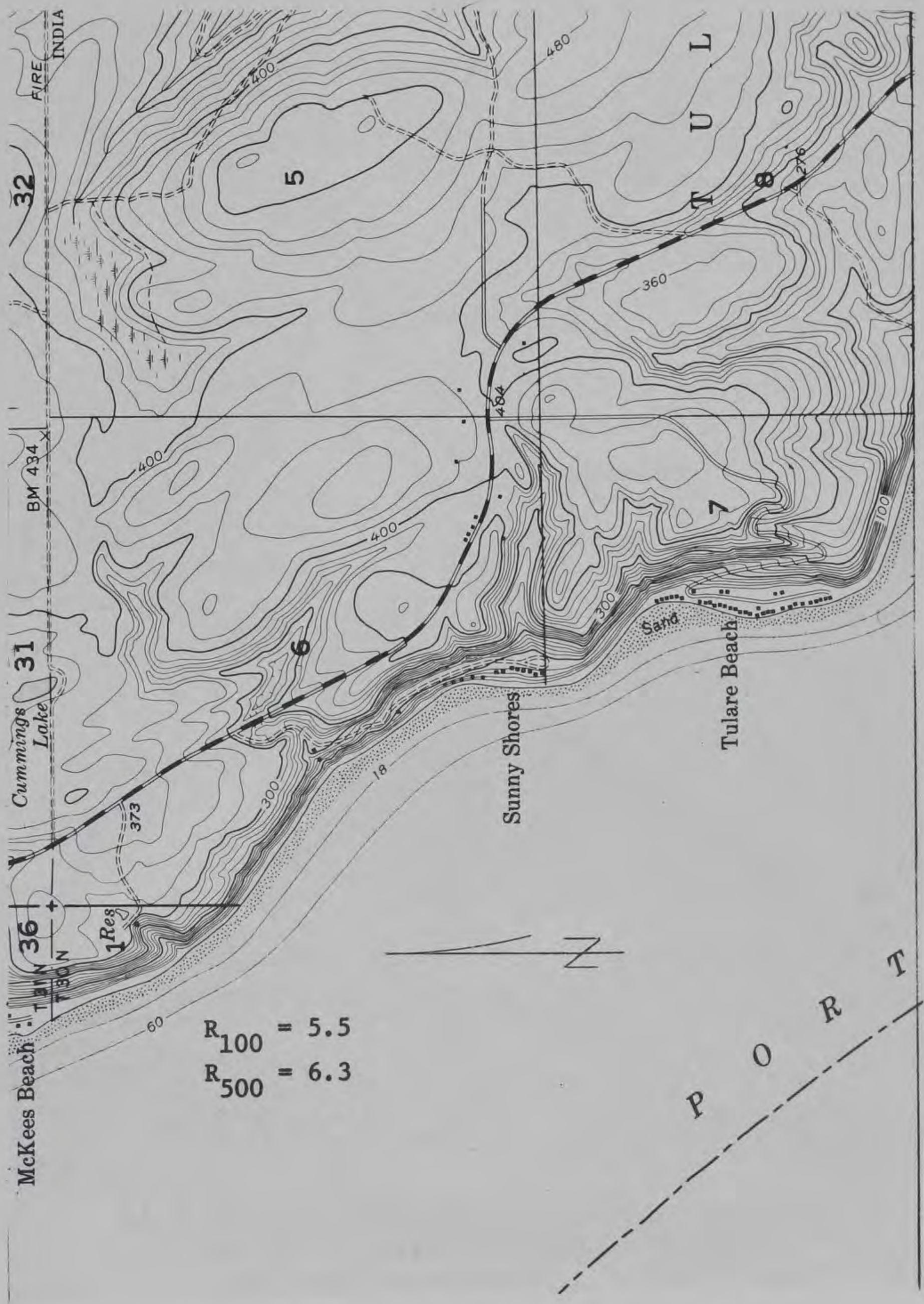

Figure 229. Tulalip, Wash., 27N to 30+N, L

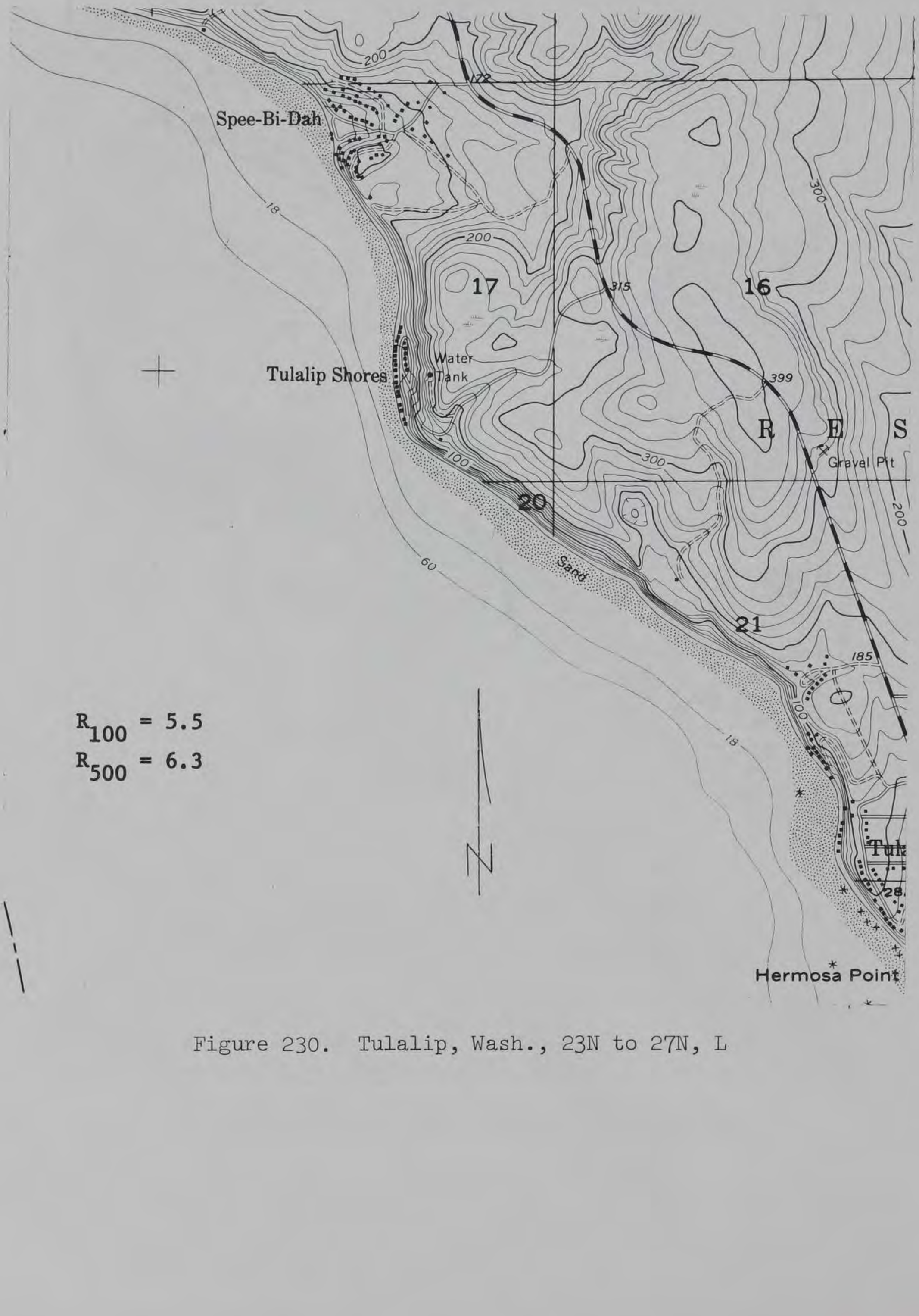

$R_{100} = 5.5$
$R_{500} = 6.3$

Figure 230. Tulalip, Wash., 23N to 27N, L

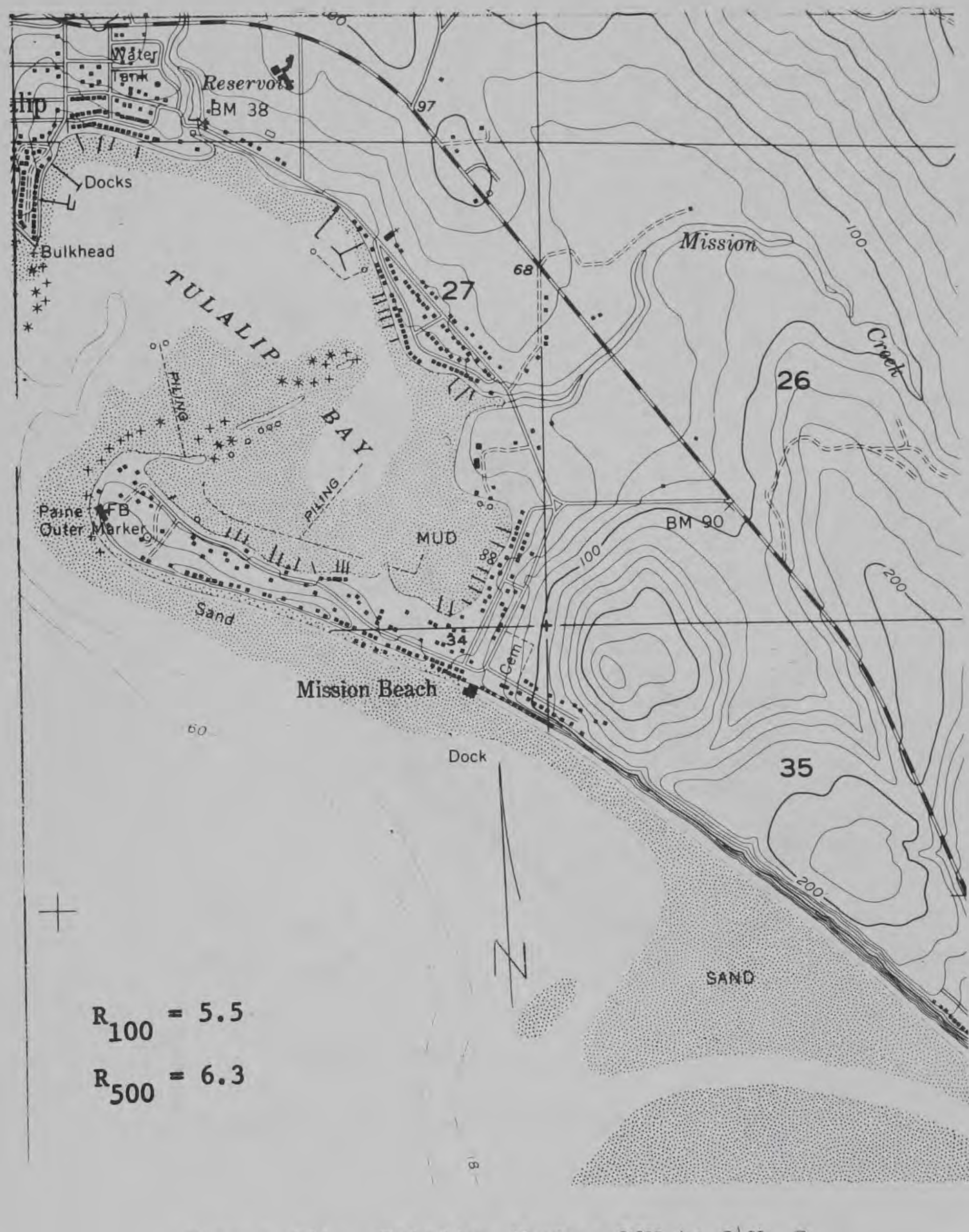

$R_{100} = 5.5$

$R_{500} = 6.3$

Figure 231. Tulalip, Wash., 20N to 24N, R

Figure 232. Tulalip, Wash., 49E to 52E, B

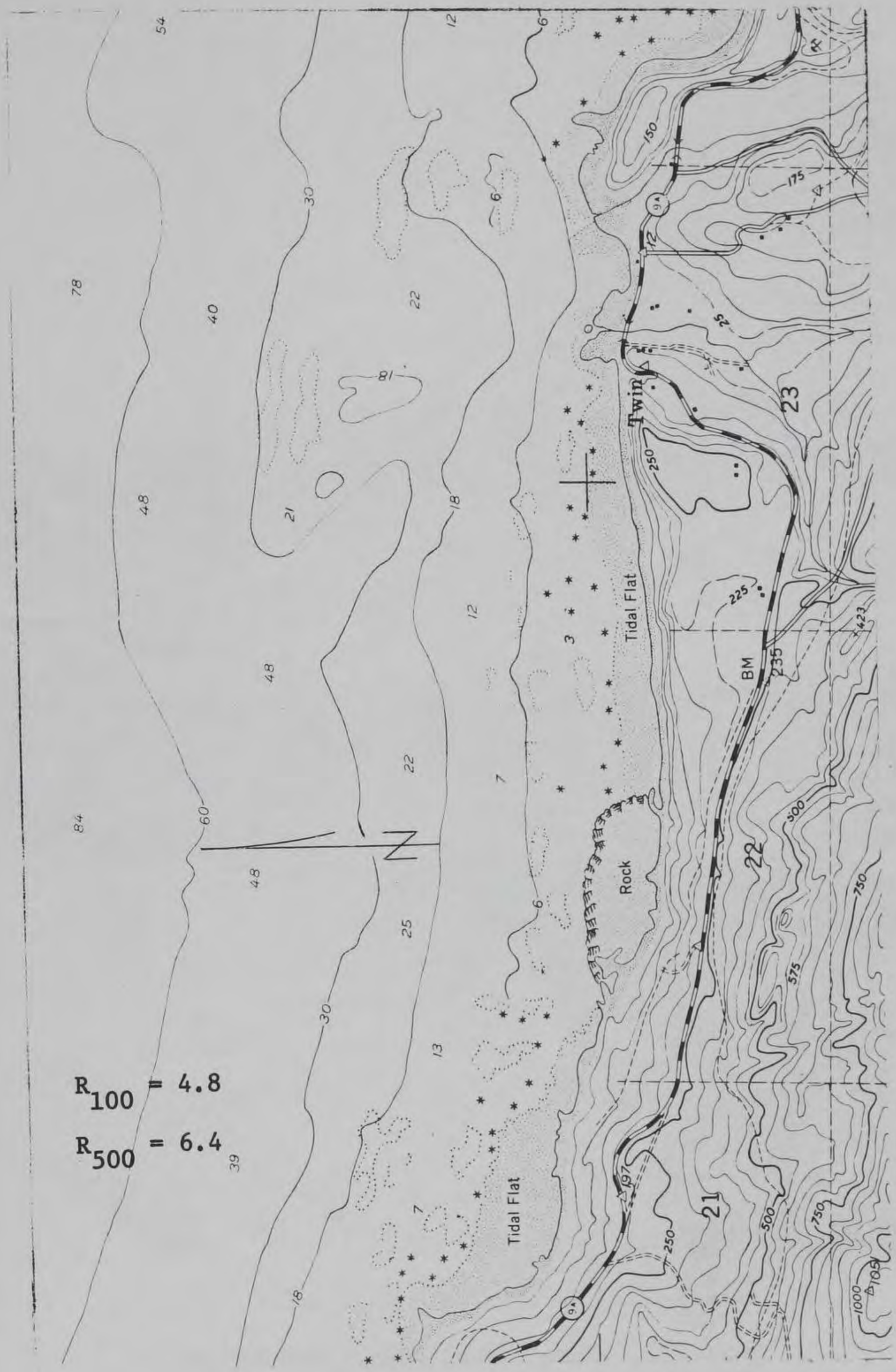

Figure 233. Twin River, Wash., 34N to 37N, R

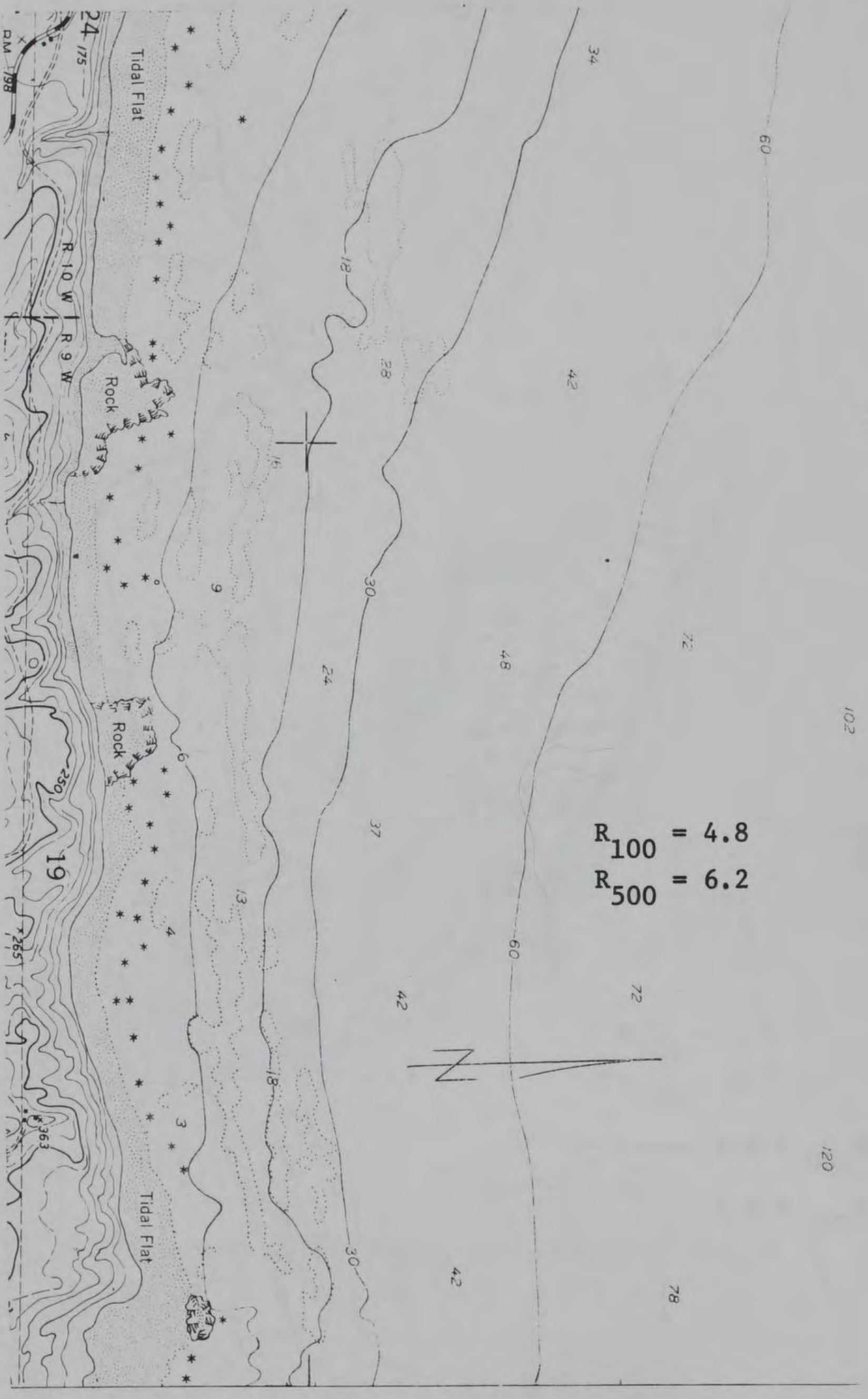

Figure 234. Twin River, Wash., 34N to 37N, R

Figure 235. Vashon, Wash., 57N to 60+N, L

Acres

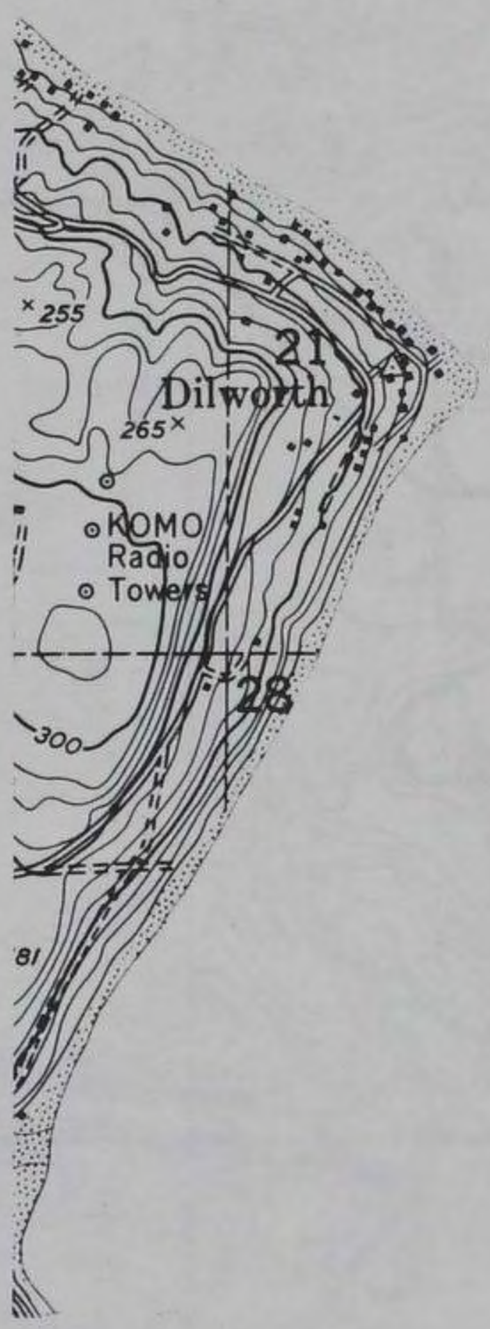

PUGET

Figure 236. Vashon, Wash., 42E to 44E, T

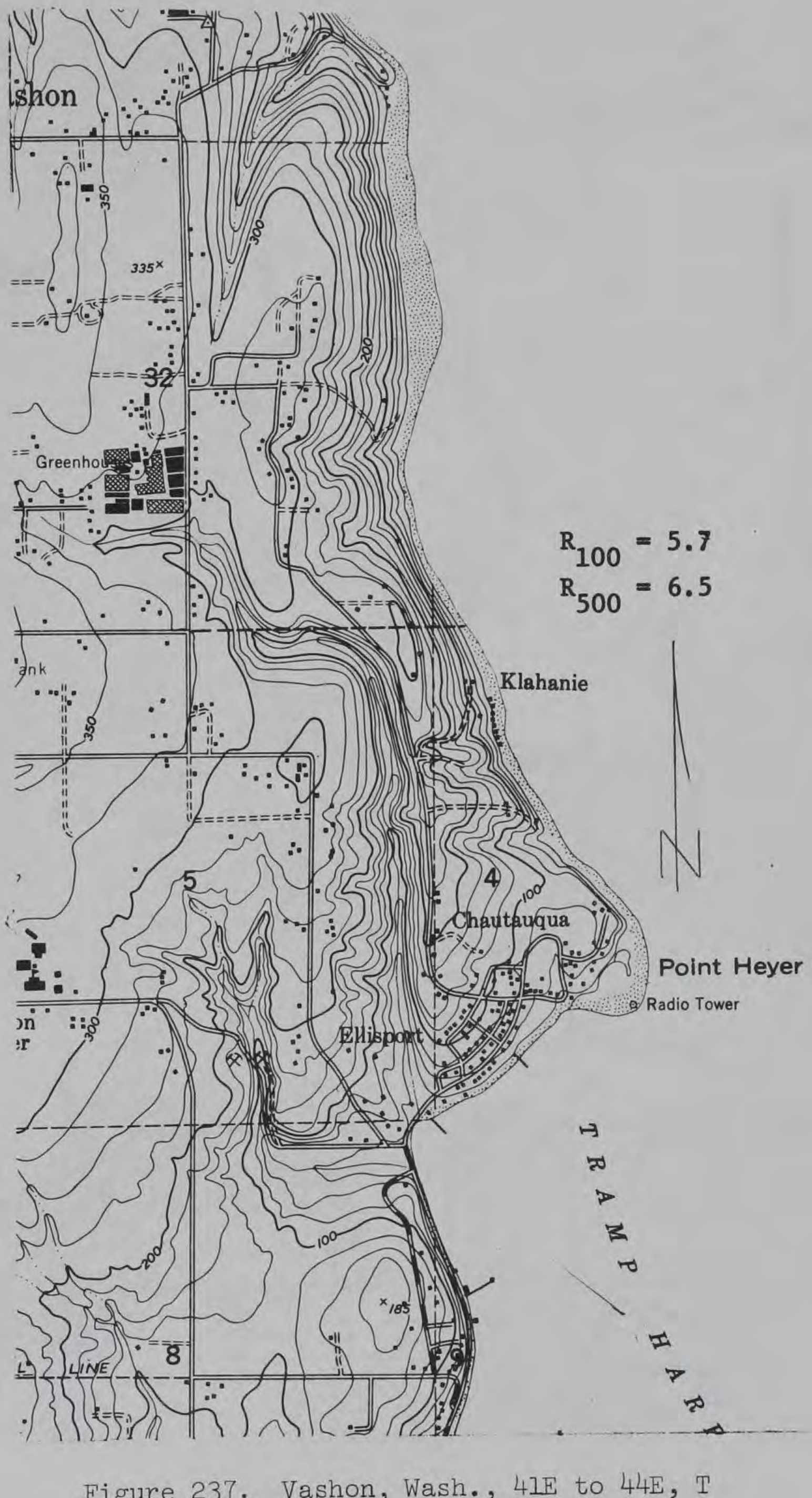

Figure 237. Vashon, Wash., 41E to 44E, T

Figure 238. Vashon, Wash., 37+E to 43E, B

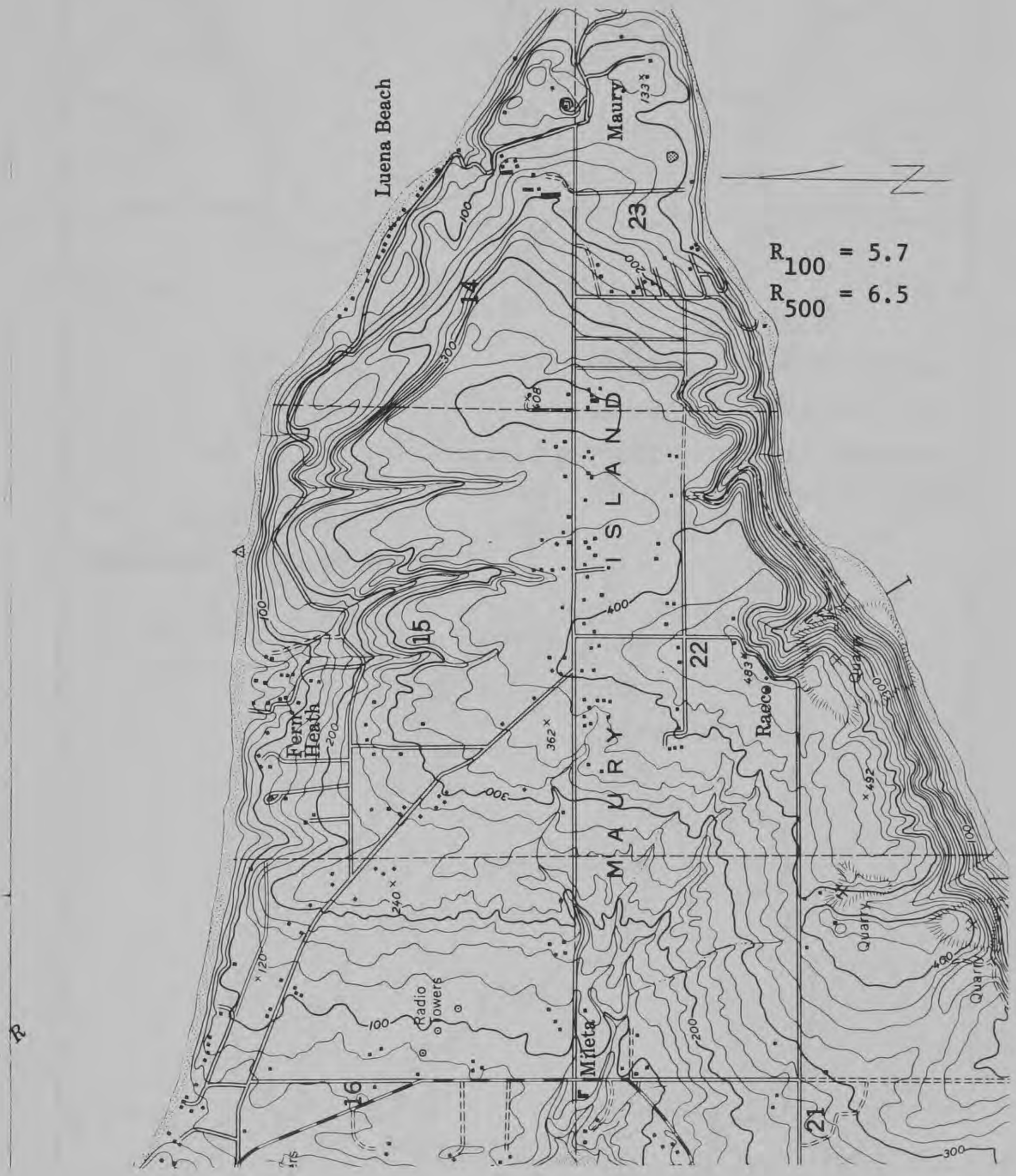

Figure 239. Vashon, Wash., 43E to 47+E, B

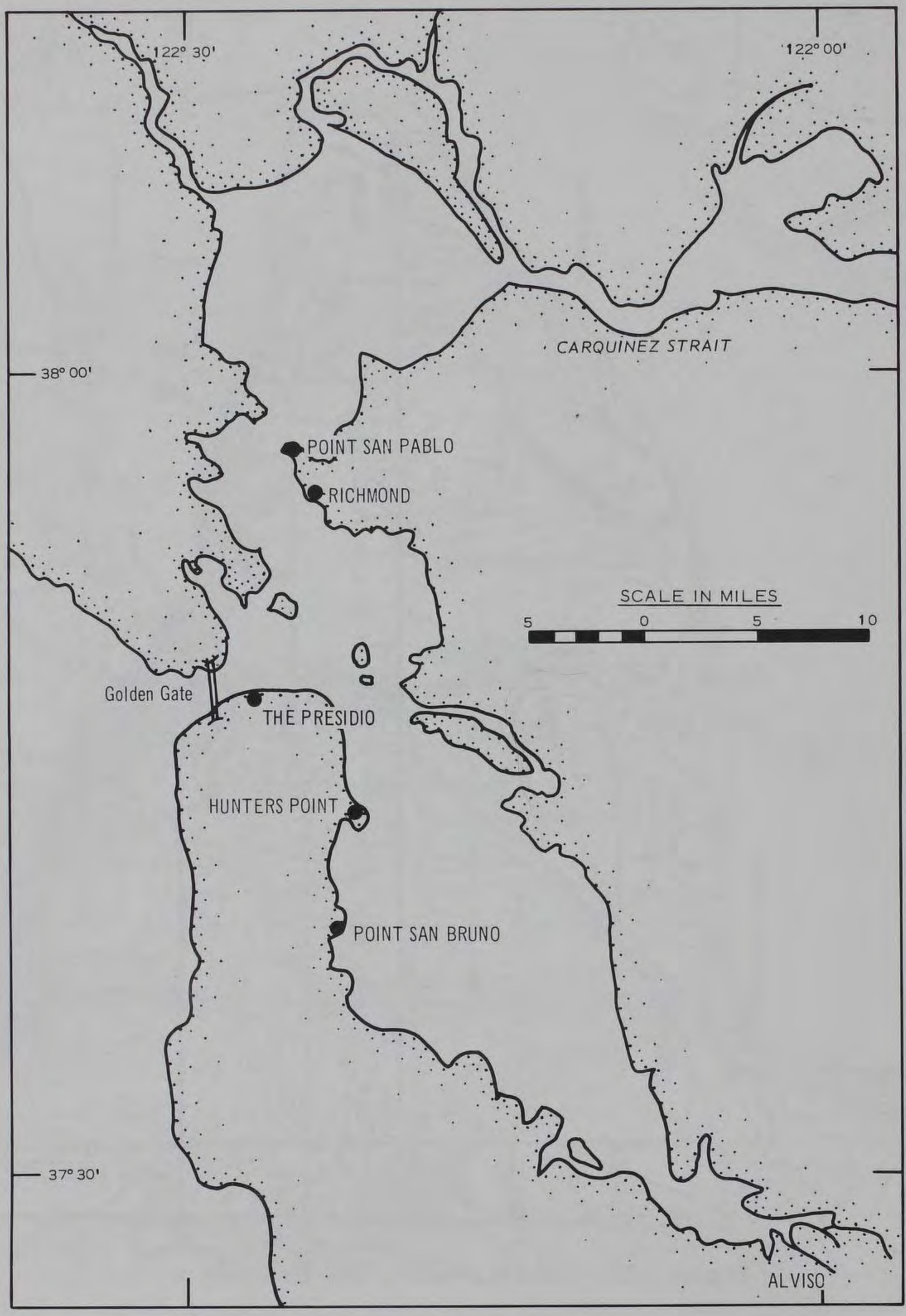

a. Vicinity map

Figure 240. San Francisco Bay (Sheet 1 of 2)

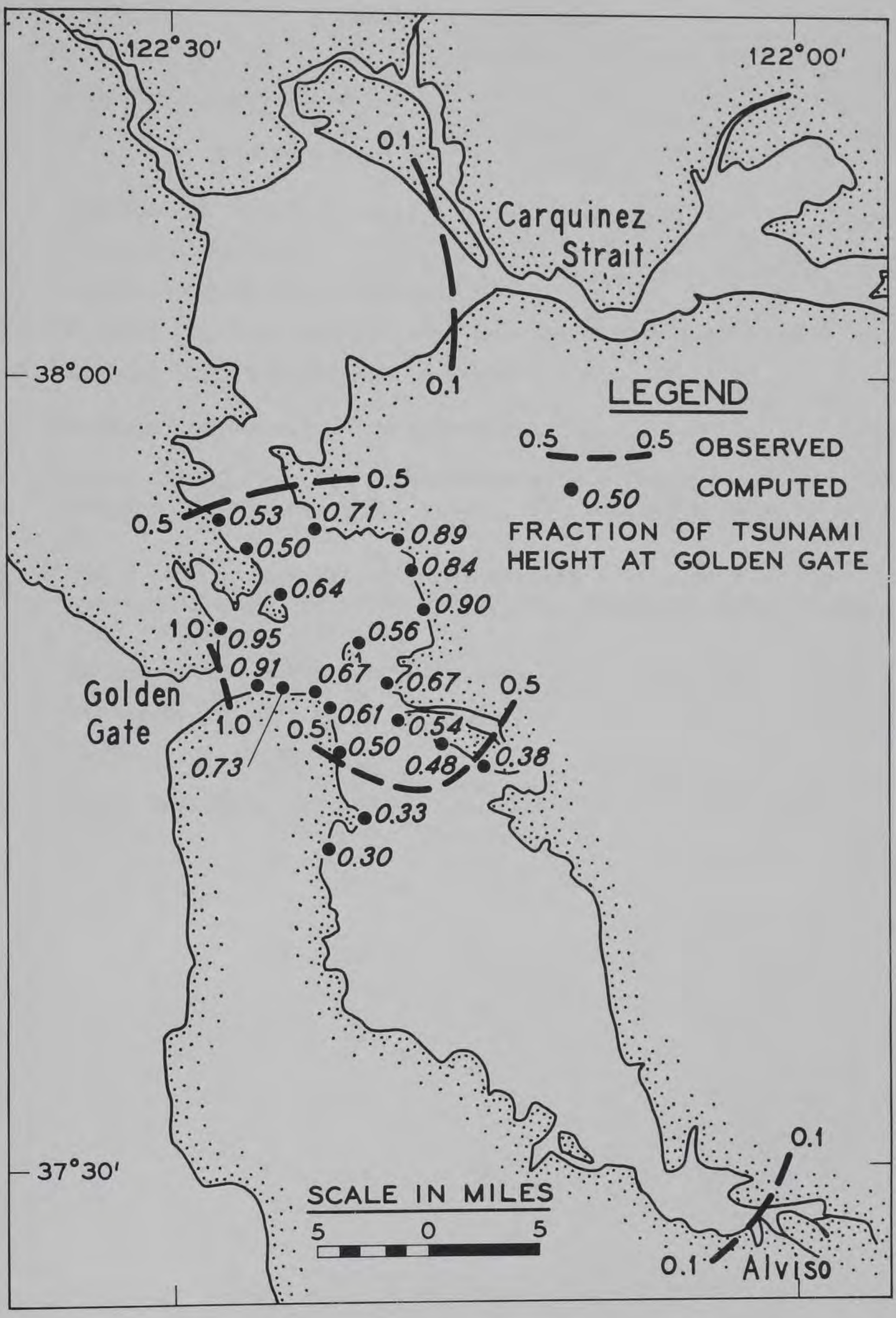

b. Tsunami attenuation (after Magoon[11])

Figure 240. (Sheet 2 of 2)

APPENDIX A: NOTATION

A	Amplitude constant
C_m	m^{th} tidal constituent
$f(\ )$	Probability density function
i	Tsunami intensity
$n(\ )$	Tsunami probability function
$P(\ )$	Probability function for combined astrotides and tsunamis
$P_S(\ )$	Probability function for tsunamis
$P_\beta(\ )$	Probability function for astrotides
R_{100}	Runup that is equaled or exceeded with a frequency on the average of once every 100 years. The reference datum is msl, ft
R_{500}	Runup that is equaled or exceeded with a frequency on the average of once every 500 years. The reference datum is msl, ft
z	Water-surface elevation above msl, ft
α	Exponential constant
λ	Variable of integration
σ^2	Tidal variance